UTILISATION OF ELECTRICAL AND ELECTRONIC PLASTIC WASTE AS REPLACEMENT FOR AGGREGATE IN CONCRETE

Lewis Alfred Parsons

A dissertation submitted to the Faculty of Engineering and the Built Environment, University of the Witwatersrand, in fulfilment of the requirements for the degree of Master of Science in Engineering.

Johannesburg, 2019

Declaration

I declare that this dissertation is my unaided work. It is being submitted to the Degree of Master of Science in Engineering to the University of the Witwatersrand, Johannesburg. It has not been submitted before for any degree or examination to any other University.

……

…….…day of…….…….year…….……...

Abstract

Waste electrical and electronic plastic (WEEP) recycling is complex due to the presence of different hazardous additives, variety in plastic types and degraded polymers among others. This often results in vast quantities of WEEP being discarded of in landfills, incinerated or stored in warehouses, whereby it could have rather been used as an aggregate replacement material in concrete.

The main aim of this research was to produce structural concrete with a minimum compressive strength of 25MPa using different types of WEEP. The different types of WEEP used include: acrylonitrile-butadiene-styrene (ABS), polycarbonate acrylonitrile-butadiene-styrene (PC/ABS), high impact polystyrene (HIPS) and an equal blend of the aforementioned WEEP types. To address the concretes strength reduction found from WEEP substitution and to improve its durability, 10% condensed silica fume and 25% metakaolin replaced cement in concrete by mass respectively. Furthermore, a superplasticiser was used to maintain a set workability. In the experimental program WEEP was used at replacement percentages of 0%, 5%, 10%, 20% and 30% in the partial replacement of both fine and coarse natural aggregates in concrete to assess its behaviour for structural applications. By performing test of compressive and tensile strength, durability performance and scanning electron microscopy analysis it has been found that all WEEP types show a real possibility for use as aggregate in concrete.

Results showed that all mixes made without and with WEEP substitution for the natural aggregate attained the minimum compressive strength of 25MPa. When concrete with a WEEP replacement of 30% was compared to the control mix there was a large decrease in strength, but when concrete with a WEEP replacement of 5% was compared with the control mix the results showed almost equal strength for all WEEP types. There was a reduction in the oxygen permeability index and water sorptivity and an increase in chloride conductivity for concrete made with a WEEP replacement of 30% compared to the control mix. It was also found that all concrete mixes made using metakaolin or condensed silica fume as partial replacement for cement had a higher strength and improved durability compared to concrete mixes made using only cement as binder material. The use of WEEP in concrete could reduce the amount of WEEP disposed of and reduce the amount of natural aggregates mined. This in turn may produce an environmentally friendly concrete.

Dedication

To my loving Mom Annémerie Kleynhans, who is always in my heart. I miss you so much.

To my loving Dad Alfred Lewis Parsons, who has been my rock in this turbulent time.

I love you both so much.

Acknowledgements

I would firstly like to acknowledge God, for without Him I would never be on this journey.

To my supervisor, Professor Nwaubani. Thank you so much for all your valuable advice, friendship, encouragement, support and guidance throughout this study.

The laboratory staff at the School of Civil and Environmental Engineering at the University of the Witwatersrand for assisting me when I required it.

The laboratory staff at Microscopy and Microanalysis Unit at the University of the Witwatersrand for training me in using the XRD and EPMA instruments.

The staff at the School of Chemical and Metallurgical Engineering at the University of the Witwatersrand for assisting me in obtaining beautiful SEM images and assisting me in preparing samples for the use on the SEM analysis.

The staff at the School of Geosciences who prepared the thin sections for the SEM analysis.

To Mr. Ckool at the Writing Centre at the University of the Witwatersrand for helping me improve my writing skills.

Post Merit Award of the University of the Witwatersrand, for providing financial support.

AfriSam who donated the natural aggregates and cement.

Anton Paar for testing the particle size distribution, surface area, relative density and pore-size distribution for some of the materials.

Kaolin-Group and Serina Trading Company for donating the metakaolin.

Sika for donating the superplasticiser and condensed silica fume.

And lastly my deepest gratitude to my family and friends who have seen so little of me during my time of this research. Thank you so much for all your love and understanding.

Table of Contents

List of Figures

List of Tables

List of Abbreviations

ABS:	Acrylonitrile-butadiene-styrene
BSE:	Backscattered Electrons
CBD:	Compact Bulk Density
CoV:	Coefficient of Variance
CSF:	Condense Silica Fume
C-S-H:	Calcium Silicate Hydrate
EEE:	Electrical and Electronic Equipment
EEP:	Electrical and Electronic Plastic
EDS:	Energy Dispersive X-ray Spectroscopy
EoL:	End of Life
EPMA:	Electron Probe Micro Analyser
e-Waste:	Electronic Waste
FESEM:	Field Emission Scanning Electron Microscope
hcp:	Hardened Cementitious Paste
HIPS:	High Impact Polystyrene
NEMA:	National Environmental Management Act
MMU:	Microscopy and Microanalysis Unit
MK:	Metakaolin
PC:	Polycarbonate
PS:	Polystyrene
SANS:	South African National Standards
S.D:	Standard Deviation
SE:	Secondary Electrons
SEM:	Scanning Electron Microscope
WDS:	Wavelength-Dispersive Spectroscopy
WEEP:	Waste Electrical and Electronic Plastic
XRD:	X-ray Diffraction
XRF:	X-ray Fluorescence

Chapter 1: Introduction

1.1 Background to the study

The e-Waste Association of South Africa (eWASA) defines e-Waste as electronic waste derived from information technology equipment, consumer electronics, small and large household appliances (eWASA, 2018).

South Africa and Algeria are some of the countries generating the largest amounts of e-Waste in Africa at 5.7kg/inh and 6.2kg/inh respectively. This is much compared to Africa's average e-Waste consumption of 1.9kg/inh (Baldé *et al*., 2017).

However, Lydall *et al*., (2017), states that only 11% of South Africa's annual e-Waste is recycled. Moreover, e-Waste volumes are expected to grow significantly in South Africa in the near future, with a growth rate of 10% per annum. This growth rate may be influenced by: social and economic development, increased consumer demand, perceived obsolescence, shorter replacement cycles and an increase in the efficiency of technology (*ibid*).

South Africa does not have any formal official governmental policy documented specific to e-Waste management, though has a progressive legislative regime in place (Baldé *et al*., 2017). Laws such as the National Environmental Management Waste Act provides measures for the prevention of pollution and ecological degradation.

However, countries with e-Waste legislations may still be vulnerable to e-Waste dumping. This may be due to improper e-Waste management, lack of recycling infrastructure, inadequate funding, lack of public awareness, unregulated disposal, collection and recycling of e-Waste (Molewa, 2015).

E-Waste companies in South Africa export approximately 90% printed circuit boards, 60% phosphorus powders and 80% waste electrical and electronic plastic (WEEP) (Lydall *et al.*, 2017). According to Godfrey (2016), much of South Africa's WEEP is exported to Belgium, Sweden, Canada and China due to the lack of reprocessing facilities in South Africa.

WEEP is the plastic component derived from e-Waste. It is frequently the least economically valuable component which is often discarded with no intent for future use

(Lydall *et al*., 2017). This may be due to the complexity faced with the recycling of WEEP, such as: degraded polymers, potentially hazardous additives and immiscible plastics found in a single electrical device (Stenvall, 2013). Therefore, less than 25% of WEEP is recycled globally (Lundstedt, 2011).

One industry in which the use of WEEP is currently being considered, is in the construction sector. Previous studies have shown that the use of WEEP as a partial replacement for aggregates in concrete is possible. However, inconsistent or incomplete results were found among some literature. Some results of these studies are as follows:

- Lakshmi and Nagan (2010), conducted *Studies on Concrete Containing e-Plastic Waste*. They found a significant decrease in the compressive strength of the control mix when 25% WEEP replaced natural coarse aggregates from 19.83MPa to 6.15MPa at 28 days of curing. They also found that replacing cement with 10% fly ash by mass increased the compressive strength of the concrete mixed with and without WEEP as replacement material from 29.79MPa to 22.42 MPa at 28 days of curing; and
- Liu *et al*., (2015), investigated the *Performance of Recycled Plastic-Based Concrete*. They replaced fine natural aggregates in percentages of 5%, 10%, 15% and 20% with PC/ABS WEEP. They used a w:c ratio of 0.36 and a water reducing admixture with a dosage of 1.5% by mass of cement. Results showed a large decrease in the compressive strength from 44.7MPa to 28.6MPa at 28 days when 20% PC/ABS WEEP replaced natural aggregates.

1.2 Motivation for the project

South Africa's population has grown from 51.58 million people in 2011 to 55.91 million people in 2016 (Trading Economics, 2018). This growth in population may result in an increase for the demand of electrical and electronic (EEE) and hence, increase the amount of e-Waste produced.

The use of WEEP in South Africa is very low, resulting in stockpiles accumulating on company sites. Utilising WEEP as a partial replacement for the natural aggregate in concrete may reduce its waste footprint (Lydall *et al*., 2017). Moreover, it may help the South African economy by using these problematic plastic fractions as a secondary resource and hence, create employment opportunities (Godfrey, 2016).

Because the use of WEEP as a partial replacement for the natural aggregate in concrete is a relatively new development in the construction sector, a lot of research is required. Therefore, this study aims to contribute to this body of knowledge.

1.3 Aim

The main aim of this research was to produce structural strength concrete (concrete used for structural applications with a minimum characteristic strength of 25MPa at 28 days of curing) using different types of WEEP in the partial replacement of both fine and coarse natural aggregates in concrete.

1.4 Objectives

The objectives of this study are as follows:

- Evaluate the physical, chemical and mineralogical properties of the materials used;
- Study the surface typography of the natural aggregate, granulated WEEP and binder materials;
- Study the workability of fresh concrete made with and without 30% WEEP replacement of both the fine and coarse natural aggregate;
- Assess the compressive strength of concrete replaced with different types of WEEP in replacements of 5%, 10%, 20% and 30% by volume at 3, 7, 28, and 90 days of curing. The different types of WEEP include: acrylonitrile-butadiene-styrene (ABS), polycarbonate acrylonitrile-butadiene-styrene (PC/ABS), high impact polystyrene (HIPS) and an equal blend of the aforementioned WEEP types;
- Evaluate the tensile splitting strength of concrete made without and with 30% WEEP replacement of both the fine and coarse natural aggregate at 28 days of curing;
- Assess the durability of hardened concrete made with and without 30% WEEP replacement of both the fine and coarse natural aggregate at 28 days of curing. These durability tests include the oxygen permeability index, water sorptivity and chloride conductivity tests;
- Repeat the above-mentioned strength and durability tests by replacing cement with 10% condensed silica fume by mass;
- Repeat the above-mentioned tests replacing cement with 25% metakaolin by mass;

- Study the effect of the micro-structure on the observed durability performance characteristics using mercury intrusion porosimetry.
- Study the interfacial transition zone between the aggregates used and the hardened cementitious paste; and
- Investigate the environmental and financial significance of concrete made using WEEP as replacement material for natural aggregates in concrete.

1.5 Layout of the dissertation

The dissertation is divided into eight chapters that are arranged as follows:

- Chapter1: Provides the background, motivation, aim and objectives for this study;
- Chapter 2: This chapter provides an in-depth review and general background pertaining to the nature of e-Waste. After which is a detailed review pertaining to WEEP which is concluded with a brief discussion regarding plastic etching;
- Chapter 3: This chapter provides detailed information regarding the binder material and aggregates used;
- Chapter 4: Provides information regarding to the experimental details and procedures followed in this study;
- Chapter 5: This chapter discusses and compares the results found from previous chapters. It also discusses the correlation (if any) between the results for the compressive strength to the tensile strength, oxygen permeability, water sorptivity and chloride conductivity;
- Chapter 6: This chapter evaluates the possible environmental and financial significance of using WEEP as partial replacement for natural aggregates in concrete;
- Chapter 7: This chapter discusses the important observations and conclusions made in previous chapters; and
- Chapter 8: Suggests possible areas for future research.

See Figure 1 for the flowchart relating to the layout of this study.

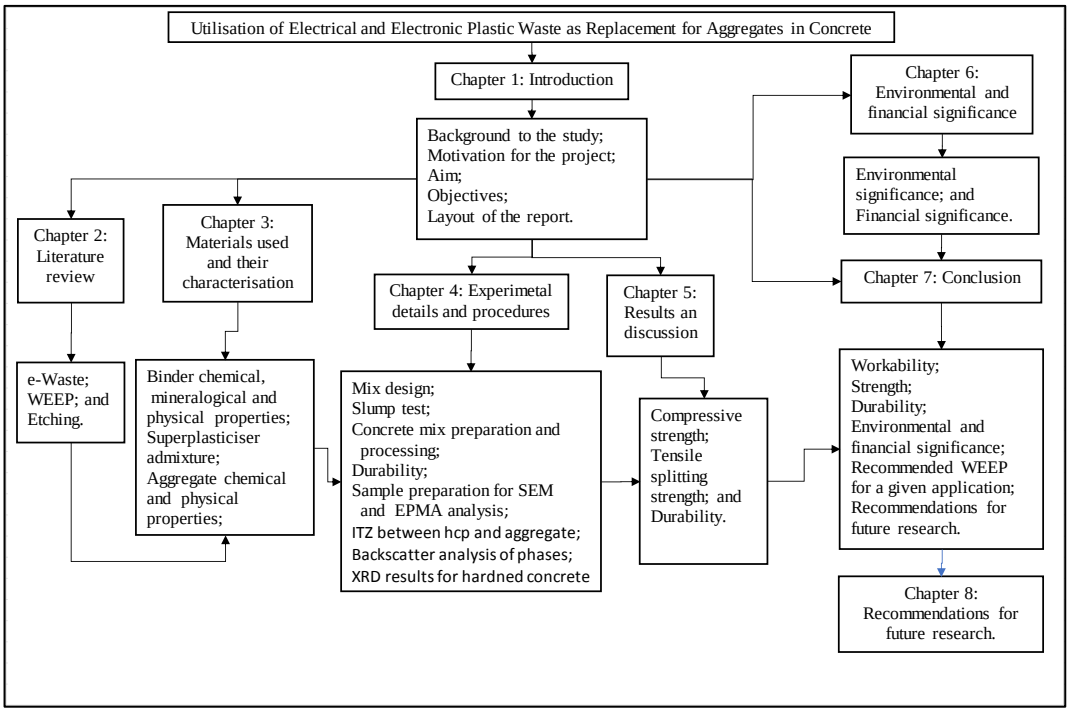

Figure 1: Flowchart for the layout of the study.

Chapter 2: Literature review

2.1 Introduction

Waste electrical and electronic plastic (WEEP) is one of the larges waste streams derived from e-Waste due to the fact that it is difficult to recycle. This in turn results in large amounts of WEEP disposed of in an un-environmentally friendly manner. It is therefore important to evaluate an alternative option to address these problematic fractions.

This literature reviewed has been organised into five sections and is presented in the following order:

- Brief discussion on the nature of e-Waste. It provides an insight into the current body of knowledge pertaining to e-Waste. This includes information on the current e-Waste legislations, transboundary movements and the managements of e-Waste;
- Detailed discussion on WEEP. This section provides a broader understanding pertaining to the mechanical properties of plastics and the challenges facing WEEP and its recycling. It also includes information pertaining to the different types of technologies available for WEEP recycling;
- An overview on previous research conducted regarding WEEP recycling in concrete;
- Brief discussion regarding the etching of plastics. This includes information on technologies available which could increase the surface area of WEEP. This in turn could improve the bonding between the WEEP and the hardened cementitious paste; and
- Brief discussion regarding cement hydration, pozzolanic reactions and the partial replacement of cement with a pozzolanic material.

2.2 E-waste

There is no official definition for e-Waste and hence, have a wide spread meaning across the world. Different countries and organisations have tried to cover aspects in defining e-Waste with some being inclusive while others are more specific.

The Official Journal of the European Union states that e-Waste is derived from waste components, sub-assemblies and consumables originating from electrical and electronic equipment (EEE) with a voltage less than 1 000V for alternating currents and 1 500V for

direct currents (Council, 2012). The Basel Convention of e-Waste Africa Program also have their own definition of e-Waste. They state that e-Waste is electrical and electronic equipment (EEE) that has reached its end of life (EoL), which will be dismantled for spare parts, material recovery or final disposal (Manhart *et al*., 2011).

These aforementioned definitions have very different meanings and could cause confusion when dealing with different types of e-Waste. One method to deal with e-Waste is by categorising it into either general waste (from which the hazardous components or substances have been removed) and hazardous wastes.

E-Waste in South Africa is categorised into eight sub-categories (Lydall *et al*, 2017):

1. Large household appliances (cookers, refrigerators, freezers and microwaves, etc.);
2. Small household appliances (vacuum cleaners and irons, etc.);
3. Office, information technology (personal computers, printers and photocopiers, etc.) and communication equipment (routers, modems and cell phones, etc.);
4. Entertainment and consumer electronics (radios, television sets and video cameras, etc.) and toys, leisure, sport and recreational equipment (video consoles, trains and electric cars, etc.) and automatic issuing machines;
5. Lighting equipment (fluorescent lamps, light emitting diode lamps, high intensity discharge lamps and high-pressure lamps);
6. Electrical tools (drills and grinding machines, etc.);
7. Security (cameras and control panels, etc), and health care equipment (cardiology equipment, radiotherapy, etc.); and
8. Mixed e-Waste.

Grouping the above-mentioned e-Waste into categories aids in sorting the products into their original function, weight, size and material composition. This helps in the logistics of collection, management, recycling, treatment and final disposal (Torres *et al*., 2016). This in turn aids in predicting the possible lifetime profile, waste quantities, economic value and potential environmental and health impacts (Baldé *et al*., 2014).

E-Waste in the abovementioned list, may also assist countries to appropriately deal with e-Waste through relevant conventions and legislations. The following section evaluates the current conventions and legislations available and how they may assist countries in dealing with e-Waste.

2.2.1 E-waste legislation

It is estimated that 4.8 billion people (66% of the world's population in 2017) were covered by an e-Waste legislation in 2017 (Baldé *et al.*, 2017). However, the scope of products covered by e-Waste legislations are different depending on the definition used. There are currently numerous different conventions available to assist membering countries in controlling the movement of hazardous wastes. These include the Basel Convention and the Bamako Convention among others, as described below.

The Basel Convention is a treaty between membering countries whereby both parties agree on the degree of hazardousness of the waste under the provisions of the national law and requires prior consent before trading of the waste product. The Basel Convention defines hazardousness as either hazardous or non-hazardous depending on the waste's chemical properties (Manhart *et al.*, 2011). The Basel Convention encourages the environmentally sound management of hazardous wastes or other wastes by ensuring that sufficient steps are taken to ensure human and environmental protection against hazardous wastes. However, different countries may interpret this definition according to their own situations and ground realities. This definition depends on both the technical status of the product and the market of the imported country. The Basel Convention does not deal with e-Waste as such, but rather as hazardous components (Baldé *et al*., 2017).

Similar to the Basel convention, the Organisation for Economic Cooperation and Development supervises and controls the transboundary movement of wastes of membering countries. However, it focuses more on wastes exported for the purpose of material recovery and aims to minimise hazardous waste shipments (Baldé *et al*., 2017).

The Bamako Convention on the Ban of the Import into Africa and the Control of Transboundary Hazardous Wastes within Africa is a treaty of African nations which prohibits the import of hazardous and radioactive wastes into Africa from contracting parties (Manhart *et al*., 2011). According to Finlay and Liechti (2008), South Africa has an interest in importing wastes for recycling in the future and has hence, not been signed.

These above-mentioned conventions could assist countries in managing the movement of hazardous wastes into and out of their respected borders. However, it may be ideal if countries already have a legislation dealing specifically with e-Waste.

South Africa does not have any e-Waste legislation, however has environmental measures in place to deal with both hazardous and non-hazardous wastes. South Africa has waste policies which encourages all wastes to be reduced, reused, recycled or recovered before landfilling. E-Waste is considered a hazardous waste in South Africa and may be very harmful to human health and the environment if not disposed of correctly (Lydall *et al*., 2017).

Acts concerning hazardous wastes in South Africa include the National Environmental Management Waste Act and the National Domestic Waste Collection Standards. These Acts describe and define hazardous wastes as being organic or inorganic compounds which have a detrimental impact to the environment or human health (NEMA, 2008).

Section 4.2.A and 4.2.B of the aforementioned Act deals with the collection and recycling of main stream and non-mainstream recyclable waste. It states that cities are obligated to provide environments whereby households are enabled to recycle domestic waste, and that wastes must be sent to well-advertised drop-off centres. It also states that electronic waste must be routed to relevant drop-off zones for suitable recycling (*ibid*). Thus, according to the Act, e-Waste can easily be collected and treated in an appropriate manner.

Section 19 of the Act deals with reduction, re-use, recycling and recovering of waste. It states that suitable infrastructure is only required when more than 100kg of hazardous waste is processed per day (*ibid*). Section 25 of the Act deals with the duties of transporting waste. It states that hazardous wastes transported other than for disposal requires prior authorisation and a written confirmation from the receiver of the waste transported, and that the receiver of the waste has the facility to safely handle the waste (*ibid*). Thus, e-Waste will only be transported and received by appropriate parties and would be treated accordingly.

The Hazardous Substances Act (Act No. 15 of 1973), provides measures on the control and the degree of substances which may be hazardous or dangerous to humans. The Act also provides measures on the manufacture, sale, use, disposal and dumping of substances among others (Act, 1973). The Act categorises electronic products as a Group 3 hazardous substance and provides regulations to deal with waste appropriately (*ibid*).

It is clear from the foresaid Acts that provided countries have joined relevant conventions and have environmental Acts in place, that appropriate trading and transboundary

movement of e-Waste is possible. However, although many countries who have joint relevant conventions and have environmental Acts in place to deal with hazardous wastes, may still fall victim to illegal e-Waste trading's and dumping's. This is partly due to the fact that they do not have the facilities to enforce such laws and hence, require a strong co-coordination between governments, such as the Ministry of Environment and the Ministry for Communication Technology. Some of the advantages and pitfalls of transboundary movements and trading of e-Waste are discussed in the following section.

2.2.2 Transboundary movements of e-Waste

The trading of e-Waste may be beneficial for both parties, provided that it is done accordingly. This is because the trading of second-hand electronics, refurbishment of EEE components or the recycling of EoL EEE in an environmentally sound manner can lower its ecological footprint. Furthermore, the trading's of second hand EEE generally makes digital technologies more affordable, thus reducing the technological gap between trading countries (Honda *et al*, 2016).

However, e-Waste is often smuggled illegally and generally from developed countries to developing countries. This may be due to the lack of a clear definition for e-Waste or legislation. Smuggling of e-Waste is a lucrative business due to the value of the components, availability and the low risk of being caught (Lundgren, 2012). Smuggling is usually done by the mislabelling of merchandise, hiding it behind other goods, concealing it as other products or by falsely declaring it as second-hand products for personal use (Honda *et al*., 2016).

The illegal trading of e-Waste can be reduced if sufficient key actors within the lifecycle of EEE improved and enforced available schemes required for the successful treatment of e-Waste. The following section provides an insight to the generation of EEE and some countermeasures available to reduce the amount of e-Waste dumping's.

2.2.3 Management of e-Waste

The lifecycle of e-Waste depends on the useful life of the equipment, the need for renewal of the equipment and on the rapid technological innovations with new products on the market at lower prices. Many manufacturers design their products to be tamper proof, resulting in a decrease in repair rate of EEE (Torris *et al*., 2016). Furthermore,

companies generally do not design their products for repair, refurbishment or ease of recycling, but rather for low-cost products.

According to Baldé *et al.,* (2017), the lifecycle of EEE can be categorised into four phases:

1. Market entry: The EEE is sold to the consumer or business. Data is obtained from sales or the apparent consumption method;
2. Stock: The EEE has entered into its place of use. This phase is also known as the products residence time regardless of owner but must stay in the country to qualify;
3. E-Waste generated: The EEE has reached its EoL; and
4. E-Waste is collected: Through either a take-back system, mixed residual waste or the collection outside the official take-back system.

The lifecycle of EEE is dependent on the type of EEE evaluated. Temperature exchange equipment, small and large equipment will have larger growth rates and in turn, longer lifecycles. Moreover, information technology is expected to grow at a slower rate, due to smaller devices being developed (*ibid*). These growth rates directly correspond to the quantity of e-Waste generated.

Other factors increasing the rate of e-Waste generated include (Baldé *el al*., 2014):

- Older technologies are discarded and replaced by newer technologies such as: old cathode ray tube screens are replaced with newer light emitting diode screens, even though the old devices are still working;
- Lower prices of EEE due to a larger pool of competitors, higher demand for information communication technologies, rapid change in technologies and hence, shorter replacement periods; and
- Growing ownership of different technologies, such as having a smartphone and a laptop.

Although there is an increase in the rate of e-Waste generation, there are currently low collection and treatment levels of e-Waste. This may be partially due to consumers disposing of it in municipal solid waste or storing the old equipment, with no intention of

future use. This storing of equipment if often due to the apparent financial or sentimental value attached to these electrical and electronic appliances (*ibid*).

According to Honda *et al.*, (2016), low levels of e-Waste collection and treatment is a result of:

- Government: There is generally inefficient technical expertise, trained personnel and resources (recyclers, recovers, collectors and economic alternatives) to implement and regulate e-Waste management. According to Torris *et al.*, (2016), governments lack specific regulatory frameworks and have conflicts with existing legislations. Lydall *et al*. (2017), states that governmental departments in South Africa are slow in granting hazardous waste licences (2 - 4 years), while the associated cost of an environmental impact assessment delays and discourages the development and expansion of e-Waste recycling by companies;
- Producer: There tends to be a lack of effort between production and scalability. According to Torris *et al.*, (2016), producers have a lack of accountability and participation in the management of e-Waste;
- Stakeholder: It generally appears that there is insufficient knowledge in the prevention of e-Waste management systems; and
- Consumer: Have inadequate consumer awareness of environmentally and sound disposal of e-Waste (*ibid*).

It is clear that there are numerous key actors which could reduce the quantity of e-Waste generation and increase its recyclability. However, waste electrical and electronic plastic (WEEP) remains one of the most problematic fractions derived from e-Waste.

This is partly because it is one of the least economically valuable component of e-Waste and is often discarded with no intent for future use. A review pertaining to the types of electrical and electronic plastics (EEP) found in EEE and its wastes are discussed in the following section.

2.3 WEEP

This study concentrates on the use of WEEP which is derived from electrical and electronic plastic (EEP). EEP is used for insulation, noise reduction, sealing, housing, structural parts, functional parts and electronic parts in EEE (Mahesh *et al*., 2012). EEP is also the second largest component of EEE which contributes to on average 30% by

weight. The most common plastics found in EEP include: acrylonitrile butadiene styrene (ABS), polypropylene (PP), polystyrene (PS), polycarbonate (PC) and polyurethane (PU), which represents more than 70% of plastics found in EEE.

Table 1 provides an overview pertaining to the quantity and type of EEP most likely used in the relevant equipment.

Table 1: Types of EEP found in EEE (Source: Delgardo *et al*., 2007).

Equipment	Plastics (%)									
	ABS	PC/ABS	ABS/SAN	HIPS	PA	PET	PP	PPE/PS	PS	PVC
Televisions		32				5		63		
Toys	70			10	5		10			5
Monitors	5	90		5						
Computer	50	35		15						

From the above-mentioned table it is clear that a single type of EEE may contain multiple different types of EEP. The choice of EEP depends on its application. EEP must therefore have sufficient mechanical strength to withstand applied forces throughout its service life, as discussed in the following section.

2.3.1 Mechanical properties of plastics

Polymetric materials found in EEP are viscoelastic. Thus, external parameters such as: straining rate, elapsed time and temperature affects the modulus of elasticity, strength, ductility and coefficient of friction of the plastic (Kumar and Gupta, 2003). There are three main types of stress-strain behaviours found for polymetric material, namely: brittle, plastic and elastic, as presented in Figure 2.

Viscoelastic materials generally have a stress-strain graph similar to that of metals. It can be seen that at low stress-strain levels the material behaves elastically. However, at elevated stress-strains the material permanently deforms. When a tensile force is initially applied, elastic deformation occurs within the amorphous regions of the semi-crystalline material. If the force is increased, the amorphous regions continue to align themselves while the crystallites experience bending and stretching of strong chain bonds (Billmeyer, 1984). If the force is furthermore increased the material changes from elastic deformation

to plastic deformation. At this stage the polymetric chains slip past one another and become more aligned with the tensile force (Callister, 2007).

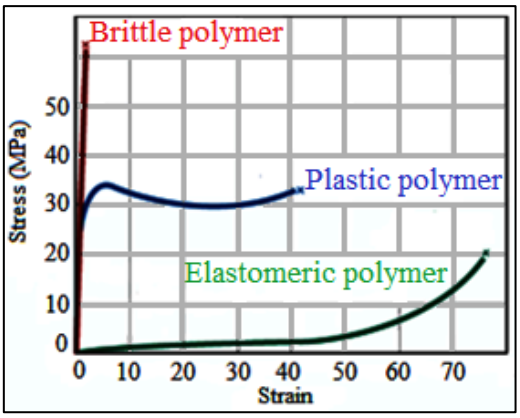

Figure 2: The stress-strain behaviour for brittle, plastic and elastomeric polymers (Source: Callister, 2007).

The response of a polymetric material to an externally applied force is dependent on its molecular structure. Polymers consist mainly of four different molecular structures, such as:

1. Linear polymers: The repeat unit of the polymer is connected by a single chain held together by Van der Waals and hydrogen bonding between the chains. Examples of materials produced include: polyethylene (PE), polyvinylchloride (PVC), PS, polymethyl-methacrylate (PMMA), nylon and fluorocarbons among others (Callister, 2007);
2. Branched polymers: These polymer structures consist of side-branch chains which are connected to the main chain. This configuration generally reduces the chain packing efficiency. Therefore, low density PE contains short chain branches which reduces the packing efficiency of the structure. By contrast, high density polyethylene (HDPE) consists primarily of linear polymers to produce a tightly packed structure (Billmeyer, 1984);
3. Crosslinked polymers: This structure occurs when linear polymer chains are joint together at various positions by covalent bonds, achieved during synthesis or non-reversible chemical reactions. This method is used to produce elastomeric materials such as rubber through a process called vulcanisation (Odian, 2004); and
4. Network polymers: This structure consist of monomers that form three or more active bonds, which produces a three-dimensional network. Highly crosslinked polymers

may also be classified as network polymers. Examples include: epoxies and phenol-formaldehyde (Callister, 2007).

These aforementioned molecular structures are presented in Figure 3.

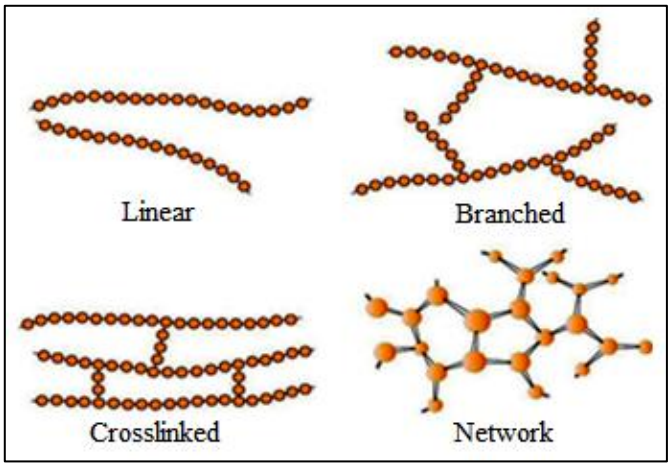

Figure 3: Molecular structures for polymers (Source: Callister, 2007).

The standards used for short-term testing of plastics are available in British Standards (BS) 2782, American Society for Testing Materials (ASTM) D638 and ASTM D790. However, care must be taken when testing as small changes in the temperature and loading rate could significantly alter the final results. Crawford (2002), states that the short-term loading of PVC at loading rates > 1mm/s resulted in a brittle failure. Alternatively, a loading rate of < 0.05mm/s of the same type of material resulted in ductile failures. Therefore, numerous tests must be performed to achieve a final result. Short-term stress-strain results are therefore not suitable to provide design data and must be obtained from long-term tests (*ibid*).

Plastics generally tend to deform when subjected to a constant loading. Thus, creep is used to measure the deformation behaviour of polymetric materials. Creep is a time-dependent change in the polymers dimension when subjected to a constant load or stress and is often plotted as strain against time (Kumar and Gupta, 2003). If creep is continued for an extended period, the material may fail. This failure is termed creep rupture and the period is dependent on the stress level, ambient temperature, fabrication method and component geometry among others (Crawford, 2002). It is believed that as the material creeps, a point is reached whereby the stress caused from the applied load causes microcracks to develop within the material. This will in turn transfer the load to the unbroken section of the material. After sufficient time has elapsed, the accumulation of

numerous microcracks will build up to the true strength of the material which will ultimately lead to the failure of the material (*ibid*).

Furthermore, polymers may behave in a rubber-like fashion at very low frequencies and exhibit a low modulus of approximately 0.1MN/m². Alternatively, polymers may behave like stiff, glass like solids at high frequencies and exhibit a high modulus of 10^3MN/m². Under fluctuating loads, the material may fail due to fatigue. This occurs as the cycle action causes cracks to develop until the cross-section cannot support the applied load any longer (*ibid*). Alternatively, fluctuating loads may cause the temperature to rise within the plastic which may soften the material. This may lead to a reduction in its mechanical properties and load bearing applications.

The response of a polymer to mechanical forces at elevated temperatures can be divided into two main polymer types, such as:

- Thermosetting polymers (thermoset): This type of polymer irreversibly cures and hence, cannot be re-softened after subjected to heat and pressure (Mahesh *et al*., 2012). This type of polymer is often discarded or used as a filler in other materials. Some thermosetting plastics include: phenol formaldehyde, melamine formaldehyde, urea formaldehyde and epoxies among others (Crawford, 2002); and
- Thermoplastic polymers (thermoplastic): This type of polymer consists of long chain-like molecules which are held together by the weak Van der Waal force. This type of polymer does not change its chemical composition when subjected to elevated temperatures (Mahesh *et al*., 2012). Crawford (2002), states that when heated sufficiently the plastic becomes soft and malleable. At elevated high temperatures it becomes viscous and melts or turns to a glassy state when cooled. According to Odian (2004), when the temperature is raised the secondary forces are diminished resulting in the relative movement of the adjacent polymer chains. However, irreversible degradation of the polymer may occur when the temperature is raised too high. This may be due to the unstable nuclei resulting from the thermal atomic vibration, which in turn disrupts the ordered molecular arrangement. Some thermoplastics include PE, PC, PVC, PS, nylon, acetate, acetal, polymethyl and methacrylate (Callister, 2007).

The melting temperature of plastic can vary significantly due to the presence of a variety of different molecular weights. Factors affecting the melting temperature include the history of the specimen and thickness of the chain-folded lamellae (Billmeyer, 1984). The chain stiffness, impurities in the polymer and imperfections in the crystal may also alter

the melting temperature. Lastly the degree of branching and the molecular weight changes the melting temperature (Odian, 2004).

2.3.2 Plastics types used in concrete

This study only concentrated on the use of ABS, PC/ABS and HIPS WEEP as partial replacement for aggregate in concrete. This is due to the fact that only granulated ABS, PC/ABS and HIPS WEEP were available in Gauteng, South Africa at the time of this study. Table 2 provides expected material parameters found for the relevant plastic types used.

Table 2: Material parameters for ABS, PS and PC. (Source: Crawford, 2002).

Parameter	Unit	ABS	PS	PC
Density	kg/m³	1 040	1 050	1 150
Flexural modulus	GN/m²	2.2	3.0	2.8
Elongation at break	%	8.0	1.5	100.0
Specific heat	kJ/kg K	1.3	1.3	1.2
Thermal conductivity	W/m/K	0.25	0.15	0.20
Coefficient of linear thermal expansion	μm/m/°C	90	80	65
Glass transition temperature	°C	115	100	149
Max operating temperature	°C	70	50	125
Moulding temperature	°C	230	230	300
Thermal diffusely	(m²/s) x 10^{-7}	1.70	0.60	1.47
Thermal diffusivity	(m²/s) x 10^{-7}	0.9	1.1	1.0
Viscosity factor	-	1.3 - 1.4	1.0	1.7 - 2.0
Poisson's ratio	υ	0.35	0.33	0.34
Tensile strength	MN/m²	38	40	65

The following sub-sections evaluates the properties of ABS, PC/ABS and HIPS plastics.

2.3.2.1 Acrylonitrile-butadiene-styrene plastic

ABS is considered to be an engineering plastic as it has superior strength, stiffness and toughness when compared to many other plastics (Crawford, 2002). ABS consists of systematic polymerisation of monomers, such as: acrylonitrile, butadiene and styrene (ABS), which can be either a continuous phase of styrene-acrylonitrile (SAN) or as a dispersed phase of polybutadiene, as seen in Figure 4 (Olivera *et al.*, 2016).

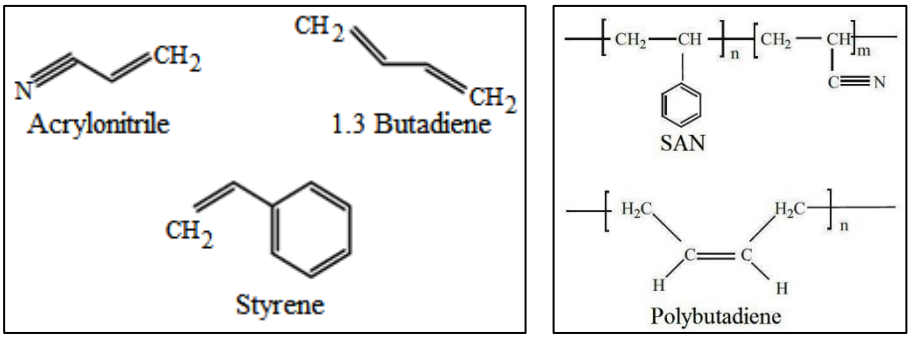

Figure 4: ABS monomers (left) and ABS in its continuous phase (right) (Source: Olivera *et al*., 2016).

The acrylonitrile monomer increases the heat deformation and chemical resistance, butadiene increases the impact strength while styrene improves processing and stiffness (Hora´K *et al.*, 2010). ABS has a chemical formula of $(C_8H_8)_X.(C_4H_6)_Y.(C_3N_3N)_Z$, which is generally mixed in proportions between (15% - 35%), (5% - 30%) and (40% - 60%) respectively (Swetham *et al.*, 2017).

ABS is an amorphous plastic. This means that ABS has polymer chains which are disordered and misaligned through twisting, kinking and coiling (Odian, 2004). ABS consist of either medium to high impact, low to high surface gloss and has high heat distortion properties (Arnold, 2003).

According to Olivera *et al.*, (2016), properties of ABS include: high toughness, adequate rigidity, thermal stability, high resistance to thermal attack, relatively cheap, low coefficient of thermal expansion and ease of moulding. However, ABS is often susceptible to chemical attacks by acids, alkalis, esters, solvents and ketones (Crawford, 2002). Furthermore, the SAN phase of ABS is particular soluble in halogenated hydrocarbons, aromatics, esters and ketones. Oxidising agents may also tend to break the polymeric chains, leading to the degradation of the polymer and the loss of toughness (Olivera *et al*., 2016).

ABS is generally used in EEE, support blocks, housewares, automobile and structural components (Pathak *et al*., 2017) and (Vezquez and Barbosa, 2017). ABS is also used in refrigerator linings, lawn and garden equipment, toys and highway safety devices. ABS has other trade names, such as: Abson, Cycolac, Kralastic, Lustran, Novodur or Tybrene among others (Callister, 2007).

2.3.2.2 Polycarbonate and acrylonitrile-butadiene-styrene plastic blends

PC is an amorphous engineering plastic and is well known for its high dimensional stability, impact resistance and low water absorption (Callister, 2007). PC has a chemical formula of $C_{16}H_{14}O_3$ and has a chemical structure unit as shown in Figure 5.

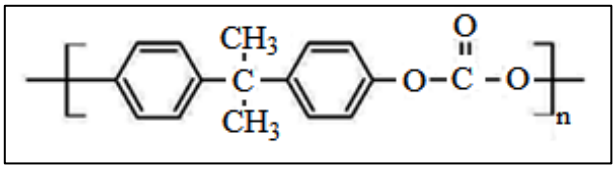

Figure 5: Structural unit of polycarbonate. (Source: Achilias *et al.*, 2012).

PC generally does not achieve the required toughness when exposed to low temperatures and is easily notched during its service life. Therefore, it is generally blended with other miscible plastics such as ABS to increase its toughness among others (Hora´K *et al.*, 2010).

PC/ABS are ternary blends mixtures consisting of chemically different PC and ABS (Delgardo *et al.*, 2007). PC/ABS has a chemical structure unit as shown in Figure 6.

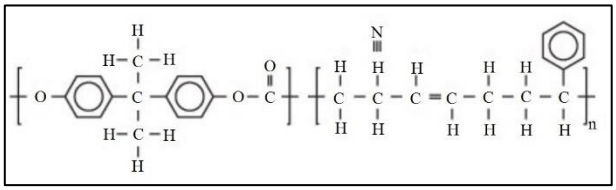

Figure 6: Structural unit of PC/ABS. (Source: Milton Plastic, 2015).

PC/ABS blends can differ from one another by alternating the amount of PC and ABS, which in turn affects their mechanical properties. Hund *et al.*, (2018), found that PC/ABS with a large amount of PC exhibited signs of splitting at the specimen surface, while ABS rich blends had highly elongated plastic zones.

PC is used in safety helmets, lenses, light globes, compact disks, bullet proof windows and food packages among others (Crawford, 2002; Callister, 2007). PC has other trade names, such as: Calibre, Lupilon, Lexan, Makrolon and Merlon (Callister, 2007).

2.3.2.3 Polystyrene plastic

PS is an amorphous engineering plastic which comprises of aromatic polymers containing styrene monomers (Crawford, 2002). PS has a chemical formula of C_8H_8 and has a chemical structure as shown in Figure 7 (Athavale, 2018).

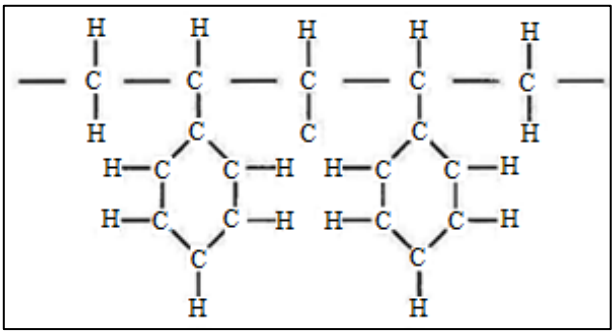

Figure 7: Structural unit of polystyrene. (Source: Crawford, 2002).

PS is used either in its expanded form as packaging material and thermal insulators or densified form as high impact polystyrene (HIPS). The difference between expanded PS and HIPS depends highly on their degree of crystallinity.

The degree of crystallinity is determined by the polymer chain configuration and the rate of cooling during solidification. At high melting temperatures, the polymer chains are highly random and entangled. Upon cooling enough time must be given to allow the polymer chains to move and align themselves. During this process nuclei form in small regions of tangle and random molecules which continue to form by ordering and alignment of additional molecular chain segments (Crawford, 2002). Crystalline polymers have a greater density than amorphous ones of the same material and molecular weight due to the packaging efficiency (Billmeyer, 1984).

PS has good strength; lightweight and durability properties, however are readily attacked by alkaline and hydrocarbon solutions. PS is also susceptible to crazing at relatively low thermal stresses which may affect the crack growth mechanism of the material (Achilias *et al*., 2012; Crawford, 2002).

PS is found in sterilisable bottles, packaging films, television cabinets and luggage bags among others. PS has trade names, such as: Herculon, Meraklon, Moplen, Poly-pro, Pro-fax, Propak and Propathene (Callister, 2007).

2.3.3 Additives found in electrical and electronic plastics

Depending on its service environment, EEP may be altered to enhance certain characteristics for a given application. This is done through the use of additives. Additives in plastics are used to modify their mechanical, chemical and/or physical properties, as described below:

- Fillers: Are often used to improve the tensile and compressive strength, abrasion resistance, toughness, dimensional or thermal stability. Fillers range in sizes from 10nm to macroscopic dimensions. These materials are generally less expensive than the virgin plastic, reducing the cost of the final product. Fillers include: sand, glass or synthetic polymers among others (Callister, 2007);
- Plasticisers: This type of additive improves the flexibility, hardness, stiffness, ductility or toughness of plastics. This is done by increasing the interchain distance between the polymer chains with the addition of small plasticiser molecules (Billmeyer, 1984). Phthalate (di-esters of 1,2 – benzenedicarboxylic acid) plasticisers are often added to ABS plastic (European Commission, 2011), however may adversely affect human health as they act as endocrine disruptors. Furthermore, some animal tests have shown negative impacts on the reproductive system, obesity and allergies when exposed to this type of plasticiser (Talsness *et al*., 2009);
- Stabilisers: Are added to polymers to counteract the deterioration process from the surrounding environments, such as the exposure to ultra violet (UV) radiation (Odian, 2004). UV radiation stabilisation is done firstly by adding a UV absorbent material into the surface and secondly by adding materials that react with the bonds broken by the UV radiation (Callister, 2007);
- Colourants: These are added in the form of pigments (filler material) or as dyes (dissolved in the polymer) to alter the colour of the plastic (*ibid*). Cadmium is used as a bright yellow to deep red pigment in plastic, as a catalyst in polymerisation reactions or as a stabilising agent in ABS (Stenvall, 2013). Moreover, lead is used in plastic as pigments and as carboxylate stabilising agents (Mahesh *et al*., 2012); and
- Flame retardants: Polymers are generally highly flammable in their pure form. The combustibility may therefore be reduced with the addition of flame retardants. EEP contains on average 26% brominated flame retardants (BFR) by weight, depending on the type of EEE (Peeters *et al.*, 2013). Antimony is generally used to catalyse the polymerisation of polyethylene tetrachloride or as a synergist to BFR. It is a suspected carcinogen and can catalyse to form brominated dioxins (PBDD/F) (Hansen and

Pergantis, 2006). Moreover, selected BFR's have also been found in food contact materials and children's toys in the European market (Ionas *et al.*, 2014).

Teuten *et al*., (2009), suggests that the migration of additives from plastics into the environment depend on the pore-size of the plastic, the molecular size of the additive and the nature of the leachate in terms of its acidity and organic content.

Some challenges facing the recycling of WEEP include the quantity and degree of hazardous additives and degradation found in WEEP, as discussed in the following section.

2.3.4 Challenges facing the recyclability of WEEP

WEEP is considered to be hazardous due to the potential presence of heavy metals. One challenge with the recycling of WEEP is to produce a high-end product with minimal negative impacts to the environment. Recycled WEEP should have similar qualities in terms of the mechanical properties of the virgin plastic they are mixed into. Hence, proper recycling is necessary to separate the different plastics types and to identify the additives and contaminants found in WEEP (Mahesh *et al.*, 2012).

Factors influencing the recyclability of WEEP include the lack of a steady stream of WEEP which depending on the source may alternate. There are also a large variety of different types of WEEP available which are generally incompatible due to their respective quality. The quality of EEP often decreases during its lifecycle as a result of polymers consuming antioxidants. This in turn results in plastics with unpredictable and insufficient properties (Stenvall, 2013).

Furthermore, weathering of EEP can cause major deterioration, whereby water exposure may have a plasticising action which could result in the embrittlement of plastic, while the exposure to UV radiation can break the polymetric chains. UV radiation and the exposure to excessive heat can also cause oxidation to occur resulting in a decrease in the materials mechanical properties (Crawford, 2002).

The rate of deterioration of plastics is therefore a function on how well they can resist attack from the external environment. A plastics permeability and absorption characteristics depends on their ability to resist the diffusion of foreign small molecules, such as: oxygen, water, carbon dioxide and methane between the plastics molecular

chain. Moreover, the rate of diffusion is often higher in amorphous than crystalline regions. This is due to the amorphous material having larger openings between molecular structures (Callister, 2007).

Some low-cost manufacturing companies recycle WEEP by blending them with virgin plastics to produce benches, utensils, plumbing pipes, building tools and the wheels in wheelbarrows. However, blending of polymers could result in a dispersed microstructure with weak interfacial adhesion between phases (Vilaplana and Karlsson, 2008).

It is clear that the recycling of WEEP is very complicated to recycle since some plastics have different grades, additives and stages of degradation. The following section evaluates different types of environmentally acceptable technologies available to recycle WEEP.

2.3.5 Recycling technologies available for WEEP

According to Stenvall (2013), there are currently two main methods used to recycle WEEP namely chemical and mechanical recycling. The following sub-sections evaluates the technologies used for both methods.

2.3.5.1 Chemical recycling

Chemical recycling is done by breaking WEEP back down to monomers through a depolymerisation process to produce virgin plastic products (Stenvall, 2013). However, these recycled plastics are generally less resilient and have lower impact strength when compared to new plastics. Furthermore, these recycled plastics are often susceptible to degradation during its service life (Achilias *et al*., 2012).

Chemical recycling of WEEP is mainly done by either feedstock or energy recycling, as described below:

- Feedstock recycling: This process converts polymers into fuels, monomers or chemicals by thermal decomposition using the following three methods (Garforth *et al*., 2005):
    1. Depolymerisation: Polymers are divided into either condensation polymers or addition polymers. Condensation polymers include materials, such as: polyamides, polyester, nylons and polyethylene tetrachloride which are depolymerised through

reversible synthesis reactions in diacids, diols or diamines. This can be done by using depolymerisation reactions, such as alcoholises, glycolysis and hydrolysis. However, addition polymers, such as: polyolefins cannot be easily depolymerised into their original monomers;

2. Partial oxidation: This entails a gasification process which is similar to direct combustion of polymer waste, but with a more environmentally friendly technology, using oxygen to create a mixture of hydrocarbons and synthesis gas;
3. Cracking: This process involves the reaction of hydrogen over a catalyst using moderate temperatures and pressures of 423K - 673K and 3MPa - 10MPa, whereby polymer chains are broken down into lower molecular weight compounds. Plastics generally processed are polyolefins, polyethylene tetrachloride, polystyrene, polyvinyl chloride and mixed polymers; and

- Energy recycling: This process uses the chemical energy from plastics to produce heat (Buekens *et al.*, 2015). However, BFR containing plastics may reduce the energy released through combustion and release toxins. The pyrolysis of polybrominated biphenyls may release toxins, such as polybrominated dibenzofurans (PBDF's) and other heavy metals. Releasing of polybrominated dibenzo-p-dioxins (PBDD's) into the environment can be dangerous to human health as they have shown to cause various types of cancers and soft-tissue sarcomas (Burke, 2007).

2.3.5.2 Mechanical recycling

This method focuses on the component recovery, pre-treatment, size reduction, separation and reprocessing of plastics without influencing the polymer length (Lydall *et al*., 2017). Vahabi *et al*., (2015), suggests however that the thermal-mechanical stresses occurring during re-smelting of plastics can lead to further degradation. There are numerous types of mechanical recycling technologies available for WEEP as described below.

- Creasolv®: In this method WEEP is broken up in a mill where metals and printed circuit boards are separated out, leaving the remaining plastics, fibres, woods and foams (Burke, 2007). A solvent is added to extract the soluble resins and plasticisers from the WEEP, leaving behind the BFR's. Therefore, this process isolates the high-grade polymers and concentrates the BFR's (Bennett *et al.*, 2009). Other applications of this technology include pigment separation in ABS WEEP (Arends *et al*., 2012);
- Near infrared sorting: WEEP is fed by a conveyor belt until it is hit by a light source. The object reflects a unique characteristic infrared spectrum, allowing the machine to

eject the required plastic. The plastic is ejected by a jet of air, pushing the selected WEEP over a splitter plate while the rejected material falls down, as shown in Figure 8 (Bennett *et al*., 2009). This method has a separation efficiency of 80% after passing the WEEP three times through the machine, and 82% after four passes. However, the payback period is 25 months with a capital expenditure of £500 000. Moreover, this method generally does not separate plastics effectively below the size of 6mm. The carbon black pigment used in most styrenic plastic used in EEE strongly absorbs the light rays and is hence, only effective for detecting lightly coloured chips (*ibid*);

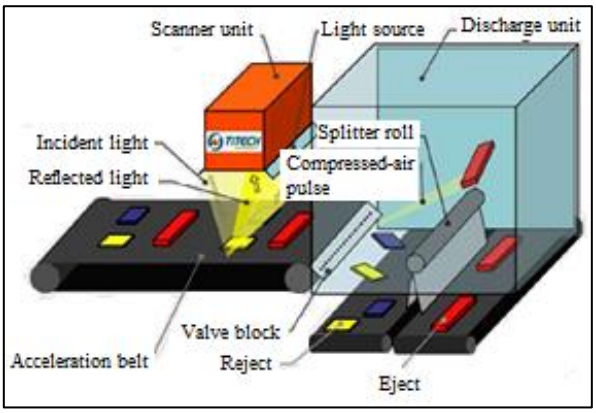

Figure 8: NIR sensor-based sorting. (Source: Bennett *et al*., 2009).

- Scanning lasers sorting: This method does not use a belt to carry the material to the sensor, but rather a vibratory feeder whereby the material falls vertically down from the feeder. It uses scanning lasers in the optical and infrared spectrum which measures the reflectance from each individual particle (Bennett *et al.*, 2009). The material slides down a Chycane-slide which falls vertically between the lasers and the detectors. Once the material has passed the sensors, it falls in front of the air jects which blows the required WEEP across the splitter plate into the ejected fractions, as shown in Figure 9 (*ibid*).

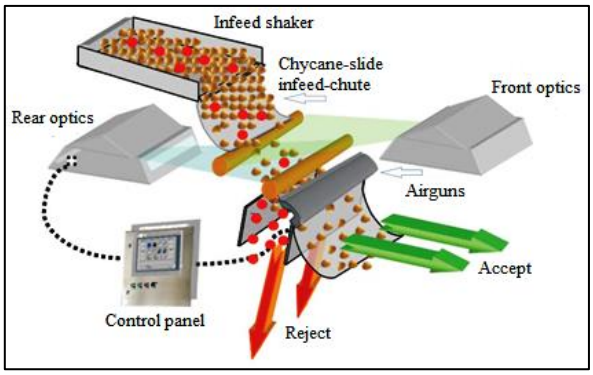

Figure 9: Scanning lasers-based sorting. (Source: Bennett *et al*., 2009).

- Wet jig sorting: This method separates WEEP by suspending it in a stream of water. The WEEP flows over a perforated bed whereby air or water pulses are ejected under the WEEP particles. WEEP passes one another and stratify into layers of similar densities. The WEEP flows over a splitter plate while the heavier fractions are diverted away, as shown in Figure 10.

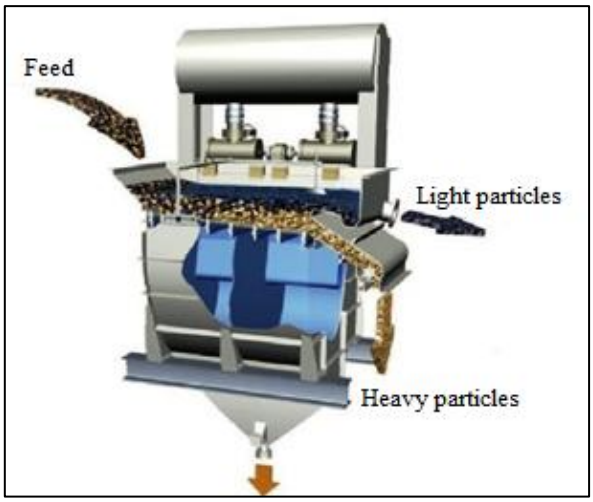

Figure 10: Wet jig. (Source: Bennett *et al*., 2009).

Using these different methods to separate WEEP could increase the quality of the recycled product. However, these machines are capital intensive and requires skilled personnel to operate them. This may deter investors in countries without a steady stream of WEEP.

The following section evaluates the technologies used to granulate WEEP used in this study.

2.3.6 Recycling technology used to granulate WEEP as aggregate in concrete

Baxter *et al.*, (2015), states that low-tech manual recycling of WEEP results in better plastic recycling compared to mechanised and automotive alternatives as it deteriorates WEEP the least. However, such low-tech recycling may impart a higher labour cost. In this study WEEP was sourced from Desco Electronic Recyclers and Monde Plastics and Services in Gauteng, South Africa. Both companies used a combination of recycling techniques whereby WEEP was manually separated into its respective plastics types and then mechanically granulated.

Granulated PC/ABS and HIPS WEEP was sourced from Desco Electronic Recyclers, while ABS WEEP was sourced from Monde Plastics and Services. Both these companies used similar techniques to granulate WEEP. This was done as Desco Electronic Recyclers could not provide granulated ABS WEEP at the time of this study while Monde Plastics and Services do not granulate HIPS WEEP.

At Desco Electronic Recyclers, plastics are manually separated into three main WEEP types, namely: ABS, PC/ABS and HIPS. After which larger plastic fractions are electrically sawed into smaller fractions, as shown in Figure 11.

Figure 11: Desco worker sawing WEEP into smaller fractions. (Source: Desco, 2019).

WEEP was belt fed to granulators with power ratings ranging between 4.0kW and 7.5kW, as shown in Figure 12. These granulators consisted of both fixed and rotating blades. The quantities and sizes of the blades vary throughout the granulating process in a three step progression. Large WEEP fractions were produced during the first stage of granulating. Here the granulators contained three rotating and two fixed blades with diameters of 450mm. The second stage further granulated WEEP into smaller fractions. Here the

granulators contained twelve rotating and four fixed blades with diameters of 150mm. Lastly, WEEP was granulated into its final fraction size using thirty rotating and two fixed blades with diameters of 80mm.

These blades span and granulated the plastics into fraction sizes of 3mm - 5mm, which was shot through a sieve. Thereafter, these plastic fractions passed through a steel separator to remove all steel fractions which may not have been previously removed from the WEEP. Thereafter, the plastic fractions were passed through a dust filtrating system whereby the final product was a relatively clean plastic fraction, as shown in Figure 13.

Figure 12: Granulators used at Desco Electronic Recyclers. (Source: Desco, 2019).

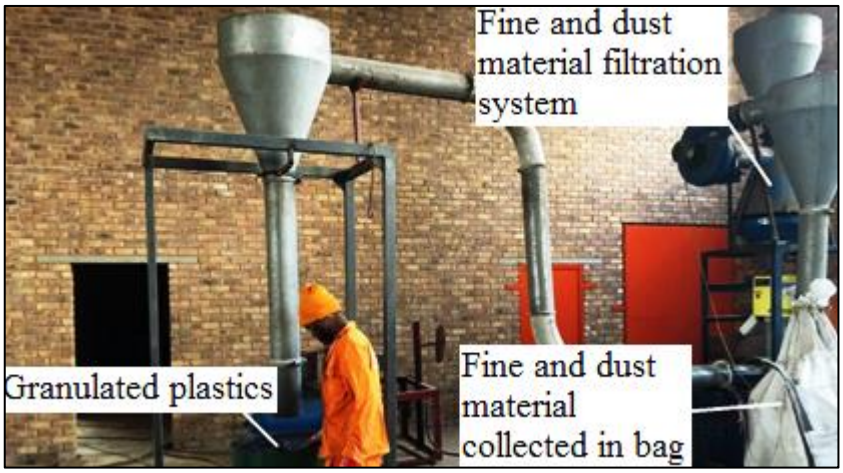

Figure 13: Outputs of granulated plastics. (Source: Desco, 2019).

2.4 Previous research done regarding the use of WEEP as aggregate replacement material in concrete

Previous research has been conducted on the use of WEEP in concrete as aggregate replacement material. This section evaluates the results found in their respective study, as described below:

- Akram *et al.*, (2015), studied *e-Waste Management by Utilisation of e-Plastics in Concrete Mixture as Coarse Aggregate Replacement*. They used an aggregate size of 20mm, 10% fly ash and 15% WEEP as partial replacement for natural coarse aggregates. Their research revealed that concrete mixed with WEEP and fly ash showed similar 28 day compressive strength results of 28MPa compared to the controlled mix. However, concrete mixed using only WEEP as aggregates had a 28 day compressive strength of 17MPa;
- Bulut and Sahin (2017), studied the *Mechanical Properties of Polymer Concrete Containing Electronic Plastic Waste*. They replaced unsaturated polyester resin as a binder in ratios of 10%, 15% and 20%. They also replaced WEEP in ratios of 5%, 15% and 25% and investigated some concrete properties. They found that replacing 20% of the polyester resin yielded the highest compressive result. However, when combining this mix with 25% WEEP, they found a notable decrease in the compressive strength from 67.50MPa to 42.80MPa, decrease in the flexural strength form 17.18MPa to 11.16MPa, decrease in the tensile splitting strength from 8.65MPa to 6.18MPa and an increase in the deflection of 1.16mm to 2.23mm at 28 days of curing. No w:c ratio was provided;
- Manjunath (2016), experimented on the *Partial Replacement of WEEP Waste as Coarse Aggregate in Concrete*. The material for the coarse aggregate was crushed coconut shell between 12.5mm and 20mm, river sand and WEEP aggregates with a maximum size of 20mm. WEEP replaced the coarse aggregates in 10%, 20% and 30% intervals. Concrete mix replacing 30% of the coarse aggregates had the highest reduction in compressive strength from 47.18MPa to 22.15MPa, reduced slump from 128mm to 75mm and had a reduced tensile split strength from 4.9MPa to 3.8MPa compared to the control mix for M20 grade concrete with a w:c ratio of 0.5 at 28 days of curing; and
- Sawant *et al.*, (2017), studied the *Combined Effect of Silica Fume and e-Waste in Concrete*. They found a drop in 28 day strength from 23.36 MPa to 20.60 MPa when 15% WEEP replaced coarse aggregates. However, they did not provide any base line

compressive strength for the cement and silica fume in the concrete mix. They did not specify what type of cement was used, w:c ratio nor whether a superplasticiser was used.

There was very little information available regarding the durability of concrete made using WEEP as aggregate replacement material and the effects different types of WEEP may have on both the fresh and hardened properties of concrete.

Part of the fact that concrete made with WEEP did not maintain high strength in previous literature is due to the low grip between WEEP and the hardened cementitious paste (hcp). One method to enhance this grip is by increasing the surface roughness of WEEP through etching, as described in the following section.

2.5 Etching of plastic

Surface treatment of plastic is done by either changing the chemical composition, modifying the surface topography or by removing contamination and weak boundary layers. Surface treatments of plastics are done by either wet or dry etching, as described in the following sections.

2.5.1 Wet etching

Wet etching is a method used whereby plastics are immersed in reactive solutions and the material is removed by either a chemical reaction or by dissolution (Walker and Tarn, 1991). According to Ottavio (1972), chemical etching is a process of deglazing the material surface without seriously roughening it. It involves the movement of the etchant species towards the plastics surface whereby a chemical reaction takes place. Following this reaction, the reactant plastics are rinsed in de-ionised water. Wet etching is generally used to etch large pattern sizes (> 2μm) with etch rate of approximately 100μm/h (Doolittle, n.d.).

One method to etch polymetric material is in the use of acid etching. Plastics are typically treated by sulfuric-chromic or trichloroethylene acid at 70°C (Blais *et al.*, 1973). Dumas *et al*., (2017), suggests however that the use of trichloroethylene can be dangerous as it readily crosses biological membranes and is classified as a human carcinogen.

Wet etching of WEEP may be complex as WEEP could have different degrees of degradation and come in a variety of sizes resulting in WEEP etched at different rates. Moreover, wet etching may be dangerous to the user and environment if it is not handled accordingly. Many etchants require high temperatures to etch efficiently and may cause serious operational injury if handled inappropriately.

2.5.2 Dry etching

Dry etching involves the removal of materials in the absence of a solvent. The following sub-sections evaluates plasma and flame treatment, and mechanical abrasion.

2.5.2.1 Plasma treatment

Plasma treatment involves polymer groups which are replaced with atoms or chemical groups from the surrounding plasma. The plasma gasses are transported to the surface whereby they are absorbed and react with the plastics surface. The gasses are then dissolved and removed from the surface (Etching and Disposition, 2017).

Plasma by-products generally do not require special handling as the excited species recombine to their original stable, non-reactive form (Kaplan and Rose, 1991). Etch rates in plasmas are much lower than wet etching ranging between 1μm/h - 10μm/h (Doolittle, n.d.).

Plasma etching is more precise, controllable, repeatable and less sensitive to temperature (Wet and Dry Etching, n.d.). Furthermore, plasma etching is clean, safe and has no waste products that need special disposal, and hence eliminates the handling of dangerous acids and solvents found in wet etching (Cui, n.d.). However, plasma etching is often more expensive compared to wet etching.

The implementation of plasma etching of WEEP for aggregates in concrete may be challenging as it requires high capital costs and skilled technicians to operate and maintain the system (Wet and Dry Etching, n.d.). Moreover, WEEP comes in different shapes, sizes and plastic types. This may affect the required etching time necessary for predictable results.

2.5.2.2 Flame and heat treatment

Flame etching requires the surface of the plastic to be exposed to an oxidising flame ranging in temperatures from 1 100°C - 3 200°C (Deurwaerder, 2006). The plastics surface characteristics are changed by passing the plastic through an oxidising portion of a gas flame. The surface is rapidly melted and quenched. This method is wildly used for PE, PP and polyphenylene surfaces (Bonding of Low-energy Plastics and Rubber, n.d.). Heat treatment of plastics at certain temperatures in ovens may change their surface characteristics. Truc *et al.*, (2015), found an increase in the hydrophilicity of the plastics after heat treating it in a thermal oven at 100°C.

Flame or heat treatment may increase the wettability or contact area of WEEP to a certain degree, however may release numerous toxins into the environment. Thus, suitable extraction fans with filters are required which may entail high capital and operational costs. Moreover, depending on the type of WEEP and direction of the applied heat, may alter the degree of wettability different for each type of WEEP.

2.5.2.3 Mechanical abrasion

This method is considered the easiest form of surface preparation. It involves a solvent swipe, abrasion of the material followed by a final solvent swipe (Bonding of Low-energy Plastics and Rubbers, n.d.). Sandblasting and grit blasting are some of the methods used in mechanical abrasion. However, they are operator sensitive, dirty and difficult to perform on small parts and may be detrimental to occupational health safety and have environmental risks if not handled properly (*ibid*).

Mechanical abrasion may be challenging to perform on WEEP. Solid or shredded WEEP have different geometries which may affect the degree of wettability, depending on the system used. This may conclude in unpredictable results when substituting it as an aggregate replacement material in concrete.

All of the above-mentioned methods may therefore increase the bond between WEEP and the cementitious paste. This may increase the strength and durability of concrete, which in turn may increase the amount of WEEP substitution in concrete. However, most of the aforementioned methods require high capital and operational costs, pose a risk to humans and the environment or result WEEP with different degrees of wettability. Hence, other

alternatives are evaluated in this study to enhance certain characteristics of concrete mixed using WEEP as aggregate.

2.6 Cement hydration, pozzolanic reactions and the partial replacement of cement with a pozzolanic material

Cement hydration involves a series of complex reactions whereby water and cement are chemically combined to produce a hardened material through the dissolution of crystal phases, surface reactions, gel formation, precipitation of new phases and textural changes (Artioli and Bullard, 2013). Alternatively, pozzolans do not chemically react with water and therefore do not hydrate but instead react with the calcium hydroxide (CH) from cement hydration to form cementing compounds of calcium silicate hydrates (C-S-H). Therefore, the pozzolanic reaction converts a weak crystalline phase of CH to a strong gel phase namely C-S-H (Fulton and Owens, 2009). Pozzolans are often used as supplementary cementitious materials which replaces part of the Portland cement in concrete mixes (Nilson *et al.*, 2010). The following sub-sections briefly discusses the chemical reactions pertaining to cement hydration resulting in the formation of free lime. Following is a brief discussion on the pozzolanic reaction between the free lime produced from the cement hydration and that of MK and CSF in concrete.

The chemical reactions presented in the following sub-sections use simplified terms whereby the abbreviations used are listed in Table 3:

Table 3: Compound abbreviation and oxide composition (Bensted and Barnes, 2008; and Neville and Brooks, 2010).

Name of the compound	Abbreviation	Oxide composition
Tricalcium silicate	C_3S	$3CaO.SiO_2$
Dicalcium silicate	C_2S	$2CaO.SiO_2$
Tricalcium aluminate	C_3A	$3CaO.Al_2O_3$
Tetracalcium aluminoferrite	C_4AF	$4CaO.Al_2O_3.Fe_2O_3$
Metakaolin	AS_2	$Al_2O_3 \cdot 2SiO_2$
Calcium hydroxide	CH	$Ca(OH)_2$
Aluminium oxide	A	Al_2O_3
Silicon dioxide	S	SiO_2
Sodium oxide	N	Na_2O
Potassium oxide	K	K_2O

2.6.1 Cement hydration

The hydration of Portland cement can be described by the following chemical reactions (Bensted and Barnes, 2008; and Fulton and Owens, 2009):

$2C_3S + 6H \rightarrow C_3S_2H_3 + 3CH$ (1)

$2C_2S + 4H \rightarrow C_3S_2H_3 + CH$ (2)

$C_3A + 3C\bar{S}H_2 + 26H \rightarrow C_6A\bar{S}_3H_{32}$ (ettringite) (3)
$C_6A\bar{S}_3H_{32} + 2C_3A + 4H \rightarrow 3C_4A\bar{S}H_{12}$ (monosulphoaluminate)
$C_4A\bar{S}H_{12} + xC_3A + xCH + 12H \rightarrow C_4A\bar{S}_xH_{12+x}$ (whereby x ranges between 0.4 and 1)

$C_4AF + 4CH + 22H \rightarrow C_4AH_{13} + C_4FH_{13}$ (4)

The product of hydration of C_3S in Equation 1 is calcium silicate hydrate ($C_3S_2H_3$) which contributes the most to the strength of hardened cement paste. During this process some lime is separated out as crystallite CH (Neville and Brooks, 2010). The reaction of C_2S in Equation 2 is similar to that of C_3S but contains less lime. C_3A hydration produces the first hydration product, namely ettringite, as shown in Equation 3. This hydration process continues until the gypsum is consumed, after which further hydration will produce tetracalcium monosulphoaluminate ($3C_4A\bar{S}H_{12}$). However, a solid solution between $C_4A\bar{S}H_{12}$ and C_4AH_{13} may form if the aluminate is consumed after monosulphoaluminate (Bensted and Barnes, 2008). Likewise, C_4AF hydration presented in Equation 4 produces hydrates similar to that of C_3A in the presence of gypsum, however may be less reactive depending on the amount of silicon dioxide, magnesium oxide and alkalis present in the cement (Fulton and Owens, 2009).

2.6.2 Pozzolanic reaction of metakaolin

MK is an amorphous purposed-made pozzolanic silica-based powdered product produced by the calcination of kaolinitic clay. MK also contains pozzolanic alumina which reacts with CH produced by cement hydration as presented by Equation 1 - 2 to produce to produce additional alumina-containing phases and C-S-H gel (Chanling *et al*., 1995). The stoichiometry of the pozzolanic reaction may be written as: (Bensted and Barnes, 2008):

$AS_2 + 5CH + 5H \rightarrow C_5AS_2H_5$ (5)

The reaction forms an additional C-S-H gel together with crystalline products whereby $C_5AS_2H_5$ represents the average composition of calcium aluminate hydrates and alumino-silicate hydrates such as: C_2ASH_8 (gehlenite hydrate) C_4AH_{13} (hydrate calcium aluminates) and C_3AH_6 (Bensted and Barnes, 2008 and Riddique, 2008). Gehlenite hydrate is a well-defined crystalline phase of variable composition, whereby large amounts of Na^+ and K^+ displaces Ca^{2+} and can affect the pore solution chemistry of cement. During the first week of curing, SiO_4^{4-} is rapidly consumed and MK reacts with CH to produce new hydrate phases (Bensted and Barned, 2008).

2.6.3 Pozzolanic reaction of condensed silica fume

Silica fume is a very fine amorphous silica by-product produced by electric arc furnaces in the production of alloys containing silica or elemental silicon. The process involves the condensation of oxidised silicon and monoxide gas into a solid, as shown in Equation 6 (Bensted and Barned, 2008):

$$2SiO\ (gass) + O_2 = 2SiO_2\ (solid) \quad (6)$$

Likewise, the chemical contribution is the chemical reaction of CH formed by cement hydration and the highly reactive silicas in silica fume (Nilson *et al*., 2010). This reaction produces secondary C-S-H which act as an additional binder which increases the hardened properties of concrete (Neville and Brooks, 2010). The non-balanced pozzolanic reaction can be written as (Fulton and Owens, 2009):

$$2S + 3CH = C_3S_2H_3 \quad (7)$$

Furthermore, the addition of alkalis improves the rate of the pozzolanic reaction of the silica fume as presented in Equation 8 (aq = aqueous and s = solid) (Bensted and Barned, 2008):

$$\begin{array}{l} S(s) + (N,K)H(aq) \quad \rightarrow (N,K)SH(aq) \\ \quad\quad\ \uparrow \qquad\qquad\qquad\quad + \\ CSH(s) + (N,K)H(aq) \leftarrow CH(aq\ or\ s) \end{array} \quad (8)$$

From Equation 8 it is clear that the cementing compounds formed by the pozzolanic reaction is similar to that of the Portland cement in Equation 1 - 2, however it is slightly different. Due to its origin, the pozzolanic reaction tend to form longer linear polysilicate anions compared to cement hydration. Moreover, with sufficient time there is a reduction of cement hydration by silica fume. This may be due to the cement grains being encapsulated by C-S-H which results in a reduction of hydration by diffusion (*ibid*).

2.6.4 Partial replacement of cement with a pozzolanic material

The partial replacement of cement with a pozzolan is very common in the construction industry. This is done to improve certain properties of concrete in either or both the fresh and hardened state (Fulton and Owens, 2009). It is achieved by physical contribution through micro-filling whereby the pozzolan fills the spaces between the cement grains and chemical contribution through a pozzolanic reaction between the pozzolan and CH obtained from cement hydration, as described in Section 2.6. The following sub-sections provide some background knowledge pertaining to the partial replacement of cement with MK and CSF in concrete.

2.6.4.1 Partial replacement of cement with condensed silica fume

CSF is mainly used in concrete as a pozzolana to enhance concretes hardened properties, such as: increasing strength and durability while reducing alkali-silica reaction (ASR) through the removal of CH produced from cement hydration and permeability due to the increase of particle packaging producing a denser concrete (Bensted and Barned, 2008). To achieve these properties, CSF is often replaced in percentages ranging between 5% - 15% by weight of the total binder material. The use of CSF as pozzolana in concrete may also enable the cement content to be reduced while maintaining a required strength. Moreover, CSF mixed in fresh concrete can significantly reduce bleeding and increase cohesiveness but reduce workability due to the higher water demand of CSF (*ibid*). Therefore, to maintain workability, CSF is often used in conjunction with a superplasticiser (Newman and Choo, 2003). The use of CSF is fresh concrete may slightly retard fresh concrete by reducing their initial and final setting time of the cement paste (Khedr and Abou-Zeid, 1994).

Previous research conducted by Alexander and Magee (1999), who investigated the *Durability Performance of Concrete Containing Condensed Silica Fume* using a CEM 1 (42.5) Portland cement with a w:b ratio of 0.56. They found that the control mix had a 28 day compressive strength of 39.0MPa , oxygen permeability index (OPI) of 10.28, water sorptivity of 5.10mm√h and a chloride conductivity of 0.95mS/cm. It was found that concrete containing the same w:b ratio and 10% CSF with a superplasticiser dosage of 0.7% by weight of cement had an increase in compressive strength to 57.0MPa and OPI of 10.42, and a decreased water sorptivity of 4.27mm√h and chloride conductivity of 0.68mS/cm. Therefore, these results confirm an overall increase in the compressive

strength and durability of concrete when using 10% CSF as a pozzolan in concrete. Furthermore, Marikunte and Nacer (2012), studied the *Interaction of Silica Fume and Water Content on Strength and Permeability of Concrete*. Using a control mix with a w:b ratio of 0.35 and superplasticiser:cementitious ratio of 0.0025 obtained 28 day compressive strength of 52.9MPa and an electrical resistivity of 1 989 Coulombs using a rapid chloride permeability test. Alternatively, when cement was replaced by 10% CSF with superplasticiser:cementitious ratio of 0.0042 increased the 28 day compressive strength to 66.1MPa and reduced the electrical resistivity to 303 Coulombs. It is therefore clear that the replacement of cement with CSF increased the compressive strength of concrete while it reduced the amount of electrical current passed through the concrete sample, increasing its durability.

2.6.4.2 Partial replacement of cement with metakaolin

Similar to CSF, MK is used to enhance the handed properties of concrete by increasing the compressive and flexural strength, prevention of ASR, increased durability and resistance to sulphate attach and reduce shrinkage. This is often achieved by replacing 5% - 25% weight of the total binder with MK (Siddique, 2008). Alternatively, MK used as a pozzolana in fresh concrete can reduce bleeding, increase levelling and provide a good surface finish, however may reduce the workability due to the increase in water demand. This is due the MK having a lower density compared to that of cement. Therefore, replacing cement with MK lowers the w:b volume ratio (Bensted and Barned, 2008). Moreover, the increase in water demand may also be the result of an increase in fineness and narrower particle size distribution. One way to maintain similar workability by be to use a superplasticiser or otherwise increase the w:b ratio. The use of MK is fresh concrete may slightly reduce the initial and final setting time of cement paste (*ibid*).

Potgieter-Vermaak and Potgieter (2006), *Investigated Metakaolin as an Extender in South African Cements*. Using a constant w:b ratio of 0.375, they replaced cement with MK in increments of 0%, 10%, 20% and 30%. They found that replacing cement with MK in the aforementioned increments resulted in an increase in the 28 day compressive strength at 50.9MPa, 101.6MPa, 98.8MPa and 99.4MPa. In addition, Poon *et al*., (2002) studied the *Pore Size Distribution of High Performance Metakaolin Concrete*. Using a w:b ratio of 0.3 and a superplasticiser dosage of 0.5L/m³ obtained a 28 and 90 day compressive strength of 96.5MPa and 102.5MPa respectively. Alternatively, when replacing cement with 20% MK and using a superplasticiser dosage of 1.0L/m³ experienced an increase in

both 28 and 90 day compressive strength of 99.6MPa and 113.8MPa respectively. Moreover, Ferreira *et al*., (2016) evaluated the *Effect of Metakaolin on the Chloride Ingress Properties of Concrete*. Using a CEM I (42.5R) cement and a constant w:b ratio of 0.45 found the electrical resistivity of the control mix at 28, 90 and 180 days of curing to be 4.80Ωm, 5.82Ωm and 5.97Ωm respectively. When replacing cement with 20% MK found an increase in resistivity at all ages of curing to be 5.93Ωm, 3.75Ωm and 4.23Ωm respectively. It is clear that the replacement of cement with 20% MK therefore increased the electrical resistivity and therefore enhanced the durability of concrete containing MK as a pozzolan.

2.7 Conclusion

It is evident that WEEP is of a growing concern. Although there are some technologies available to deal with WEEP, they are often capital intensive and require skilled technicians to operate them.

Based on previous literature, substituting natural aggregates with WEEP generally decreases the strength and workability of concrete. This could be the result of the surface interaction between the WEEP and hcp as WEEP is often hydrophilic. However, etching WEEP is either dangerous to humans and the environment, capital and/or operational intensive.

Lastly, it is clear that the optimal substitution of cement with either MK or CSF can enhance the strength and durability of concrete.

Chapter 3: Materials used and their characterisation

3.1 Introduction

This chapter provides information pertaining to the materials used in this study. The material used and their characterisations have been arranged into three sections and are presented in the following order:

- Detailed description of the binder materials used. This includes the oxide composition, phase composition, particle size distribution, specific density, BET surface area and the surface typography results for all the binder materials used;
- Brief overview pertaining to the superplasticiser used; and
- Detailed information pertaining to the aggregates used. This includes the sieve analysis, elemental composition of WEEP, particle relative density, compact bulk density and the surface typography of the aggregates.

3.2 Binder chemical, mineralogical and physical properties

Different cementitious materials were used in this study. The cement used was a CEM I 52.5R donated by AfriSam, metakaolin (MK) by Kaolin-Group and Serina Trading Company and condensed silica fume (CSF) by Sika, South Africa. The powders for the aforementioned binder materials are presented in Figure 14.

CEM I 52.5R cement Metakaolin Condensed silica fume

Figure 14: Binder materials.

A high strength, rapid hardening ordinary Portland cement (CEM I 52.R) was used to ensure structural concrete with a minimum compressive strength of 25MPa was achieved at 28 days of curing owing to the negative effect on the compressive strength with the

increased volume addition of WEEP. Replacement of cement with CSF or MK was done to compensate for any further loss in strength and to increase the durability of concrete made using WEEP as partial replacement for the natural aggregate. Furthermore, the use of CSF and MK incorporated by replacing cement by mass. In this study CSF replaced 10% of cement, while metakaolin replaced 25% of cement respectively. The amount of CSF and MK replaced is based on optimal replacement levels found by Bensted and Barnes, (2008); Ghutke and Bhandari (2014); and Oriol and Pera (1995).

The energy-dispersive X-ray spectroscopy (EDS), wavelength-dispersive spectroscopy (WDS), X-ray mapping and X-ray diffraction (XRD) was performed by the author at the MMU department, at the University of the Witwatersrand. The scanning electron microscopy was performed with the assistance from the staff at the School of Chemical and Metallurgical Engineering, at the University of the Witwatersrand. The X-ray fluorescence (XRF) was outsourced and analysed by Sci-Ba. The specific area, density and particle-size distribution of all the binder materials were tested by Anton Paar.

3.2.1 Elemental composition using EDS

Before any analysis of the chemical or oxide composition was done, an EDS analysis was performed on all the binder materials. This was accomplished by using a "Compagnie des Applications Mécaniques et Électroniques au Cinéma et à l'Atomistique" (CAMECA) SX5-FE electron probe micro analyser (EPMA), as shown in Figure 15.

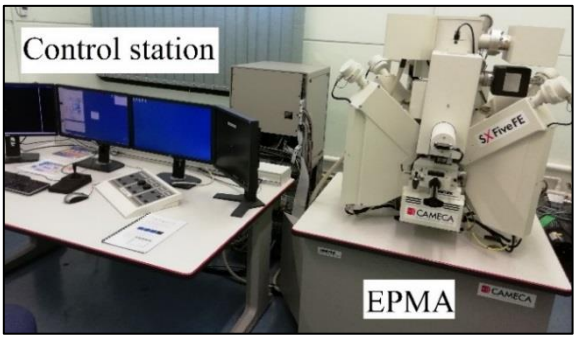

Figure 15: CAMECA EPMA at the MMU department at the University of the Witwatersrand.

The EDS analysis separated the emitted X-rays according to their respective energies. The EPMA used silicon drift detectors which measured X-ray photons emitted at different energies which resulted in a rapid semi-quantitative analysis. This method was

used to identify the major elements present in the sample as it struggled to identify peaks from minor trace elements (Heath and Taylor, 2015).

Therefore, the EDS analysis only gave information pertaining to the elemental composition contained within the binder, whereby qualitative work was performed using the WDS function on the EPMA.

3.2.2 Oxide composition of the binder material using WDS and XRF

The oxide compositions shown in Table 4 were obtained using WDS and XRF. The WDS analysis was conducted after identifying the major elemental peaks from the EDS analysis. The WDS analysis separated the emitted X-rays according to their respective wavelengths and was used to quantify a complete composition of the materials evaluated.

Table 4: Oxide composition of binders.

Oxide	Percentage oxide			
	Cement (WDS)	CSF (WDS)	CSF (XRF)	MK (XRF)
Al_2O_3	1.01	0.24	1.45	42.65
CaO	67.05	-	0.02	0.06
Cr_2O_3	-	-	1.45	0.07
Fe_2O_3	0.68	0.30	2.46	0.41
K_2O	-	1.29	2.14	0.17
MgO	1.23	0.68	1.14	0.29
MnO	-	-	0.77	0.09
Na_2O	-	0.11	0.55	< 0.01
P_2O_5	-	0.04	0.13	0.07
SiO_2	23.52	85.77	87.80	54.02
SO_3	0.07	0.05	< 0.01	< 0.01
TiO_2	-	-	< 0.01	1.39
Total	99.56	88.70	99.66	100.10

The WDS analysis compared the elements found in the material to pre-defined crystalline mineralogical standards. Evaluating amorphous material, such as CSF and MK resulted in lower final elemental totals, as shown by CSF (WDS) in Table 4. Hence, XRF analysis was used to analyse the CSF and MK powders. The detailed results pertaining to the elemental composition for WDS analysis for all the binder materials are available in Appendix G, Tables G1 - G3. The oxide compositions for the cement and CSF found were similar to those suggested by Fulton and Owens (2009), while the oxide composition for MK was similar to those recommended by the manufacturer (Kaolin-Group, 2017).

3.2.3 XRD for binder materials

X-ray diffraction (XRD) is a non-destructive technique used to study the crystal structure and atomic spacing of a material (Bunaciu *et al.*, 2015). This method was used in a semi-qualitative manner to identify some relevant phases in the binder materials used in this study.

This was done using the fundamentals of Bragg's law which related the X-ray wavelengths and interatomic spacings to the angle of the diffracted beam, as described below (Callister, 2007):

$$n\lambda = 2d \cdot \sin(\theta) \quad (9)$$

$n =$ order of reflection (integer);
$\lambda =$ wavelength of the electromagnetic radiation on the order of the atomic spacing for solids;
$d =$ lattice spacing in the crystalline sample; and
$\theta =$ diffraction angle.

The X-rays were generated by a cathode ray tube which was filtered to produce a monochromatic X-ray beam. The interference of the X-ray beam with the sample was scattered in all directions by the electrons associated with each atom in the beams path which was detected, processed and counted (*ibid*).

A D2 Phaser diffractometer was used to determine the angles at which diffraction occurred for all the powdered samples using target material of copper k-alpha. It consists of three main parts, namely: the X-ray tube, sample mount and detector, as shown in Figure 16. The solar slits on the left-hand side corrected the angular divergence, while the divergence slit controlled the beam spread. The anti-scatter split on the right-hand side reduced the diffusion or scatter amount. The solar slits on the right-hand side also limited the beam height. The receiving slit known as the height divergence limiting slit removed the diffused scattered X-rays that occurred from the previous elements in the secondary optics.

The results for the semi-quantitative XRD analysis of the binder material was analysed using Deffrac.Eva software. This software removed the background noise and assisted in determining the phases of the binder materials using a chemical filter function. Using the

acquired information, Origin 85 software was used to plot the data, name and number the relevant peaks.

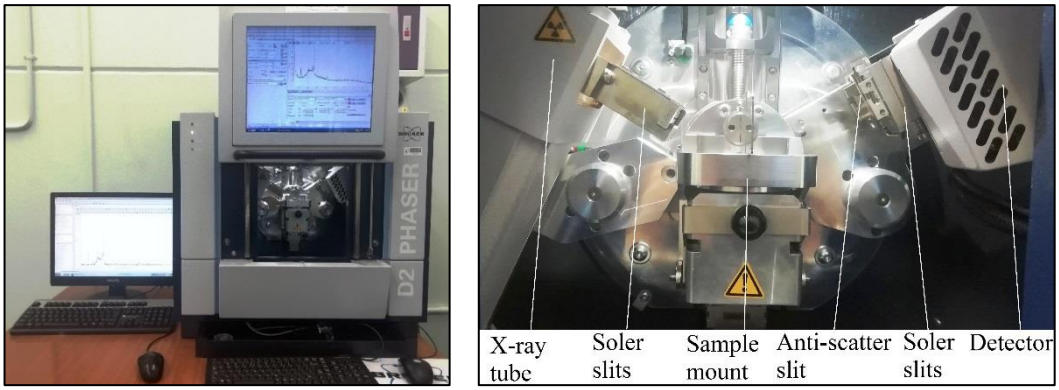

Figure 16: D2 Phaser diffractometer (left) and its internal arrangements (right) at the MMU department at the University of the Witwatersrand.

The results were plotted on an XRD graph. The peak intensity (y-axis) was based on the atoms that were present while the diffracting angle (x-axis) provided the information pertaining to the elements which were present in the sample. The width and the shape of the diffraction peaks were based on the Scherrer's equation (Pallon, *et al.*, 2015), as shown:

$$B(2\theta) = \frac{k\lambda}{L \cdot \cos(\theta)} \tag{10}$$

$B =$ peak width (rad);
$k =$ constant dependant on the analysed plane; and
$L =$ crystallite size along the normal of the plane.

The following sub-sections evaluates the XRD results for the binder materials used in this study.

3.2.3.1 XRD results for cement

Results from previous literature was used to compare relevant intensities and angles. These include data from Jadhav and Debnath (2011); Kontoleontos *et al.*, (2013); and Stutzman *et al.,* (2016). Furthermore, the peaks were confirmed using the database in the Diffrac.Eva software. The PDF's corresponding to the relevant peaks are available in Appendix I, Figures I1 - I2.

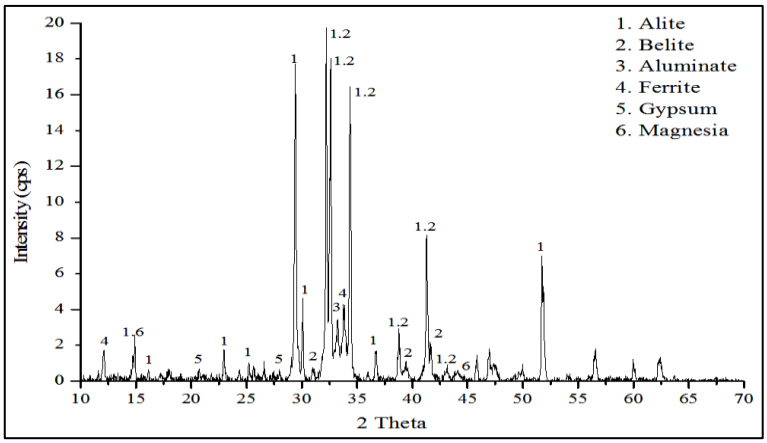

Figure 17: XRD results for cement.

From the data presented in Figure 17, it can be seen that the cement had numerous amounts of both alite (tricalcium silicate) and belite (dicalcium silicate). Smaller amounts of aluminate (tricalcium aluminate) and ferrite (tricalcium aluminoferrite) were also found. Very small peaks of gypsum was found for this cement. This may account for some of the rapid hardening characteristics associated with this type of cement.

3.2.3.2 XRD for MK

Results from previous literature was used to compare relevant intensities and angles. These include data from Barbhuiya *et al*., (2015); Bodogiannis *et al*., (2005); and Diffo *et al.*, (2015). The relevant PDF's corresponding to the relevant peaks are available in Appendix I, Figure I3. From the XRD graph presented in Figure 18, it can be seen that MK had numerous amounts of amorphous material. The three phases detected include: illite, quartz and amorphous kaolinite.

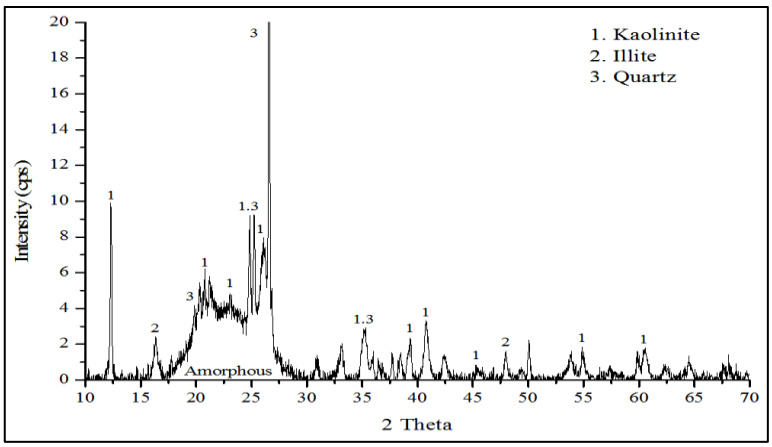

Figure 18: XRD results for metakaolin.

3.2.3.3 XRD for CSF

Results from previous literature was used to compare relevant intensities and angles for the XRD graph in Figure 19. These include data from Arroudj *et al.*, (2011); Bortrill (1991); and Souza *et al.*, (2014). The relevant PDF's corresponding to certain peaks can be found in Appendix I, Figure I4.

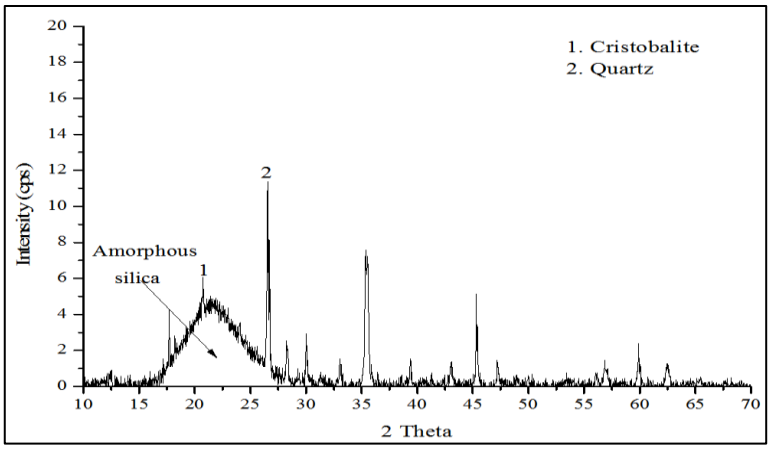

Figure 19: XRD results for condensed silica fume.

From the data presented in Figure 19, it can be seen that CSF had numerous amounts of cristobalite, quartz and amorphous silica.

3.2.4 Particle size distribution of binders

The particle size distribution of the binder material has a profound effect on the performance of concrete as it affects its workability, curing, strength and durability among others. Malvern (2016), states that as the particle size of the material decreases, so will the surface area also increase. This in turn will result in a higher area which will increase the rate of hydration. Furthermore, Wang *et al.*, (1999), states that a wider particle size distribution curve will also result in a higher packaging density which in turn, lowers the water demand.

The Anton Paar PSA 1190 particle size analyser was used to study the upper nanometre to millimetre particle size of the binder material used in this study. The machine used a dry desperation, venturi free fall setup using a compressor to circulate the air. A laser beam was directed into the dispersed material, causing the light to diffract. This diffracted light was sensed by a detector and evaluated using programming.

The particle size distribution test was conducted on the cement, MK and CSF powders. The D-sizes shown in Tables 5 - 7 correspond to the percentage of material passing a particular size. In other words, D10 represents the particle size that corresponds to 10% of the material.

Each binder material was analysed for 10 seconds. Each material was also tested three times. Figure 20 shows the average results of three tests for the particle size distribution of the binder materials used. See Appendix K, Tables K1 - K3 for the raw data.

From Figure 20 it is clear that the cement was more fine-grained compared to CSF which was coarse grained. The cement also had a poorly-graded particle size distribution as it contained a narrow size range. The cement had a small flat zone between 2μm - 3μm and thus, had missing particles in that size range. Conversely, MK had a well graded particle size distribution as it contained a broad range of particle sizes.

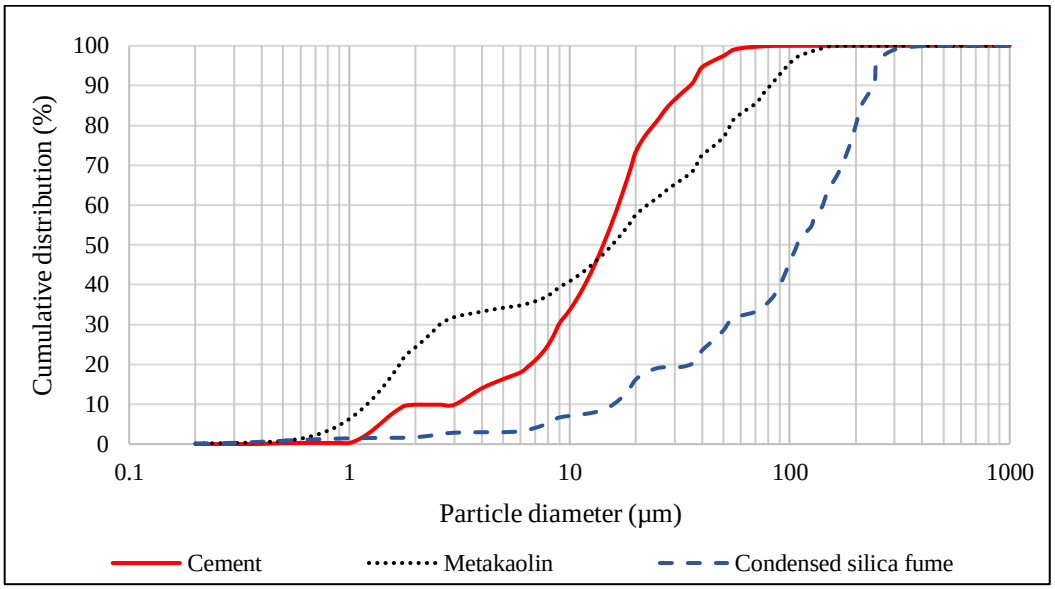

Figure 20: Particle size distribution for cement, MK and CSF.

The following sub-sections evaluates each binder material in more detail.

3.2.4.1 Particle size distribution of cement

Cements should have approximately 60% - 70% of its material ranging in sizes between 3μm - 30μm for it to perform adequately as a binder material (Malvern, 2016). Moreover, particles > 60μm generally only have filling effects in concrete and thus have little contribution to its strength (*ibid*). Alternatively, cement with excessive fines (3μm) often

have reduced rheological properties and undesirable volume changes (Škvára *et al.*, 1981).

From Figure 20, it is clear that 87% of the cement had a size < 30μm and 9.9% had a size < 3μm, indicating a very fine cement. This correlates well to the results found for cement in this study whereby cement had a mean particle size of 16.2μm, as shown in Table 5. This results in the high strength and rapid hardening properties generally associated with CEM I 52.5R cements.

Table 5: Particle size distribution results for cement.

D-sizes	D10 (μm)	D50 (μm)	D90 (μm)	Mean size (μm)
Average value	3.117	12.260	33.183	16.199
Standard deviation (%)	0.030	0.363	2.167	0.839
*CoV (%)	0.962	2.961	6.530	5.179

*CoV = Coefficient of variance.

3.2.4.2 Particle size distribution of metakaolin

According to Siddique (2008), 99.9% of MK should be finer than 16μm, while Bodogiannis (2005), states that MK has a mean particle size of approximately 5μm. This fine material inherently increases the water demand but also acts as a fine filler (*ibid*). From Table 6 it is clear that MK had a very high mean particle size of 27.0μm, which was higher compared to the cement.

Table 6: Particle size distribution results for MK.

D-sizes	D10 (μm)	D50 (μm)	D90 (μm)	Mean size (μm)
Average value	1.128	73.184	72.570	27.011
Standard deviation (%)	0.016	0.583	1.002	0.258
CoV (%)	1.418	0.800	1.381	0.955

3.2.4.3 Particle size distribution of CSF

According to Holland (2005), silica fume has approximately 95% of its particles with sizes < 1μm. This is beneficial for particle packaging, but may affect the water demand of concrete (Marikunte and Nacer, 2012). The mean particle size of CSF used was 167.0μm, which was much higher compared to cement or MK. This is due to the fact that the silica fume was densified by an electrostatic furnace which allowed the particles to agglomerate into pellets to produce condensed silica fume. This method is often used to ease its

usability (Fulton and Owens, 2009). This may result in CSF not improving the physical packaging of concrete by means of micro-filling. It may also not have effective pozzolanic activities at early ages.

Table 7: Particle size distribution results for CSF.

D-sizes	D10 (μm)	D50 (μm)	D90 (μm)	Mean size (μm)
Average value	11.739	131.576	324.919	167.008
Standard deviation (%)	4.078	8.429	14.561	6.394
CoV (%)	34.739	6.406	4.481	3.829

It is clear from Table 7 that there were very large differences between the tests as seen by the standard deviations and CoV. This indicates that there were a wide range of random particle sizes found in CSF.

3.2.5 Specific density of the binder materials

The specific density of the binder material used will influence the amount of bleeding that occurs in fresh concrete. This is due to the fact that the dense cement particles tend to segregate to the bottom while the water migrates to the top (Fulton and Owens, 2009). Furthermore, replacing the dense cement particles with lighter MK or CSF particles by mass will inherently increase the total volume and surface area of the binder material which in turn increases the water demand.

Therefore, replacing cement with MK or CSF in concrete with a set w:b ratio may reduce the workability of the fresh concrete. The specific volume and density of the binder materials used in this study were evaluated using a Pentrapyc 5200e gas pycnometer. Three concurrent tests were performed using helium gas with a flow time of one minute each. Table 8 shows the results for all the binder materials.

The cement had a specific density of 3.63g/cm³ which is much compared to the recommended data from AfriSam which suggests that CEM I 52.5R has a specific density of 3.12g/cm³ (AfriSam, 2017). MK had a specific density of 2.47g/cm³. This is similar to other studies performed by Dhinakaran *et al*., (2012) and Guneyisi and Mermerda (2007), which found MK to have specific densities of 2.5g/cm³ - 2.6g/cm³. CSF has a specific gravity of 2.071g/cm³. This is similar to the results suggested by Holland (2005) of 2.2g/cm³.

Table 8: Specific volume and density of the binder materials.

Tests	Cement		MK		CSF	
	Volume (cm^3)	Density (g/cm^3)	Volume (cm^3)	Density (g/cm^3)	Volume (cm^3)	Density (g/cm^3)
Test 1	0.931	3.657	1.050	2.413	1.649	2.073
Test 2	0.942	3.614	1.008	2.513	1.647	2.076
Test 3	0.939	3.626	1.018	2.487	1.656	2.064
Average	0.938	3.632	1.025	2.471	1.651	2.071
S.D* (%)	0.006	0.022	0.022	0.052	0.005	0.006
CoV* (%)	0.006	0.006	0.021	0.021	0.003	0.003

*S.D = standard deviation.

From the above-mentioned table, it is clear that MK and CSF had much lighter specific densities compared to that of the cement. Replacements of the cement by mass with MK or CSF will therefore increase the amount of binder by volume and may therefore reduce the workability of the fresh concrete.

3.2.6 BET surface area

Mehta and Monteiro (2006), states that a finer cement will react more rapidly with water compared to coarser cements due to the increased surface area. This increases the rate of hydration which in turn increases the intensity of heat evolved and strength development occurring from the chemical reaction. Furthermore, finer cements also have higher water demands as it has larger surface areas (*ibid*).

The Brunauer-Emmett-Teller (BET) test is based on the amount of gas absorbed on the surface of a material at a given pressure (Pennell, 2016). It is therefore commonly used to measure the surface area of porous and non-porous material.

The NOVAtouch LX gas sorption analyser was used to evaluate the BET surface area for cement, MK and CSF in this study. The sorption analyser achieved this by recording various pressures of gas in the sample cell due to adsorption and desorption and used software to calculate relevant parameters. This machine further analysed the surface areas ranging from $0.01m^2$ and above using nitrogen gas. See Appendix F, Section F.4 for the equations used to calculate the surface area of all the binder materials.

From Table 9 it is clear that CSF had the largest surface area at 16.443 m^2/g, followed by MK and cement. Silica fume is a very fine amorphous silica by-product produced in electric arc furnaces in the production of alloys containing silica or elemental silicon.

This is similar to the surface area suggested by Fulton and Owens of 20 m^2/g (Fulton and Owens, 2009). This increased surface area of MK and CSF in the fresh concrete may adversely affect the workability and reduce the setting time of fresh concrete (Arel, 2016).

Table 9: Results for BET test.

Material	Mass (g)	Duration (min)	Intercept	Slope	C (constant)	Surface area (m^2/g)
Cement	0.7030	58.9	64.682	1 736.200	27.842	1.934
MK	0.8302	60.5	2.223	210.185	202.487	7.736
CSF	0.7715	62.0	1.610	447.948	131.565	16.443

3.2.7 Surface typography of the binder materials using SEM

A Carl Zeiss Sigma Field Emission Scanning Electron Microscope (FESEM) was used to evaluate the surface typography of all the binder materials using secondary electron (SE), as shown in Figures 21 - 22. This machine used an Oxford X-act EDS detector which provided very high resolution imaging.

Figure 21: Carl Sigma FESEM at the Chemical and Metallurgical Department at the University of the Witwatersrand.

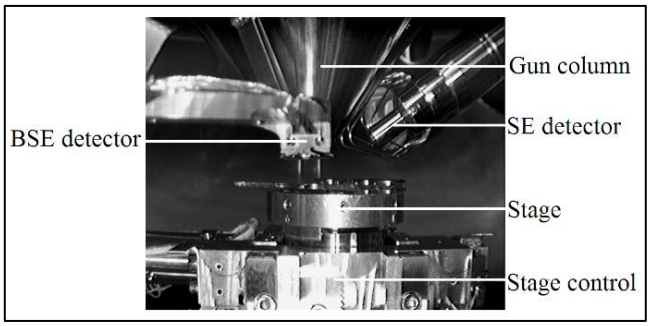

Figure 22: Carl Sigma FESEM internal arrangement.

Electrons were produced and accelerated by the electron gun, which was mounted on top of the column structure of the FESEM. Electromagnetic lenses consisted of ring shaped coils which generated a magnetic field. These lenses were used to focus the electron beam which passed through the hollow centre (Zhou *et al*., 2006). A high vacuum environment between 10^{-7}mbar and 10^{-10}mbar was required to prevent the scattering of electrons through the collisions with gas molecules. This in turn produced higher resolution imagery.

Image formation was depended on the interaction between the electron beam generated between the primary beam and specimen. The SE produced between the interaction of the specimen and electron beam were released from the specimen which escaped into the vacuum inside the FESEM chamber, where it was detected by an Everhart Thornley detector.

This detector used both a scintillator and Faraday cage. The Faraday cage was used to attract the electrons to the scintillator, while the scintillator converted the electrons to photons. The photons travelled through a light conducting pipe which was converted back to electrons. The output signal was amplified and displayed on a screen (Egerton, 2005, and Zhou *et al*., 2006).

The following sub-sections evaluates the typographical features for each binder material used in this study.

3.2.7.1 Surface typography of the cement using SEM

Figure 23 graphically illustrates the difference in the particle sizes of the cement used in this study. It is clear that there were numerous amounts of large particles with some smaller particles in between, as was found using the particle size analyser.

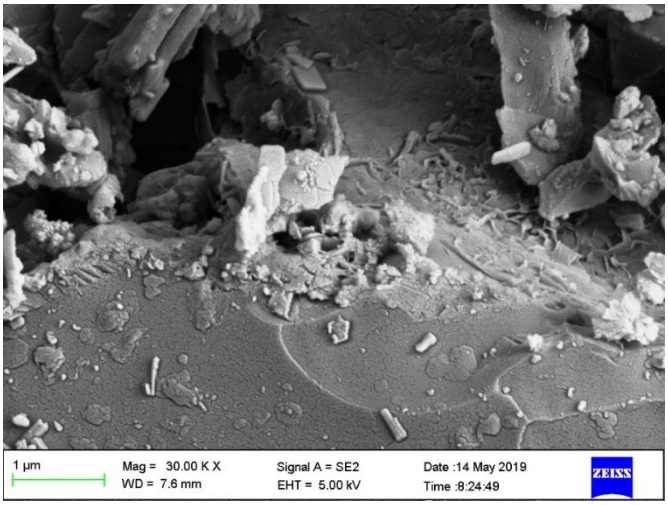

Figure 23: SEM image of cement magnified at 30 000 times.

3.2.7.2 Surface typography of metakaolin using SEM

Figure 24 graphically illustrates the difference in the particle sizes of the MK used in this study. Here it can be seen that there were numerous amounts of small plate like MK particles clumped together.

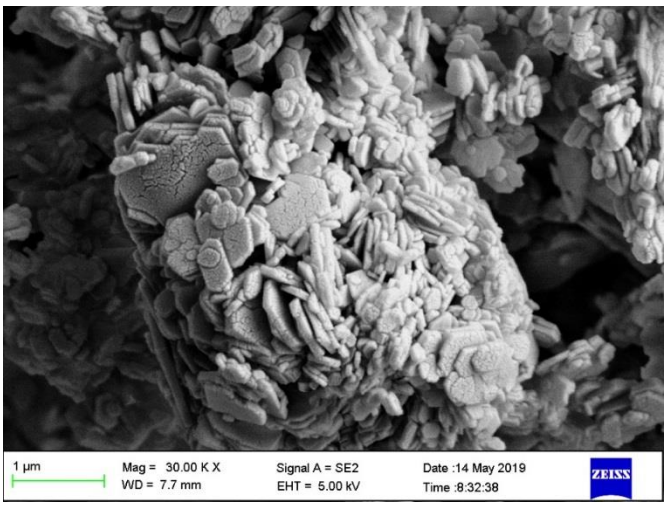

Figure 24: SEM image of metakaolin, magnified at 30 000 times.

3.2.7.3 Surface typography of condensed silica fume using SEM

Figure 25 graphically illustrates the difference between the particle sizes of CSF. It is clear that the CSF used was indeed very fine. However, since it was densified it

conglomerated to such a high degree that it had a very high mean particle size as detected in the particle size distribution test.

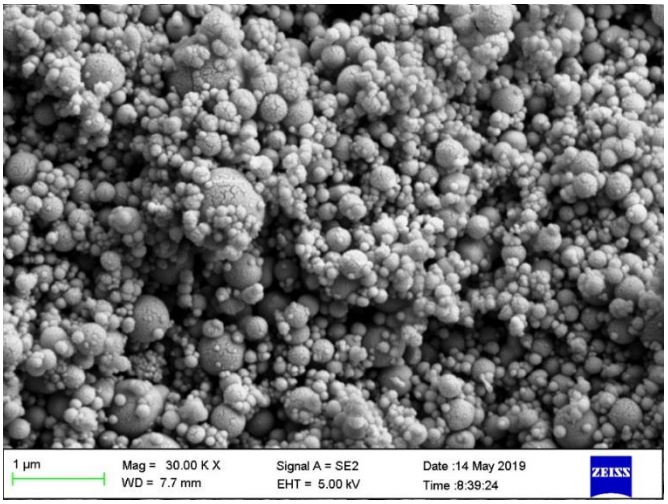

Figure 25: SEM image of condensed silica fume, magnified at 30 000 times.

3.3 Superplasticiser admixture

A superplasticiser admixture is often used to increase concretes workability or to reduce the w:c ratio of concrete. It works on the principal whereby it is absorbed into the cements surface and interacts with one another by electrostatic repulsion or steric stabilisation. This causes a uniformly distribution of the cement particles (Newman and Choo, 2003). The superplasticiser Sika®ViscoCrete®-3088 was used in this study and is chemically based on an aqueous solution of modified polycarboxylate ethers (Sika 3088, 2012). It was used to maintain a slump of 80mm $\pm$ 25mm when MK, CSF or WEEP was used as replacement material for the natural aggregate in concrete.

3.4 Aggregates chemical and physical properties

The natural aggregates used were mined at the Eikenhof quarry in Gauteng and is classified as an andesite rock. Furthermore, the granulated PC/ABS and HIPS WEEP was bought from Desco Electronic Recyclers while granulated ABS WEEP was bought from Monde Plastics and Services, as shown in Figures 26 - 27. WEEP used as aggregate was tested for its elemental composition, using EDS and WDS analysis. This was done to evaluate whether or not WEEP used contained any heavy elements, as literature suggests.

Furthermore, a sieve analysis, particle size distribution and bulk density tests were performed on both the natural aggregates and granulated WEEP.

ABS WEEP PC/ABS WEEP

Figure 26: Granulated ABS (LHS) and PC/ABS WEEP (RHS).

HIPS WEEP

Figure 27: Granulated HIPS WEEP.

3.4.1 Sieve analysis for aggregates

This section evaluates the sieve analysis and densities of both the coarse and fine natural aggregates and granulated WEEP.

3.4.1.1 Sieve analysis for natural aggregates (coarse and fine)

A sieve analysis was performed in accordance to SANS 201:2008 using sieves ranging in sizes from 19mm - 0.075mm as presented in Table 11 using a mallet, cleaning brush and

a mechanical sieve shaker. Both 13.2mm and 9.5mm coarse natural aggregates were initially tested.

This was done as WEEP was granulated into a single sized aggregate and its replacement as aggregate in concrete could be done using either size. Thus, as presented in Appendix B, trial mixes were conducted to assess the change in workability and strength. From the data below the fineness modulus and dust content were calculated according to SANS 1083:2014. The results are presented in Table 10.

Table 10: Fineness modulus and dust content for the natural aggregates.

	13.2mm Stone	9.5mm stone	Sand
Fineness modulus	n/a	n/a	3.4
Dust content (%)	2.1	0.6	8.3

Table 11 presents the results for the average cumulative percentage material passing for the sieve analysis. A grading curve is presented in Figures 28 - 29. The minimum and maximum grading limits for the fine and coarse natural aggregates were obtained from BS 822:1992. See Appendix A, Tables A1 - A3 for the detailed sieve results for the natural aggregates.

Table 11: Results for the sieve analysis of natural aggregates.

	Cumulative % passing		
Sieve opening (mm)	13.2mm stone	9.5mm stone	Sand
19.000	100.0	100.0	100.0
16.000	98.4	88.3	100.0
13.200	71.0	13.4	100.0
9.500	10.5	1.9	100.0
6.700	2.3	0.7	100.0
4.750	2.1	0.4	96.6
2.360	2.1	0.4	62.0
2.000	2.1	0.4	55.5
1.180	2.1	0.4	39.8
0.600	2.1	0.4	27.6
0.425	2.1	0.4	22.9
0.300	2.1	0.4	19.7
0.150	2.1	0.4	14.5
0.075	2.1	0.4	11.4
Pan			

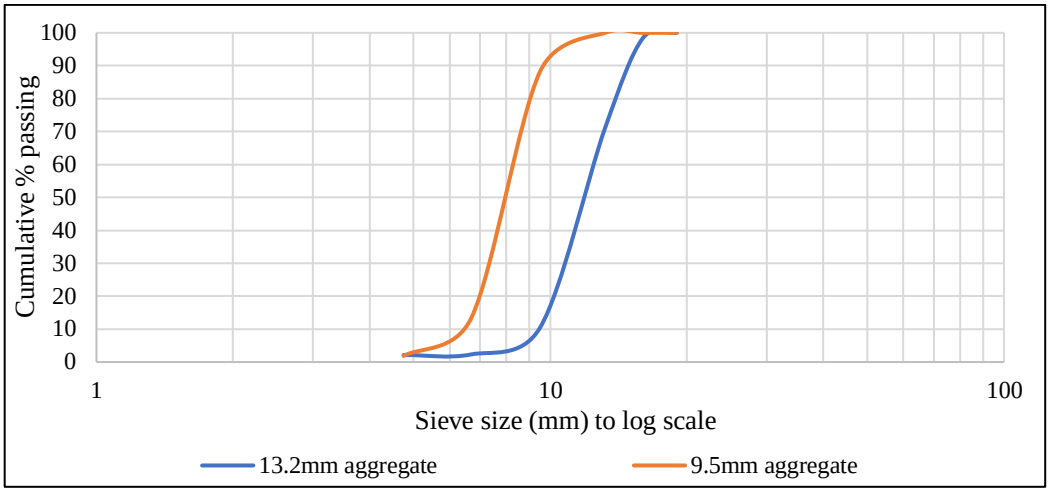

Figure 28: Grading curve for the 13.2mm and 9.5mm coarse aggregates.

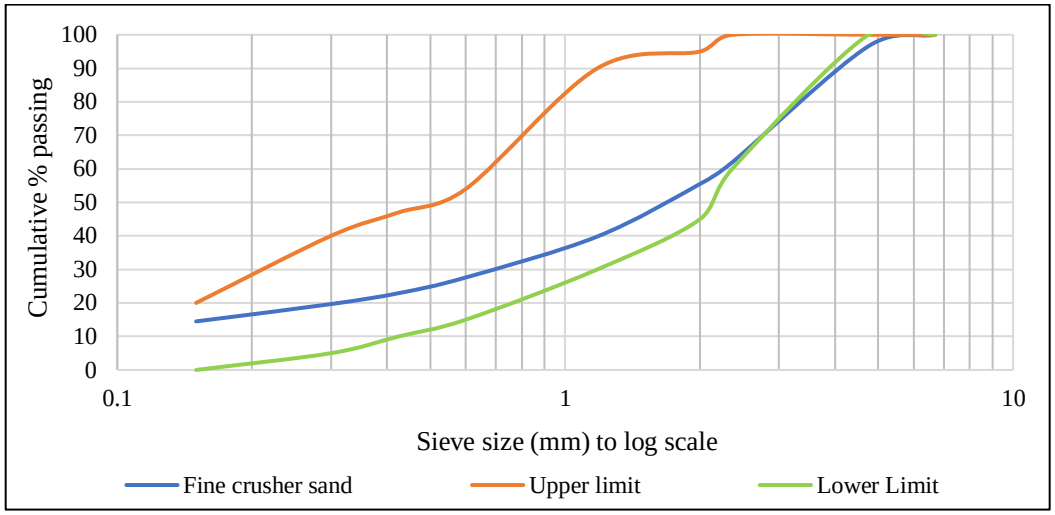

Figure 29: Grading curve for the fine natural aggregates.

3.4.1.2 Sieve analysis for granulated WEEP

A sieve analysis for the granulated WEEP was performed in accordance to SANS 201:2008. The granulated WEEP were relatively clean and free from dust and dirt. The average of three sieve test results were used and their average cumulative percentage passing is presented in Table 12. Figure 30 provides the grading curves for ABS, HIPS and PC/ABS WEEP. See Appendix A, Tables A4 - A6 for the detailed sieve test results for the granulated WEEP.

Table 12: Results of sieve analysis for WEEP aggregates.

	Cumulative % passing		
Sieve opening (mm)	PC/ABS	HIPS	ABS
9.500	100.00	100.00	100.00
6.700	99.20	99.50	96.20
4.750	74.35	77.90	67.50
2.360	4.85	7.60	11.20
2.000	2.45	0.50	11.10
1.180	0.35	0.30	4.60
0.600	0.15	0.30	1.60
0.425	0.10	0.20	1.00
0.300	0.10	0.20	0.70
0.150	0.10	0.10	0.50
0.075	0.10	0.50	0.30
Pan			

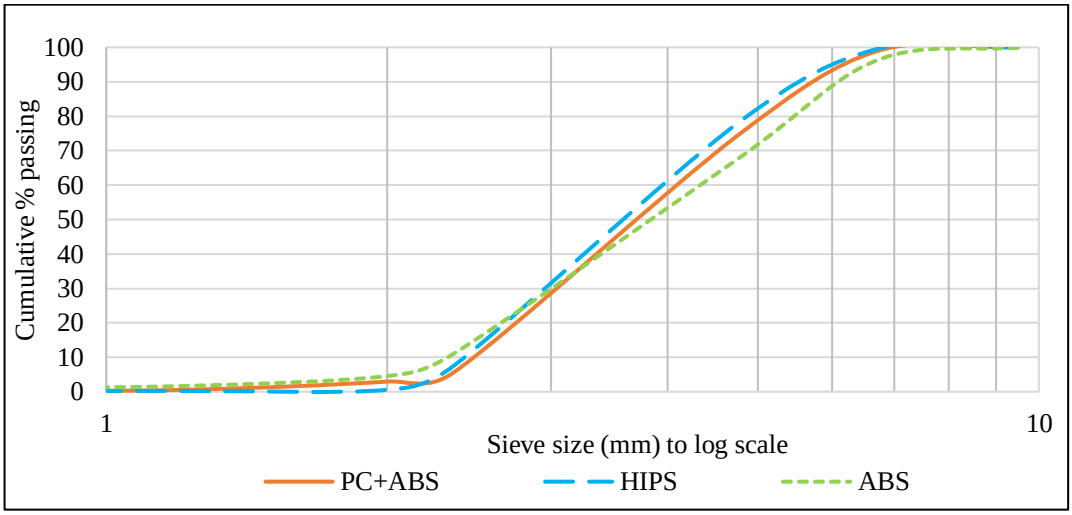

Figure 30: Grading curve for ABS, HIPS and PC/ABS WEEP.

From the sieve test results, it can be seen that HIPS WEEP had the highest percentage material passing the larger sieve openings. It is interesting to note that that ABS WEEP had the widest grading curve, which may have decreased when PC was added to produce PC/ABS in manufacturing. Thus, from the grading curve it can be seen that the addition of PC in ABS reduced the plasticity of ABS WEEP. Furthermore, HIPS WEEP was more brittle when compared to PC/ABS and ABS WEEP. Thus, when granulated it snapped into smaller pieces and passed the blades more readily. ABS WEEP was more resilient compared to PC/ABS and HIPS WEEP. Hence, when ABS WEEP was granulated the plastic either got pushed through the blades, producing larger fractions or it bounced on top of the blades producing finer fractions, until it finally passed the blades.

However, the question arose as to which natural aggregates (coarse or fine) should WEEP replace? It was hence decided to test which aggregate replacement would yield the

highest compressive strength at 28 days of curing. Thus, trial mix designs replaced coarse and fine aggregates separately and both coarse and fine simultaneously. More information pertaining to the trial mix designs are provided in Appendix B.

3.4.2 Elemental composition of WEEP

The EDS analysis was performed using a CAMECA EPMA to evaluate all the elements present in WEEP. After which the WDS analysis was performed calculating the normal weights in percentages for each WEEP type, as shown in Table 13. See Appendix G, Tables G4 - G16 for the detailed results found for ABS, PC/ABS and HIPS WEEP.

Table 13: Elemental composition of WEEP.

WEEP type	Normal weight (%) of elements (WDS)						
	C	O	Cl	Br	Sb	N	Total
ABS	77.19	3.26	1.76	14.49	3.30	0.00	100.00
PC/ABS	91.65	1.03	0.00	0.00	0.00	7.33	100.00
HIPS	81.47	17.55	0.97	0.00	0.00	0.00	100.00

From the above table, it is clear that ABS WEEP contained heavy elements in its polymetric matrix, namely: bromine (Br) and antimony (Sb). Both of which are used as a flame retardant in EEP as stated by: Gutman *et al*., (2005); Hansen and Pergantis (2006); and Imai *et al*., (2002).

3.4.3 Density analysis for aggregates

The particle density for the natural aggregates were performed according to SANS 5844:2014, while the compact bulk density was performed according to SANS 5845:2006. This method used the "rodding procedure" to calculate the densities, as shown in Table 14.

Table 14: Particle densities of natural aggregates.

	13.2mm Stone	9.5mm Stone	Sand
Particle density (kg/m³)	2 890	2 930	2 580
Compact bulk density (kg/m³)	1 660	1 600	2 060

Granulated WEEP was evaluated using the same codes used for the natural aggregates. The uncompacted bulk density (UBD) was performed according to SANS 5845:2006. From Table 15 it is clear that PC/ABS and HIPS WEEP had the same UBD, while ABS WEEP had the lowest.

Table 15: Particle densities of WEEP aggregates.

	ABS	PC/ABS	HIPS
Particle density (kg/m³)	940	1 190	1 390
Uncompact bulk density (kg/m³)	520	580	580

3.4.4 Typography of the aggregates using SEM

This section evaluates the typography of both the natural aggregates and granulated WEEP using a Carl Sigma FESEM. The surface roughness of the natural aggregate and WEEP used may explain the bonding strength between the aggregate and hardened cementitious paste (hcp), which in turn affects the overall strength and durability of concrete. An aggregate with a very smooth surface may reduce the bonding area between the aggregate and hcp, reducing the bonding strength. Alternatively, an aggregate with a rough surface may increase the bonding area between the aggregate and hcp, increasing the bonding strength.

The natural aggregate was sampled at random and was approximately 2.3mm in diameter. The aggregate was blown with compressed air to remove the excess dust from the surface. Prolonged investigations of the surface typography of WEEP were often prone to damage from the electron beam, which sometimes resulted in the charging of the surface.

The following sub-sections evaluates the results of the surface typography of the natural aggregate and granulated WEEP at magnifications of 5 000 times.

3.4.4.1 Crushed natural aggregate

Figure 31 shows the typography of the natural aggregate used in this study. Here it is seen that the surface was very rough and contained numerous crevasses in which cementitious paste could flow and harden. It was also seen that there were small grains of dust attached to the aggregates surface. It is however believed that these dust grains would be mixed into the fresh cementitious paste and would not significantly affect the strength, provided that mixing was done optimally and for long enough periods.

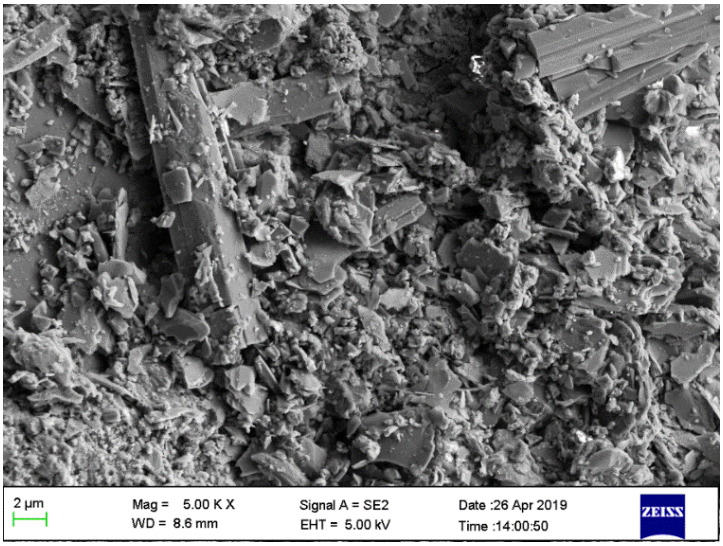

Figure 31: SEM image of the natural aggregate, magnified at 5 000 times.

3.4.4.2 ABS WEEP

Figure 32 shows the typography of ABS WEEP. There were parallel lines on the surface of the ABS WEEP. As these lines were protruding out from underneath the plastic, it is believed that it was produced when it was originally moulded.

It is clear that the surface of ABS WEEP was very smooth compared to that of the natural aggregate. The smooth surface of the ABS WEEP may reduce the bonding area of the hcp which in turn may reduce the strength and durability of hardened concrete.

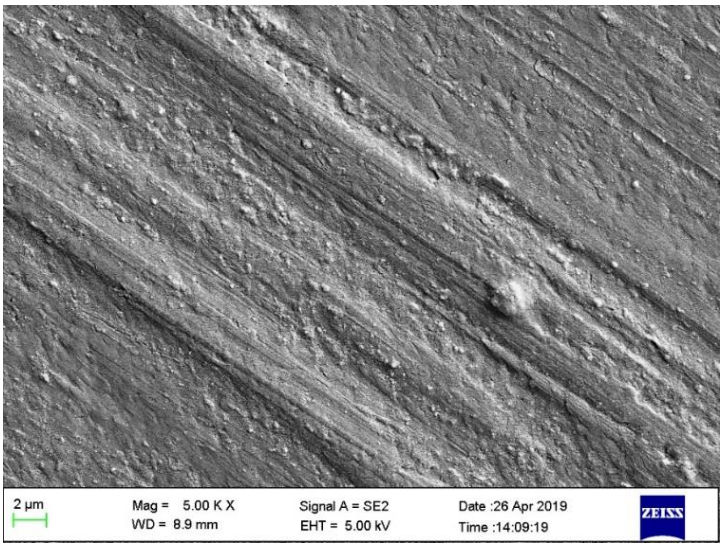

Figure 32: SEM image of granulated ABS WEEP, magnified at 5 000 times.

3.4.4.3 PC/ABS WEEP

Figure 33 shows the typography of PC/ABS WEEP. Comparing magnifications between PC/ABS and ABS WEEP, it is clear that there was a visible difference in their surface texture. PC/ABS WEEP had a rougher surface with numerous random protrusions coming out from underneath the plastic. This may in turn act as small anchorages and provide holdings for the hcp, which in turn could increase the strength more compared to that of the ABS WEEP.

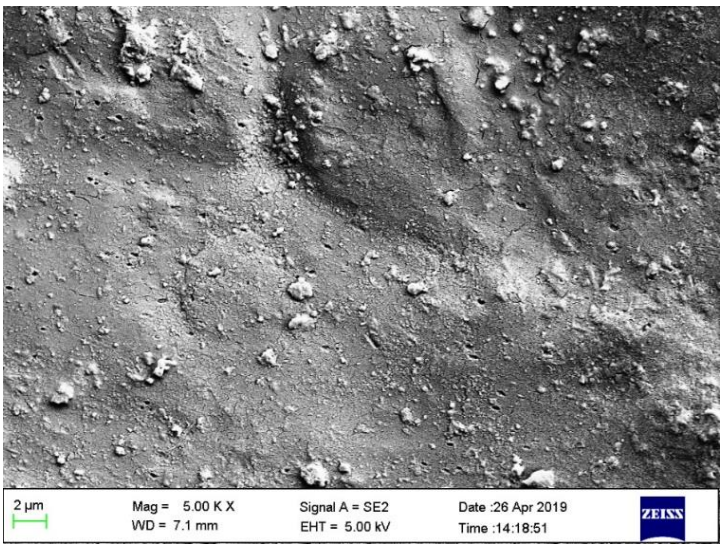

Figure 33: SEM image of granulated PC/ABS WEEP, magnified at 5 000 times.

3.4.4.4 HIPS WEEP

Figures 34 - 35 shows the typography of HIPS WEEP at 5 000 and 1 000 times magnification. HIPS WEEP used had cylindrically shaped particles protruding out from the bottom of the plastic.

These cylinders were blended into the plastic as it is clearly different compared to the surrounding plastic which was very flat. Furthermore, the cylinders had a very rough exterior which could increase the bonding area between HIPS WEEP and the hcp. This in turn could increase the strength and durability of concrete more compared to other types of WEEP.

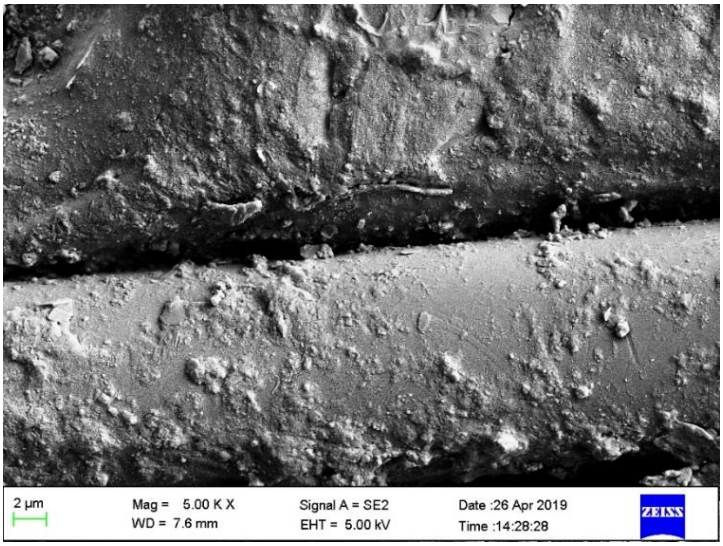

Figure 34: SEM image of granulated HIPS WEEP, magnified at 5 000 times.

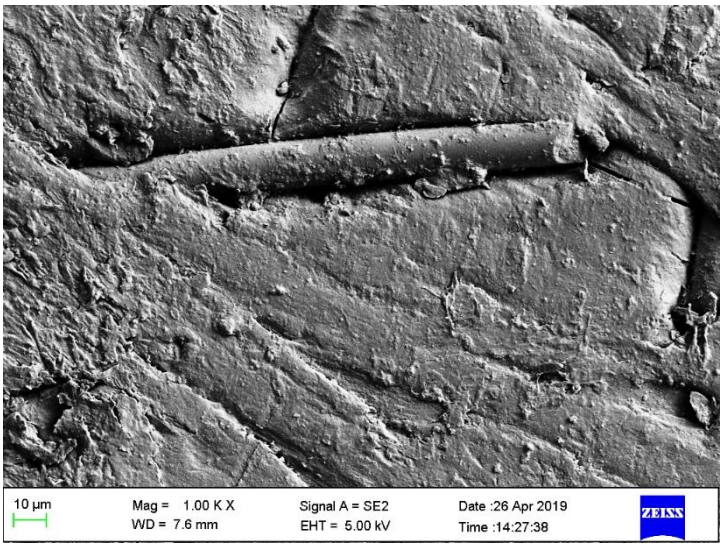

Figure 35: SEM image of granulated HIPS WEEP, magnified at 1 000 times.

3.5 Summary

This chapter has provided the material properties of both the binder materials and aggregates used in this study. The following chapter presents the experimental details and procedures conducted in this study.

Chapter 4: Experimental details and procedures

4.1 Introduction

This chapter presents the experimental details and procedures conducted in this study. From previous literature, it was found that WEEP decreased the compressive strength of concrete by as much as 50%, even at low replacements. This generally resulted in concrete that was not suitable for structural usage. It was the aim of this study to produce structural concrete with a compressive strength > 25MPa using different types of WEEP in the partial replacement for the natural aggregate. One way to achieve the aforementioned strength was by using a CEM I 52.5R ordinary Portland cement which generally provides concrete with a compressive strength in excess of 52.5MPa (Owens and Addis, 2012) which took the strength reduction associated with the volume addition of WEEP into consideration. Furthermore, a superplasticiser was used to maintain a slump of 80mm $\pm$ 25mm to ensure a workable mix was maintained.

The experimental details and procedures has been arranged into three sections and are presented in the following order:

- Details pertaining to the mix design;
- Details relating to the procedures followed for the mixing and curing of concrete; and
- Test details and procedures followed to evaluate both fresh and hardened concrete.

4.2 Mix design

The mix design was based on experiments conducted on trial mixes using the Cement and Concrete Institute (C&CI) method, as presented in Appendix B. Concrete was produced for each mix design by maintaining a constant water:binder (w:b) ratio and water content. Furthermore, superplasticiser was added to maintain a slump of 80mm $\pm$ 25mm. WEEP replaced both the coarse (13.2mm) and fine natural aggregates by volume.

Three main mix designs were evaluated all consisting of the partial replacement of ABS, PC/ABS, HIPS WEEP and an equal blend of PC/ABS, HIPS and ABS WEEP in ratios of 1:1:1. The replacement levels were done at 5%, 10%, 20% and 30%. The first mix design (control mix) replaced both the fine and coarse aggregates with the aforementioned WEEP replacements. The second mix design was based on the first, whereby cement was

replaced by 25% MK by mass. The third mix was also based on the first mix, whereby cement was replaced with 10% CSF by mass. See Table 16 for all the mix design acronyms used. Figure 36 graphically illustrates the description for the acronyms in the aforementioned table.

Table 16: Acronyms used for the different concrete mix designs.

Acronym	Description	Acronym	Description
PC	Control mix	PC(**PC/ABS**-5)	Replacement of the natural aggregate with PC/ABS WEEP.
PC**M**	Based on the control mix whereby metakaolin replaces 25% of the cement.	PC(**HIPS**-5)	Replacement of the natural aggregate with HIPS WEEP.
PC**S**	Based on the control mix whereby condensed silica fume replaces 10% of the cement.	PC(**Blend**-5)	Replacement of the natural aggregate with WEEP in a ratio of 1:1:1 (ABS: PC/ABS:HIPS) WEEP.
PC(**ABS**-5)	Replacement of the natural aggregate with ABS WEEP.	PC(ABS-**5**)	5% Replacement of natural aggregates with WEEP.

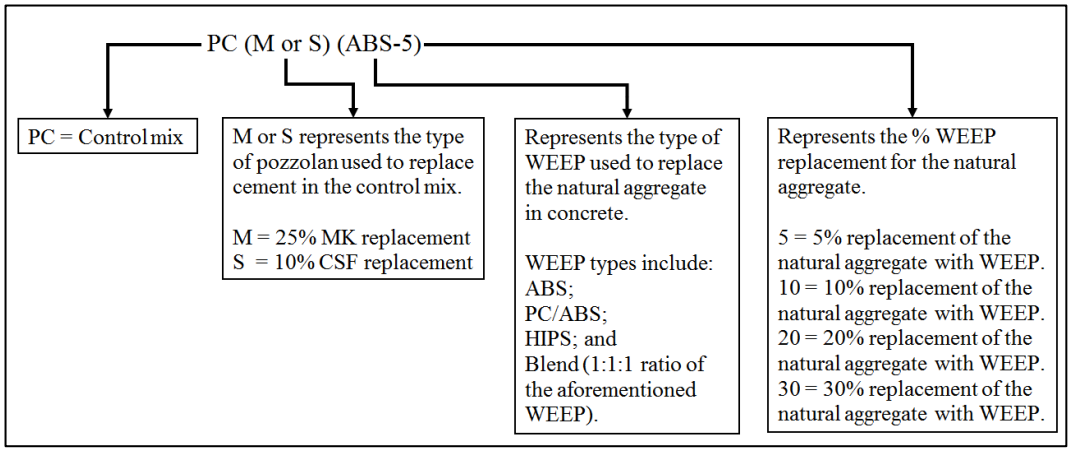

Figure 36: Acronyms used for the different concrete mix designs.

The compressive strengths were evaluated for all the mix designs shown in Table 19. However, the durability and tensile splitting strength were only evaluated for the mix designs shown in Table 17. Therefore, all WEEP types were tested at their maximum WEEP replacements. This represents the "peak values" whereby smaller substitutions of WEEP could be estimated between the mix replaced with 30% WEEP and those without.

Table 17: Mix designs tested for tensile strength and durability.

Control mix design replacing the natural aggregates with 30% WEEP	Control mix design replacing 25% cement with MK and replacing the natural aggregates with and without 30% WEEP	Control mix design replacing 10% cement with CSF and replacing the natural aggregates with and without 30% WEEP
PC (Control mix)	PCM	PCS
PC (ABS-30)	PCM (ABS-30)	PCS (ABS-30)
PC (PC/ABS-30)	PCM (PC/ABS-30)	PCS (PC/ABS-30)
PC (HIPS-30)	PCM (HIPS-30)	PCS (HIPS-30)
PC (Blend-30)	PCM (Blend-30)	PCS (Blend-30)

Exactly 612 cubes were used for the mix designs presented in Table 19 and had their respected compressive strengths tested at 3, 7, 28 and 90 days after curing. A further 90 cubes were cast to test the 28 day durability tests (OPI, water sorptivity and chloride conductivity). Lastly, 45 cylinders were cast to test the 28 day tensile splitting strength, as presented in Table 18.

Table 18: Number of specimens required per test.

Test	Number of mix designs tested	Specimens required per test	Age at which specimens were tested
Compressive strength test	51	12 cubes	3, 7, 28 and 90 days
Durability index	15	6 cubes	28 days
Tensile splitting strength test	15	3 cylinders	28 days

Table 19: Mix proportions of the various mix designs (w:b = 0.52).

Mix design	Sand (kg/m³)	Stone (kg/m³)	WEEP (kg/m³)	Water (kg/m³)	Cement (kg/m³)	MK (kg/m³)	CSF (kg/m³)	Total mass (kg/m³)	Superplasticiser (% binder)	Slump (mm)	Nominal proportions*
PC (Control mix)	931	706	0	231	444	0	0	2312	0.00	80	1:2.1:1.6:0.0
PC(ABS-5)	908	688	14	231	444	0	0	2285	0.00	75	1:2.0:1.5:0.0
PC(ABS-10)	884	671	28	231	444	0	0	2259	0.00	70	1:1.9:1.5:0.1
PC(ABS-20)	838	635	57	231	444	0	0	2205	0.09	65	1:1.9:1.4:0.1
PC(ABS-30)	791	600	85	231	444	0	0	2152	0.16	68	1:1.8:1.4:0.2
PC(PC/ABS-5)	908	688	18	231	444	0	0	2289	0.00	80	1:2.0:1.5:0.0
PC(PC/ABS-10)	884	671	36	231	444	0	0	2266	0.00	80	1:1.9:1.5:0.1
PC(PC/ABS-20)	838	635	72	231	444	0	0	2220	0.00	55	1:1.9:1.4:0.1
PC(PC/ABS-30)	791	600	108	231	444	0	0	2174	0.12	55	1:1.8:1.4:0.2
PC(HIPS-5)	908	688	21	231	444	0	0	2292	0.00	75	1:2.0:1.5:0.0
PC(HIPS-10)	884	671	42	231	444	0	0	2272	0.00	75	1:1.9:1.5:0.1
PC(HIPS-20)	838	635	84	231	444	0	0	2232	0.04	60	1:1.9:1.4:0.1
PC(HIPS-30)	791	600	126	231	444	0	0	2193	0.12	60	1:1.8:1.4:0.2
PC(Blend-5)	908	688	18	231	444	0	0	2289	0.00	65	1:2.0:1.5:0.0
PC(Blend-10)	884	671	36	231	444	0	0	2266	0.00	65	1:1.9:1.5:0.1
PC(Blend-20)	838	635	71	231	444	0	0	2219	0.06	60	1:1.9:1.4:0.1
PC(Blend-30)	791	600	107	231	444	0	0	2173	0.18	65	1:1.8:1.4:0.2
PCM	931	706	0	231	333	111	0	2312	0.33	80	1:2.1:1.6:0.0
PCM(ABS-5)	908	688	14	231	333	111	0	2285	0.67	70	1:2.0:1.5:0.0
PCM(ABS-10)	884	671	28	231	333	111	0	2259	0.67	65	1:1.9:1.5:0.1
PCM(ABS-20)	838	635	57	231	333	111	0	2205	0.87	75	1:1.9:1.4:0.1
PCM(ABS-30)	791	600	85	231	333	111	0	2152	0.94	70	1:1.8:1.4:0.2
PCM(PC/ABS-5)	908	688	18	231	333	111	0	2289	0.33	80	1:2.0:1.5:0.0
PCM(PC/ABS-10)	884	671	36	231	333	111	0	2266	0.33	70	1:1.9:1.5:0.1
PCM(PC/ABS-20)	838	635	72	231	333	111	0	2220	0.33	65	1:1.9:1.4:0.1
PCM(PC/ABS-30)	791	600	108	231	333	111	0	2174	0.67	75	1:1.8:1.4:0.2

Mix design	Sand (kg/m³)	Stone (kg/m³)	WEEP (kg/m³)	Water (kg/m³)	Cement (kg/m³)	MK (kg/m³)	CSF (kg/m³)	Total mass (kg/m³)	Superplasticiser (% binder)	Slump (mm)	Nominal proportions*
PCM(HIPS-5)	908	688	21	231	333	111	0	2292	0.37	70	1:2.0:1.5:0.0
PCM(HIPS-10)	884	671	42	231	333	111	0	2272	0.45	70	1:1.9:1.5:0.1
PCM(HIPS-20)	838	635	84	231	333	111	0	2232	0.52	65	1:1.9:1.4:0.1
PCM(HIPS-30)	791	600	126	231	333	111	0	2193	0.57	60	1:1.8:1.4:0.2
PCM(Blend-5)	908	688	18	231	333	111	0	2289	0.45	70	1:2.0:1.5:0.0
PCM(Blend-10)	884	671	36	231	333	111	0	2266	0.60	60	1:1.9:1.5:0.1
PCM(Blend-20)	838	635	71	231	333	111	0	2219	0.64	65	1:1.9:1.4:0.1
PCM(Blend-30)	791	600	107	231	333	111	0	2173	0.69	60	1:1.8:1.4:0.2
PCS	931	706	0	231	400	0	44	2312	0.00	75	1:2.1:1.6:0.0
PCS(ABS-5)	908	688	14	231	400	0	44	2285	0.04	70	1:2.0:1.5:0.0
PCS(ABS-10)	884	671	28	231	400	0	44	2259	0.10	65	1:1.9:1.5:0.1
PCS(ABS-20)	838	635	57	231	400	0	44	2205	0.22	55	1:1.9:1.4:0.1
PCS(ABS-30)	791	600	85	231	400	0	44	2152	0.22	55	1:1.8:1.4:0.2
PCS(PC/ABS-5)	908	688	18	231	400	0	44	2289	0.00	65	1:2.0:1.5:0.0
PCS(PC/ABS-10)	884	671	36	231	400	0	44	2266	0.00	60	1:1.9:1.5:0.1
PCS(PC/ABS-20)	838	635	72	231	400	0	44	2220	0.19	60	1:1.9:1.4:0.1
PCS(PC/ABS-30)	791	600	108	231	400	0	44	2174	0.27	60	1:1.8:1.4:0.2
PCS(HIPS-5)	908	688	21	231	400	0	44	2292	0.00	60	1:2.0:1.5:0.0
PCS(HIPS-10)	884	671	42	231	400	0	44	2272	0.00	55	1:1.9:1.5:0.1
PCS(HIPS-20)	838	635	84	231	400	0	44	2232	0.10	70	1:1.9:1.4:0.1
PCS(HIPS-30)	791	600	126	231	400	0	44	2193	0.15	65	1:1.8:1.4:0.2
PCS(Blend-5)	908	688	18	231	400	0	44	2289	0.00	60	1:2.0:1.5:0.0
PCS(Blend-10)	884	671	36	231	400	0	44	2266	0.07	55	1:1.9:1.5:0.1
PCS(Blend-20)	838	635	71	231	400	0	44	2219	0.10	55	1:1.9:1.4:0.1
PCS(Blend-30)	791	600	107	231	400	0	44	2173	0.19	55	1:1.8:1.4:0.2

*Ratio: cement:sand:stone:WEEP

4.3 Mixing procedure and curing regime

Concrete cubes of size 100mm x 100mm x 100mm were cast for each of the mix designs listed in Table 19 while cylinders of size 150mm x 30mm were cast for mixes listed in Table 17. All the solid materials and potable water were batched by weight using an electrical scale with an accuracy of 1g, while the superplasticiser was volume batched using a graduated cylinder. Mixing was carried out using a 50L pan mixer in the following steps:

- Add the stone, binder and sand. In the use of WEEP as replacement for the natural aggregate, WEEP was added before the stone. This was done to prevent the granulated WEEP from bouncing out of the pan during the initial mixing. The dry materials were mixed for approximately 2 - 3 minutes, after which the potable water was added.
- The fresh concrete was mixed for approximately 2 - 3 minutes. A slump test was performed according to SANS:5862-1 (2006), using a mould, base plate and tamping rod, directly after the machine was switched off. The mould was filled with concrete in three layers of equal depth, tamping each layer with 25 strokes of the tamping rod evenly over the concrete. If the mix did not have a slump of 80mm $\pm$ 25mm, a superplasticiser was added directly into the fresh concrete and mixed for 1 - 2 minutes. This procedure was repeated until the required slump was obtained.

Compaction was carried out using a vibrating table. Concrete cube moulds were filled with approximately one third fresh concrete. They were then vibrated for approximately 5 - 8 seconds, after which they were filled with another third of the cubes volume and vibrated again.

This was done until the mould was full and nearly all the bubbles stopped coming out. The total time of vibration for the cubes ranged between 15 - 24 seconds. Concrete cylinder moulds were filled with fresh concrete in three layers. Each of the layers were vibrated between 5 - 10 seconds. The total time of vibration ranged between 20 - 30 seconds.

After compaction, the concrete cubes and cylinders were covered with a plastic sheet and de-moulded approximately 22h $\pm$ 2h after casting. The concrete cubes and cylinders were placed in a water curing tank at temperatures ranging between $23°C \pm 2°C$, as described in SANS:5861-3 (2006).

4.4 Test methods

The following sub-sections evaluates both the tests and procedures followed for the fresh and hardened concrete.

4.4.1 Tests on fresh concrete (workability/slump)

The slump test results for PC (Control mix), PCM and PCS were compared to its respected replacement with 30% WEEP for the natural aggregate. Only 30% replacements were compared as lower percentages had the least effect on the fresh concrete. The slump test results and percentage superplasticiser used for all mix designs are available in Table 19. The slump test images for PC (Control mix) and its WEEP replacements for the natural aggregates are shown in Figure 37. These images illustrate how different types of WEEP affected the shape and cohesiveness of each concrete mix.

PC (Control mix) PC(ABS-30) PC(HIPS-30) PC(PC/ABS-30)

Figure 37: Slump for PC (Control mix), PC(ABS-30), PC(HIPS-30) and PC(PC/ABS) mixes.

From Figure 37 it can be seen that PC (Control mix) had a good slump with little bleed water at the base of the slump. PC(ABS-30) and PC(PC/ABS-30) provided some resistance on the tamping rod during compaction. However, PC(HIPS-30) provided more resistance on the tamping rod. There was also more bleed water accumulating at the base of this slump when compared to the other mixes made using WEEP. The slump test images for PCM and its WEEP replacements are shown in Figure 38.

PCM PCM(ABS-30) PCM(HIPS-30) PCM(PC/ABS-30)

Figure 38: Slump for PCM, PCM(ABS-30), PCM(HIPS-30) and PCM(PC/ABS-30).

The slump of PCM looks similar to that of PC (Control mix). However, more superplasticiser was added to achieve a similar slump, as shown in Table 19. It can be seen that PCM(ABS-30) and PCM(HIPS-30) accumulated bleed water at the base of the concrete slump. These mixes provided large amounts of resistance against the tamping rod when compacting the concrete. PCM(PC/ABS-30) was the most challenging mix as it struggled to attain the required slump of 80mm $\pm$ 25mm. Small quantities of superplasticiser were continuously added, until segregation occurred, as shown in Figure 39. However, its slump remained in the range of 5mm - 10mm.

Figure 39: Segregation of aggregates of PCM(PC/ABS-30).

More superplasticiser was added to the mix to obtain the required slump until it sheared, as shown in Figure 38.

The slump test images for PCS and its WEEP replacements are shown in Figure 40. Here it can be seen that PCS had a good slump shape with little bleed water accumulating at the bottom of the slump. PCS(ABS-30) and PCS(PC/ABS-30) had similar workability. However, PCS(HIPS-30) had more bleed water accumulating at the bottom of the slump compared to the other mixes.

PCS PCS(ABS-30) PCS(HIPS-30) PCS(PC/ABS-30)

Figure 40: Slump for PCS, PCS(ABS-30), PCS(HIPS-30) and PCS(PC/ABS-30).

4.4.2 Tests on hardened concrete (compressive, tensile, durability, backscatter analysis, XRD, SEM, EPMA and pore-size distribution)

The following sub-sections evaluates the tests on hardened concrete.

4.4.2.1 Compressive strength of concrete cubes

The compressive strength test was performed by applying a compressive load perpendicular to the direction of casting for three cubes from a sample of concrete. SANS:5863 (2006), was used to determine the compressive strength of hardened concrete for all the mixes presented in Table 19. A cube press-foote test machine manufactured by Concrete Testing Equipment was used to evaluate the compressive strength of hardened concrete, as shown in Figure 41. It is a fully automated machine which automatically

stops once it detects that the cube has failed. The machine has a maximum loading capacity of 1 000kN. The cubes were loaded at a rate of 150kN/min (0.25MPa/s).

Figure 41: Cube press-foote machine (LHS) and a concrete cube between the steel platens (RHS).

4.4.2.2 Tensile splitting strength of cylinders

SANS:6256 (2006), provided the standards required to test the tensile splitting strength of concrete. The tests were performed on the cylindrical concrete specimens with mix designs presented in Table 17. The cylinders were tested at 28 days of curing using an Amsler Compression Machine, as shown in Figure 42.

Figure 42: Amsler 2 000kN .

The machine has a maximum loading capacity of 2 000kN. The cylinders were loaded at a rate of 67.5kN/min (0.025MPa/s).

4.4.2.3 Tests for durability

Three laboratory durability tests were performed according to SANS codes and relevant standards, namely: oxygen permeability index (SANS:3001-C03-2, 2015), chloride conductivity (SANS:3001-C03-3, 2015) and water sorptivity (Durability Index Manual, 2017).

Durability tests were performed for all the mixes shown in Table 17. These mixes had the highest replacement of granulated WEEP and was hence the best representative of concrete mixed with WEEP.

Preparation of concrete disks

At 28 days of curing, concrete cubes were cored with a high speed, water-cooled core drill machine with a core barrel with an inner diameter of 70mm. Drilling was performed perpendicular to the casting direction, after which 5mm were cut away from both exterior faces of the core with a diamond tip water-cooled circular saw blade. The concrete disks were cut into a thickness of 30mm $\pm$ 2mm from either sides of the core and marked on the interior faces. The disks were placed in a ventilated oven at temperatures maintained at $50°C \pm 2°C$ for 7 - 8 days, to remove excess moisture from the concrete.

On the day of testing, the disks were removed from the oven and placed in a desiccator to cool down for 2 - 4 hours. The disks thickness and diameters were recorded using a vernier calliper at four different points.

Oxygen permeability test

The oxygen permeability index (OPI) test is based on deriving the Darcy's coefficient of permeability. Thus, it evaluates the falling pressure head whereby one side of a pre-conditioned sample is exposed to an internal pressure, while the opposed side is exposed to atmospheric pressure.

Therefore, the OPI test measures the pressure decay of oxygen through the sample which is expressed as "the negative log of the coefficient of permeability (K(m/s))" (Fulton and Owens, 2009, p181). As the log is used in the calculations, a small difference in the OPI value may result in a large permeability difference. OPI values generally range between 8.5 - 10.5 in South Africa and the equivalent coefficient of permeability (k-value) range

between $3.2x10^{-9}$ - $3.2x10^{-11}$. A higher OPI value corresponds to a concrete with a higher impermeability while a higher k-value corresponds to a concrete with a higher permeability (*ibid*).

OPI tests can be used to predict carbonation depths in various concretes, assess the micro and macrostructure of the outer surface which corresponds to the state of compaction, presence of bleed voids and channels and the interconnectedness of the concrete pore structure (*ibid*).

Four preconditioned disks were placed in compressible collars within ridged sleeves, as shown in Figure 43. With the test surface of the specimen facing the bottom, the units were secured on top of the permeability cells to cover the chamber holes. The apparatuses were clamped down on top of the chambers, as shown in Figures 44 - 45.

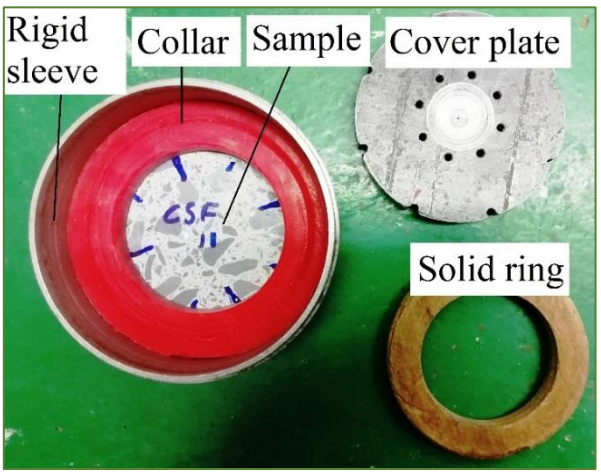

Figure 43: Oxygen permeability sample unit.

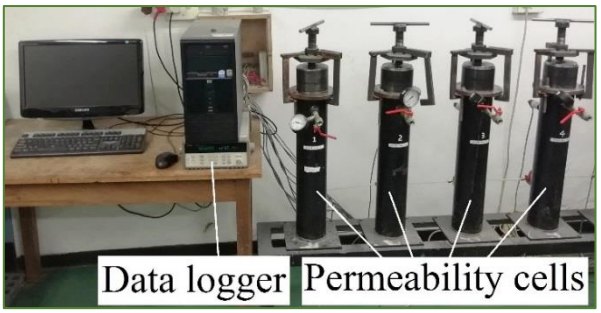

Figure 44: Oxygen permeability experimental setup.

The permeability cells were initially pressurised between 100kPa - 120kPa and immediately reopened for approximately 5 seconds to remove all other gasses, except for oxygen. The tank was re-pressurised to approximately 100kPa $\pm$ 5kPa. The cells were

checked to ensure that no gas leakages were occurring. A data logger was used to record the pressure decay at intervals of 15 minutes and was stopped after 6 hours or after the pressure dropped to 50kPa $\pm$ 2.5kPa.

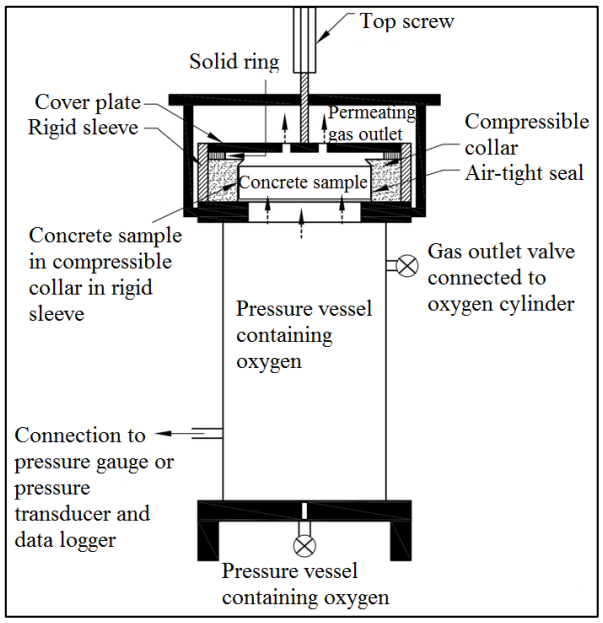

Figure 45: Schematic representation of a permeability cell. (Source: SANS 3001-2:2015).

The analysis of the OPI and k-values were calculated using an excel spreadsheet obtained from The Concrete Institute (2018). See Appendix F, Section F.1 for the required equations to manually calculate the OPI and k-values.

Water sorptivity test

The water sorptivity test involves the determination of sorptivity and porosity values of a pre-conditioned disk. Water sorptivity results may be used as a site control parameter as it is less dependent on the concrete material composition and more dependent on construction factors, such as curing (Alexander *et al.*, 2008).

Sorptivity values range from between 5mm/√h - 15mm/√h for well cured Grade 30 - Grade 50 concrete and 15mm/√h - 20mm/√h for poorly cured Grade 20 concrete (*ibid*)

Two to three layers of cello tape were tightly wrapped around the lower half of the circumference of the disk, exposing only the outer face of the specimen to a uni-directional absorption of water. This allowed water to penetrate the concrete disk, as shown in Figure 46.

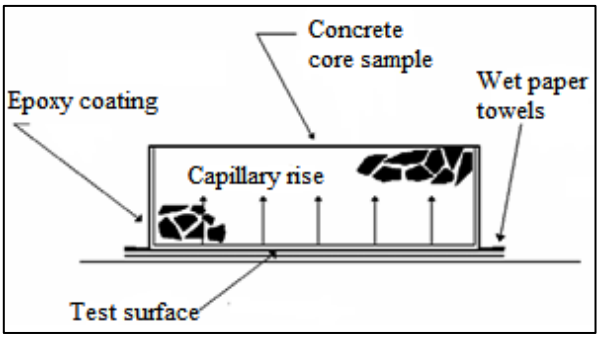

Figure 46: Capillary rise in water sorptivity test. (Source: Alexander, 2004).

Five grams of calcium hydroxide was mixed for each liter of potable water and was poured into a tray lined with 10 layers of absorbent paper, to a height no more than 2mm up the side of the disks. The disks were patted once on a damp paper towel and weighed on an electronic balance to the nearest 0.01g at 3, 5, 7, 9, 12, 16, 20 and 25 minutes to measure the rate of absorption, as seen in the experimental setup in Figure 47.

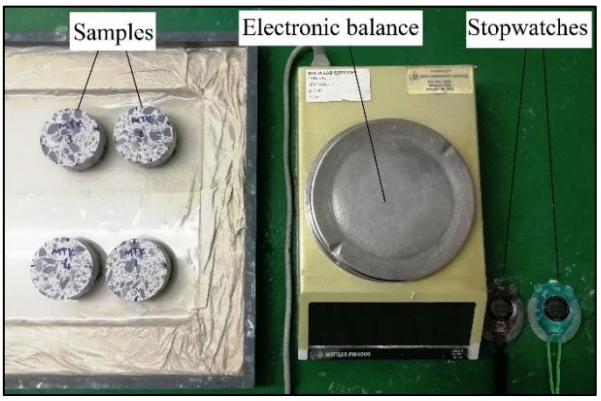

Figure 47: Samples tested for water sorptivity.

After which, the disks were placed in a vacuum tank and depressurised between -75kPa and -80kPa for 3 hours. Thereafter, calcium hydroxide solution was allowed to enter the tank for 1 hour at the aforementioned pressures. The pressure was then released, and the disks were left to soak for 18 hours and weighed in their saturated surface dry condition. Vacuum saturating the samples can provide an approximation of the total pore volume of the concrete, as shown in Figure 48.

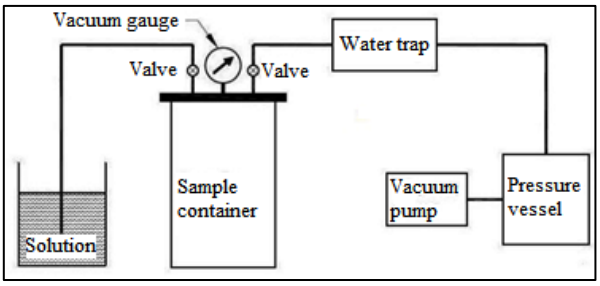

Figure 48: Vacuum saturation facility. (Source: Durability Index Manual, 2017).

The calculations were performed using an excel spreadsheet from The Concrete Institute (2018), which calculated the sorptivity in mm/√hr and porosity in %. See Appendix F, Section F.2 for the equations required to manually calculate the water sorptivity and porosity.

Chloride conductivity test

The chloride conductivity test is often used to specify concrete performance in seawater environments (Alexander *et al.*, 2008). This is achieved by subjecting a pre-conditioned sample to a vacuum saturation in a highly ionic chloride solution for a pre-determined period and then measuring its resistance at a given potential. Chloride conductivity values for concrete made with CEM I and CSF in ratios of 90:10 should range between 1.2mS/cm - 0.35mS/cm for concretes exposed to airborne salt, but not directly in contact with water and for concrete permanently submerged and exposed to abrasion (*ibid*).

Sodium chloride solution (5M) was prepared by mixing 2.93kg of chemical pure sodium chloride salt to 10 litres of potable water, 3 days before testing. The specimens were pre-conditioned. The disks dry mass was measured before testing to an accuracy of 0.01g. The disks were placed in a vacuum saturation tank under pressures ranging between -75kPa and -80kPa for approximately 3 hours. After which sodium chloride solution was allowed to enter the tank and cover approximately 40mm above the disk, all without allowing any air to enter the system.

The pressure was re-established, and further vacuum saturation was done for 1 hour. Thereafter, the vacuum was released, and the specimen soaked for 17 - 18 hours. Following, every specimen was removed from the tank and patted with a paper towel to its surface dry condition, and its mass recorded, as described earlier. Directly after

measuring the mass, each disk was transferred separately to the chloride conduction rig and placed into a compressible rubber collar, as shown in Figures 49 - 50.

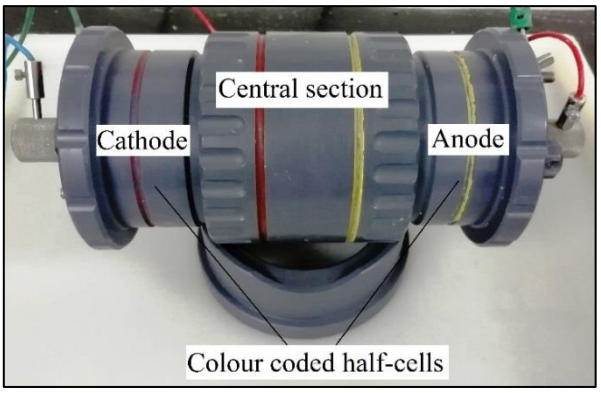

Figure 49: Complete chloride conduction rig.

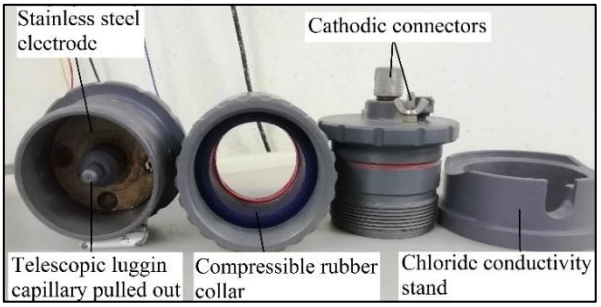

Figure 50: Components of chloride conduction rig.

One half of the conduction cell was closed, and the sodium chloride solution was poured into the cell. The cell was bled to remove all entrapped air with the bleed screws and the connectors were tightened. Similar procedure was followed for the other half of the cell. The ammeter and volt meter were connected and adjusted at a DC power supply until the voltage across the disk reached approximately 10V. At this stage both the current and voltage was measured respectively, as shown in Figure 51.

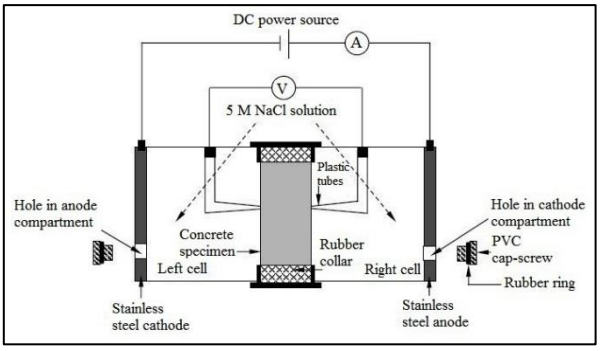

Figure 51: Simple cell arrangement. (Source: SANS 3001-CO3-3, 2015).

The calculations were performed using an excel spreadsheet from The Concrete Institute (2018), which calculated the chloride conductivity in mS/cm and porosity in %. See Appendix F, Section F.3 for the equations required to manually calculate the chloride conductivity and porosity.

4.4.2.4 Sample preparation for scanning electron microscopy

The sample preparations for SEM analysis were done at the School of Geosciences, at the University of the Witwatersrand. Different sample preparations were required, depending on the test performed.

Hardened concrete samples were prepared as thin sections, with thicknesses ranging between 80μm - 100μm. These thin sections were the same samples tested for the OPI test at 28 days of curing. Once the OPI tests were complete, the samples were cling-wrapped to prevent any damage from occurring due to carbonisation. The samples were cut into rectangular shapes with dimensions of 45mm x 30mm x 25mm. The lower half of the samples surface was placed directly into the EpoFix epoxy, while the other was open to atmospheric air. EpoFix epoxy was mixed in ratios of 1:8 with EpoFix resin and EpoFix hardener. The samples were then placed in a vacuum chamber at 6 bar for 12 hours, to ensure that the epoxy was drawn into the concretes structure. After which the samples were ground using 400, 600, 800 and 1 000 grit silicon carbide paper at 300 rounds per minute for approximately 8 minutes per grit. After which they were mounted on a glass slide using a mounting press at 34$°C$ for 8 - 12 hours. The test surface was then ground further using silicon carbide powder, with a similar grit to those used for the silicon carbide paper. Thereafter, the samples were polished using a diamond polishing paste of 15μm, 9μm, 6μm and 3μm.

Materials analysed were required to be conductive in order to conduct relevant analysis. This in turn also reduces charging and thermal damage of the sample. All the materials evaluated were non-conductive and hence required coating with an electrically conductive material. The coatings were done at the MMU department, at the University of the Witwatersrand. The type and thickness of the coating depended on the type of material coated. Coating of materials were done as recommended by the MMU staff. The thin sections were coated with a 30nm carbon layer.

4.4.2.5 ITZ test and results

The interfacial transition zone (ITZ) is found between the aggregate and hcp in hardened concrete. The structure of the hcp at the ITZ is entirely different compared to the bulk hcp (Bensted and Barnes, 2002). The ITZ is often the weak link in concrete and may therefore have a negative influence on the strength, durability and permeability of hardened concrete. The ITZ is formed during the compaction of fresh concrete. A film of water forms around the aggregate, leading to higher w:b ratios close around the aggregate, as shown in Figure 52 (Li, 2011).

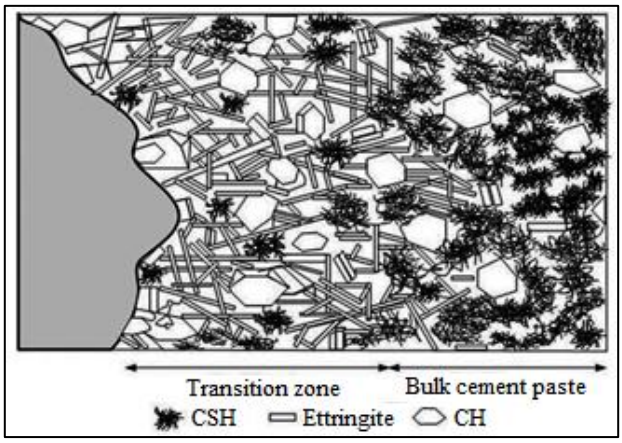

Figure 52: Interfacial transition zone in concrete (Source: Li, 2011).

This section evaluates the ITZ, size and distribution of pores around the ITZ of concrete at 28 days of curing. This is done for both concrete made without WEEP and 30% replacement of WEEP for the natural aggregate. The "Blend-30" mix was chosen as it contained all three WEEP types, i.e. ABS, PC/ABS and HIPS WEEP mixed in either PC (Control mix), PCM or PCS.

High magnification of the concrete matrix was required to evaluate the bonding of the hcp to the aggregate. This was done at 5 000 times magnification.

Polished thin section slides were used to analyse the pore-size and ITZ using the backscatter function on the FESEM. This was done as the grey scale level allowed different phases in the concrete matrix to be easily distinguished. Heavy elements have a high atomic mass and appeared more bright, while lighter elements appeared more dark. Thus, the pores which are epoxy impregnated appeared very dark and allowed them to be easily identified in the concrete matrix (Zhao and Darwin, 1990).

ITZ between the natural aggregate and the cement paste for PC (Control mix)

Figure 53 represents the interface between the natural aggregate and the hcp for PC (Control mix). Here the ITZ is noticeable by the clear dark-sheath band between the aggregate and hcp. This band was approximately 4μm - 6μm thick and stretched parallel between the aggregate and the hcp. It was noticed that within this band there were numerous dark patches (pores) ranging in sizes of between < 1μm and 1.5μm. This band contained less hcp and more pores. However, it was seen that there was contact between the aggregate and the hcp.

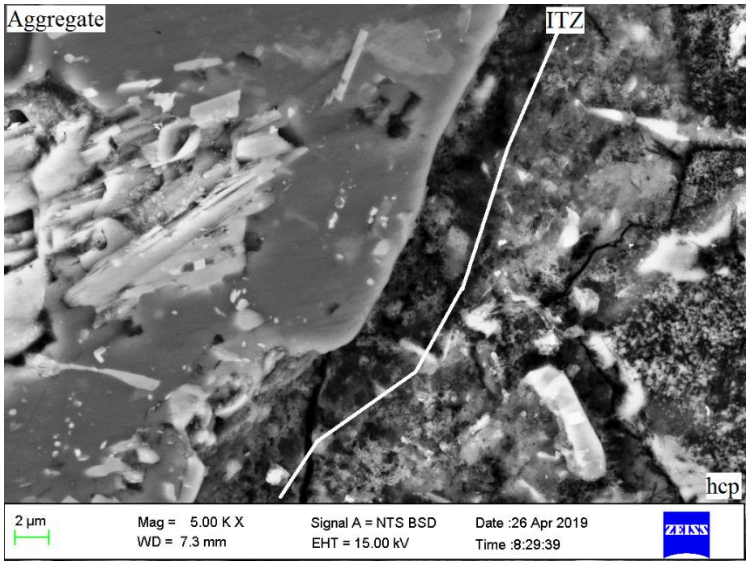

Figure 53: BSE image of the ITZ of the natural aggregate in PC (Control mix) at 5 000 times magnification.

ITZ between ABS WEEP and the cement paste for PC(Blend-30)

Figure 54 represents the interface between ABS WEEP and hcp in PC(Blend-30). As WEEP contained mainly carbon in its chemical structure, it had a low backscattering coefficient and thus appeared dark on the BSE image. There was no noticeable ITZ between the ABS WEEP and hcp. However, as indicated by "1" in Figure 54, there were numerous amounts of crystal formations between the ABS WEEP and hcp. The EDS analysis revealed that it contained numerous amounts of calcium and silicon in atomic ratios indicating a phase between belite and calcium silicate hydrate (C-S-H). The EDS results are available in Appendix J, Table J1.

Figure 54: BSE image of ABS WEEP in PC(Blend-30) at 5 000 times magnification.

ITZ between PC/ABS WEEP and the cement paste for PC(Blend-30)

Figure 55 represents the interface between PC/ABS WEEP and the hcp in PC(Blend-30). There was no clear ITZ between the PC/ABS WEEP and the hcp. There were noticeably more pores in the hcp compared to Figure 54. These pores also seemed to have a higher degree of connectiveness. It also seemed that there was some smearing between the hcp and the PC/ABS WEEP. This could be as a consequence of polishing during sample preparation, whereby the hcp was smeared into the softer PC/ABS WEEP as these smears were prominent to flow in a single direction.

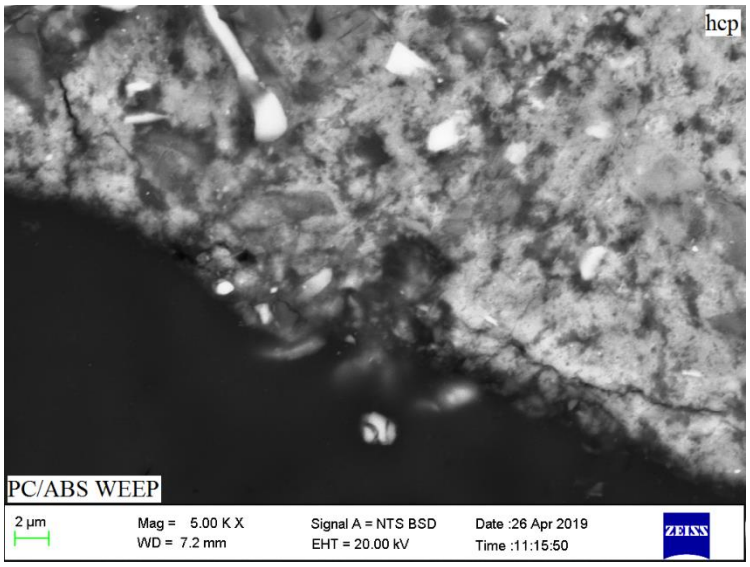

Figure 55: BSE image of PC/ABS WEEP in PC(Blend-30) at 5 000 times magnification.

ITZ between HIPS WEEP and the cement paste for PC(Blend-30)

Figure 56 represents the interface between HIPS WEEP and the hcp in the PC(Blend-30). Here it was seen that there was no distinguishable ITZ between the HIPS WEEP and the hcp. There was a very large pore indicated by "2" measuring more than 3μm in diameter. Moreover, it seemed that there were more connected pores in the hcp between the HIPS WEEP compared to the PC/ABS WEEP, as indicated by the yellow lines. Similar to Figure 55, there was some smearing transition between the hcp and the WEEP.

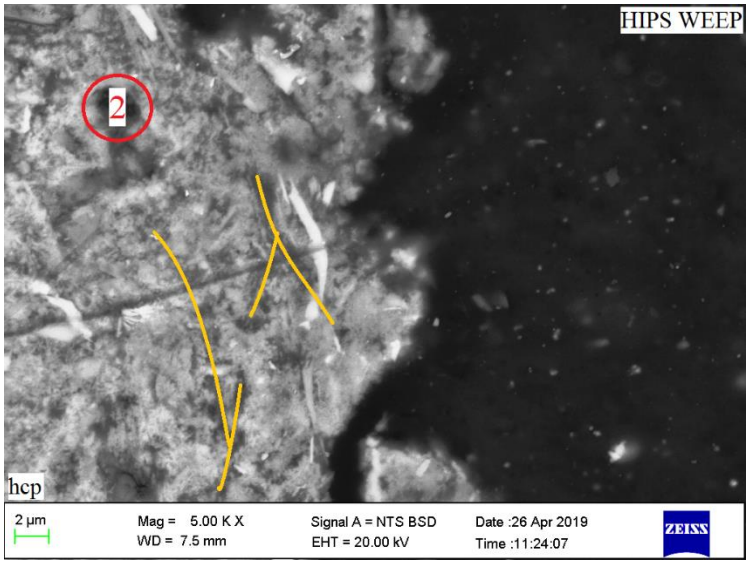

Figure 56: BSE image of the ITZ of HIPS in PC(Blend-30) mix at 5 000 times magnification.

ITZ between natural aggregate and the cementitious paste for PCM

Figure 57 represents the interface between the natural aggregate and the hcp in PCM. There were numerous amounts of connective pores within the hcp. This is clearly seen inside the red circle numbered "3". Furthermore, these connective pores ran parallel between the ITZ line and the natural aggregate. This could be as a result of high quantities of bleed water accumulating between the hcp and aggregate when compacted in the fresh state.

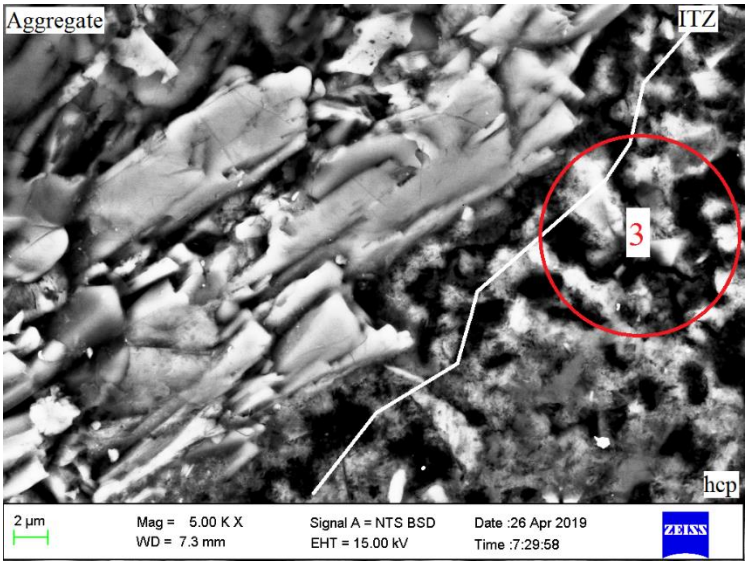

Figure 57: BSE image of the ITZ of stone in PCM at 5 000 times magnification.

ITZ between ABS WEEP and the cementitious paste for PCM(Blend-30)

Figure 58 represents the interface between the ABS WEEP and the hcp in PCM(Blend-30). Similar types of crystal formations were found between the ABS WEEP and the hcp as in PC(Blend-30), indicated by "4". The crystals were just under 2μm thick. Unlike the hcp around the ABS WEEP in the PC(Blend-30), there were very few visible pores in the hcp.

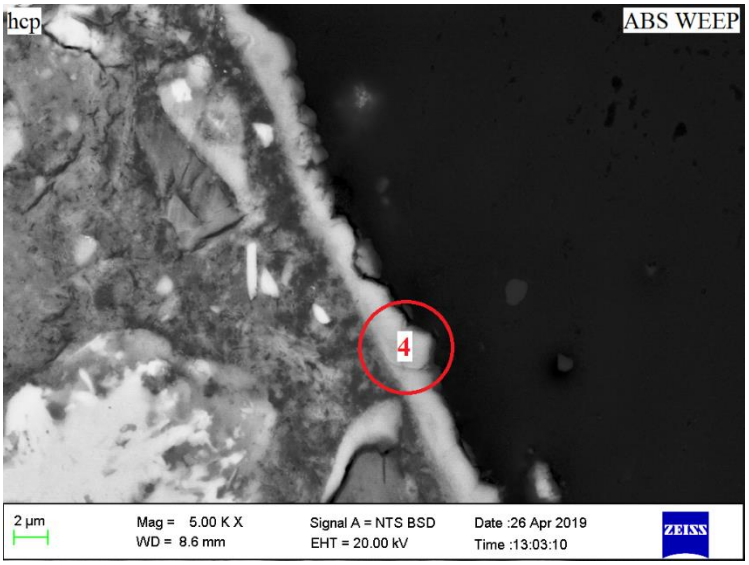

Figure 58: BSE of ABS WEEP in PCM(Blend-30) at 5 000 times magnification.

ITZ between PC/ABS WEEP and the cementitious paste for PCM(Blend-30)

Figure 59 represents the interface between the PC/ABS WEEP and the hcp in PCM(Blend-30). Similar to the PC/ABS and HIPS WEEP replacement in PC(Blend-30), there was no distinguishable ITZ. There was some smearing between the PC/ABS WEEP and the hcp. This is similar to the results shown in Figure 55 (p.82). There were small cracks in the paste as indicated by "5", but this is believed to have been introduced during the sample preparation.

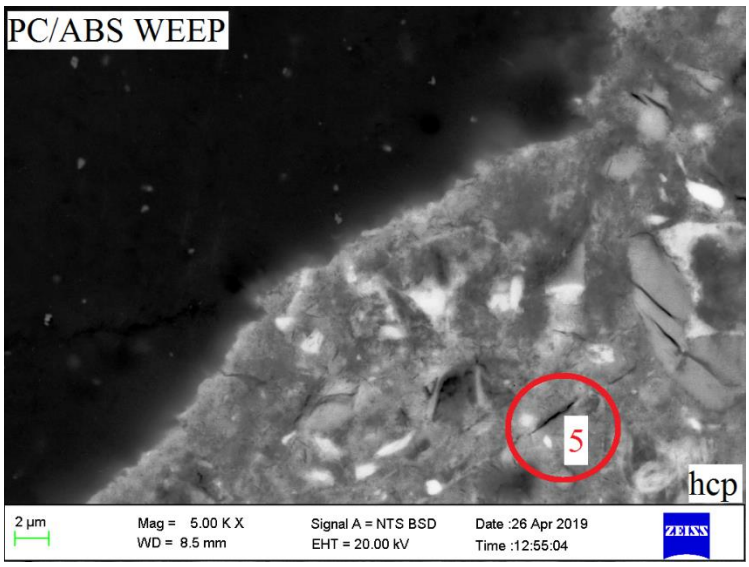

Figure 59: BSE of PC/ABS WEEP in PCM(Blend-30) at 5 000 times magnification.

ITZ between HIPS WEEP and the cementitious paste for PCM(Blend-30)

Figure 60 represents the interface between HIPS WEEP and the hcp in PCM(Blend-30). There was no distinguishable ITZ between the hcp and the HIPS WEEP. The hcp contained large pores which were over 2μm wide as numbered "6".

The bonding between HIPS WEEP and the hcp had less smearing compared to HIPS WEEP used in PC(Blend-30) (p.83). This could be as a result of HIPS WEEP having different hardness's depending on its source and original application.

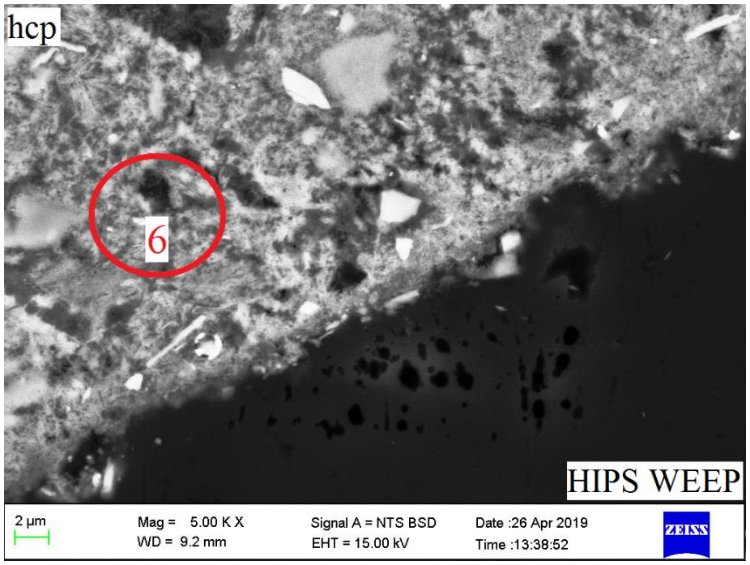

Figure 60: BSE of HIPS WEEP in PCM(Blend-30) at 5 000 times magnification.

ITZ between the natural aggregate and the cementitious paste for PCS

Figure 61 represents the interface between the natural aggregate and hcp in PCS. There was a clear ITZ of approximately 1μm - 3μm thick between the natural aggregate and the hcp. There were numerous amounts of pores in the hcp as indicated by "7". These pores were larger than 2μm in diameter. There were a lot of connecting pores within the hcp whereby the yellow line represents a connection which was greater than 15μm in length.

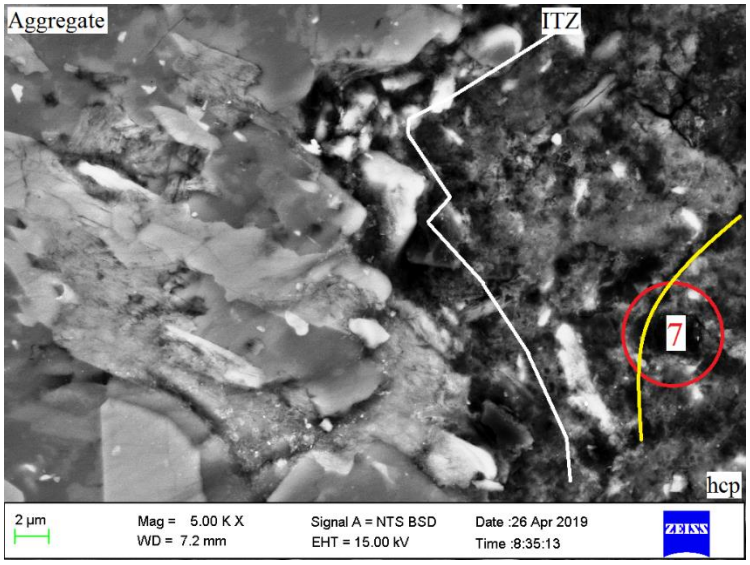

Figure 61: BSE image of the ITZ of stone in PCS at 5 000 times magnification.

ITZ between ABS WEEP and the cementitious paste for PCS (Blend-30)

Figure 62 represents the interface between the ABS WEEP and the hcp in PCS(Blend-30). It was seen that there was an ITZ between the ABS WEEP and the hcp. This is seen by the small amounts of crystals accumulated between the interface of the ABS WEEP and the hcp. There were also less visible pores in the hcp compared to Figure 54 (p.82).

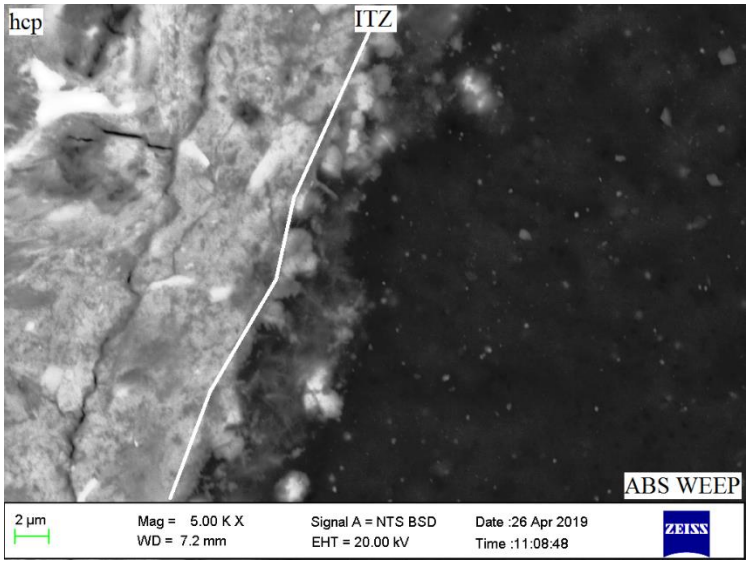

Figure 62: BSE image of ABS WEEP in PCS(Blend-30) at 5 000 times magnification.

ITZ between PC/ABS WEEP and cementitious paste for PCS (Blend-30)

Figure 63 represents the interface between the PC/ABS WEEP and the hcp in PCS(Blend-30). There was a clear ITZ region between the PC/ABS WEEP and the hcp. This was noted as there was a lot less unhydrated material on the right hand side of the ITZ line, compared to the left. It was also seen that there were some closed pores just under 2μm in diameter as indicated by “8”.

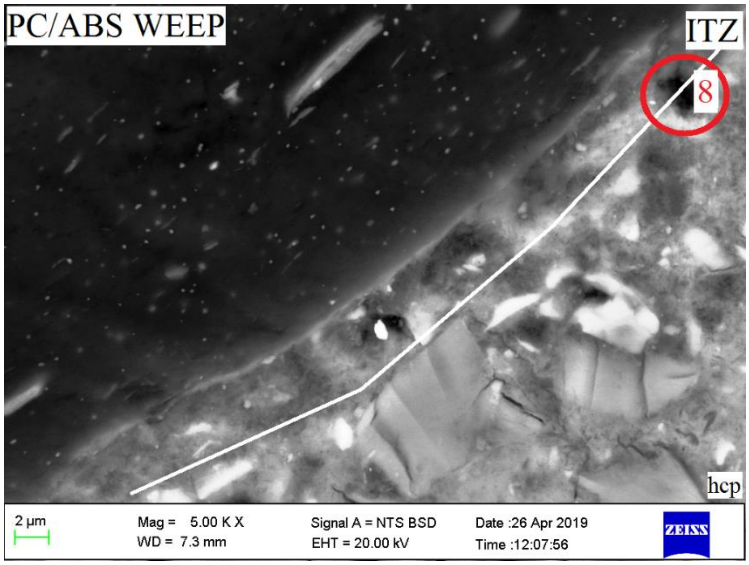

Figure 63: BSE of PC/ABS WEEP in PCS(Blend-30) at 5 000 times magnification.

ITZ between HIPS WEEP and cementitious paste for PCS (Blend-30)

Figure 64 represents the interface between the HIPS WEEP and the hcp in PCS(Blend-30). There were noticeably fewer connected pores compared to previous mixes made using HIPS WEEP as aggregate replacement material for the natural aggregate. It was also seen that there were small amounts of smearing between the hcp and the HIPS WEEP. The bright pigments found in the HIPS WEEP is believed to be the hcp which had been smeared into the HIPS WEEP during the sample preparation.

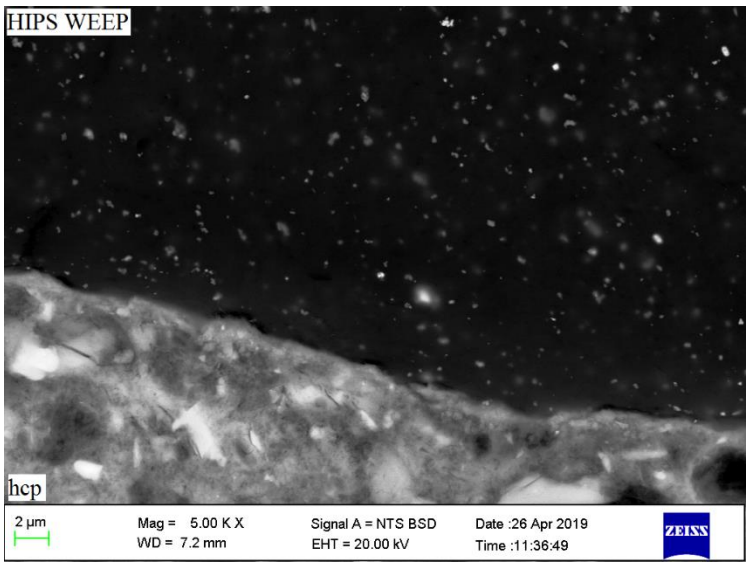

Figure 64: BSE of HIPS WEEP in PCS(Blend-30) at 5 000 times magnification.

4.4.2.6 Phase analysis of hardened concrete using BSE

As stated earlier, BSE provides atomic number contrast. Thus, a denser material exhibits a higher intensity BSE signal and appears brighter on the display screen. This may help distinguish specific phases within the hcp, such as: unhydrated cement particles, calcium hydroxide, calcium silicate hydrate (C-S-H), voids and cracks based on the relative intensities of their respective BSE signals (Zhao and Darwin, 1990). BSE investigation was mainly used as qualitative analysis as the apparent intensities measured during examination of the individual phases as they are subjective as adjustments on the FESEM instrument changes according to the user.

Table 20 presents the backscattering coefficients for the phases analysed. The equations used to calculate the mean atomic numbers and backscattering coefficients are available in Appendix F, Section F.5. Here it was seen that alite and belite had very similar backscattering coefficients and was difficult to differentiate from one another just by looking at their brightness on the screen. Thus, EDS analysis was used to distinguish these two phases from one another by analysing their relative mean atomic percentage and comparing them to Table 20. The X-ray mapping function on the FESEM was also used to identify areas of interest, which is available in Appendix H, Figures H1 - H3.

Table 20: Backscattering coefficients for phases analysed.

Phases	Mean atomic number	Backscattering coefficient	Scale (100)
Free lime	16.56	0.1882	98
Ferrite	16.65	0.1860	96
Alite	15.06	0.1716	80
Belite	14.56	0.1662	74
Aluminate	14.34	0.1639	71
Calcium hydroxide	14.30	0.1618	69
Calcium silicate	12.39	0.1456	51
Silicon dioxide	10.80	0.1254	28
Illite	10.87	0.1252	28

As seen in Table 21, alite, belite and calcium silicate hydrate had similar atomic masses, however their atomic percentage differed vastly from one another. Using the ratio of their atomic mass to atomic percentage, it was found that alite had a silicon:calcium ratio of 0.23, belite had a ratio of 0.34 and C-S-H had a silicon to calcium ratio of 0.70. Thus, the backscattering coefficients were only used as a guide to select the possible phases, while

the EDS analysis studied the selected phases. In this study, the phases of PC (Control mix), PCM and PCS were evaluated.

Table 21: Atomic mass and percentage of elements found in alite, belite and C-S-H (Source: Ebbing and Gammon, 2009)

Material	Element	Atomic mass	Atomic percentage
Alite	Si	28	12
	Ca	40	53
	O	16	35
Belite	Si	28	16
	Ca	40	47
	O	16	37
C-S-H	Si	28	21
	Ca	40	30
	O	16	1
	H	1	48
Metakaolin	Al	27	21
	O	16	56
	Si	28	22

BSE phase analysis of PC (Control mix)

Figure 65 presents the BSE image of the different phases found in PC (Control mix) at 28 days of curing. It can be seen that there were areas containing well-crystallised C-S-H. Belite occurred in small to large crystal sizes, ranging between 9μm - 15μm in width. Ferrite had slightly elongated shapes ranging between 1μm - 5μm in width. Aluminate was found to be between ferrite and had a width of approximately 8μm. See Appendix J, Figure J2 and Tables J2 - J3 for the EDS results.

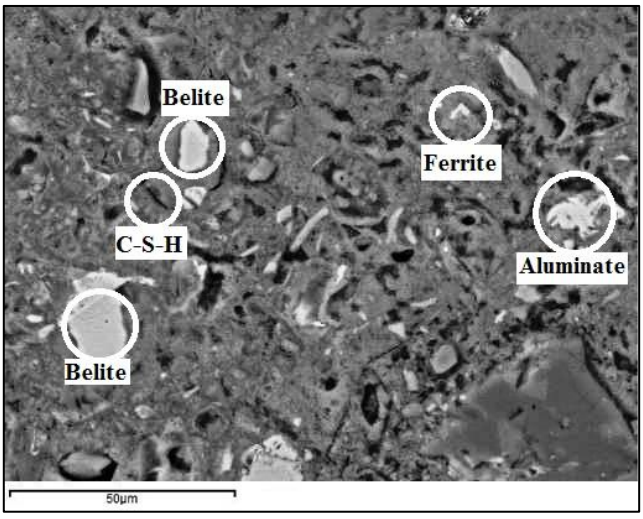

Figure 65: Phase identification using BSE and EDS analysis for PC (Control mix) at 28 days of curing.

BSE phase analysis of PCM

Figure 66 presents the BSE image of the different phases found in PCM at 28 days of curing. The unreacted MK particle was mainly identified using EDS analysis and had a width of approximately 21μm. The aluminate crystal was spherical in shape and had a diameter of approximately 3μm. Ferrites were triangular in shape and had widths of approximately 15μm. Well crystallised C-S-H had created long bands around other crystals. Belite had an irregular shaped crystal with a width of approximately 8μm. Curiously, there was a large crystal with smaller crystal growth inside it. EDS analysis revealed that these crystals had phases between that of belite and C-S-H. Figure 67 shows higher magnifications of this crystal. See Appendix J, Figure J3 and Tables J4 - J5 for the EDS results.

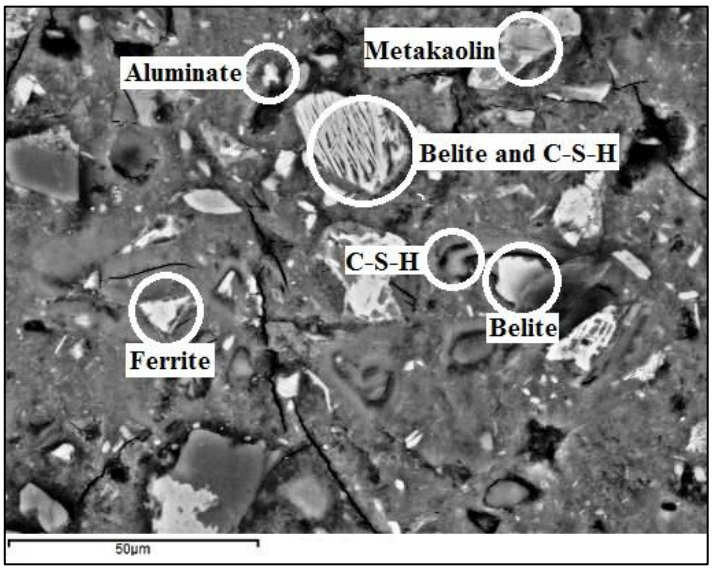

Figure 66: Phase identification using BSE and EDS analysis for PCM at 28 days of curing.

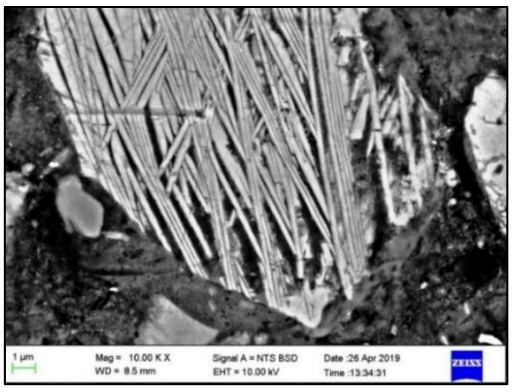

Figure 67: Crystal formation of belite and C-S-H at 10 000 times magnification.

BSE phase analysis of PCS

Figure 68 presents the BSE image of the different phases found in PCS at 28 days of curing. There was a small patch of CSF that seemed to have clumped into an elongated particle with a width of approximately 6μm. The belite crystal had a semi-spherical shape and a width of approximately 8μm. There were multiple patches of semi-crystallised C-S-H. The aluminates had a size of approximately 8μm. Similar crystal growth was found compared to Figure 66 (p.91), whereby a large crystal contained smaller crystals inside, but not as well defined. Cracks in the paste is believed to have been introduced during the preparation of the sample. See Appendix J, Figure J3 and Tables J6 - J7 for the EDS results.

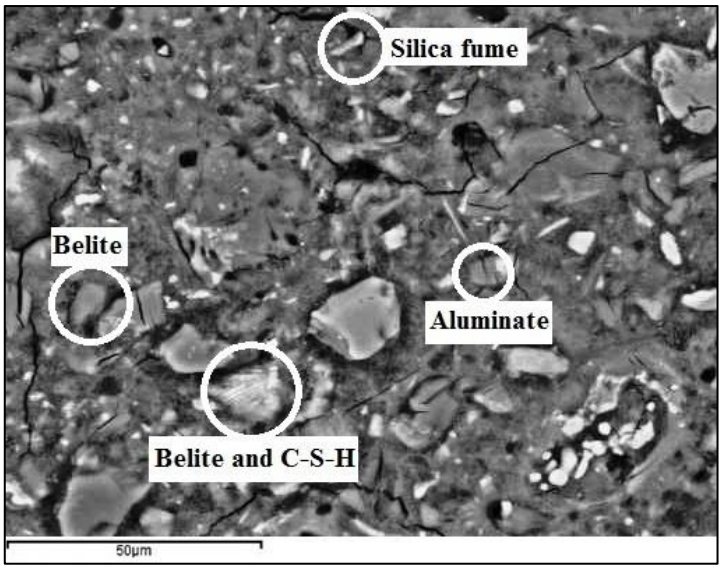

Figure 68: Phase identification using BSE and EDS analysis for PCS at 28 days of curing.

4.4.2.7 XRD phase analysis results for hardened concrete samples

XRD analysis was performed on the same samples used for the OPI tests. After the OPI tests were complete, the disks were cling-wrapped and stored. One day before the XRD test, the disks were crushed into smaller fragments. Pieces from the centre of the disk was collected and was further crushed into a powder using a mortar and pestle. Small amounts of potable water was added to lubricate the material and further grinding was continued. The material was placed in an oven maintained at a temperature ranging between $50°C \pm 2°C$ overnight. On the day of testing, these ground fragments were sieved through a 75μm sieve and collected in the pan below.

Results from the analysis performed on cement, MK and CSF in Section 3.2.3 (p.42), was used to evaluate and compare relevant intensities and angles. The intensity and angle of C-S-H was found using external sources by Arroudj *et al.*, (2015); Heikal *et al.*, (2004); and Hunnicutt (2013).

The above-mentioned intensities and positions were confirmed using the Diffrac.Eva software. The PDF's are available in Appendix I, Figures I5 - I10. The following sub-sections evaluates the results obtained from the XRD test performed on PC (Control mix), PCM and PCS.

XRD analysis for PC (Control mix) at 28 days of curing

Figure 69 presents the XRD results for PC (Control mix) at 28 days of curing. It is clear that alite had been consumed while small amounts of belite, aluminate and ferrite remained. This was the results of these mineral compounds hydrating much slower compared to alite and generally provides strength after 28 days of curing (Bensted and Barned, 2002 and Wild *et al.*, 1995). Furthermore, results showed that C-S-H had an intensity of approximately 2.9cps. The PDF's for PC (Control mix) are available in Appendix I, Figures I5 - I6.

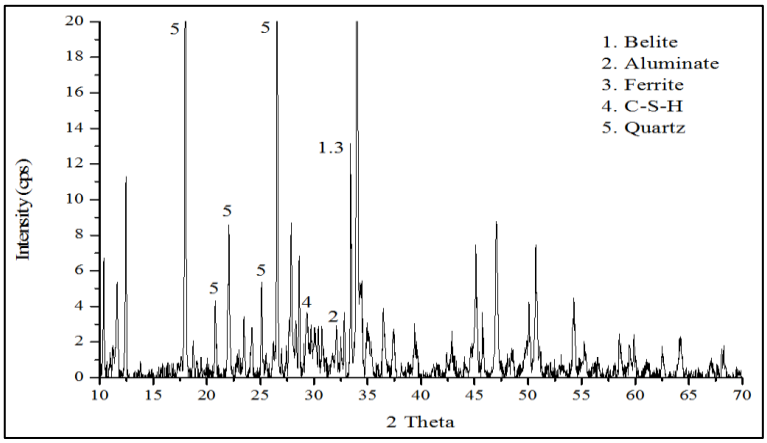

Figure 69: XRD result for PC (Control mix) tested at 28 days of curing.

XRD analysis for PCM at 28 days of curing

Figure 70 presents the XRD results for PCM at 28 days of curing. It is clear that MK was consumed during hydration as the intensity of C-S-H was much higher at 3.9cps, compared to PC (Control mix) which had 2.9cps.

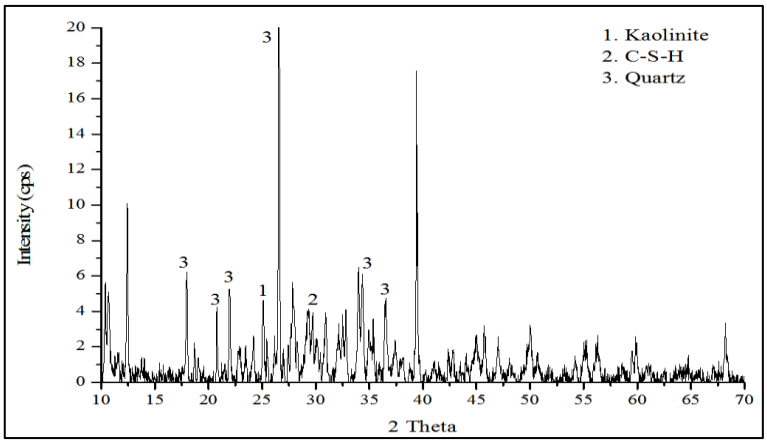

Figure 70: XRD result for PCM mix design tested at 28 days of curing.

Thus, there were more C-S-H crystals in PCM, compared to that of PC (Control mix). The PDF's for PCM are available in Appendix I, Figures I7 - I8.

XRD analysis for PCS at 28 days of curing

Figure 71 presents the XRD results for PCS at 28 days of curing. It was difficult to distinguish between the phases of quartz and CSF as they both contain silicon dioxide. However, it was clear that PCS had a slightly higher intensity of C-S-H at 3.1cps, compared to PC (Control mix) at 2.9cps. As the difference is not much higher, it can be suggested that CSF was not very reactive as little amount of secondary C-S-H were formed during hydration. The PDF's for PCS are available in Appendix I, Figures I9 - I10.

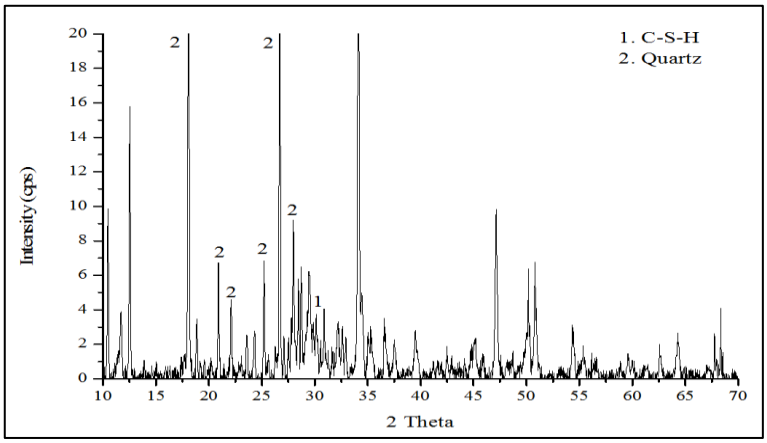

Figure 71: XRD result for PCS mix design tested at 28 days of curing.

4.4.2.8 Pore-size and distribution of concrete

The permeability of hardened concrete is a function of the interconnection of pores, pore sizes and distributions. Alternatively, porosity represents the fraction of material that is filled by voids. These voids or pores may be found in both the aggregate, mortar matrix and the ITZ (Richardson, 2002).

Concrete contains a wide range of different pore sizes, namely:

- Micro-pores or gel pores: These types of pores range in sizes of between 1nm - 100nm which are created during the hydration process. The sizes of these pores depend on the cement, paste age, w:b ratio and chemical properties of the C-S-H and the calcium hydroxide (Gong, 2006);

- Meso-pores or capillary pores: These pores range in sizes of between 0.1μm - 10μm and are caused by the heterogeneous component system with fine and coarse aggregates (*ibid*). These pores are the remanence of the originally water filled spaces in the concrete matrix which have not been filled with hydration gel (Bensted and Barnes, 2002); and

- Macro-pores: These pores range in sizes of between 10μm - 10 000μm and are commonly found in concretes with coarse aggregates (Gong, 2006).

Macro and meso-pores are commonly responsible for the decrease in strength and porosity of hardened concrete. An applied force of 70% or more of the concretes ultimate strength will cause these larger pores to experience excessive stress concentrations, resulting in localised strain. With an increase in the applied force, the mortar paste gradually cracks at these localisations, transferring the load to other regions within the concrete matrix. Cracks gradually spread and join around the ITZ which results in the ultimate failure of the concrete (Li, 2011).

The pore-size and distribution of hardened concrete can be measured using a technique called Mercury Intrusion Porosimetry (MIP). This test serves as a porosity index and connectivity index respectively (Ma, 2014). The process entails the removal of gasses from the porous material and then pushing mercury into the porous material by an externally applied pressure (Gong, 2013).

The pore-size and distribution of PC (Control mix), PCM and PCS were tested complimentary by Anton Paar by the use of MIP using a Quantachrome Poremaster. The mercury used had a surface tension of 480erg/cm², contact angle of 140° and a density of 13.5g/cm³. Table 22 presents a summary of the results for PC (Control mix), PCM and PCS tested at 28 days of curing.

Figures 72 - 73 represents the combined results for PC (Control mix), PCM and PCS tested at 28 days of curing.

Table 22: Summary for the pore-size and distribution test for PC, PCM and PCS.

	PC (Control mix)	PCM	PCS
Core weight (g)	30.293	29.902	29.090
Pressure range (PSIA)	3.736 - 57 204.094	4.674 - 59 765.184	4.200 - 49 132.797
Pore range (μm)	57.093 - 0.004	45.636 - 0.004	50.786 - 0.004

Figure 72 presents the volume of mercury intruded against the pore diameter. Here it can be seen that PC (Control mix) initially had a flat linear line until 5μm indicating little amounts of open pores above that size range were present in the concrete matrix. It then experienced a sudden increase between 5μm - 3μm, indicating that it contained some open pores ranging in that size. It continued to gradually increase between 3μm - 0.1μm, indicating more open pores became available in that size range for the mercury to flow into. It then experienced a rapid increase between 0.1μm - 0.08μm indicating vast amounts of open pores were found in that size range.

PCM initially had some macro-pores, however remained flat until 1μm, indicating very little amounts of open pores above that size range were present in the matrix. It then had a gradual increase in the amount of open pores available between 1μm - 0.06μm. There was a rapid increase between 0.06μm - 0.03μm, however these pore-sizes have very little impact on the strength of hardened concrete.

PCS remained very flat and linear until 1μm, indicating little amounts of open pores of that size range and above were present. However, it then experienced a rapid increase in the amount of open pores between 1μm – 0.1μm. Thereafter, it experienced a very rapid increase in the amount of open pores present in the size range of between 0.1μm – 0.03μm. This indicated that there were vast amounts of open pores in those size ranges.

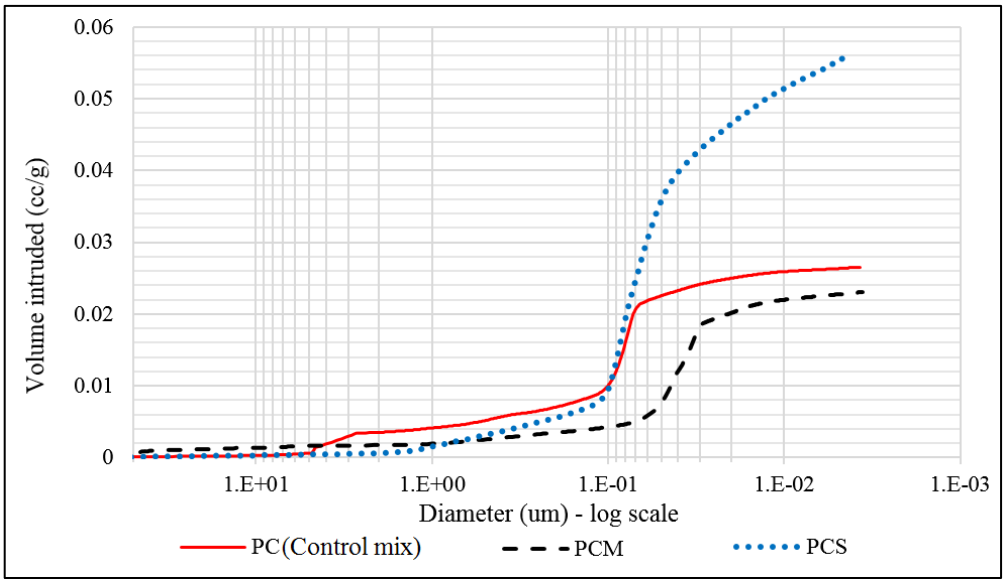

Figure 72: Volume mercury intruded against the pore diameter for PC (Control mix), PCM and PCS at 28 days of curing.

It is clear that PCM had the least amount of capillary pores, followed by PCS and PC (Control mix). This can also be seen from Figure 73 which represents the pore volume distribution over the pore diameter. Here it is clear that PC (Control mix) had the highest amount of open pores between 10μm - 1μm. PCS had the highest amount of open pores between 0.1μm - 0.05μm and PCM had the highest amount of open pores between 0.04μm - 0.03μm. The raw data for the MIP tests are available in Appendix L, Table L1.

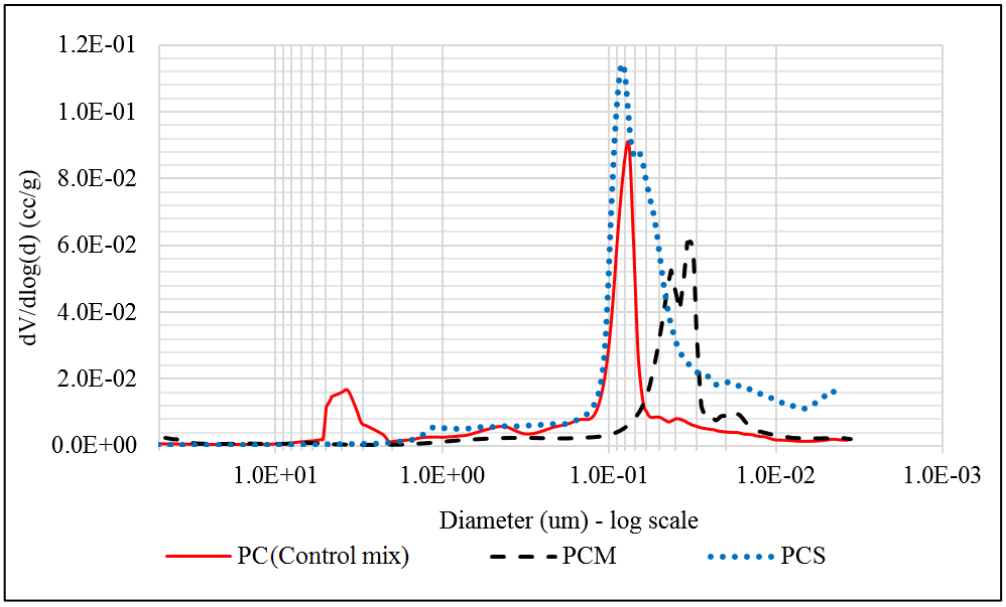

Figure 73: Pore volume distribution over pore diameter for PC (Control mix), PCM and PCS at 28 days of curing.

This chapter has provided the experimental details and procedures used. The following chapter discusses the results and analysis found in this study.

Chapter 5: Results and discussion

5.1 Introduction

This chapter presents the results and discussions found for the experimental work conducted and has been arranged into four sections and is presented in this order:

- Slump test results for concrete mixes made without and with 30% WEEP replacement for the natural aggregate;
- The compressive strength results for concrete mixed without and with 5%, 10%, 20% and 30% WEEP replacement for the natural aggregate by volume at 3, 7, 28 and 90 days of curing;
- The tensile splitting strength results for concrete mixed without WEEP and those mixed with 30% WEEP replacements for the natural aggregate at 28 days of curing. Moreover, this section evaluates the correlation (if any) between the average tensile splitting strength and the compressive strength for concrete mixed without WEEP and those with 30% WEEP ; and
- The durability results (OPI, water sorptivity and chloride conductivity) for concrete made without WEEP replacement and those with 30% WEEP replacement for the natural aggregate at 28 days of curing.

This chapter concentrates highly on concrete made using different types of WEEP replaced at 30%. This is due to the fact that 30% replacement of WEEP represents the percentage at which the most WEEP replaced the natural aggregate in this study and had thus the greatest influence on the concretes fresh and hardened properties.

5.2 Slump test for the fresh concrete

The following sub-sections evaluates and discusses the slump test results for concrete mixed without and with 30% replacement of WEEP for the natural aggregate in fresh concrete.

5.2.1 Slump test for the fresh concrete made without WEEP

Table 19 (p.66) and Figures 37, 38 and 40 (p.69 - 71) presents the slump test results for PC (Control mix), PCM, PCS. It was found that the slump of the fresh concrete was

reduced when replacing cement with 25% MK or 10% CSF by mass. The MK reduced the slump of the fresh concrete the most and required the greatest dosage of superplasticiser to attain the required slump range. This could be explained by the results found for the specific density of MK. From Table 8 (p.49) it can be seen that MK had a specific density of 2.5g/cm³ which was much less compared to cement which had a specific density of 3.6g/cm³. As cement replaced MK by mass, more MK was added by volume. This additional volume in turn increased the water demand and the slump. Furthermore, from Table 9 (p.50) it can be is seen that MK had a specific surface area of 7.7m²/g which was much compared to that of cement which had a surface area of 1.9m²/g. This additional surface area also contributed to the increase in water demand and reduction in slump. Similar results were found by Dhinakaran *et al.*, 2012; Guneyisi and Mermerda, 2007; and Siddique, 2008.

Only small quantities of superplasticiser was required to attain the required slump range for fresh concrete when replacing cement with 10% CSF as it did not readily affect the slump. This is in contrast to the results found when replacing cement with silica fume, found by Kadri *et al*., (2012) and Khedr and Abou-Zeid (1994). This is due to the fact that CSF could not effectively be broken down from its densified form during initial mixing. Moreover, because CSF had a lower density at 2.1g/cm³ compared to cement at 3.6g/cm³ as shown in Table 8 (p.49), replacing cement by mass resulted in more CSF being added by volume. This in turn slightly increased the water demand, and hence required only a small dose of superplasticiser to attain the required slump range.

5.2.2 Slump test for the fresh concrete made using WEEP as aggregate replacement material for the natural aggregate

Table 19 (p.66) and Figures 37, 38 and 40 (p.69 - 71) presents the slump test results for PC (Control mix), PCM, PCS and its replacements with 30% WEEP for the natural aggregate. It was found that the slump of concrete decreased with WEEP replacements. This is similar to results found by Kumar and Baskar (2015) and Manjunath (2016). This may be due to the fact that WEEP contained single sized aggregates, as shown in Figure 30 (p.57). Therefore, replacement of WEEP affected the particle size distribution by reducing the range of particle sizes and hence, became poorly-graded. Therefore, a superplasticiser was added to increase the slump. However, signs of overdosage occurred for concrete made using WEEP at low dosages of 0.12% - 0.64% by weight of the binder

material. This could be due to the interaction between the fresh cementitious paste and the WEEP aggregate.

From the typography images for the aggregates used, as shown in Figures 31 - 35 (p.60 - 62), it is clear that the surface of the natural aggregate was more rough compared to the granulated WEEP. Therefore, the fresh cementitious paste could not effectively adhere to the WEEP aggregates. This in turn may have reduced the recommended maximum dosage of the superplasticiser. This overdosage can explain the bleed water found at the bottom of the slump for concrete made using WEEP, as shown in Figures 37, 38 and 40 (p.69 - 71). This overdosage resulted in the accumulation of water around the WEEP aggregate, which in turn created crystal formations of calcium and silicon between ABS WEEP and the hcp, as shown in Figures 54 (p.82), 58 (p.84) and 62 (p.87).

5.3 Strength of hardened concrete

This section discusses the compressive and tensile splitting strength of hardened concrete made without WEEP and with WEEP replacement for the natural aggregate. In addition, it also addresses some of the mechanisms behind the respective results obtained by linking them to results found in previous chapters.

5.3.1 Compressive strength results of concrete mixes

Table 23 represents the average cube compressive strength (fcu ave) in MPa, standard deviation (S.D) and coefficient of variance (CoV). The average compressive strengths indicate that most concrete mixes made with WEEP replacement for the natural aggregate had a reduced compressive strength, compared to concrete made without. Some cases arose whereby 5% and 10% WEEP replacements had a slight increase in its average compressive strength, compared to its respective mix made without WEEP. However, these marginal strength gains could be contributed by the increase in superplasticiser, as shown in Table 19 (p.66). It was also found that PCM performed the overall best, yielding higher average compressive strengths compared to PC (Control mix) and PCS. The variability measured by the CoV indicated good consistency for the majority of the concrete mixes indicating that the samples were well prepared. The individual compressive strength results are available in Appendix C, Table C1.

Table 23: Average compressive strength, SD, CoV and confidence interval results of the various concrete mix designs at different ages of curing.

Concrete mix label	3 Day results				7 Day results				28 Day results				90 Day results			
	fcu (Ave) (MPa)	S.D*	CoV (%)	Confidence interval	fcu (Ave)	S.D	CoV (%)	Confidence interval	fcu (Ave)	S.D	CoV (%)	Confidence interval	fcu (Ave)	S.D	CoV (%)	Confidence interval
PC (Control mix)	37.5	0.8	2.2	2.1	46.4	0.4	0.9	1.0	57.6	1.0	1.7	2.4	60.1	1.8	3.0	4.4
PC(ABS-5)	35.2	2.4	6.9	6.0	42.6	1.4	3.2	3.4	49.6	0.4	0.8	1.0	53.3	1.2	2.2	2.9
PC(ABS-10)	31.5	0.9	2.8	2.2	37.8	0.6	1.7	1.6	44.2	1.1	2.6	2.8	49.2	1.7	3.4	4.2
PC(ABS-20)	28.8	0.5	1.9	1.4	34.0	0.6	1.7	1.4	38.1	0.8	2.1	2.0	42.1	0.5	1.1	1.2
PC(ABS-30)	19.1	0.3	1.6	0.8	22.1	1.4	6.3	3.5	25.1	1.4	5.7	3.6	27.0	1.6	6.1	4.1
PC(PC/ABS-5)	37.4	1.2	3.2	3.0	43.5	1.1	2.5	2.7	50.4	1.1	2.2	2.7	53.1	0.8	1.4	1.9
PC(PC/ABS-10)	36.3	0.4	1.1	1.0	40.7	0.6	1.6	1.6	46.5	0.5	1.1	1.3	46.6	0.3	0.6	0.6
PC(PC/ABS-20)	34.2	0.5	1.5	1.2	37.5	2.2	5.8	5.4	41.6	0.7	1.8	1.8	43.8	1.5	3.5	3.8
PC(PC/ABS-30)	33.2	2.2	6.6	5.4	36.4	1.5	4.2	3.8	40.5	1.6	3.8	3.9	40.9	1.0	2.5	2.5
PC(HIPS-5)	37.0	0.9	2.5	2.3	42.2	2.5	5.9	6.2	50.5	0.9	1.8	2.2	51.1	0.5	1.0	1.2
PC(HIPS-10)	34.0	0.2	0.5	0.4	39.5	0.4	0.9	0.9	46.1	0.1	0.2	0.3	46.7	1.4	3.1	3.5
PC(HIPS-20)	32.3	0.7	2.2	1.8	35.5	0.7	1.8	1.6	39.8	1.7	4.3	4.2	41.1	0.7	1.8	1.8
PC(HIPS-30)	34.0	0.7	2.0	1.7	38.5	1.9	4.9	4.7	39.5	0.8	2.1	2.1	40.7	1.9	4.7	4.7
PC(Blend-5)	37.1	0.1	0.3	0.2	42.9	0.6	1.5	1.6	49.4	1.0	1.9	2.4	53.3	1.4	2.6	3.4
PC(Blend-10)	34.9	0.9	2.5	2.1	41.4	0.4	1.0	1.0	46.5	0.6	1.4	1.6	49.9	1.2	2.4	3.0
PC(Blend-20)	31.3	0.3	0.9	0.7	36.8	0.7	1.9	1.8	42.0	0.9	2.1	2.2	42.5	0.4	1.0	1.1
PC(Blend-30)	31.6	0.5	1.6	1.2	34.9	1.6	4.5	3.9	37.5	1.2	3.1	2.9	37.5	1.9	5.1	4.7
PCM	41.2	0.6	1.4	1.5	59.3	0.4	0.8	1.1	70.2	1.3	1.9	3.3	73.5	0.6	0.8	1.5
PCM(ABS-5)	39.5	0.7	1.7	1.7	54.0	0.8	1.4	1.9	63.3	1.4	2.3	3.6	65.2	1.5	2.4	3.8
PCM(ABS-10)	33.0	1.7	5.2	4.2	46.4	1.6	3.5	4.1	52.4	1.0	2.0	2.6	54.8	1.5	2.8	3.8
PCM(ABS-20)	28.2	0.6	2.0	1.4	34.1	0.5	1.5	2.8	41.3	0.2	0.5	0.5	43.4	1.3	3.1	3.3
PCM(ABS-30)	26.8	0.3	1.0	0.6	23.0	0.8	3.3	1.8	38.8	0.8	2.2	2.1	40.9	3.0	7.4	7.5
PCM(PC/ABS-5)	40.2	0.8	2.0	2.0	50.8	1.6	3.1	3.9	60.0	1.4	2.4	3.6	62.1	0.7	1.2	1.8
PCM(PC/ABS-10)	41.7	0.7	1.8	1.9	52.1	1.6	3.0	3.9	61.0	1.7	2.7	3.6	61.8	3.3	5.4	1.8
PCM(PC/ABS-20)	37.5	0.7	2.0	1.9	46.7	1.2	2.5	3.9	53.1	0.5	1.0	4.2	54.6	0.5	1.0	8.2

Concrete mix label	3 Day results				7 Day results				28 Day results				90 Day results			
	fcu (Ave) (MPa)	S.D*	CoV (%)	Confidence interval	fcu (Ave) (MPa)	S.D	CoV (%)	Confidence interval	fcu (Ave) (MPa)	S.D	CoV (%)	Confidence interval	fcu (Ave) (MPa)	S.D	CoV (%)	Confidence interval
PCM(PC/ABS-30)	36.3	1.1	3.1	2.8	44.5	0.7	1.6	1.7	49.1	1.3	2.6	3.2	50.9	2.0	3.9	4.9
PCM(HIPS-5)	41.0	0.1	0.2	0.2	56.4	1.1	1.9	2.6	62.6	1.4	2.3	3.5	57.2	0.4	0.8	1.1
PCM(HIPS-10)	35.2	0.7	2.0	1.7	49.1	0.9	1.8	2.2	56.0	0.4	0.7	1.0	56.4	2.3	4.1	5.7
PCM(HIPS-20)	35.2	1.6	4.5	3.9	47.6	1.4	2.9	3.4	52.7	0.5	1.0	1.3	53.3	2.1	4.0	5.2
PCM(HIPS-30)	38.7	0.8	2.0	1.9	45.8	1.4	3.0	3.4	49.0	1.3	2.7	3.3	50.8	1.3	2.5	3.2
PCM(Blend-5)	41.0	0.4	1.1	1.1	56.9	0.5	0.9	1.3	66.1	1.5	2.3	3.7	69.8	1.4	1.9	3.4
PCM(Blend-10)	42.1	0.3	0.7	0.7	54.5	3.1	5.6	7.6	61.7	1.0	1.6	2.5	63.6	1.8	2.8	4.5
PCM(Blend-20)	36.4	0.5	1.4	1.3	45.4	1.4	3.0	3.4	50.3	2.3	4.7	5.8	51.0	0.5	1.0	1.2
PCM(Blend-30)	34.2	1.4	4.2	3.5	43.7	2.0	4.6	5.0	47.5	1.9	4.1	4.8	47.4	1.0	2.2	2.6
PCS	36.7	1.9	5.2	4.8	47.6	0.2	0.5	0.6	59.5	0.6	1.0	1.5	63.7	2.3	3.5	5.6
PCS(ABS-5)	30.7	0.8	2.6	2.0	39.3	0.3	0.7	0.7	52.8	0.7	1.4	1.8	57.1	2.4	4.2	5.9
PCS(ABS-10)	28.4	0.4	1.5	1.1	37.2	0.5	1.3	1.2	48.1	0.2	0.5	0.6	51.4	0.3	0.6	0.8
PCS(ABS-20)	25.3	0.4	1.4	0.9	26.1	0.5	2.0	1.3	40.2	1.0	2.4	2.4	42.1	0.8	1.8	1.9
PCS(ABS-30)	17.3	0.4	2.2	0.9	23.0	0.8	3.3	1.9	32.0	1.2	3.8	3.0	33.0	0.7	2.1	1.7
PCS(PC/ABS-5)	31.9	0.6	1.9	1.5	40.0	0.8	2.0	2.0	54.8	1.2	2.1	2.9	55.8	2.1	3.8	5.2
PCS(PC/ABS-10)	34.2	0.6	1.8	1.5	43.9	0.0	0.0	0.0	55.5	0.9	1.6	2.2	56.4	1.2	2.1	2.9
PCS(PC/ABS-20)	31.2	0.8	2.6	2.0	39.7	0.8	2.0	1.9	46.6	2.3	5.0	5.7	48.3	1.9	4.0	4.8
PCS(PC/ABS-30)	27.3	1.0	3.7	2.5	37.1	0.3	0.9	0.8	40.0	0.5	1.3	1.2	42.1	5.4	12.9	13.5
PCS(HIPS-5)	34.3	0.3	0.9	0.8	42.8	0.8	1.9	2.0	52.8	1.9	3.5	4.6	56.5	0.3	0.5	0.7
PCS(HIPS-10)	32.7	1.0	3.0	2.5	43.6	0.2	0.6	0.6	52.5	3.4	6.5	8.5	54.7	0.3	0.5	0.7
PCS(HIPS-20)	29.5	0.6	2.2	1.6	37.1	0.8	2.2	2.0	46.4	0.6	1.2	1.4	46.4	1.0	2.1	2.4
PCS(HIPS-30)	28.6	0.7	2.6	1.8	38.5	1.1	2.8	2.6	41.7	0.9	2.1	2.2	43.0	0.7	1.7	1.9
PCS(Blend-5)	33.5	0.9	2.7	2.2	41.3	0.7	1.6	1.7	52.6	0.5	0.9	1.1	56.4	1.9	3.4	4.7
PCS(Blend-10)	33.4	0.3	0.8	0.7	40.3	0.2	0.5	0.5	49.9	0.3	0.5	0.7	53.1	0.8	1.5	2.0
PCS(Blend-20)	31.2	0.3	1.0	0.8	37.3	0.1	0.3	0.3	43.9	0.9	2.1	2.3	46.4	2.5	5.4	6.2
PCS(Blend-30)	27.7	0.3	1.0	0.7	32.7	0.4	1.1	0.9	38.6	2.0	5.1	4.9	40.3	0.9	2.3	2.3

*Standard deviation

The following sub-sections analyses the results found in Table 23. It compared the average compressive strengths of PC (Control mix), PCM and PCS mixed without WEEP to PC (Control mix), PCM and PCS mixed with ABS, PC/ABS, HIPS and Blend WEEP respectively at 3, 7, 28 and 90 days of curing.

The use of inferential error bars were used to display the confidence interval of 95% in a data set. The confidence interval of 95% provides a range around the mean where 95% of the values may occur if these test were to be performed multiple times. These error bars therefore indicate whether a given result was statistically significant or uncertain compared to another result.

For example, if two results had overlapping error bars then one could not confidently state that these results were different from one another as they may have over lapping results when tested multiple times. However, when comparing the results from two non-overlapping error bars one can confidently state that the results were statistically significant as these results would have no overlapping results. Moreover, a very long error bar indicates that the data is highly variable and less reliable. See Table 23 (p.102) for the confidence intervals for all the mixes and Appendix F, Equation F.21 for the equation used to calculate the range of the error bars.

5.3.1.1 Compressive strength for concrete made using ABS WEEP

Figures 74 - 77 compares the average compressive strengths of PC (Control mix), PCM and PCS at different ages of curing and percentage replacement levels with ABS WEEP for the natural aggregate. The average compressive strength results clearly show that concrete containing no ABS WEEP substitution had higher average compressive strengths, compared to when it was replaced by ABS WEEP for the natural aggregate.

The average compressive strengths of the mixtures containing ABS WEEP were observed to decrease as the percentage substitution increased.

The mixtures containing 30% ABS WEEP had average compressive strengths in the following order at 28 days of curing:

PCM > PCS > PC (Control mix) > PCM(ABS-30) > PCS(ABS-30) > PC(ABS-30).

i.e. (70.2 > 59.5 > 57.6 > 38.8 > 32.0 > 25.1)MPa.

Here it is clear that mixtures containing MK and CSF as replacement for cement increased the average compressive strength of both concrete mixed with and without ABS WEEP.

At 90 days of curing, the mixtures containing 30% ABS WEEP had a very marginal increase in its average compressive strength over that obtained at 28 days of curing in the following order:

PCM > PCS > PC (Control mix) > PCM(ABS-30) > PCS(ABS-30) > PC(ABS-30).

i.e. (73.5 > 63.7 > 60.1 > 40.9 > 33.0 > 27.0)MPa.

Another important observation is that even at 30% substitution with ABS WEEP, the average compressive strengths obtained were above 25MPa which is the minimum requirement for structural concrete based on its compressive strength.

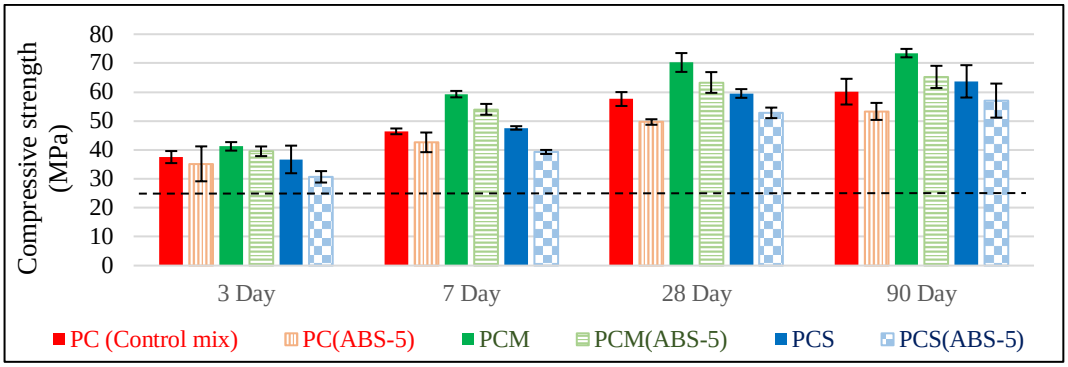

Figure 74: Compressive strength of 5% replacement for ABS in PC(Control), PCM and PCS.

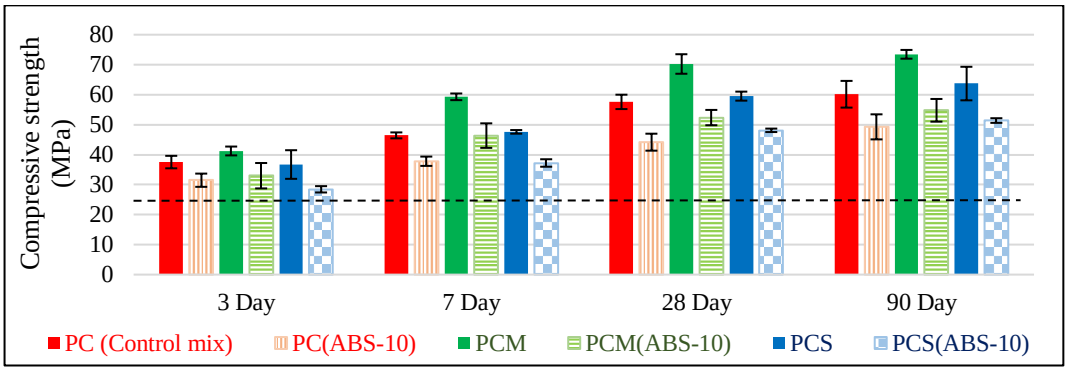

Figure 75: Compressive strength of 10% replacement for ABS in PC (Control), PCM and PCS.

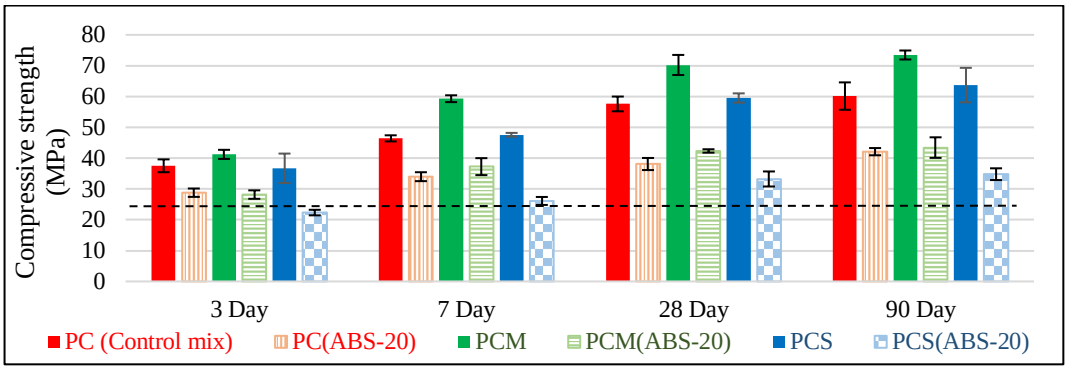

Figure 76: Compressive strength of 20% replacement for ABS in PC (Control), PCM and PCS.

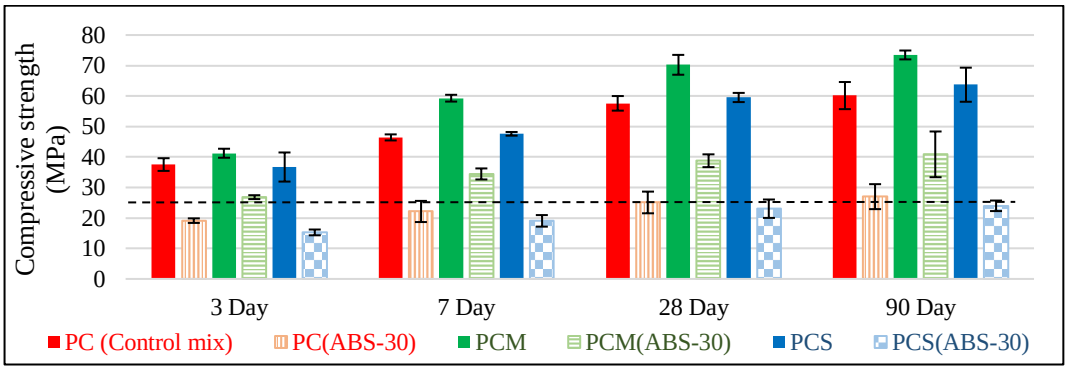

Figure 77: Compressive strength of 30% replacement for ABS in PC (Control), PCM and PCS.

5.3.1.2 Compressive strength for concrete made using PC/ABS WEEP

Figures 78 - 81 compares the average compressive strengths of PC (Control mix), PCM and PCS at different ages of curing and percentage replacement levels with PC/ABS WEEP for the natural aggregate.

Similar trends of average compressive strength reduction was found for PC/ABS WEEP, compared to ABS WEEP replacements. However, replacements with 30% PC/ABS WEEP had a much lower average compressive strength reduction in concrete compared to replacements of 30% ABS WEEP.

At 28 days of curing, the mixtures containing 30% PC/ABS WEEP had average compressive strengths in the following order:

PCM > PCS > PC (Control mix) > PCM(PC/ABS-30) > PC(PC/ABS-30) > PCS(PC/ABS-30).

i.e. (70.2 > 59.5 > 57.6 > 49.1 > 40.5 > 40.0)MPa.

Here it is seen that PC(PC/ABS-30) and PCS(PC/ABS-30) had nearly identical average compressive strengths. This indicates that replacements of CSF for cement had little effect on the 28 day compressive strength.

At 90 days of curing, the mixtures containing 30% PC/ABS WEEP had a very marginal increase in its average compressive strength over that obtained at 28 days of curing, in the following order:

PCM > PCS > PC (Control mix) > PCM(PC/ABS-30) > PCS(PC/ABS-30) > PC(PC/ABS-30).

i.e. (73.5 > 63.7 > 60.1 > 50.9 > 42.1 > 40.9)MPa.

Here it is seen that PCS(PC/ABS-30) attained a higher average compressive strength compared to PC(PC/ABS-30). This indicates that replacements of CSF for cement did indeed increase the average compressive strength of concrete, but at a later day, i.e. 90 days of curing. It is also seen that concrete made with 30% PC/ABS WEEP attained the minimum strength requirements of > 25MPa for structural concrete based on its compressive strength.

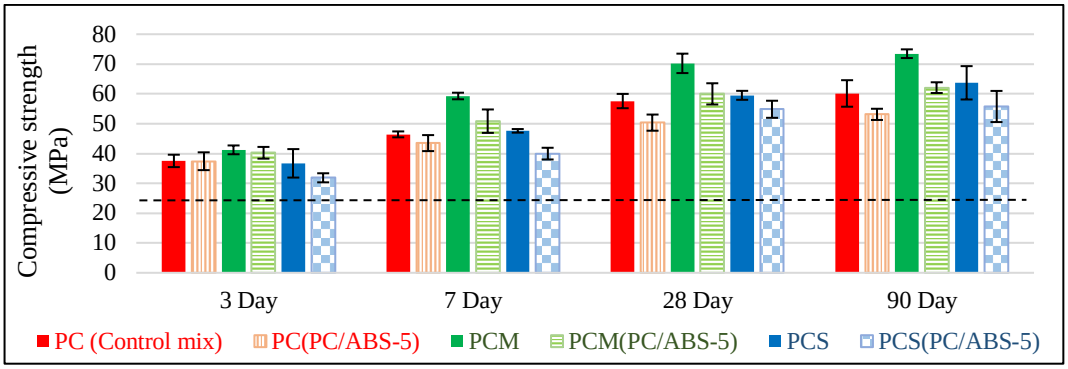

Figure 78: Compressive strength of 5% replacement for PC/ABS in PC (Control), PCM and PCS.

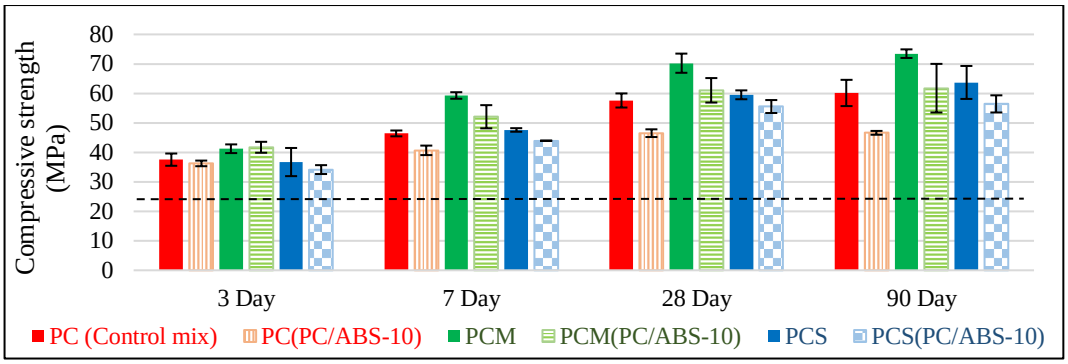

Figure 79: Compressive strength of 10% replacement for PC/ABS in PC (Control), PCM and PCS.

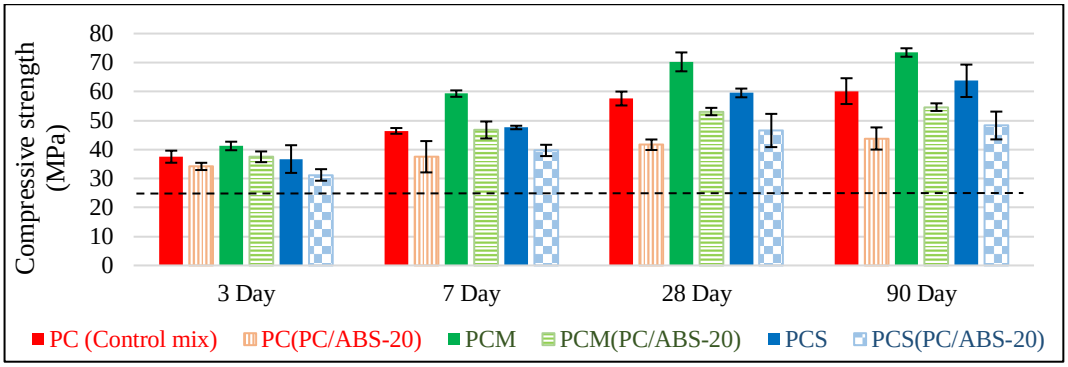

Figure 80: Compressive strength of 20% replacement for PC/ABS in PC (Control), PCM and PCS.

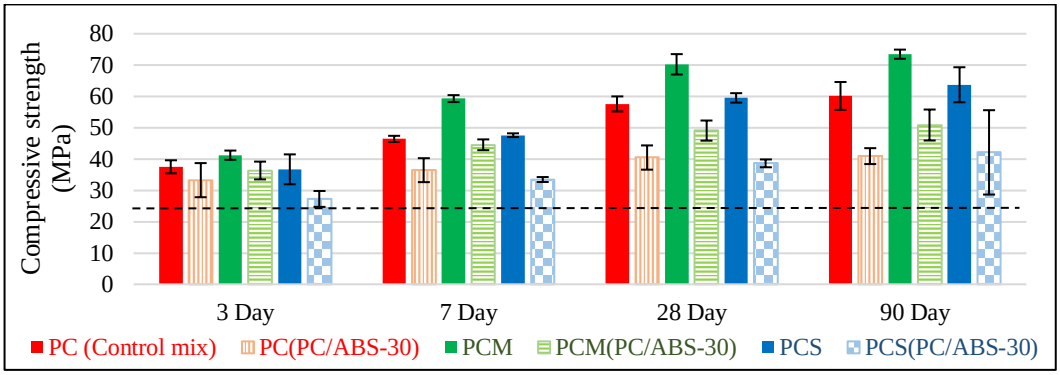

Figure 81: Compressive strength of 30% replacement for PC/ABS in PC (Control), PCM and PCS.

5.3.1.3 Compressive strength for concrete made using HIPS WEEP

Figures 82 - 85 compares the average compressive strengths of PC (Control mix), PCM and PCS at different ages of curing and percentage replacement levels with HIPS WEEP for the natural aggregate.

Replacements of 30% HIPS WEEP yielded a similar average compressive strength reduction pattern, compared to replacements of 30% PC/ABS WEEP. At 28 days of curing, mixtures containing 30% HIPS WEEP had average compressive strengths in the following order:

PCM > PCS > PC (Control mix) > PCM(HIPS-30) > PCS(HIPS-30) > PC(HIPS-30).

i.e. (70.2 > 59.5 > 57.6 > 49.0 > 41.7 > 39.5)MPa.

Here it is seen that replacements of MK and CSF for cement increased the average compressive strengths of both concrete mixed with and without WEEP. It is also seen that replacements with HIPS WEEP yielded a similar 28 day compressive strength compared to replacements with PC/ABS WEEP.

At 90 days of curing, mixtures containing 30% PC/ABS WEEP had a slight increase in its average compressive strength compared to concrete tested at 28 days, in the following order:

PCM > PCS > PC (Control mix) > PCM(HIPS-30) > PCS(HIPS-30) > PC(HIPS-30).

i.e. (73.5 > 63.7 > 60.1 > 50.8 > 43.0 > 40.7)MPa.

From the above-mentioned results, it is clear that 30% substitution of WEEP attained the minimum strength requirements of > 25MPa for structural concrete based on its compressive strength.

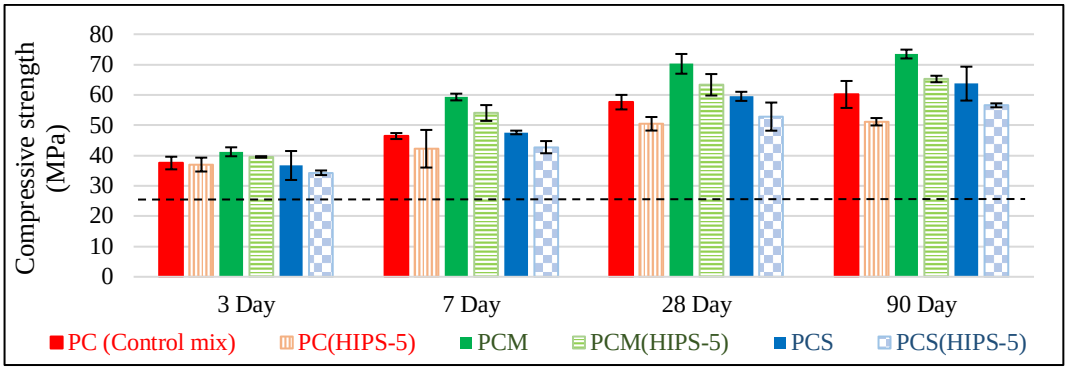

Figure 82: Compressive strength of 5% replacement for HIPS in PC (Control), PCM and PCS.

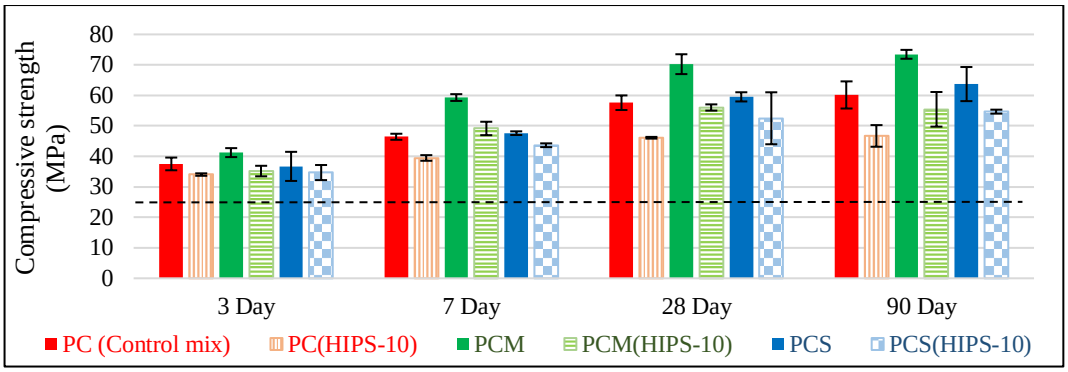

Figure 83: Compressive strength of 10% replacement for HIPS in PC (Control), PCM and PCS.

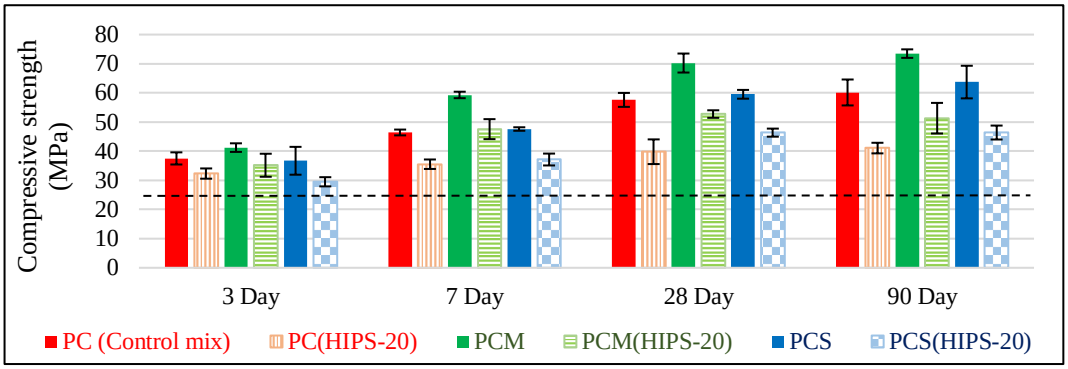

Figure 84: Compressive strength of 20% replacement for HIPS in PC (Control), PCM and PCS.

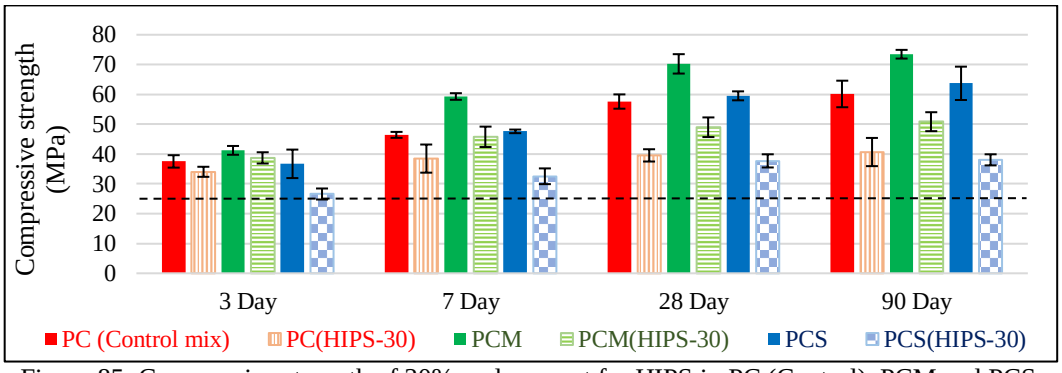

Figure 85: Compressive strength of 30% replacement for HIPS in PC (Control), PCM and PCS.

5.3.1.4 Compressive strength for concrete made using Blend WEEP

Figures 86 - 89 compares the average compressive strengths of PC (Control mix), PCM and PCS at different ages of curing and percentage replacement levels with Blend WEEP for the natural aggregate. Replacements of 30% Blend WEEP yielded a higher average compressive strength reduction compared to PC/ABS or HIPS WEEP replacement, but was higher compared to ABS WEEP replacement.

At 28 days of curing, the mixtures containing 30% Blend WEEP had average compressive strengths in the following order:

PCM > PCS > PC (Control mix) > PCM(Blend-30) > PCS(Blend-30) > PC(Blend-30).

i.e. (70.2 > 59.5 > 57.6 > 47.5 > 38.6 > 37.5)MPa.

Here it is seen that PCS(Blend-30) and PC(Blend-30) had very little differences in their average compressive strengths.

At 90 days of curing, the mixtures containing 30% PC/ABS WEEP had a very marginal increase in their average compressive strengths over that obtained at 28 days of curing, in the following order:

PCM > PCS > PC (Control mix) > PCM(Blend-30) > PCS(Blend-30) > PC(Blend-30).

i.e. (73.5 > 63.7 > 60.1 > 47.4 > 40.3 > 37.5)MPa.

Here it is clear that PCS(Blend-30) attained a later day strength as the gap in the average compressive strength between itself and PC(Blend-30) widened. It was also noted that there was no difference between the average 28 and 90 day compressive strength for PC(Blend-30).

All mixes attained an average compressive strength > 25MPa which is the minimum strength requirement for structural concrete based on its compressive strength.

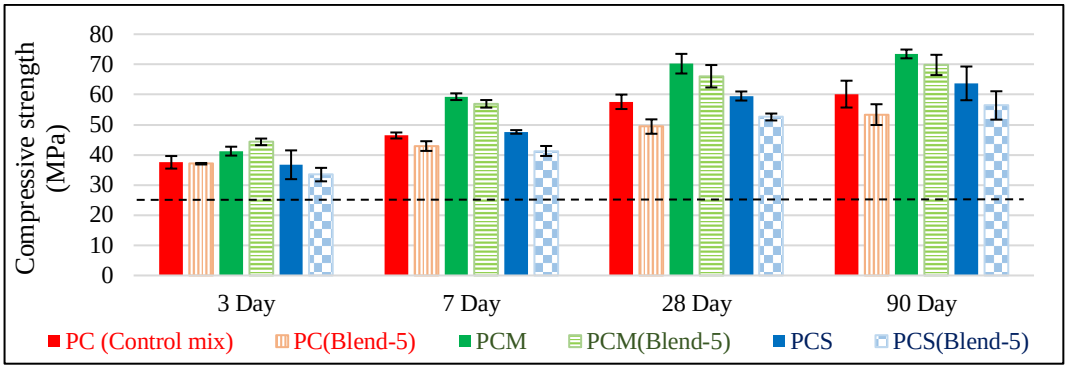

Figure 86: Compressive strength of 5% replacement for Blend in PC (Control), PCM and PCS.

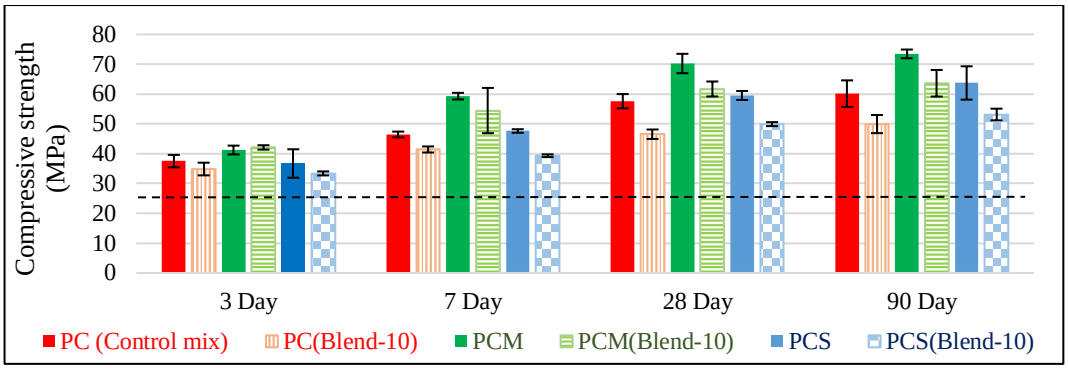

Figure 87: Compressive strength of 10% replacement for Blend in PC (Control), PCM and PCS.

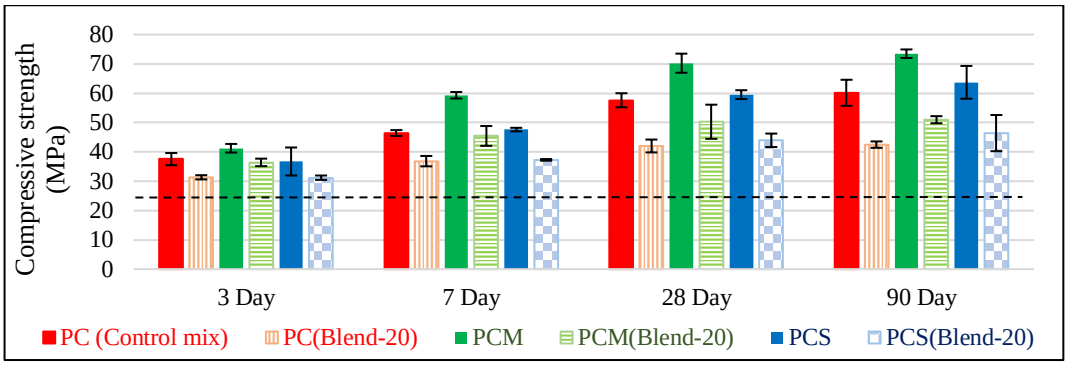

Figure 88: Compressive strength of 20% replacement for Blend in PC (Control), PCM and PCS.

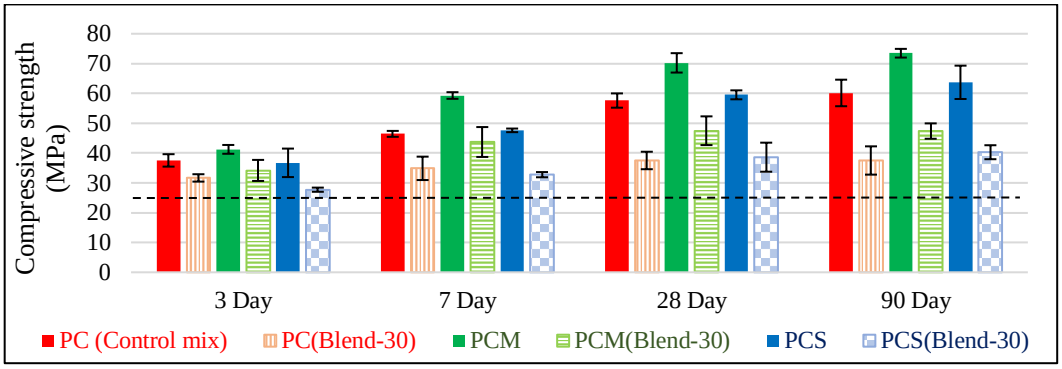

Figure 89: Compressive strength of 30% replacement for Blend in PC (Control), PCM and PCS.

The following sub-sections evaluates the average compressive strengths of PC (Control mix), PCM and PCS with the substitution of different types of WEEP at different percentage replacements for the natural aggregate.

5.3.1.5 Compressive strength for PC (Control mix) replaced with WEEP

Figures 91 - 94 compares the average compressive strengths of PC (Control mix) at different ages of curing, types of WEEP and percentage replacement levels. The average compressive strength results showed that PC (Control mix) containing no WEEP substitution had the highest strength at all ages of curing.

The compressive strength of the mixtures containing WEEP were observed to decrease as the percentage of substitution increased. Furthermore, it is interesting to note that there was little difference in the compressive strength of concrete made with WEEP at 20% replacement. However, there was a large drop in strength for concrete made using ABS WEEP at 30% replacement.

At 28 days of curing, the mixtures containing 30% WEEP had average compressive strengths in the following order:

PC (Control mix) > PC(PC/ABS-30) > PC(HIPS-30) > PC(Blend-30) > PC(ABS-30).

i.e. (57.6 > 40.5 > 39.5 > 37.5 > 25.1)MPa.

Here it is seen that replacements of ABS WEEP significantly reduced the compressive strength of PC (Control mix) by 56.4%, Blend WEEP by 34.9%, HIPS WEEP by 31.3% and PC/ABS WEEP by 29.7%.

At 90 days of curing, the mixtures containing 30% WEEP had a very marginal increase in average compressive strength over that obtained at 28 days of curing, in the following order:

PC (Control mix) > PC(PC/ABS-30) > PC(HIPS-30) > PC(Blend-30) > PC(ABS-30).

i.e. (60.1 > 40.9 > 40.7 > 37.5 > 27.0)MPa.

It is clear that there was no difference in the average compressive strengths for concrete made with PC(Blend-30) compared to 28 days of curing.

Furthermore, it was found that replacements of 30% ABS WEEP continued to significantly reduce the compressive strength of PC (Control mix) by 55.1%, Blend WEEP by 37.7%, HIPS WEEP by 32.4% and PC/ABS WEEP by 32.0%.

All mixes made with WEEP substitution for the natural aggregate and without MK or CSF replacement for cement attained a compressive strength > 25MPa which is the minimum requirement for structural concrete based on its compressive strength.

Figure 90 presents the typical correlations between PC and its ABS WEEP replacements at different ages and substitution percentages. It is clear that there was a strong negative linear relationship between PC (Control mix) and its percentage ABS WEEP replacements as its correlation coefficient (R^2) was very close to 1 at different ages of curing. Therefore, the compressive strength of concrete made with WEEP decreased with an increase in ABS WEEP replacement for all ages. See Appendix D, Figures D1 - D12 for the correlations between PC, PCM, PCS and its WEEP replacements.

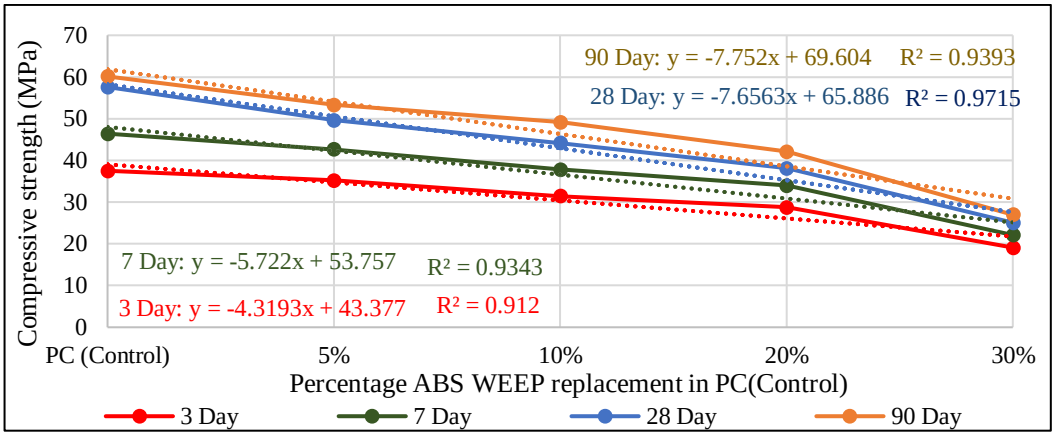

Figure 90: Correlation between PC (Control) and ABS WEEP at different ages of curing.

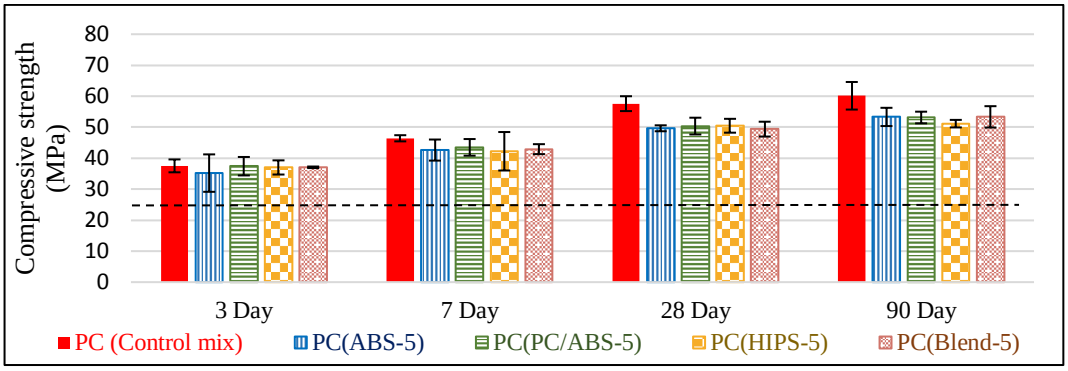

Figure 91: Compressive strength for PC (Control) with and without 5% WEEP replacement.

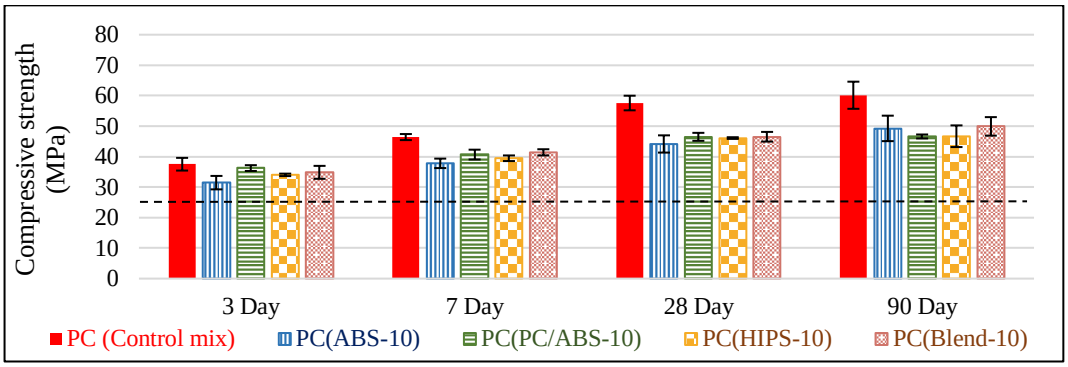

Figure 92: Compressive strength for PC (Control) with and without 10% WEEP replacement.

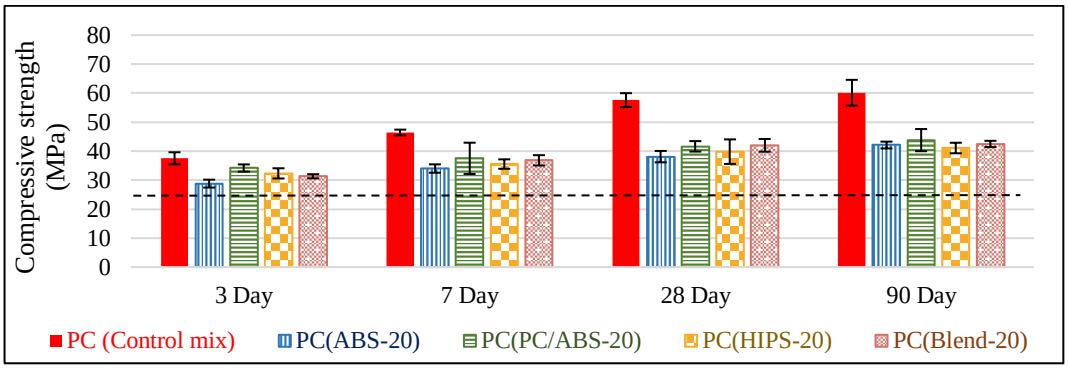

Figure 93: Compressive strength for PC (Control) with and without 20% WEEP replacement.

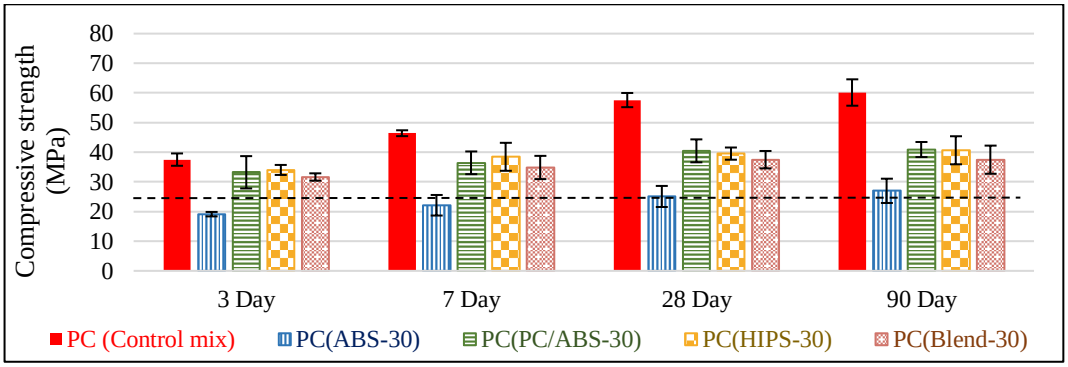

Figure 94: Compressive strength for PC (Control) with and without 30% WEEP replacement.

5.3.1.6 Compressive strength for PCM replaced with WEEP

Figures 95 - 98 compares the average compressive strengths of PCM at different ages of curing, types of WEEP and percentage replacement levels. The average compressive strength results clearly showed that PCM containing no WEEP substitution for the natural aggregate had the highest average compressive strength at all ages of curing.

It is clear that the average compressive strength of concrete decreased as the percentage of WEEP replacement increased. It was noted that although ABS WEEP reduced the average compressive strength of concrete mixed with WEEP the most, it had a smaller overall decrease in the average compressive strength for PCM, compared to PC (Control mix).

At 28 days of curing, the mixtures containing 30% WEEP had average compressive strengths in the following order:

PCM > PCM(PC/ABS-30) > PCM(HIPS-30) > PCM(Blend-30) > PCM(ABS-30).

i.e. (70.0 > 49.1 > 49.0 > 47.5 > 38.8)MPa.

Here it can be seen that replacement of ABS WEEP significantly decreased the average compressive strength of PCM by 44.8%, Blend WEEP by 32.4%, HIPS WEEP by 30.3% and PC/ABS WEEP at 30.1%. Here it can also be seen that replacements of PC/ABS and HIPS WEEP had very little difference in its average compressive strength.

At 90 days of curing, the mixtures containing 30% WEEP had a very marginal increase in the average compressive strength over that obtained at 28 days of curing, in the following order:

PCM > PCM(PC/ABS-30) > PCM(HIPS-30) > PCM(Blend-30) > PCM(ABS-30).

i.e. (73.5 > 50.9 > 50.8 > 47.4 > 40.9)MPa.

Here it can be seen that replacement of ABS WEEP significantly decreased the average compressive strength of PCM by 44.8% (identical to 28 days of curing), Blend WEEP by 35.5%, HIPS WEEP by 30.8 % and identically PC/ABS WEEP by 30.8%. All mixes made with WEEP substitution for the natural aggregate and made with MK replacement for cement attained structural strength > 25MPa.

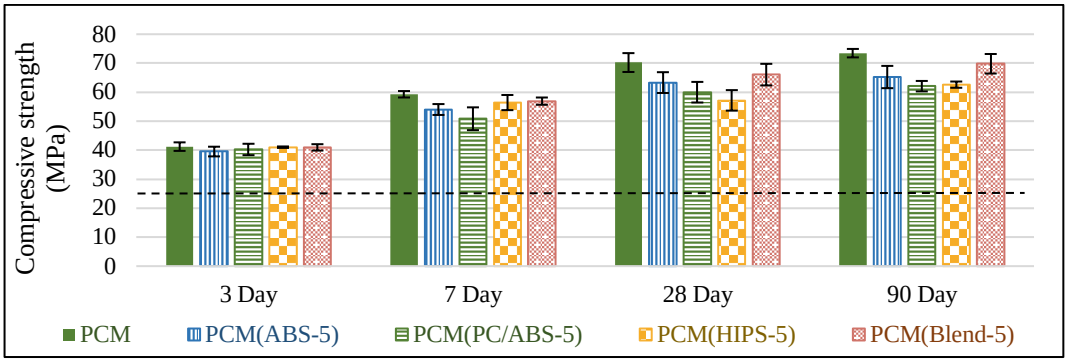

Figure 95: Compressive strength for PCM mix with and without 5% WEEP replacement.

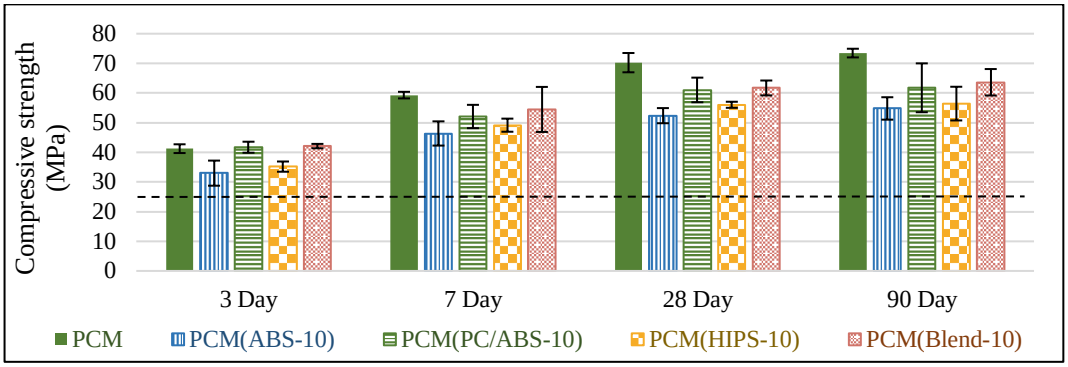

Figure 96: Compressive strength for PCM mix with and without 10% WEEP replacement.

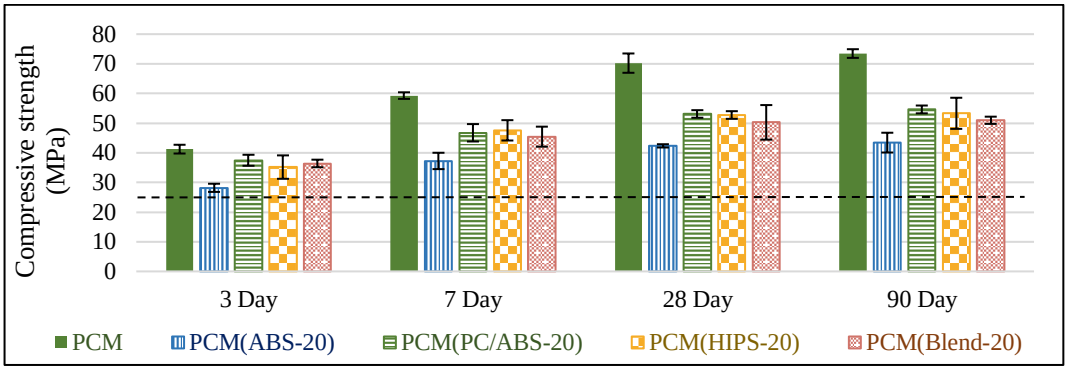

Figure 97: Compressive strength for PCM mix with and without 20% WEEP replacement.

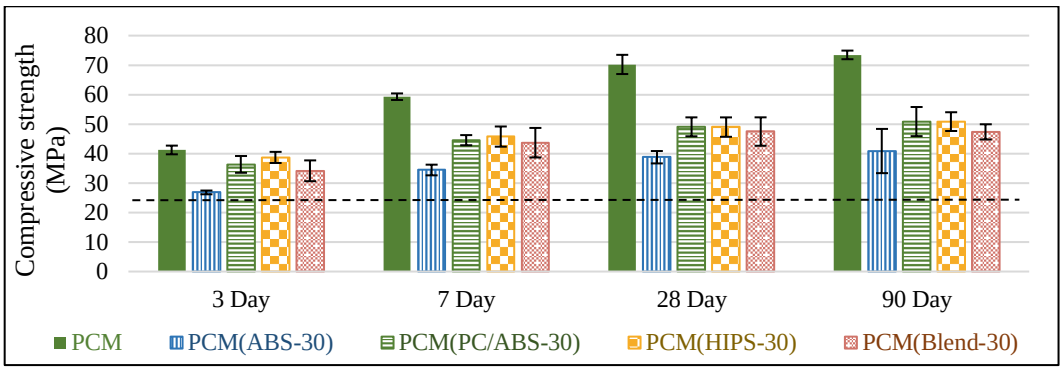

Figure 98: Compressive strength for PCM mix with and without 30% WEEP replacement.

5.3.1.7 Compressive strength for PCS replaced with WEEP

Figures 99 - 102 compares the average compressive strengths of PCS at different ages of curing, types of WEEP and replacement levels. It was clear that PCS containing no WEEP substitution had the highest average compressive strength at all ages of curing. It was also noted that the average compressive strength reduction from ABS WEEP substitution at 30% replacement for the natural aggregate had a smaller decrease in the average compressive strength in PCS, compared to PC (Control mix) alone. Furthermore, the average compressive strength of concrete decreased as the percentage WEEP increased.

At 28 days of curing, the mixtures containing 30% WEEP had average compressive strengths in the following order:

PCS > PCS(HIPS-30) > PCS(PC/ABS-30) > PCS(Blend-30) > PCS(ABS-30).

i.e. (59.5 > 41.7 > 40.0 > 38.6 > 32.0)MPa.

Here it can be seen that replacement of ABS WEEP significantly decreased the average compressive strength of PCS by 46.2%, Blend WEEP by 35.1%, HIPS WEEP by 32.9 % and PC/ABS WEEP at 29.9%. It is seen that replacement of HIPS WEEP yielded the highest average compressive strength for concrete made using WEEP. This is different compared to WEEP replacement in PC (Control mix) and PCM whereby replacements of PC/ABS WEEP yielded the highest average compressive strengths.

At 90 days of curing, the mixtures containing 30% WEEP had a small increase in the average compressive strength over that obtained at 28 days of curing, in the following order:

PCS > PCS(HIPS-30) > PCS(PC/ABS-30) > PCS(Blend-30) > PCS(ABS-30).

i.e. (63.7 > 43.0 > 42.1 > 40.3 > 33.0)MPa.

Here it can be seen that replacement of ABS WEEP for the natural aggregate continued to decrease the average compressive strength of PCS by 48.2%, Blend WEEP by 36.8%, PC/ABS WEEP by 33.9% and HIPS WEEP by 32.4%. All mixes made with WEEP substitution for the natural aggregate and made with CSF replacement for cement attained structural strength > 25MPa.

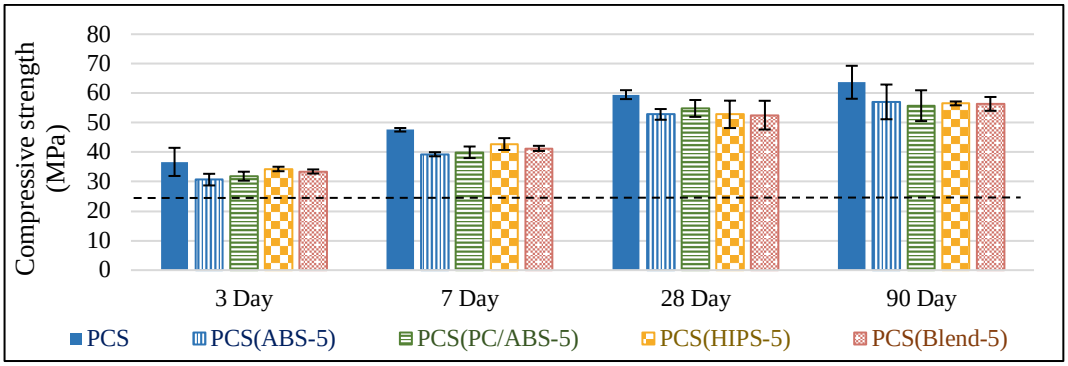

Figure 99: Compressive strength for PCS mix with and without 5% WEEP replacement.

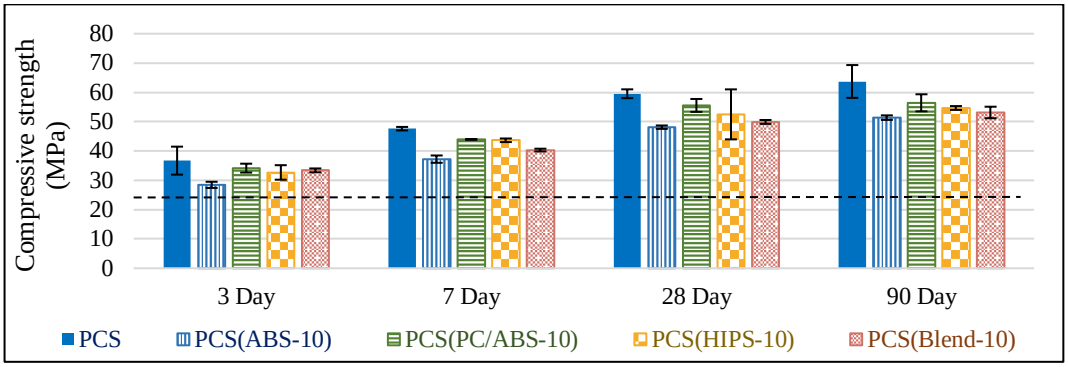

Figure 100: Compressive strength for PCS mix with and without 10% WEEP replacement.

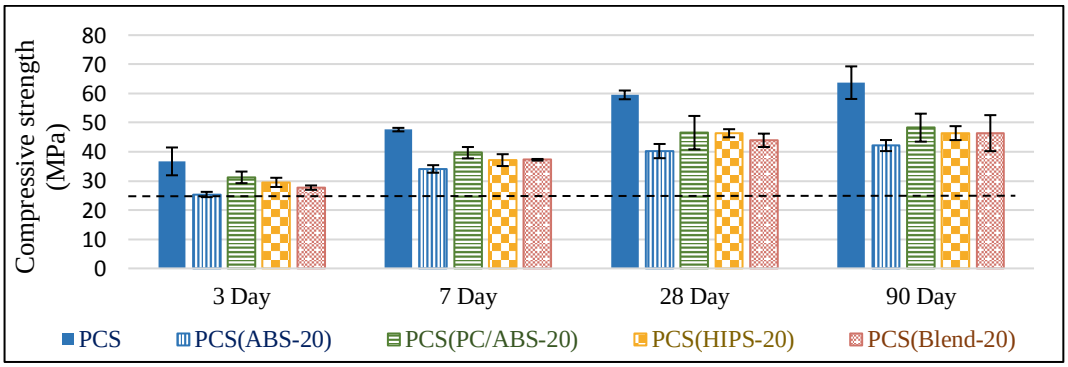

Figure 101: Compressive strength for PCS mix with and without 20% WEEP replacement.

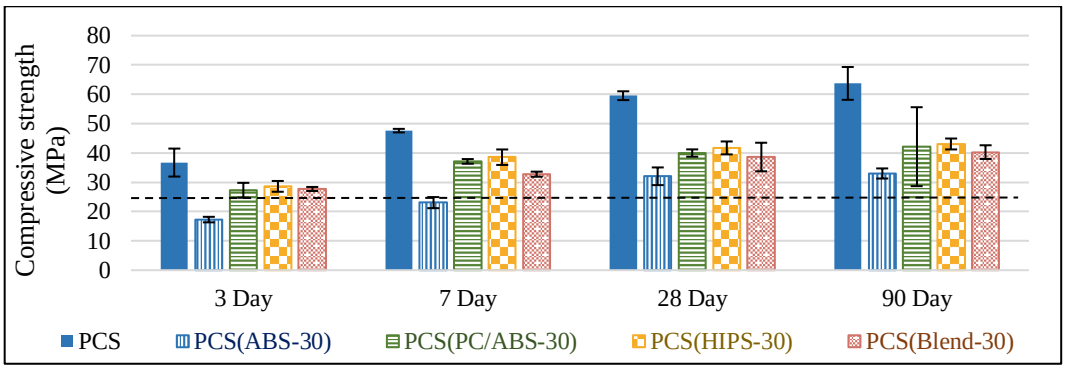

Figure 102: Compressive strength for PCS mix with and without 30% WEEP replacement.

5.3.1.8 Concrete made without WEEP substitution for the natural aggregate

It is clear from Figure 103 that PCM had the highest average compressive strength, followed by PCS and PC (Control mix) at 28 days of curing, i.e. 70.2MPa, 59.5MPa and 57.6MPa respectively. Similar results were obtained at 90 days of curing, whereby PCM had an average compressive strength of 73.5MPa, PCS with 63.7MPa and PC (Control mix) with 60.1MPa.

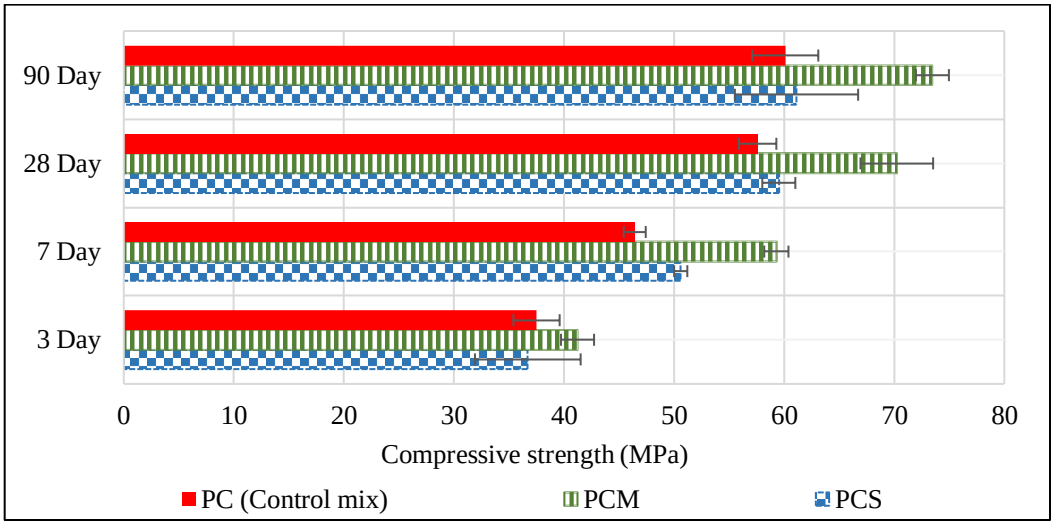

Figure 103: Average compressive strength of concrete made without WEEP at 3, 7, 28 and 90 days of curing.

It is seen that there was a small difference of 1.9MPa in the average compressive strength between PC (Control mix) and PCS at 28 days of curing and 3.6MPa at 90 days of curing. Therefore, the replacement of cement with CSF did not greatly increase the compressive strength of concrete. This could be the result of CSF used having a very large mean particle size of 167μm, as shown in Table 7 (p.48). This is much compared to the mean particle size of cement at 16.2μm and the mean particle size of MK at 27.0μm. Therefore, CSF may not have sufficiently reacted with the calcium hydroxide formed during the initial hydration process nor acted as an effective fine filler. From the pore-size and distribution curve for hardened concrete presented in Figures 72 - 73 (p.97), it is clear that PC (Control mix) had the largest amount of open capillary pores at 28 days of curing. These types of pores are responsible for the reduction in compressive strength of concrete (Li, 2011). It also showed that PCM had the smallest quantity of open pores and the smallest pore-sizes. Thus, from these results it is clear that PC (Control mix) should have the lowest average compressive strength followed by PCS and lastly, PCM with the highest average compressive strength.

The results from the pore-size distribution is confirmed by evaluating the ITZ results found in this study. The ITZ is responsible for the reduction in compressive strength found in concrete (Bensted and Barnes, 2002). From Figure 53 (p.81), it was found that PC (Control mix) had an ITZ around the aggregate ranging between 4μm - 6μm. This is much compared to PCM which had an ITZ ranging between 1μm - 4μm while PCS which had an ITZ ranging between 2μm - 3μm around the natural aggregate, as shown in Figure 57 (p.84) and 61 (p.86). This additional size in the ITZ for PC (Control mix) could also explain why PC (Control mix) had the lowest average compressive strength at 28 and 90 days of curing.

From Figure 104 it can be seen that PCM had the highest percentage rate increase in average compressive strength at 7 days of curing relative to its initial 3 day average compressive strength increasing by 43.8%, followed by PCS at 37.8% and PC (Control mix) at 23.7%. PC (Control mix) had a slight increase at 28 days of curing relative to its 7 day average compressive strength at 24.1%, while PCM and PCS increased with 18.5% and 17.6% respectively. At 90 days of curing it was found that the rate in average compressive strength slowed down to 7.0%, 4.6% and 4.4% for PCM, PCS and PC (Control mix).

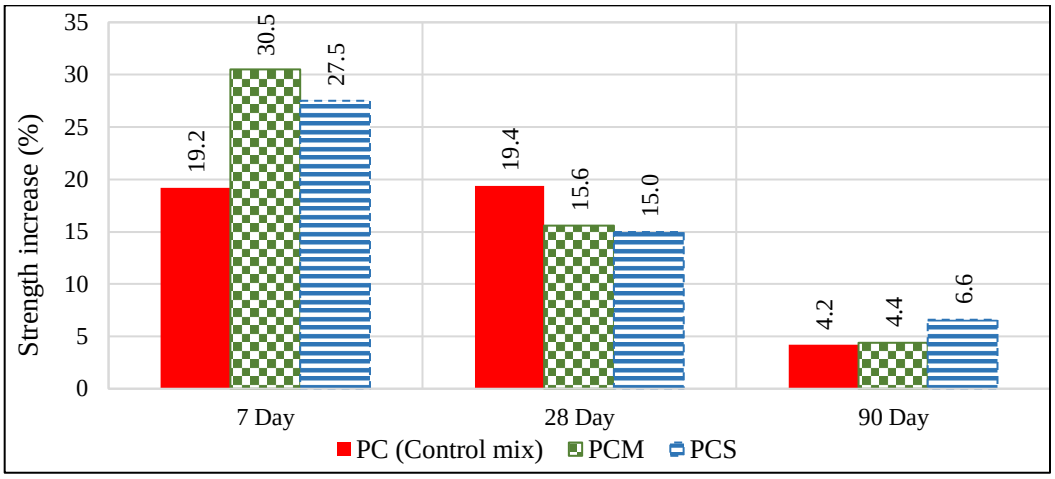

Figure 104: Percentage compressive strength increase for PC (Control mix), PCM and PCS at 7, 28 and 90 days of curing.

This indicates that the pozzolanic reaction created by the replacement of cement with MK or CSF experienced an initial burst in the rate of the average compressive strength which slowed down between 28 and 90 days of curing. PC (Control mix) however experienced a gradual increase in its average compressive strength, but also slowed down between 28 and 90 days of curing. This decrease in the rate of compressive strength gain between 28

and 90 days of curing could be explained by referring back to the XRD results for hardened concrete found in Section 4.4.2.7 (p.92).

Alite hydration is responsible for the early day strength while belite, ferrite and aluminate hydrations are responsible for the later day strength (Wild *et al.*, 1995). The XRD results confirmed that there was no alite found in PC (Control mix), PCM or PCS, indicating that it was all consumed to form C-S-H. Furthermore, it was found that there were still detectable amounts of MK available in PCM. This indicated that the available calcium hydroxide was consumed to form secondary C-S-H and that some MK remained unreacted. From the XRD graphs it was also seen that PCM had the highest intensity of C-S-H at 3.9cps, followed by PCS at 3.1cps and PC (Control mix) with 2.9cps. This indicates that PCM had the highest amount of C-S-H which are responsible for the strength of hardened concrete (Richardson, 2002). Thus, from the XRD results it is clear that PCM should have the highest average compressive strength, followed by PCS and PC (Control mix). Furthermore, results from the BSE phase analysis also found that there were no alite minerals in either PC (Control mix), PCM or PCS. Unreacted MK was found in Figure 70 (p.94), while unreacted CSF was found in Figure 71 (p.94).

5.3.1.9 Concrete made with WEEP

All mixes who had their natural aggregates replaced with 30% WEEP for the natural aggregate had a decrease in average compressive strength, as shown in Table 23 (p.102). Similar results were found by Kumar and Baskar (2015); Lui *et al.*, (2015); and Manjunath (2016). It was found that the replacement of different types of WEEP yielded higher average compressive strengths compared to others depending on the type of binder used, as shown in Table 24.

Table 24: WEEP type producing the highest and lowest average compressive strength at 28 and 90 days of curing.

Mix design	30% WEEP replacement for the natural aggregate			
	WEEP producing the highest compressive strength		WEEP producing the lowest compressive strength	
	28 Day	90 Day	28 Day	90 Day
PC (Control mix)	PC/ABS	PC/ABS	ABS	ABS
PCM	PC/ABS	PC/ABS	ABS	ABS
PCS	HIPS	HIPS	ABS	ABS

From Table 24 it is clear that replacements of ABS WEEP produced concrete with the lowest average compressive strength. PC/ABS WEEP replacement produced the highest average compressive strength in PC (Control mix) and PCM while replacements of HIPS WEEP produced the highest average compressive strength in PCS. The average compressive strength drop in concrete when different types of WEEP substituted for the natural aggregate could be linked to the interaction between be aggregate and hcp in the concrete matrix. Figure 54 (p.82) presents the interface between the ABS WEEP and the hcp in PC(Blend-30) at 28 days of curing. Here it is seen that there were crystals formed between the ABS WEEP and hcp. Using EDS analysis, it was found that these crystals mainly contained calcium and silicon elements among others. These crystals were formed during hydration, whereby calcium hydroxide formed between the aggregate and the bulk paste when critical saturation was reached. The crystals formed due to the dissolution of calcium silicate, forming calcium and hydroxyl ions. Calcium hydroxide then grew into very large plate like crystals. Excess water around the aggregate produced a more porous system. As hydration continued these pores were filled with poorly crystallised calcium silicate hydrates, small crystals of ettringite and calcium hydroxide between the framework (Li, 2002).

These crystals reduced the bond between the hcp and ABS WEEP, which in turn reduced the concretes compressive strength. Similar crystals were also found around the ABS WEEP in both the PCM(Blend-30) and PCS(Blend-30), as presented in Figures 58 (p.84) and 62 (p.87). Furthermore, the aggregates with rougher surfaces provided higher bonding between the aggregate and hcp. The compressive strength of concrete was therefore compromised by replacing the rough natural aggregates with smooth WEEP, as shown in Figures 31 - 35 (p.60 - 62).

5.3.2 Tensile splitting strength results for concrete mixes

Table 25 presents the cylinder tensile splitting strength in MPa, standard deviation (S.D) and coefficient of variance (CoV) in percentage for concrete made using 30% WEEP replacement for the natural aggregate. The average tensile splitting strength results in Table 25 are graphically illustrated in the bar chart in Figure 105. The average tensile splitting strengths indicate that the concretes average tensile strength decreased for all the mixes which had their natural aggregates replaced with WEEP, regardless of the type of WEEP. It was also found that PCM mix designs performed the overall best, yielding

average tensile strengths greater when compared to PC (Control mix) and PCS. The variability measured by the CoV indicated a good consistency for the majority of the concrete mixes indicating that the samples were well prepared. The following sub-sections analyses the average tensile splitting strength results for each mix.

Table 25: 28 Day tensile splitting strength test results.

Concrete mix label	28 Day results						
	Test 1 (MPa)	Test 2 (MPa)	Test 3 (MPa)	Average (MPa)	S.D (%)	CoV (%)	Confidence interval
PC (Control mix)	4.24	3.98	3.97	4.06	0.16	3.87	0.39
PC(ABS-30)	3.53	3.48	3.42	3.48	0.06	1.60	0.54
PC(PC/ABS-30)	3.83	3.73	3.66	3.74	0.09	2.38	0.42
PC(HIPS-30)	3.76	3.71	3.49	3.65	0.14	3.89	0.06
PC(Blend-30)	3.74	3.61	3.53	3.63	0.11	2.94	0.09
PCM	5.56	5.46	5.14	5.39	0.22	4.00	0.14
PCM(ABS-30)	4.03	3.98	3.91	3.97	0.06	1.54	0.11
PCM(PC/ABS-30)	4.67	4.51	4.42	4.53	0.12	2.73	0.15
PCM(HIPS-30)	4.57	4.27	4.46	4.43	0.15	3.49	0.31
PCM(Blend-30)	4.57	4.51	4.22	4.43	0.18	4.17	0.38
PCS	4.73	4.61	4.40	4.58	0.17	3.67	0.46
PCS(ABS-30)	3.78	3.73	3.73	3.75	0.03	0.75	0.07
PCS(PC/ABS-30)	4.16	4.00	3.86	4.00	0.15	3.75	0.37
PCS(HIPS-30)	4.10	3.80	3.90	4.00	0.17	4.27	0.42
PCS(Blend-30)	3.90	3.80	3.66	3.79	0.12	3.25	0.31

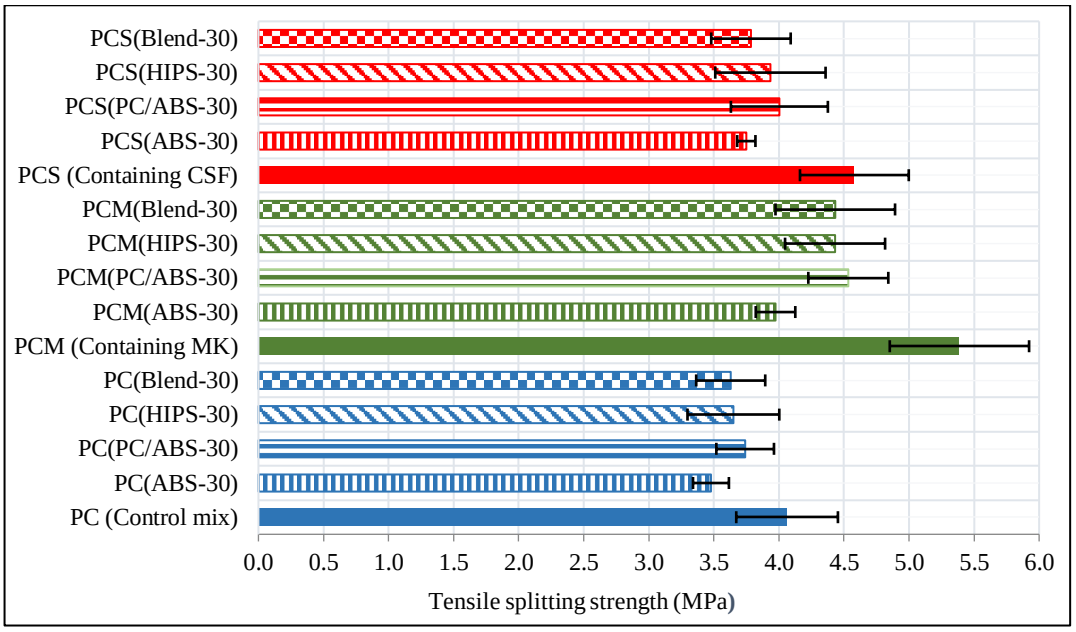

Figure 105: Average 28 day tensile splitting strength test results for concrete made without and with 30% WEEP replacement for the natural aggregate.

5.3.2.1 Tensile strength for PC (Control mix) replaced with WEEP

From Figure 105 it is clear that PC (Control mix) had the highest average tensile splitting strength compared to PC (Control mix) who had 30% of its natural aggregates replaced with WEEP. The average tensile splitting strength results for 28 days of curing are:

PC (Control mix) > PC(PC/ABS-30) > PC(HIPS-30) > PC(Blend-30) > PC(ABS-30).

i.e. (4.06 > 3.74 > 3.65 > 3.63 > 3.48)MPa.

It was noticed that there was little to no difference in the average tensile splitting strength between substitutions of HIPS or Blend WEEP. As with the average compressive strength of concrete, replacements with ABS WEEP yielded the lowest average tensile splitting strength results. Here it is clear that ABS WEEP substitution decreased the average tensile splitting strength of concrete mixed with ABS WEEP the most at 14.4%, followed by Blend WEEP at 10.7%, HIPS WEEP at 10.2% and PC/ABS WEEP at 7.9%.

5.3.2.2 Tensile splitting strength for PCM replaced with WEEP

Similar to PC (Control mix), the average tensile splitting strength of PCM was reduced when replacing natural aggregates with 30% WEEP. The average tensile splitting strength results for 28 days of curing are:

PCM > PCM(PC/ABS-30) > PCM(HIPS-30) = PCM(Blend-30) > PCM(ABS-30).

i.e. (5.39 > 4.59 > 4.43 = 4.43 > 3.94)MPa.

There were no differences in the average tensile splitting strengths between replacements of HIPS and Blend WEEP in concrete. Here it was also noticed that replacements of ABS WEEP reduced the average tensile splitting strength of PCM the most at 26.2% followed by HIPS and Blend WEEP at 17.7% and PC/ABS WEEP at 15.9%. It is clear that replacements of WEEP in PCM reduced the average tensile splitting strength of concrete the most, compared to replacements of WEEP in PC (Control mix). However, as PCM had a very high initial average tensile splitting strength, replacements of WEEP in PCM still attained higher 28 day tensile splitting strengths compared to replacements of WEEP in PC (Control mix).

5.3.2.3 Tensile splitting strength for PCS replaced with WEEP

The average tensile strength of PCS mixed with and without WEEP for the natural aggregate generally fell between the average tensile splitting strengths of PC (Control mix) and PCM. The average tensile splitting strength results for 28 days of curing are:

PCS > PCS(PC/ABS-30) > PCS(HIPS-30) > PCS(Blend-30) > PCS(ABS-30).

i.e. (4.58 > 4.00 > 3.93 > 3.79 > 3.75)MPa.

Here it is seen that there were very little difference in the average tensile splitting strength between replacements of PC/ABS and HIPS WEEP. Furthermore, it is clear that ABS WEEP replacement decreased the average tensile splitting strength of concrete the most at 18.1%, Blend WEEP at 17.4%, HIPS WEEP at 14.1% and PC/ABS WEEP at 12.6%. Figure 106 illustrates the crack formed at failure for PC(Blend-30) and the internal distribution of the aggregates inside the cylinder.

Figure 106: Tensile splitting of PC(Blend-30) (LHS) and the internal distribution of PC(Blend-30) (RHS).

5.3.2.4 Concrete made without WEEP

From Figure 105, it is clear that PCM had the highest average tensile splitting strength at 5.4MPa, followed by PCS at 4.6MPa and PC (Control mix) at 4.1MPa. These values are much lower compared to the average compressive strengths. This is due to concrete being much weaker in tension and stronger in compression (Li, 2011).

From the pore-size distribution curve shown in Figures 72 – 73 (p.97), it can be seen that PC (Control mix) had the highest amount of meso pores in its matrix, followed by PCS and PCM. When a tensile load was applied, the forces were much higher around these large pores. When the tensile load was increased the failure occurred due to high localised

straining occurring at these larger pores. Therefore, PC (Control mix) who had the largest pore-sizes failed at lower tensile forces, followed by PCS and finally PCM which failed at higher tensile forces.

5.3.2.5 Correlation between compressive and tensile splitting strength

Figures 107 - 109 correlates the average compressive and tensile splitting strengths of the different mixes at 28 days of curing. It is seen that PC (Control mix), PCM, PCS and their WEEP replacements had a correlation coefficient (R^2) of 0.9635, 0.9922 and 0.9539 respectively, indicating a strong positive linear relationship. This indicates that some of the mechanisms responsible for concrete failure in compression such as a weak ITZ between the WEEP and hcp, as described in Section 4.4.2.5 (p.80) strongly relates to those for the tensile splitting strength of concrete made using WEEP as natural aggregate replacement material. It is further noticed that as the compressive strength increased, the tensile splitting strength also increased but at a slower rate.

From Figure 107, it was seen that PC(ABS-30) simultaneously had the lowest average compressive and tensile splitting strength. Furthermore, PC(PC/ABS-30), PC(HIPS-30) and PC(Blend-30) all had similar compressive strengths. However, PC(PC/ABS-30) had a slightly reduced tensile splitting strength compared to PC(HIPS-30) and PC(Blend-30). It is further noticed that the distribution of the samples on the x-axis were very narrow indicating small differences in tensile strengths between the mixes.

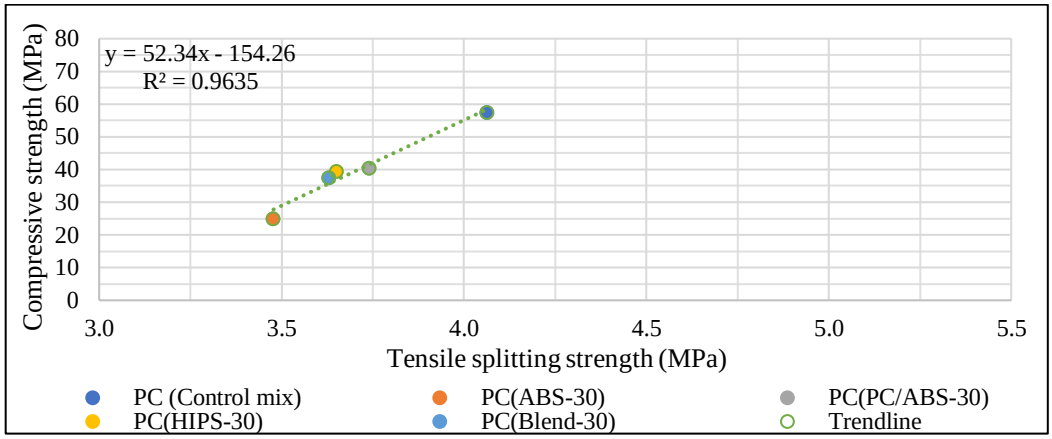

Figure 107: Correlation between the average compressive and tensile splitting strength for PC (Control mix) mixes at 28 days of curing.

From Figure 108, it was seen that similar to PC (Control mix) replacement with ABS and PCM(ABS-30) WEEP produced concrete with the lowest average compressive and

tensile splitting strengths. It was also found that there was little difference in both the average tensile splitting and compressive strength for PCM(HIPS-30) and PCM(Blend-30) while PCM(PC/ABS-30) had a slightly higher average tensile splitting strength. It was also clear that PCM had the highest average compressive and tensile splitting strengths for all mixes. In contrast to findings in Figure 107, the distribution of the tensile splitting strength relative to its compressive strength have shifted to the right hand side of the graph, indicating an overall increase in the tensile splitting strength. It is further noticed that the distribution of the tensile strength relative to its compressive strength have widened, indicating a broader range of tensile splitting strengths for PCM concretes mixed with WEEP.

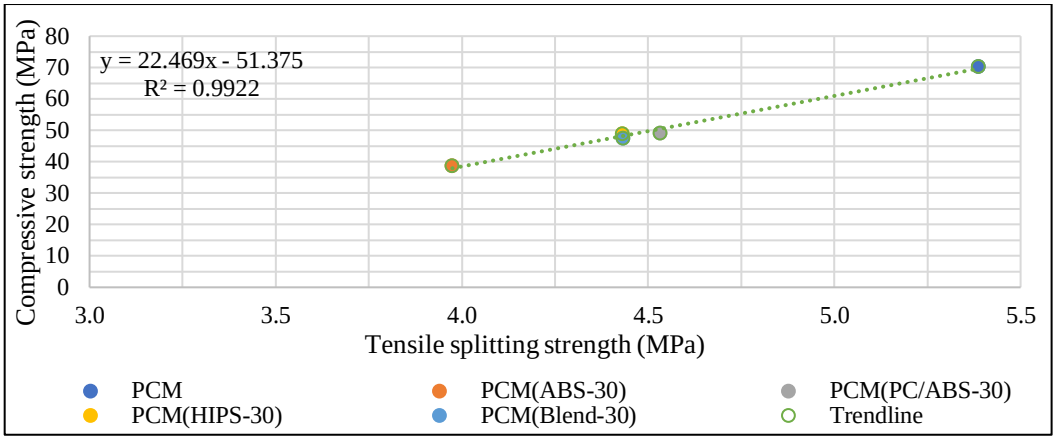

Figure 108: Correlation between the average compressive and tensile splitting strength for PCM mixes at 28 days of curing.

From Figure 109, it can be seen that PCS(ABS-30) produced concrete with the lowest average compressive and tensile splitting strengths. This is similar to results found when replacing ABS WEEP in PC (Control mix) and PCM mixes. It was also seen that PCS(Blend-30) and PCS(HIPS-30) had similar average compressive and tensile splitting strengths. This is similar to the results found in Figure 108 whereby replacements of HIPS WEEP produced similar results, compared to replacement with Blend WEEP. It was also seen that PCS produced the highest average compressive and tensile splitting strengths. It is further noticed that the distribution width of the tensile splitting strength fell in the range between that of Figure 107 - 108. This indicates that there was an overall increase in the tensile splitting and compressive strength for concrete made using CSF compared to concrete made using only cement as binder material.

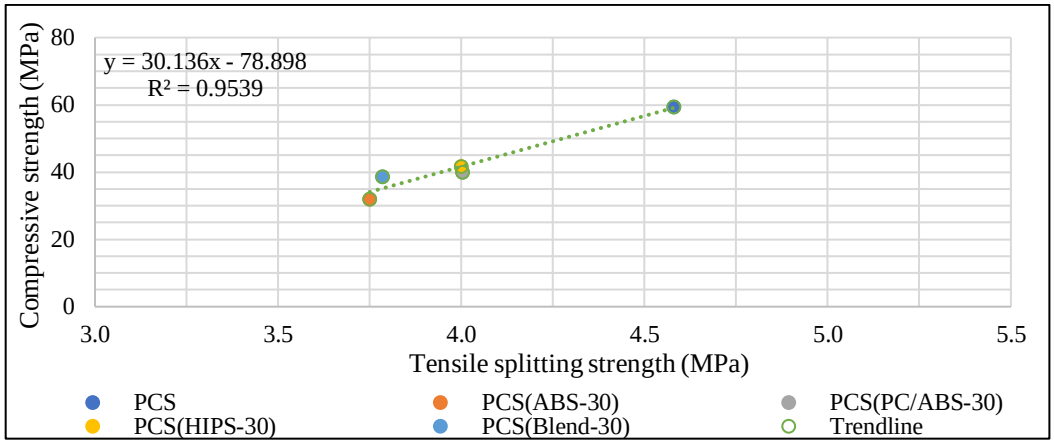

Figure 109: Correlation between the average compressive and tensile splitting strength for PCS mixes at 28 days of curing.

5.4 Durability test results for concrete mixes

The durability of concrete in South Africa can be measured by the oxygen permeability, water sorptivity and porosity, and chloride conductivity tests. The indexing values obtained can be used to determine the rational design life of a certain structure, and optimise material and construction processes (Fulton and Owens, 2009). The limiting index values can be used to provide certain concrete qualities for an expected design life and environment (Beushausen and Alexander, 2008). The durability indices are also empirically related to service life prediction models (Fulton and Owens, 2009). Concrete tested should meet the acceptable limits for durability indexes, as presented in Table 26.

Table 26: Suggested ranges for durability of concrete. (Source: Alexander *et al.*, 2011).

Durability class	OPI (log scale)	Sorptivity (mm/√h)	Conductivity (mS/cm)
Excellent	> 10	< 6	< 0.75
Good	9.5 - 10	6 - 10	0.75 - 1.50
Poor	9.0 - 9.5	10 - 15	1.50 - 2.50
Very poor	< 9	> 15	> 2.50

The following sections evaluates the oxygen permeability, water sorptivity and chloride conductivity for the mixes described in Table 17 (p.65).

Similar to the analysis of the strength of concrete, inferential error bars were used to display a 95% confidence interval in a data set and thus indicate the range where 95% of the results may fall in multiple tests. Overlapping error bars indicate the values that could overlap one another after numerous tests were done and are therefore statistically

uncertain while non-overlapping bars indicate that the compared values are statistically significant.

5.4.1 Oxygen permeability index results

The average OPI and k-value results are shown in Table 27. These measurements were taken at 28 days of curing and were tested on either 7 - 8 days after oven drying and preconditioning. Each of the results shown in Table 27 represents the average of four disks. See Appendix E, Tables E1 - E2 for the individual results. Some disks had an abnormally low result compared to the other in the same batch and its results were omitted from the final result. This could be the product of small flaws within the concrete matrix brought on during cutting or coring of the disks.

The OPI value is generally used more than the k-value to classify the quality of concrete. The OPI has an indexing value, ranging from high (good concrete) to low (poor concrete). Poor concrete is believed to have a high number of connected pores which allows the oxygen to escape more readily through the concrete matrix.

This allows unwanted ingress of external contaminants to the reinforcing steel in concrete much easier. This results in the rapid degradation of the concrete structure and hence, low durability. Concrete with low OPI values have higher k-values. This is as a result of oxygen moving faster through the concrete matrix.

The OPI results are graphically presented in Figure 110. It illustrates the relationship of the average OPI values of different mixes at 28 days of curing and compares the results to other concrete mix designs.

Moreover, the OPI test is sensitive to compaction (Alexander, 2004). As WEEP had a smaller specific weight compared to the other concrete constituents, it tends to move up through the concrete when vibrated. This may explain the variance in the test results.

According to Table 26, concrete with an OPI value > 10 indicates a concrete with an excellent durability. Moreover, concrete with an OPI value ranging between 9.5 - 10 indicates a concrete with a good durability. The following sub-sections evaluates the average results for the oxygen permeability of each mix described in Table 17 (p.65).

Table 27: Average OPI test results for concrete made without WEEP and with 30% WEEP replacement for the natural aggregate at 28 day of curing.

Mix design	OPI test data						
	k(m/s)			OPI			
	Mean	S.D	COV (%)	Mean	S.D	COV (%)	Confidence interval
PC (Control mix)	6.00E-11	3.36E-12	5.6	10.22	0.02	0.23	0.06
PCM	1.14E-11	6.22E-13	5.5	10.95	0.02	0.22	0.06
PCS	3.15E-11	6.50E-12	20.6	10.51	0.09	0.81	0.21
PC(ABS-30)	1.17E-10	1.57E-11	13.4	9.59	0.03	0.29	0.27
PC(PC/ABS-30)	2.58E-10	1.63E-11	6.3	9.93	0.06	0.59	0.14
PC(HIPS-30)	8.80E-11	6.39E-12	7.3	10.06	0.03	0.31	0.08
PC(Blend-30)	2.66E-10	2.96E-11	11.1	9.58	0.05	0.52	0.08
PCM(ABS-30)	4.01E-10	1.07E-10	26.8	9.83	0.11	1.15	0.28
PCM(PC/ABS-30)	2.45E-11	1.02E-11	41.4	10.63	0.18	1.69	0.45
PCM(HIPS-30)	4.20E-11	8.86E-12	21.1	10.38	0.10	0.94	0.24
PCM(Blend-30)	4.43E-11	3.99E-12	9.0	10.36	0.04	0.39	0.10
PCS(ABS-30)	2.04E-10	2.06E-11	10.1	9.69	0.04	0.45	0.11
PCS(PC/ABS-30)	9.72E-11	1.29E-11	13.3	10.01	0.06	0.60	0.15
PCS(HIPS-30)	8.29E-11	1.06E-11	12.8	10.08	0.06	0.57	0.14
PCS(Blend-30)	1.10E-10	1.72E-11	15.7	9.96	0.07	0.73	0.18

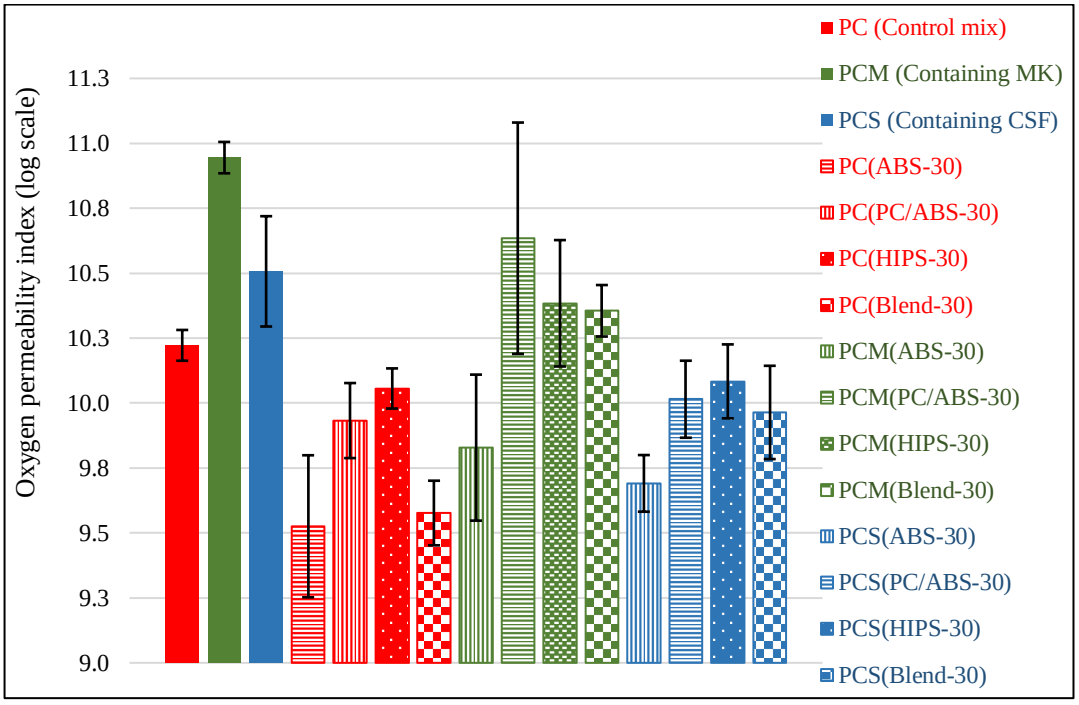

Figure 110: Average OPI test results for concrete made without WEEP and with 30% WEEP replacement for the natural aggregate at 28 days of curing.

5.4.1.1 Oxygen permeability index for PC (Control mix) replaced with WEEP

From Figure 110 it is clear that PC (Control mix) had a higher average OPI value, compared to concrete mixed with WEEP substitution at 30% for the natural aggregate. The average OPI results for 28 days of curing are:

PC (Control mix) > PC(HIPS-30) > PC(PC/ABS-30) > PC(ABS-30) > PC(Blend-30).

i.e. 10.22 > 10.06 > 9.93 > 9.59 > 9.58.

According to Table 26 (p.129), only PC (Control mix) and PC(HIPS-30) had OPI values > 10, which indicated excellent durability. Other mixes made with WEEP replacement fell between 9.5 and 10 which classifies them as having good durability. It must however be remembered that these mixes were all water cured under laboratory conditions and may have lower OPI values when used in practice. It was also seen that there were little differences in the OPI values between the replacements of ABS and Blend WEEP and thus had very similar durability.

5.4.1.2 Oxygen permeability index for PCM replaced with WEEP

From Figure 121 it can be seen that PCM and its WEEP replacements had the highest overall average OPI values compared to relevant WEEP replacements in PC (Control mix) and PCS. The average OPI results for 28 days of curing are:

PCM > PCM(PC/ABS-30) > PCM(HIPS-30) > PCM(Blend-30) > PCM(ABS-30).

i.e. 10.95 > 10.63 > 10.38 > 10.36 > 9.83.

It is clear that replacements of ABS WEEP decreased the OPI value of PCM the most compared to all other WEEP replacements. It is seen that PCM mixes had the overall highest average OPI values compared to relevant mixes made with the same type of WEEP. All mixes except for PCM(ABS-30) had average OPI values > 10, indicating excellent durability. PCM(ABS-30) had an OPI value ranging between 9.5 and 10, indicating good durability.

5.4.1.3 Oxygen permeability index for PCS replaced with WEEP

From Figure 110 it can be seen that PCS and its WEEP replacements had average OPI values between that of PCM and PC (Control mix) compared to relevant WEEP replacements. The average OPI results for 28 days of curing are:

PCS > PCS(HIPS-30) > PCS(PC/ABS-30) > PCS(Blend-30) > PCS(ABS-30).

i.e. 10.51 > 10.08 > 10.01 > 9.96 > 9.69.

It is clear that PCS, PCS(PC/ABS-30) and PCS(HIPS-30) had an average OPI value > 10, indicating excellent durability. Other mixes made with WEEP all had OPI values ranging between 9.5 - 10, indicating good durability. Replacing 30% PC/ABS or HIPS WEEP produced concretes with very similar average OPI values of 10.08 and 10.01 and thus have similar durability.

From Table 28 it can be seen that different types of WEEP yielded higher and lower OPI values for PC (Control mix), PCM and PCS.

Table 28: WEEP type producing the highest and lowest OPI values at 28 days of curing.

Mix design	30% Replacement of WEEP for the natural aggregate	
	WEEP type producing the highest average water sorptivity result	WEEP type producing the lowest average water sorptivity result
PC (Control mix)	HIPS	ABS
PCM	PC/ABS	ABS
PCS	HIPS	ABS

It is clear that HIPS WEEP produced the highest average OPI value for WEEP replacement in PC (Control mix) and PCS, while PC/ABS WEEP had the highest for replacement in PCM. It was also seen that ABS WEEP had the lowest average OPI value for both PC (Control mix), PCM and PCS mixes. This could be due to the formation of calcium and silicon crystals between the aggregate and hcp, as shown in Figures 54 (p.82), 58 (p.84) and 62 (p.87). These crystals were less dense compared to the surrounding hcp matrix allowing more oxygen to escape through the disk when pressurised, resulting in lower OPI values.

5.4.1.4 Oxygen permeability index for concrete made without WEEP

From Figure 110 it can be seen that PCM had the highest average OPI value followed by PCS and lastly PC (Control mix). Therefore, the replacement of cement with MK or CSF increased the durability of concrete. This is similar to results found by Bakera and Alexander (2018) and Alexander and Magee (1999). This clearly indicates that there were less interconnected pores throughout the concrete matrix, impeding the flow of oxygen.

This can be seen by the pore-size distribution in Figures 72 - 73 (p.97). PCM had a lot less open capillary pores, compared to PCS and PC (Control mix). This is also confirmed by the ITZ analysis between the aggregate and hcp in Figures 54 (p.82), 58 (p.84) and 62 (p.87). If the open pores connect to one another, they can form a percolation pathway through which the oxygen could pass through the concrete and reduce the OPI value and thus reduce the durability of hardened concrete (Snyder *et al*, 1992).

5.4.2 Water sorptivity test results

Table 29 represents the average water sorptivity test results of four disks. The disks were tested at 28 days of curing. In this table the water sorptivity test results are presented as sorptivity (mm/√h) and porosity as (%). The test was performed according to the Durability Index Testing Procedure Manual (2017). Note that different core samples were used to those in the OPI test. This was done to test multiple concrete mix designs concurrently and to reduce the possibility of confusion between the multiple tests. Appendix E, Table E3 - E4 presents the individual disk results.

The average water sorptivity test results shown in Table 29 are graphically illustrated in Figure 111 while the average porosity is graphically illustrated in Figure 112. The confidence interval error bars were calculated using Equation F.21 in Appendix F with a confidence index of 95%. It compares the average sorptivity and porosity values of concretes made with and without WEEP replacement for the natural aggregate to one another at 28 days of curing. Thus, the sorptivity results were used to evaluate the durability of concrete as it is one of the major mechanisms which transport harmful aggressive agents into the concrete matrix.

Table 29: Average water sorptivity test results for concrete made without WEEP and with 30% WEEP replacement for the natural aggregate at 28 day of curing.

Mix design	Water sorptivity test data							
	Sorptivity (mm/√hr)				Porosity (%)			
	Mean	S.D	COV (%)	Confidence interval	Mean	S.D	COV (%)	Confidence interval
PC (Control mix)	9.57	0.36	3.78	0.50	11.91	0.31	2.64	0.12
PCM	6.41	0.38	5.95	0.57	8.70	0.36	4.14	0.14
PCS	7.80	0.30	3.79	0.08	15.19	0.05	0.32	0.02
PC(ABS-30)	8.47	0.65	7.73	0.30	11.41	0.19	1.66	0.07
PC(PC/ABS-30)	8.02	0.93	11.63	2.16	10.12	1.36	13.42	0.52
PC(HIPS-30)	8.09	0.39	4.81	0.65	10.48	0.41	3.91	0.16
PC(Blend-30)	8.33	0.80	9.55	0.77	9.83	0.48	4.90	0.18
PCM(ABS-30)	5.50	0.23	4.11	0.57	12.77	0.36	2.81	0.14
PCM(PC/ABS-30)	4.88	0.67	13.67	1.62	9.33	1.02	10.89	0.39
PCM(HIPS-30)	4.01	0.64	15.98	1.42	11.75	0.89	7.61	0.34
PCM(Blend-30)	5.42	0.24	4.39	0.82	13.33	0.51	3.86	0.20
PCS(ABS-30)	7.35	0.49	6.64	0.33	7.48	0.21	2.79	0.08
PCS(PC/ABS-30)	6.20	0.28	4.53	0.14	10.17	0.09	0.86	0.03
PCS(HIPS-30)	6.23	0.21	3.35	3.24	12.19	2.04	16.73	0.78
PCS(Blend-30)	6.94	0.63	9.08	0.50	8.26	0.31	3.80	0.12

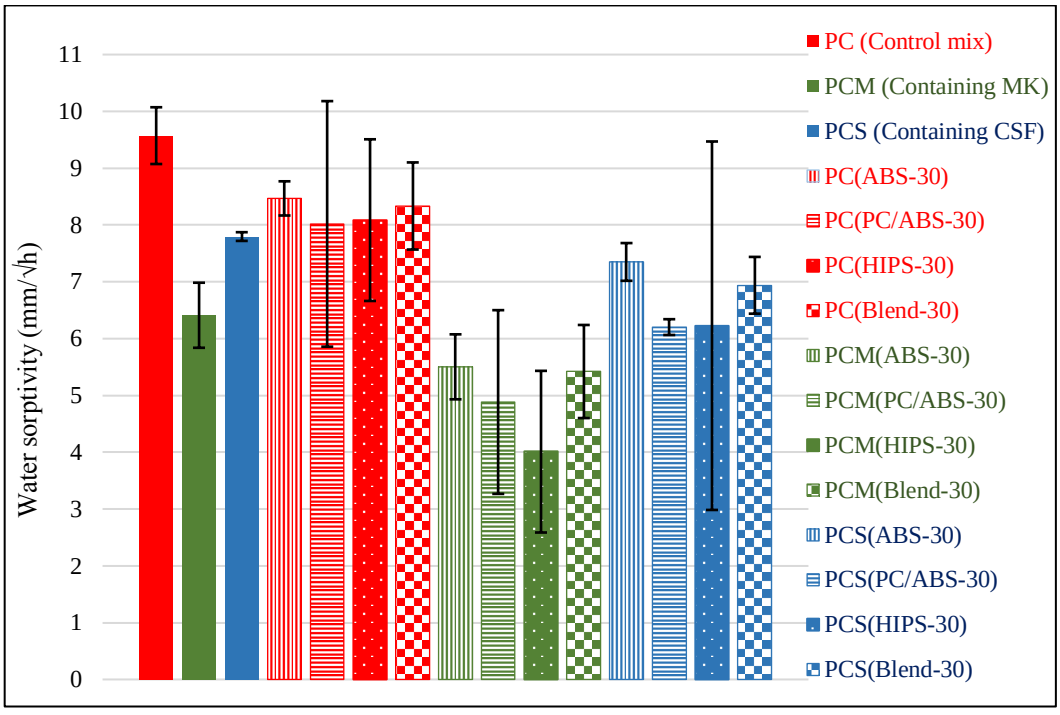

Figure 111: Average water sorptivity test results for concrete made without WEEP and with 30% WEEP replacement for the natural aggregate at 28 days of curing.

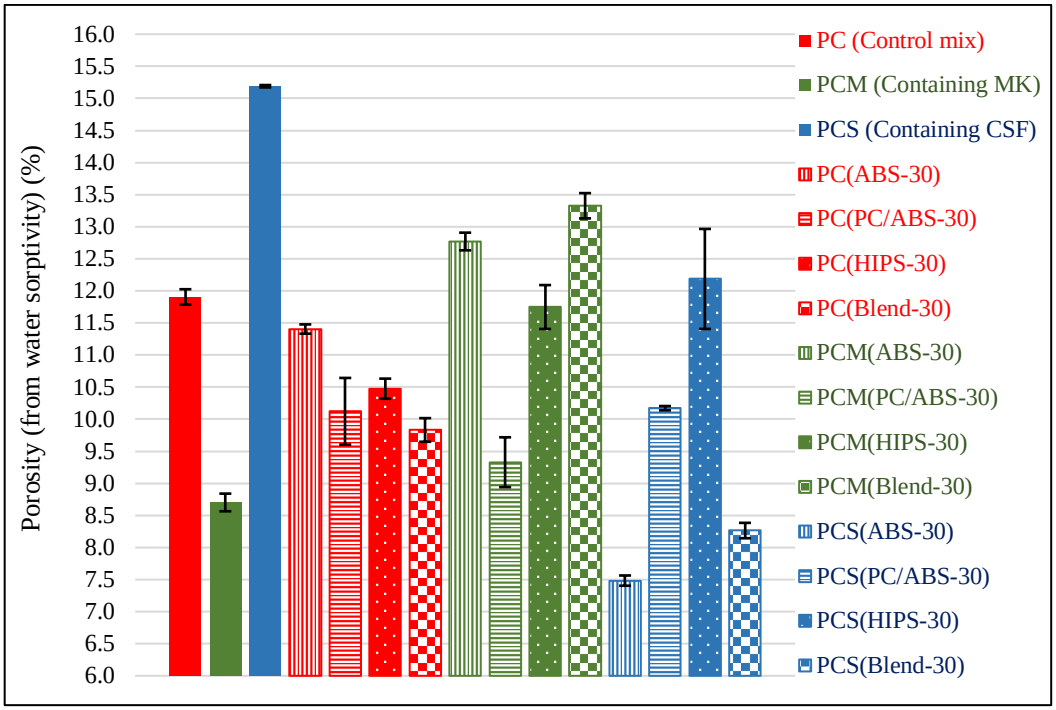

Figure 112: Average porosity results for concrete made without WEEP and with 30% WEEP replacement for the natural aggregate at 28 days of curing.

Sorptivity values represent the rate of water penetrating into the concrete matrix while porosity evaluates absorption properties and provides a measurement of the total volume of pores in the concrete matrix that can be filled with water (Li, 2001). Generally, concrete with low w:b ratios tend to have lower sorptivity and porosity values and thus absorb less water into the concrete matrix. A direct comparison of the average water sorptivity and porosity may be misleading. This is due to the fact that the majority of the error bars from the water sorptivity graph overlap one another and is therefore statistically uncertain. This may be due to the long error bars of each result indicating values with higher variabilities and which are less reliable. On the other hand, the porosity values have less overlapping error bars between the relevant mixes and may therefore be more reliable when comparing different mixes to one another.

Concretes with high w:b ratios tend to have higher sorptivity and porosity values and thus absorb more water into the concrete matrix. According to Table 26 (p.129), concrete with water sorptivity ranging between 6mm/√h - 10mm/√h have good durability while concrete with water sorptivity < 6mm/√h have excellent durability. The following sub-sections evaluates the average sorptivity results for concrete made with and without WEEP as replacement for the natural aggregate.

5.4.2.1 Water sorptivity and porosity for PC replaced with WEEP

From Figure 111 it can be seen that the average water sorptivity of PC (Control mix) made without WEEP had a higher average water sorptivity compared to concrete made without WEEP replacement for the natural aggregate.

The average water sorptivity results for 28 days of curing are:

PC (Control mix) > PC(ABS-30) > PC(Blend-30) > PC(HIPS-30) > PC(PC/ABS-30).

i.e. (9.57 > 8.47 > 8.33 > 8.09 > 8.02)mm/√h.

The average porosity results for 28 days of curing are:

PC (Control mix) > PC(ABS-30) > PC(HIPS-30) > PC(PC/ABS-30) > PC(Blend-30).

i.e. (11.91 > 11.41 > 10.48 > 10.12 > 9.83)%.

It is clear that all mixes made with WEEP replacement for the natural aggregate had an improved durability compared to PC (Control mix) alone. All mixes had average water sorptivity values ranging between 6mm/√h - 10mm/√h, indicating good durability.

5.4.2.2 Water sorptivity and porosity for PCM replaced with WEEP

From Figure 111 it was clear that the replacements of WEEP for the natural aggregate in PCM had the overall lowest average water sorptivity results, compared to relevant replacements of WEEP in PC(Control mix) and PCS.

The average water sorptivity results for 28 days of curing are:

PCM > PCM(ABS-30) > PCM(Blend-30) > PCM(PC/ABS-30) > PCM(HIPS-30).

i.e. (6.41 > 5.50 > 5.42 > 4.88 > 4.01)mm/√h.

The average porosity results for 28 days of curing are:

PCM (Blend-30) > PCM(ABS-30) > PCM(HIPS-30) > PCM(PC/ABS-30) > PCM.

i.e. (13.33 > 12.77 > 11.75 > 9.33 > 8.70)%.

It is seen that PCM had average water sorptivity values ranging between 6mm/√h - 10mm/√h, indicating good durability. All PCM mixes made with WEEP replacement for the natural aggregate had water sorptivity values < 6 mm/√h indicating excellent durability.

5.4.2.3 Water sorptivity and porosity for PCS replaced with WEEP

The average water sorptivity results for PCS and its WEEP replacement for the natural aggregate at 28 days of curing are:

PCS > PCS(ABS-30) > PCS(Blend-30) > PCS(PC/ABS-30) > PCS(HIPS-30).

i.e. (7.80 > 7.35 > 6.94 > 6.26 > 6.20)mm/√h.

The average porosity results for 28 days of curing are:

PCS > PCS(HIPS-30) > PCS(PC/ABS-30) > PCS(Blend-30) > PCS(ABS-30).

i.e. (15.19 > 12.19 > 10.17 > 8.26 > 7.48)%.

It is clear that all mixes had average water sorptivity values ranging between 6mm/√h and 10mm/√h, indicating good durability. There were very little differences in the average water sorptivity values between PCS(PC/ABS-30) and PCS(HIPS-30) and thus had very similar durability.

From Figure 111, it is clear that concrete made with WEEP replacement for the natural aggregate had a reduced sorptivity, compared to concrete made without. This indicates that the overall durability increased for the majority of concretes made with WEEP. This is contradictory to the results found for the OPI tests. One reason may be due to WEEP being overall impermeable to water, compared to that of natural aggregates. This can be seen by comparing the images of the exposed surface of the disks of concrete made with and without WEEP, as shown in Figure 113.

It is clear that the exposed surface of the concrete disk made with WEEP replacement for the natural aggregate prevented water from being readily absorbed into the aggregates surface which in turn, lowered the overall water sorptivity results. It was also seen that WEEP replacement for the natural aggregate in PCM had the lowest average water sorptivity followed by WEEP replacement in PCS.

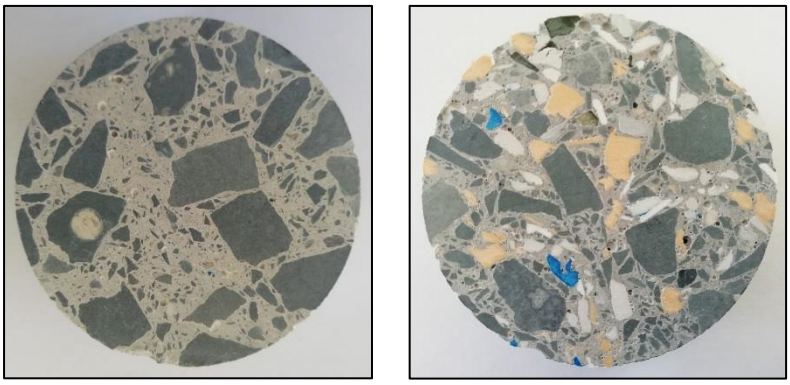

Figure 113: PC disk (LHS) and PC(Blend-30) disk (RHS).

From the results for concrete made with WEEP replacement presented in Figure 111, it is clear that different types of WEEP yielded higher average water sorptivity values compared to other mixes, as shown in Table 30.

Table 30: WEEP type producing the highest and lowest average water sorptivity at 28 days of curing.

Mix design	30% Replacement of WEEP for the natural aggregate	
	WEEP type producing the highest average water sorptivity result	WEEP type producing the lowest average water sorptivity result
PC (Control mix)	ABS	PC/ABS
PCM	ABS	HIPS
PCS	ABS	PC/ABS

From Table 30 it is clear that there was no specific type of WEEP which produced the lowest average water sorptivity. However, it was noticed that ABS WEEP yielded the overall highest average sorptivity and thus had the lowest durability. This may be due to the formation of calcium and silicon crystals between the ABS WEEP and the hcp previously discussed in Section 5.3.1.9 (p.122). These crystals of calcium and silicon may be very porous, resulting in high capillary suction at the ITZ. This in turn may have increased the water sorptivity more compared to other WEEP replacements.

Due to the hydrophilic nature of WEEP, little to no water was absorbed into the WEEP surface. This altered the mechanics of the water sorptivity test, resulting in a reduction in water sorptivity for concrete made with WEEP as partial replacement for the natural aggregate.

5.4.2.4 Water sorptivity for concrete made without WEEP

PC (Control mix) had the highest average water sorptivity results, followed by PCS and lastly PCM. Thus, PC (Control mix) absorbed more water into its matrix by capillary suction compared to PCM or PCS. This is due to the amount of connected pores throughout its matrix. The concretes pore-size and distribution determined the degree of capillary suction. Meso and capillary pores increased the permeability of PC (Control mix) which in turn increased its water sorptivity.

From Figures 72 – 73 (p.97) it was seen that PC (Control mix) had the highest amount of capillary pores which in turn corresponded to the high sorptivity values found for PC (Control mix). Furthermore, PCM had the least amount of open capillary pores and thus, absorbed the least amount of water into its matrix due to capillary suction which reduced the water sorptivity of PCM (Escadeillas and Maso, 1991).

5.4.3 Chloride conductivity test results

The average chloride conductivity test results are shown in Table 31. It represents the average of four disks tested at 28 days of curing and preconditioning. The test results are represented as chloride conductivity (mS/cm) and porosity (%). Appendix E, Table E5 - E6 presents the individual disk results.

The data shown in Table 31 is graphically illustrated in Figures 114 - 115, which compares the average chloride conductivity and porosity values of different mixes to each other. The confidence interval error bars were calculated using Equation F.21 in Appendix F with a confidence index of 95%. According to Table 26 (p.129), concrete with excellent durability have chloride conductivity values of < 0.75mS/cm, while concrete with poor durability have chloride conductivity values > 2.50mS/cm.

It is noted that the porosity results from the chloride conductivity tests were less compared to that of the water sorptivity test. This is due to the fact that the porosity from the chloride conductivity was measured after the specimens were impregnated with NaCl solution. The chloride binding produced new products which blocked the pores in the concrete matrix, reducing the specimen's conductivity. Moreover, it is clear that PCM had the lowest porosity. This is as a results of its chloride binding capacities due to its high alumina content. The alumina reacts with the chloride ions from the calcium chloroaluminate reducing the free chloride ions in the pore system (Tomas *et al*., 2012).

Table 31: Average chloride conductivity test results for concrete made without WEEP and with 30% WEEP replacement for the natural aggregate at 28 day of curing.

Mix design	Chloride conductivity test data							
	Conductivity (mS/cm)				Porosity (%)			
	Mean	S.D	COV (%)	Confidence interval	Mean	S.D	COV (%)	Confidence interval
PC (Control mix)	1.05	0.05	4.95	0.08	3.68	0.11	2.85	0.17
PCM	0.66	0.04	6.31	0.06	3.37	0.13	3.82	0.21
PCS	0.94	0.03	3.46	0.05	3.54	0.09	2.58	0.14
PC(ABS-30)	3.11	0.20	6.53	0.32	4.58	0.11	2.37	0.17
PC(PC/ABS-30)	1.85	0.11	5.94	0.18	5.22	0.29	5.45	0.45
PC(HIPS-30)	2.45	0.29	5.45	0.45	4.02	0.14	3.54	0.23
PC(Blend-30)	2.63	0.14	5.27	0.22	4.53	0.30	6.49	0.47
PCM(ABS-30)	1.04	0.07	6.80	0.11	4.39	0.14	3.24	0.23
PCM(PC/ABS-30)	0.74	0.04	5.28	0.06	3.55	0.17	4.87	0.28
PCM(HIPS-30)	0.79	0.06	7.72	0.10	3.08	0.10	3.20	0.16
PCM(Blend-30)	0.85	0.03	4.59	0.05	3.57	0.19	5.35	0.30
PCS(ABS-30)	1.27	0.05	4.29	0.08	5.20	0.24	4.52	0.38
PCS(PC/ABS-30)	1.13	0.05	4.71	0.08	4.89	0.29	3.92	0.46
PCS(HIPS-30)	1.03	0.05	5.31	0.08	4.54	0.19	4.24	0.31
PCS(Blend-30)	1.12	0.06	5.55	0.10	4.95	0.24	4.75	0.37

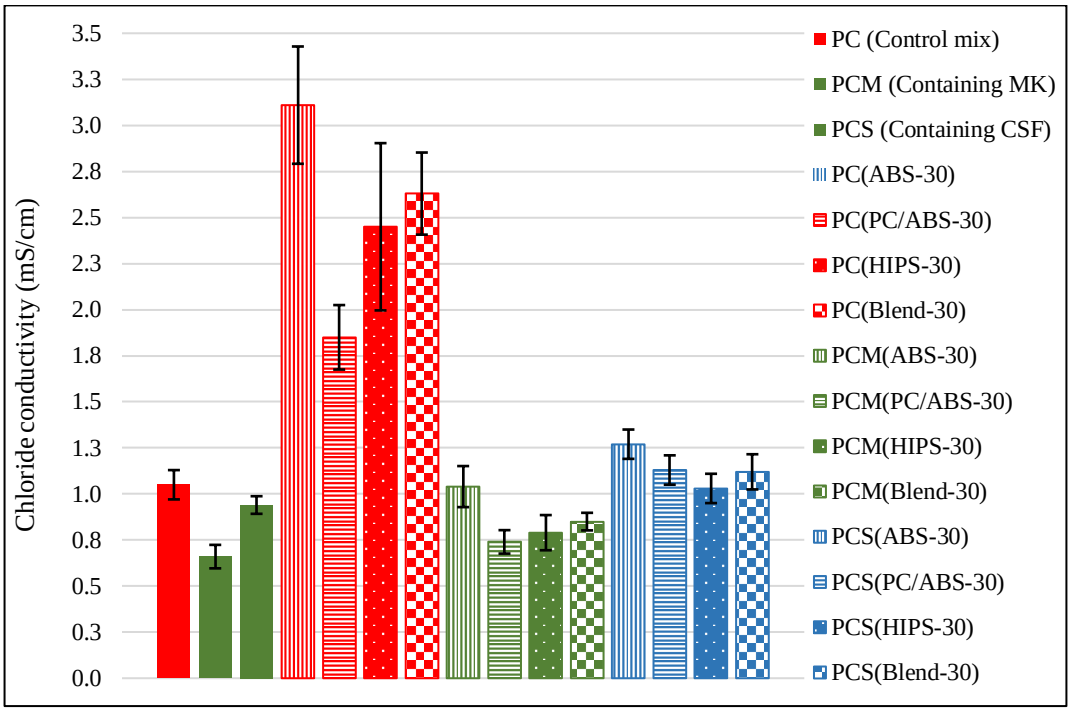

Figure 114: Average chloride conductivity test results for concrete made without WEEP and with 30% WEEP replacement for the natural aggregate at 28 days of curing.

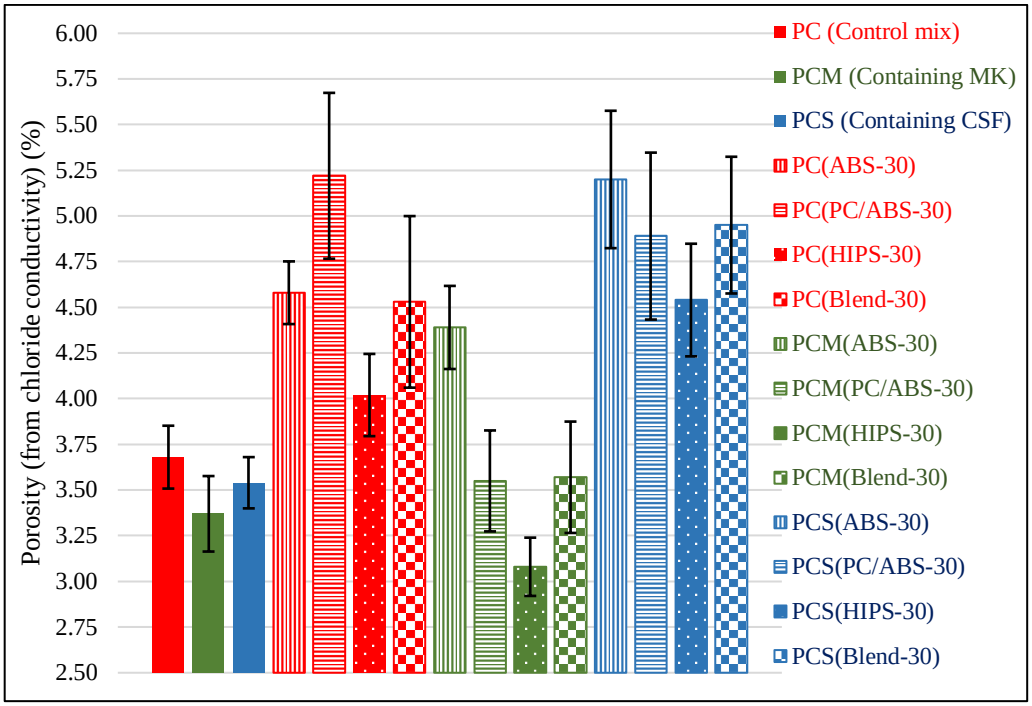

Figure 115: Average porosity results for concrete made without WEEP and with 30% WEEP replacement for the natural aggregate at 28 days of curing.

The following sub-sections evaluates the average chloride conductivity results of concrete made with and without WEEP as replacement material for the natural aggregate at 28 days of curing.

5.4.3.1 Chloride conductivity for PC (Control mix) replaced with WEEP

From Figure 114 it is seen that the average chloride conductivity of PC (Control mix) made with WEEP replacement had a higher average chloride conductivity compared to concrete made without WEEP replacement.

The average chloride conductivity results at 28 days of curing are:

PC(ABS-30) > PC(Blend-30) > PC(HIPS-30) > PC(PC/ABS-30) > PC (Control mix).

i.e. (3.11 > 2.63 > 2.45 > 1.85 > 1.05)mS/cm.

The average porosity results at 28 days of curing are:

PC(PC/ABS-30) > PC(ABS-30) > PC(Blend-30) > PC(HIPS-30) > PC (Control mix).

i.e. (5.22 > 4.58 > 4.53 > 4.02 > 3.68)%.

It was seen that all mixes made with WEEP replacement increased its average chloride conductivity, compared to PC (Control mix). Here it was found that replacing the natural aggregate with WEEP resulted in average chloride conductivities > 1.50mS/cm resulting in poor durability. However, PC (Control mix) mixed with no WEEP resulted in concrete with a chloride conductivity ranging between 0.75mS/cm - 1.50mS/cm indicating good durability.

5.4.3.2 Chloride conductivity for PCM replaced with WEEP

From Figure 114 it is clear that replacements of WEEP for the natural aggregate in PCM yielded the overall best average chloride conductivity results, compared to relevant replacements of WEEP in PC (Control mix) and PCS.

The average chloride conductivity results at 28 days of curing are:

PCM(ABS-30) > PCM(Blend-30) > PCM(HIPS-30) > PCM(PC/ABS-30) > PCM.

i.e. (1.04 > 0.85 > 0.79 > 0.74 > 0.66)mS/cm.

The average porosity results at 28 days of curing are:

PCM(ABS-30) > PCM(Blend-30) > PCM(PC/ABS-30) > PCM > PCM(HIPS-30).

i.e. (4.39 > 3.57 > 3.55 > 3.37 > 3.08)%.

It was clear that replacements of ABS, Blend and HIPS WEEP for the natural aggregate produced concrete with an average chloride conductivity value ranging between 0.75mS/cm - 1.50mS/cm indicating good durability. Replacements of PC/ABS WEEP and concrete with no WEEP had chloride conductivity values < 0.75 indicating excellent durability.

5.4.3.3 Chloride conductivity for PCS replaced with WEEP

From Figure 114 it is seen that the average chloride conductivity of PCS mix designs ranged between that of PC (Control mix) and PCM for the relevant WEEP replacement types.

The average chloride conductivity results for PCS and its WEEP replacements at 28 days of curing are:

PCS(ABS-30) > PCS(PC/ABS-30) > PCS(Blend-30) > PCS(HIPS-30) > PCS.

i.e. (1.27 > 1.13 > 1.12 > 1.03 > 0.94)mS/cm.

The average porosity results at 28 days of curing are:

PCS(ABS-30) > PCS(Blend-30) > PCS(PC/ABS-30) > PCS(HIPS-30) > PCS.

i.e. (5.20 > 4.95 > 4.89 > 4.54 > 3.54)%.

It is clear that all mixes had average chloride conductivity values ranging between 0.75mS/cm - 1.50mS/cm indicating good durability.

From Figure 114 it is clear that both PC (Control mix), PCM and PCS mixed with WEEP had an increase in average chloride conductivity. It was also found that the replacement of different types of WEEP for the natural aggregate in PC (Control mix), PCM and PCS yielded different average chloride conductivity values.

From Table 32 it is clear that there was no specific WEEP type which produced the lowest average chloride conductivity. However, it is clear that ABS WEEP had the overall highest chloride conductivity and thus, lowest durability.

Table 32: WEEP types producing the highest and lowest average chloride conductivity at 28 days of curing.

Mix design	30% Replacement of WEEP for the natural aggregate	
	WEEP type producing the highest average chloride conductivity result	WEEP type producing the lowest average chloride conductivity result
PC (Control mix)	ABS	PC/ABS
PCM	ABS	PC/ABS
PCS	ABS	HIPS

It is clear that replacements of ABS WEEP had the highest average chloride conductivity indicating that replacements of ABS WEEP yielded the lowest durability when replaced in PC (Control mix). This may be due to the formation of calcium and silicon crystals between ABS WEEP and hcp, as shown in Figures 54 (p.82), 58 (p.84) and 62 (p.87). If the ITZ overlap one another they create a pathway for the chloride ions to pass through when a voltage is applied across the specimen. Thus, increasing the chloride conductivity of concrete mixed with ABS WEEP the most compared to other WEEP types.

5.4.3.4 Chloride conductivity for concrete made without WEEP replacement

PCM yielded the lowest average chloride conductivity followed by PCS and PC (Control mix). Therefore, PCM had the highest durability. This is due to PCM having the least amount of interconnecting pores through which ions could pass through the concrete matrix.

This can be explained by referring back to the pore-size and distribution curve, as shown in Figures 72 - 73 (p.97). Here it was seen that PCM had the lowest amount of open capillary pores. This resulted in less ions passing through the concrete matrix, reducing the chloride conductivity compared to PC (Control mix) and PCS.

5.5 Conclusion

The overall results and discussions showed that both concrete made with and without WEEP replacement for the natural aggregate attained structural strength. There was little strength difference at 28 days of curing between replacements of 30% HIPS or Blend WEEP in either PC (Control mix), PCM and PCS. However, replacements of ABS WEEP yielded the overall lowest average compressive and splitting tensile strength at 28 days of curing.

Furthermore, the durability results indicate that certain WEEP types can have similar or even higher durability results compared to concrete made without WEEP replacement for the natural aggregate.

Chapter 6: Environmental and financial significance

6.1 Introduction

In our information driven world, the use of EEE have become a prime source of communication and entertainment. However, the pursuit for faster and more efficient technologies have resulted in the increase of e-Waste. These wastes are often difficult to recycle as they contain numerous amounts of toxins that require strictly controlled recycling measures to prevent contamination from occurring (Lydall, *et al*., 2017).

WEEP is considered to be one the least economically valuable material of e-Waste and is often discarded, used as a filler material or as a plastic extender (Delgardo, *et al*., 2007). Replacing natural aggregates with granulated WEEP in concrete could encapsulate this problematic waste product while reducing the amount of natural aggregates mined.

This section assesses the possible environmental and financial significance of using WEEP as replacement material for the natural aggregate in concrete.

6.2 Environmental significance

The following sub-sections evaluates both the saving of natural resources and the reduction in the amount of WEEP discarded when using WEEP as an aggregate in concrete.

6.2.1 Saving of natural resources

The mining of natural aggregates can have a negative influence on the surrounding environment due to certain engineering activities performed during the extraction of the aggregates. This may cause a change in the geomorphology and visual scene which can permanently destroy the habitation in the surrounding environment (Mineral Economics, 2008).

Table 33 provides information pertaining to the quantity of natural aggregates and granulated WEEP required to produce 1m³ concrete for the PC (Control mix) designs and is then graphically illustrated in Figures 116.

Table 33: Total granulated WEEP used, and total natural aggregate saved per 1m³ concrete.

Mix design	Sand (kg/m³)	Stone (kg/m³)	WEEP (kg/m³)	Total natural aggregate saved (kg/m³)
PC (Control mix)	931	706	0	0
PC(ABS-5)	908	688	14	41
PC(ABS-10)	884	671	28	82
PC(ABS-20)	838	635	57	164
PC(ABS-30)	791	600	85	246
PC(PC/ABS-5)	908	688	21	41
PC(PC/ABS-10)	884	671	42	82
PC(PC/ABS-20)	838	635	84	164
PC(PC/ABS-30)	791	600	126	246
PC(HIPS-5)	908	688	18	41
PC(HIPS-10)	884	671	36	82
PC(HIPS-20)	838	635	72	164
PC(HIPS-30)	791	600	108	246
PC(Blend-5)	908	688	18	41
PC(Blend-10)	884	671	36	82
PC(Blend-20)	838	635	71	164
PC(Blend-30)	791	600	107	246

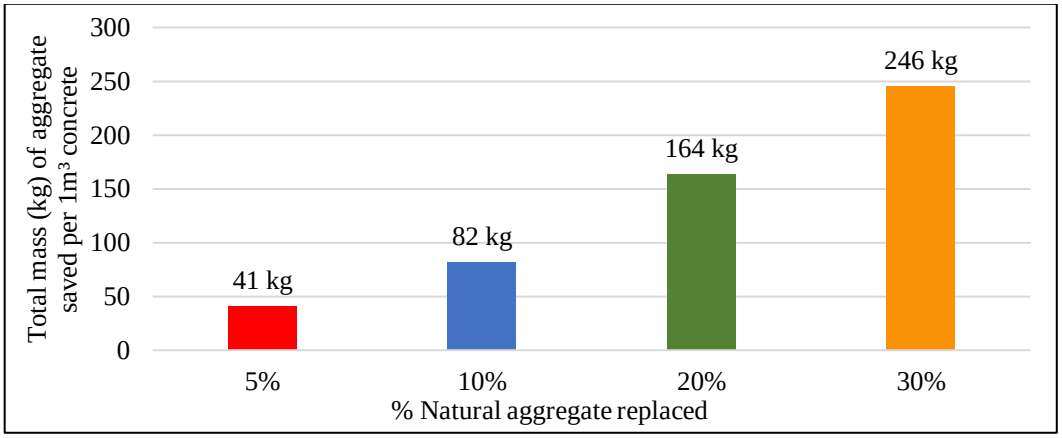

Figure 116: Total mass of natural aggregate saved per 1m³ concrete when replaced by 5%, 10%, 20% and 30% WEEP.

From Figure 116 it is clear that 30% WEEP replacement for the natural aggregate yielded the highest natural aggregate material savings at 246kg/m³.

6.2.2 Reducing the amount of WEEP discarded

As reviewed in Chapter 2, environmentally friendly recycling of WEEP is very challenging. Using WEEP as replacement for the natural aggregate may reduce the amount of WEEP dumped or incinerated, saving the natural environment.

Different quantities of WEEP were required to produce 1m³ of concrete depending on the type of WEEP substituted, as shown in Table 33 and Figure 117. This was the result of different WEEP types having different densities, as shown in Table 15 (p.59). Therefore, more PC/ABS WEEP was used to produce concrete and will hence be the most environmentally friendly concrete, compared to identical replacements by ABS or HIPS WEEP.

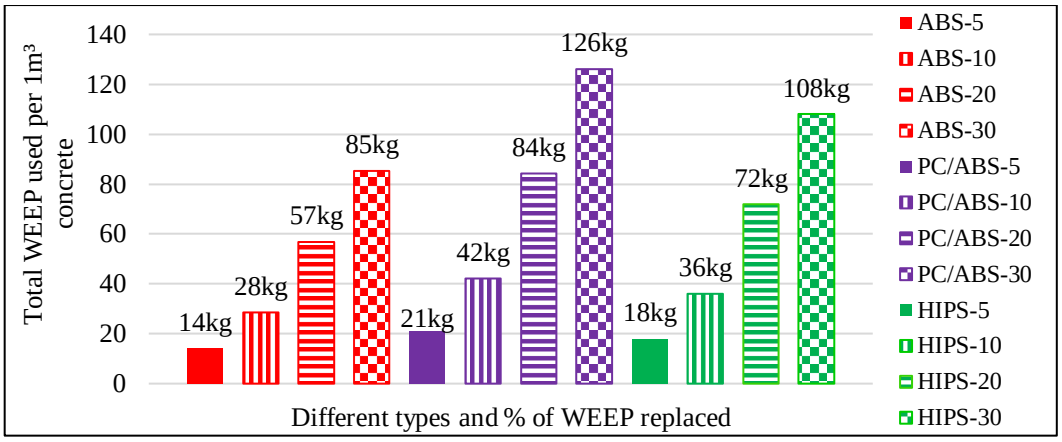

Figure 117: Total mass of different types WEEP used per 1m³ concrete.

6.3 Financial significance

It was not the aim of this study to perform a detailed cost analysis including the distance travelled from the quarry or granulation plant to the construction site. It was also not the aim to calculate the feasibility of implementing the use of WEEP as partial replacement for the natural aggregate in concrete. This section however evaluates the present cost of concrete made with and without WEEP replacement for the natural aggregate.

Moreover, it evaluates the cost of selective granulated WEEP namely ABS, PC/ABS and HIPS WEEP used in this study and as a blend of unknown quantities and types produced from mechanical recycling of e-Waste. Table 34 presents the cost of material per kg excluding VAT. at the end of April 2019 in Rands. It is clear that using selective granulated WEEP had a high financial cost, compared to sand and stone.

According to Newman and Choo (2003), a standard concrete mix typically uses 330kg/m³ cement and has a compressive strength ranging between 30MPa - 40MPa. This study used a cement content of 444kg/m³. This quantity of cement falls in the range of concrete made using plastic as aggregate replacement material. Lui *et al*. (2015), evaluated the *Performance of Recycled-Based Concrete* using a cement content of 555kg/m³. On the other hand, Kumar and Baskar (2015), investigated the *Recycling of E-plastic Waste as Construction Material in Developing Countries* and used a cement content of 376kg/m³. This is due to the fact that a high strength concrete is initially required as WEEP reduces the compressive strength of concrete.

However, if concrete containing WEEP would be used to replace structural concrete based on a compressive strength > 25MPa in the construction industry, then it should be compared to a conventional mix design. Therefore, the mix design and results from Alhassan (2014), who investigated *The Effects of Materials and Micro-Climate Variations on Predictions of Carbonation Rate in Reinforced Concrete in the Inland Environment* was used. Alhassan used a mix design using a w:c ratio = 0.75 and material quantities: CEM I 52.5R cement = 300kg/m³, coarse aggregates = 1050kg/m³, fine aggregates = 810kg/m³ and water = 225L/m³. The concrete had a 28 day compressive strength of 36MPa, OPI of 9.5 and a water sorptivity of 12.2mm√hr. These strength and durability results are similar to those obtained in this study and will therefore be used as a comparison. Using the material costs in Table 34, it was calculated that the cost of the concrete amounts to R941.40 per m³ concrete. This mix design is termed 'Comparison M35'.

Table 34: Material costs per kg (Rand).

Material	Sand	Stone	ABS	PC/ABS	HIPS	CEM	MK	CSF	SP	Water
Rand per kg or L	0.24	0.20	10.00	9.50	9.00	1.76	7.50	9.54	23.0	0.04

These high prices of selective WEEP may be the result of initial equipment expenses (plastic granulator), intense labour costs and machine operational and maintenance costs. If WEEP could be sourced from companies who mechanically recycle e-Waste, then these materials would be much cheaper.

Mechanical recycling of e-Waste involves the mechanical shredding of e-Wastes as whole components and uses different mechanisms to extract the valuable materials from the mix (Lydall *et al*., 2017). This produces an end-product WEEP which contain

unknown types and quantity of WEEP which cannot easily be recycled. The performance of this mix WEEP as replacement for the natural aggregate in concrete may however be more difficult to predict as different types of WEEP affect the strength and durability of concrete. Table 35 provides details pertaining to the cost per mix design made in this study.

Table 35: Cost of mix designs per m³ in Rand.

Mix design	Cost per m³ (Rand)	Additional cost (Rand)	Cost of mixed WEEP (Rand)	Reduction in cost (Rand)
Comparison (M35)	941	0		
PC (Control mix)	1 156	215		
PC(ABS-5)	1 289	348		
PC(ABS-10)	1 422	481		
PC(ABS-20)	1 697	756		
PC(ABS-30)	1 971	1 030		
PC(PC/ABS-5)	1 347	406		
PC(PC/ABS-10)	1 537	596		
PC(PC/ABS-20)	1 918	977		
PC(PC/ABS-30)	2 312	1 371		
PC(HIPS-5)	1 309	368		
PC(HIPS-10)	1 462	521		
PC(HIPS-20)	1 771	830		
PC(HIPS-30)	2 085	1 144		
PC(Blend-5)	1 288	347	1 147	9
PC(Blend-10)	1 376	435	1 138	18
PC(Blend-20)	1 691	750	1 125	30
PC(Blend-30)	1 968	1 027	1 119	36
PCM	1 827	0		
PCM(ABS-5)	1 995	168		
PCM(ABS-10)	2 128	301		
PCM(ABS-20)	2 414	587		
PCM(ABS-30)	2 688	861		
PCM(PC/ABS-5)	2 017	191		
PCM(PC/ABS-10)	2 208	381		
PCM(PC/ABS-20)	2 589	763		
PCM(PC/ABS-30)	3 005	1 179		
PCM(HIPS-5)	1 984	157		
PCM(HIPS-10)	2 145	318		
PCM(HIPS-20)	2 458	631		
PCM(HIPS-30)	2 768	942		
PCM(Blend-5)	1 971	144	1 830	-3
PCM(Blend-10)	2 074	247	1 836	-9
PCM(Blend-20)	2 388	561	1 822	5
PCM(Blend-30)	2657	831	1 808	18
PCS	1 501	0		
PCS(ABS-5)	1 639	138		
PCS(ABS-10)	1 778	277		
PCS(ABS-20)	2 057	555		

Mix design	Cost per m³ (Rand)	Additional cost (Rand)	Cost of mixed WEEP (Rand)	Reduction in cost (Rand)
PCS(ABS-30)	2 323	821		
PCS(PC/ABS-5)	1 661	160		
PCS(PC/ABS-10)	1 828	327		
PCS(PC/ABS-20)	2 150	649		
PCS(PC/ABS-30)	2 478	977		
PCS(HIPS-5)	1 654	153		
PCS(HIPS-10)	1 807	306		
PCS(HIPS-20)	2 124	622		
PCS(HIPS-30)	2 434	933		
PCS(Blend-5)	1 633	132	1 492	9
PCS(Blend-10)	1 721	220	1 483	18
PCS(Blend-20)	2 051	549	1 485	17
PCS(Blend-30)	2 323	822	1 474	27

From Table 35 it was clear that concrete made using WEEP to replace the natural aggregate in concrete was more expensive, compared to concrete made without WEEP. It is clear that the additional strength from the Control mix was R215 more per m³ compared to the Comparison (M35) mix. The use of PC/ABS WEEP in the PC (Control mix) doubled the price per m³ concrete, while it increased the price of both PCM and PCS. As PC/ABS WEEP had the highest density, more mass of PC/ABS WEEP was required to fill the same volume compared to HIPS or ABS WEEP. This resulted in the increased price of concrete made with PC/ABS WEEP. Although ABS WEEP was the most expensive per kg, less was required per m³ concrete, reducing the cost compared to PC/ABS and HIPS WEEP. It was also seen that concrete made with cement extenders had a higher financial cost, compared to using cement alone. The following sub-sections evaluates the financial cost for PC (Control mix), PCM and PCS mixed with and without WEEP.

6.3.1 Financial cost of using WEEP in PC (Control mix)

The data found in Table 35 is graphically presented in Figure 118 for PC (Control mix) made with and without WEEP replacement for the natural aggregate. The financial comparison of concrete made with and without sorted WEEP clearly showed that concrete made without WEEP had the lowest cost.

The cost of concrete containing sorted WEEP was observed to increase as the substitution increased. At 30% replacement of WEEP for the natural aggregate, the cost of concrete is shown in the following order:

PC(PC/ABS-30) > PC(HIPS-30) > PC(ABS-30) > PC (Control mix) > Comparison (M35).

i.e. R(2 312 > 2 085 > 1 971 > 1 156 > 941).

Here it is clear that replacements of ABS WEEP yielded concrete with the lowest cost followed by HIPS and PC/ABS WEEP.

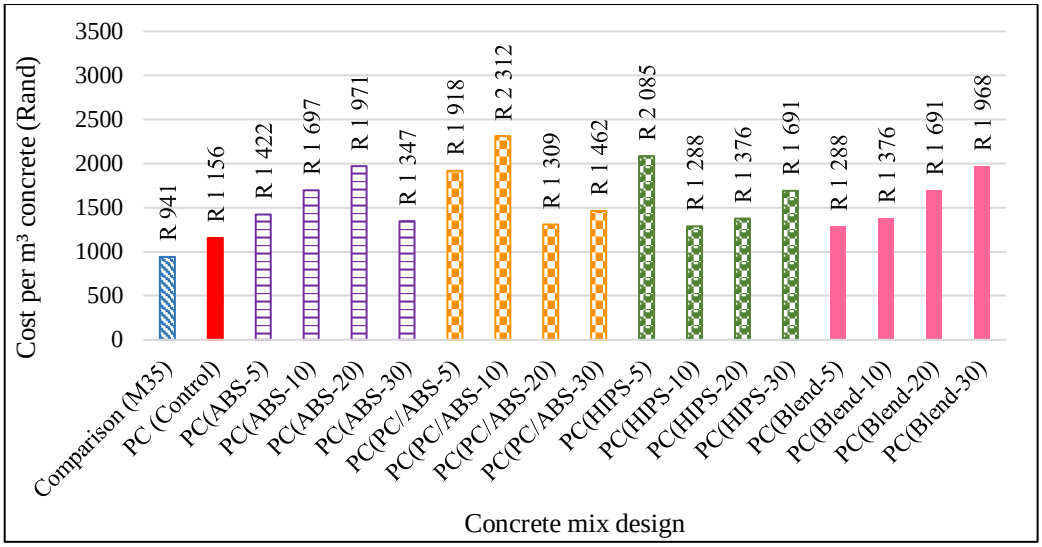

Figure 118: Concrete cost in Rand per m³ for PC with and without WEEP replacement for the natural aggregate.

6.3.2 Financial cost of using WEEP in PCM

The data found in Table 35 is graphically illustrated in Figure 119 for PCM mix designs made with and without WEEP replacements for the natural aggregate. As the total mass of WEEP replacements are the same as for PC (Control mix), the increase in price was dependent on the cost of MK and the superplasticiser used. It is therefore clear that concrete made using MK had a much higher financial cost. At 30% replacement of WEEP, the cost of concrete is shown in the following order:

PCM(PC/ABS-30) > PCM(HIPS-30) > PCM(ABS-30) > PCM > PC (Control mix) > Comparison (M35).

i.e. R(3 005 > 2 768 > 2 688 > 1 827 > 1 156 > 941).

Similar to the results found for the replacement of ABS WEEP in PC (Control mix), replacements of ABS WEEP in PCM yielded the lowest financial cost for concrete made using WEEP compared to other types of WEEP replacements.

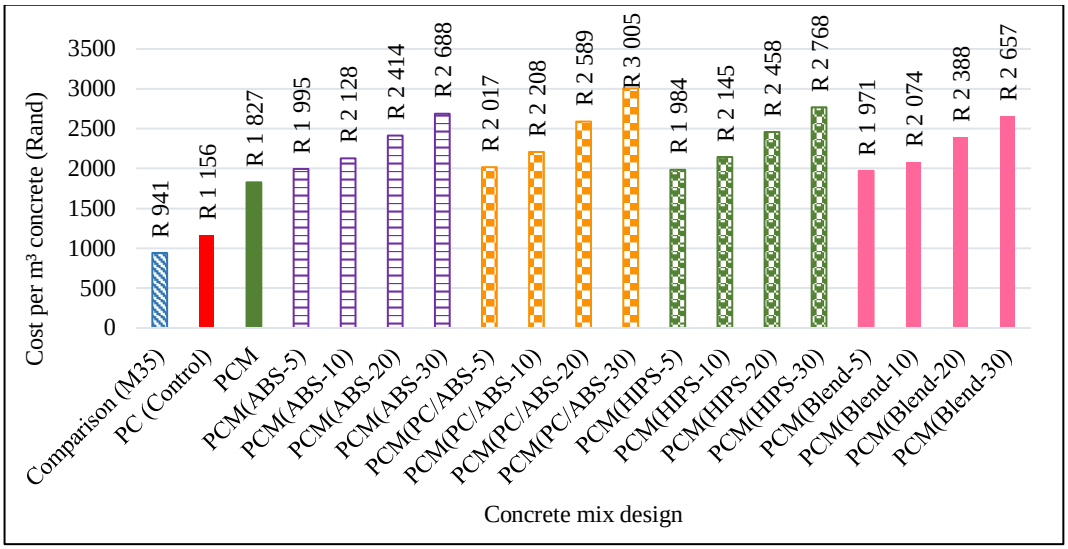

Figure 119: Concrete cost in Rand per m³ for PCM with and without WEEP replacement for the natural aggregate.

6.3.3 Financial cost of using WEEP in PCS

The data found in Table 35 is graphically illustrated in Figure 120 for PCS mix designs made with and without WEEP replacements. The financial cost of PCS made with WEEP was less compared to replacements of WEEP in PCM, but higher compared to replacements of WEEP in PC (Control mix). At 30% replacement of WEEP, the cost of concrete is shown in the following order:

PCS(PC/ABS-30) > PCS(HIPS-30) > PCS(ABS-30) > PCS > PC > Comparison (M35).

i.e. R(2 478 > 2 434 > 2 323 > 1 501 > 1 156 > 941).

Here it is seen that replacements of ABS WEEP yielded the lowest financial cost for concrete made using WEEP.

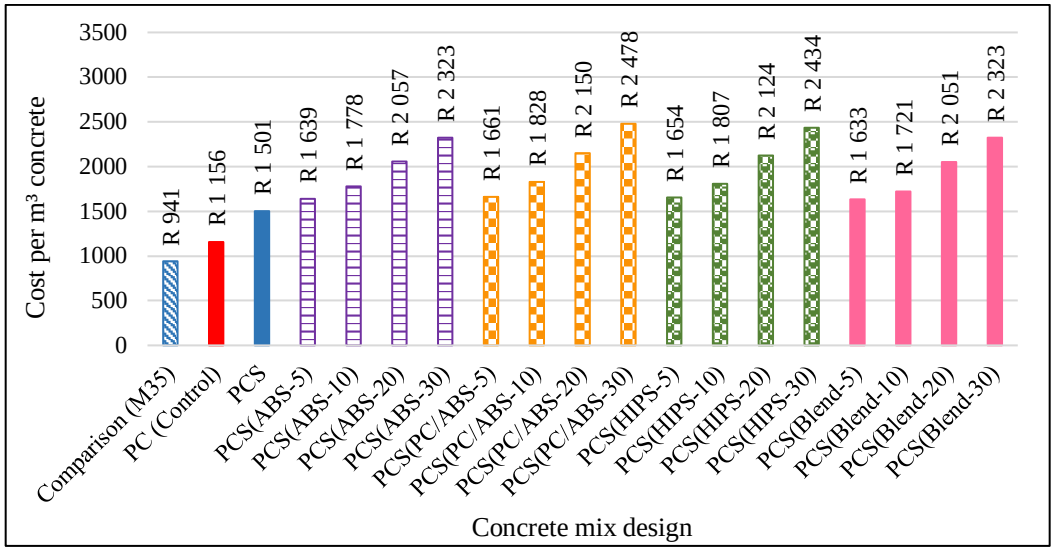

Figure 120: Concrete cost in Rand per m³ for PCS with and without WEEP replacement for the natural aggregate.

6.3.4 Financial cost of using mixed WEEP in concrete

Unlike experiments conducted in this study which evaluated the strength and durability of different types of WEEP in concrete, WEEP sourced from mechanical recyclers would have a mixture of ABS, PC/ABS and HIPS WEEP among others, in unknown ratios. As this material is not separated prior into its respective types, it is generally discarded and thus, has no monitory value.

However, using data found in this study certain assumptions could be made. If the batch of e-Waste destined for mechanical recycling had a lot of ABS WEEP in its EEE design, then a relationship between ABS and Blend WEEP mix designs could be made. This is similar to e-Waste consisting of a majority of PC/ABS or HIPS WEEP.

Data shown in Table 35 is graphically illustrated in Figure 121. Here it was seen that using mixed WEEP from a mechanical shredder may reduce the cost of concrete. This cost was calculated by excluding the price of WEEP from the concrete mix design.

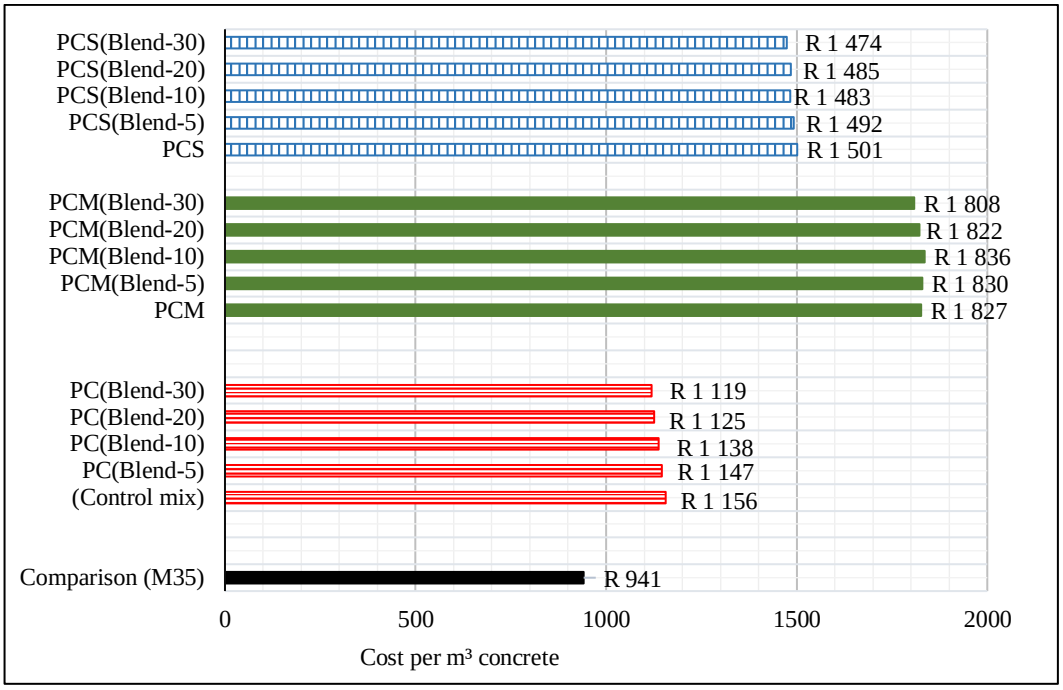

Figure 121: Concrete cost in Rand per m³ for concrete made with a blend of WEEP in unknown ratios derived from mechanical shredding.

From Figure 121 it is clear that substituting CSF and MK significantly increased the price compared to PC (Control mix) mixed with and without WEEP replacement for the natural aggregate.

6.3.5 Indirect financial significance of WEEP replacement in concrete

Figure 122 presents the reduction of mass in percentage for the different types of WEEP replacement in PC (Control mix). It is clear that replacement of 30% ABS WEEP yielded the highest reduction in mass at 6.9%. This is followed by replacements of 30% HIPS and 30% PC/ABS WEEP at 5.9% and 5.2%. This reduction in mass could reduce the dead load of a structure and in turn reduce the required member sizes.

This in turn may decrease the material quantities required during construction and hence reduce the overall project cost. Furthermore, the densities of WEEP are much lighter compared to the natural aggregates. This may reduce the fuel cost associated with hauling heavy natural aggregates from the quarry to the site.

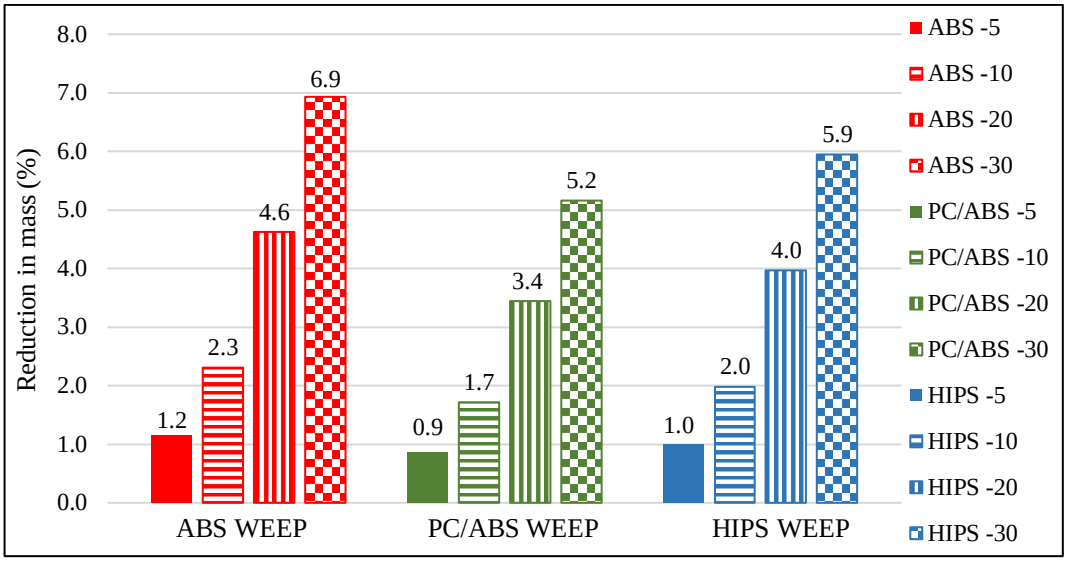

Figure 122: Reduction in mass using different types of WEEP.

6.4 Summary and conclusion

The partial replacement of WEEP for the natural aggregate has many environmental advantages. Not only could it reduce the amount of WEEP discarded, it could also reduce the amount of natural aggregates mined. It is however noted that concrete containing WEEP has a much higher financial cost compared to concrete containing no WEEP with similar strength and durability such as the 'Comparison (M35)' mix. This in turn may discourage investors from using WEEP as aggregate replacement material in concrete. However, the use of WEEP in concrete can be an environmentally friendly alternative compared to that of natural aggregates.

Chapter 7: General conclusion

7.1 Introduction

The increase in electrical and electronic equipment has resulted in vast quantities of WEEP discarded with no intention of re-use. The recycling of WEEP in concrete has the potential to reduce the amount of waste disposed of in landfills and to preserve natural resources with minimal environmental disturbances.

This chapter concludes the results found for the workability, strength, durability and the environmental and financial significance of using WEEP as partial replacement for coarse and fine natural aggregates in concrete.

This study has confirmed that ABS, PC/ABS, HIPS and an equal combination of the aforementioned WEEP can be used to partially replace both fine and coarse aggregates in percentages of 0%, 5%, 10%, 20% and 30% and attain the minimum compressive strength requirements for structural concrete set in the aim of this study of > 25MPa.

It was found that there was a negative linear relationship between the compressive strength of concrete and the percentage replacement of WEEP for the natural aggregate. It was also found that WEEP replacement for the natural aggregate reduced both the tensile splitting strength, OPI and water sorptivity but increased the chloride conductivity.

Substituting cement with MK or CSF increased both the strength and durability performance of concrete containing WEEP, however large quantities of superplasticiser was required to attain a suitable slump range. It was noticed that concrete containing 30% WEEP substitution for the natural aggregate resulted in reduced slump. At small dosages of superplasticiser, it was found that concrete containing WEEP had excessive bleeding. This was the results of the interaction of the smooth WEEP and the fresh concrete.

During initial mixing a film of water formed between the WEEP and the cement paste increasing the w:c ratio near the WEEP surface. This resulted in a weak microstructure forming between the WEEP and hcp. EDS analysis found that concrete containing ABS WEEP contained small crystals of calcium and silicon between the ABS WEEP and hcp which were responsible for the decrease in strength and durability performance.

7.1.1 Concluding remarks on workability

- Replacements of WEEP for the natural aggregates reduced the workability of concrete;
- The use of a superplasticiser increased the slump of concrete mixed with WEEP to the required slump; and
- The use of a superplasticiser in concrete replaced by 30% WEEP for natural aggregates experienced large amounts of bleeding.

7.1.2 Concluding remarks on strength

- Replacement of WEEP for the natural aggregate reduced the compressive strength of concrete at all ages of curing;
- All mixes made with and without WEEP as partial replacement for the natural aggregates attained structural strength at 28 days of curing;
- Replacing cement with CSF or MK increased the 28 and 90 day compressive and tensile splitting strength of all mixes made with and without WEEP replacement for the natural aggregate;
- The strength of PC (Control mix), PCM and PCS significantly decreased at 30% WEEP replacement for the natural aggregate at all ages of curing;
- Replacement of 30% ABS WEEP significantly decreased the compressive and tensile splitting strength of concrete the most, followed by 30% Blend WEEP. Replacements of 30% HIPS and 30% PC/ABS WEEP yielded the highest compressive and tensile splitting strengths for concrete made using WEEP as substitute material for the natural aggregate in concrete; and
- The compressive and tensile splitting strength of concrete made with and without WEEP replacement had a strong linear positive correlation.

7.1.3 Concluding remarks on durability

- Replacements of cement with MK or CSF increased the durability of all mixes compared to mixes made with only cement as binder material in concrete;
- All PC (Control mix) made without and with 30% WEEP replacement for the natural aggregates had a lower durability compared to PCM and PCS mix designs made with and without 30% WEEP replacements;

- Concrete made using ABS WEEP as replacement material for the natural aggregate had the overall lowest durability compared to mixes replaced with Blend, PC/ABS or HIPS WEEP; and

7.1.4 Concluding remarks on environmental and financial implications

- The use of WEEP has the potential to reduce the amount of WEEP disposed of in landfills or incinerated, preserve natural resources and reduce the degree of environmental disturbances;
- The high financial costs associated with the processing of WEEP may discourage the usage of the material in large scale projects. However, as the demand for the nations EEE and infrastructure grows, so will the potential for the use of WEEP as aggregate increase; and
- WEEP sourced from mechanical recycling of e-Waste may reduce the cost of concrete. However, it may have unpredictable strength and durability depending on the type and quality of WEEP used as replacement material for the natural aggregate.

7.2 Recommended WEEP replacement for an application

The recommended WEEP types replaced at 30% for natural aggregates at 28 days of curing are presented in Table 36. These results are based on the type of WEEP which performed the overall best in a particular test.

These WEEP types could be used to create concrete structures for both inland environments and coastal regions. These include road barricades, dolosse, foundations, retaining walls and pavements among others. The type of WEEP used will however depend on the type of binder material used and the environment it is exposed to.

Table 36: Recommended WEEP for a particular test.

Mix	Test				
	Compressive strength	Tensile strength	Oxygen permeability	Water sorptivity	Chloride conductivity
PC (Control mix)	PC/ABS	PC/ABS	HIPS	PC/ABS	PC/ABS
PCM	PC/ABS	PC/ABS	PC/ABS	HIPS	PC/ABS
PCS	HIPS	PC/ABS	HIPS	PC/ABS	HIPS

Chapter 8: Recommendations for future research

- Replace WEEP with a similar aggregate grading to those of the control mix. This in turn may improve the workability of concrete in the fresh state;
- Evaluate the fire resistance of concrete made with WEEP as aggregate replacement material. This may allow concrete to be used where fire resistance is required, such as in buildings used as hospitals, schools and office blocks among others;
- Evaluate the response of concrete made with WEEP when subjected to a dynamic loading. This will allow modelling of concrete behaviour in structures generally subjected to dynamic loading, such as bridges; and
- Study the erosion processes of concrete made with WEEP as natural aggregate replacement material. As WEEP is much softer compared to the natural aggregate, it may erode more easily in some environments.

References

Achilias, D.S, L Andriotis, I.A Koutsidis, D.A Louka, N.P Nianias, P Siafaka, I Tsagkalias, and G Tsintzou. 2012. *Recent Advances in the Chemical Recycling of Polymers (PP, PS, LDPE, HDPE, PVC, PC, Nylon, PMMA).* Material Recycling - Trends and Perspectives. http://www.intechopen.com/books/material-recycling-trends-and-perspectives/recent-advances-in-thechemical-recycling-of-polymers.

ACI:211.1-91. 1999. *Standard Practice for Selecting Proportions for Normal, Heavyweight, and Mass Concrete.* Farmington Hills, Michigan: American Concrete Institute.

Act, Hazardous Substances. 1973. "Hazardous Substances Act, 1973." *Government Gazette Republic of South Africa* 94 (3834). Accessed August 7, 2018. https://www.gov.za/sites/www.gov.za/files/Act%2015%20of%201973.pdf.

AfriSam. 2017. *Afrisam Technical Reference Guide.*

Akram, Amiya, C Sasidhar, and K Mehraj Pasha. 2015. "e-Waste Management by Utilisation of e-Plastics in Concrete Mixture as Coarse Aggregate Replacement." *International Journal of Innovative Research in Science* 5087-5095.

Alexander, M.G. 2004. "Durability Indexes and their Use in Concrete Engineering." *International RILEM Symposium on Concrete Science and Engineering: A Tribute to Arnon Bentur.* http://demo.webdefy.com/rilem-new/wp-content/uploads/2016/10/pro036-002.pdf.

Alexander, M.G, Y Ballim, and K Stanish. 2008. "A Framework for use Oof Durability Indexes in Performance Based Design and Specifications for Reinforced Concrete Structures." *Materials and Structures* 921–936.

Alexander, M.G., and B.J Magee. 1999. "Durability Performance of Concrete Containing Condensed Silica Fume." *Cement and Concrete Research* (Pergamon) 917–922. doi:PII: S0008-8846(99)00064-2.

Alexander, M.G., J Mackechnie, and Y Ballim. 2011. "Use of Durability Indexes to Achieve Durable Cover Concrete in Reinforced Concrete Structures." *Materials Science of Concrete* (American Ceramic Society Westerville).

Alhassan, Y.A. 2014. *The Effects of Materials and Micro - Climate Variations on Predictions of Carbonation Rate in Reinforced Concrete in the Inland Environment.* Johannesburg: The University of the Witwatersrand.

Arel, H.S. 2016. "Effects of Curing Type, Silica Fume Fineness, and Fiber Length on the Mechanical Properties and Impact Resistance of UHPFRC." *Results in Physics* 664–674.

Arends, D, M Schlummer, and A Ma¨urer. 2012. *Removal of inorganic colour pigments from acrylonitrile butadiene styrene by dissolution-based recycling.* J Mater Cycles Waste Manage.

Arnold, J.R. 2003. "High Quality Copper-Nickel-Chromium Plating on Plastics: A Continuous Process and its Challenges." *Plat Surf Finish* 91: 355–379.

Arroudj, K, A Zenati, M.N Oudjit, A Bali, and A Tagnit-Hamou. 2011. "Reactivity of Fine Quartz in Presence of Silica Fume and Slag." *Scientific Research* 569-576.

Arroudj, K, M Lanez, M.N Oudjit, and A Tagnit-Hamou. 2015. "Comparative Study of Chemical Activity of Different Ultrafine Cementitious Additions." *International Journal of Advanced Materials Research* 45-52.

Artioli, G, and J.W Bullard. 2013. "Cement Hydration: The Role of Adsorption and Crystal Growth." *Crystal Research and Technology* 903–918.

ASTM:D638. 2014. *Standard Test Method for Tensile Properties of Plastics.* West Conshohocken: ASTM International.

ASTM:D790. 2017. *Standard Test Methods for Flexural Properties of Unreinforced and Reinforced Plastics and Electrical Insulating Materials.* West Conshohocken: ASTM International.

Athavale, S.P. 2018. *Handbook of Printing, Packages and lamination.*

Bakera, A.T, and M.G Alexander. 2018. "Properties of Western Cape Concretes with Metakaolin." *MATEC Web of Conferences.* Creative Commons Attribution License. 1-14. https://doi.org/10.1051/matecconf/201819911011.

Baldé, C.P, F Wang, R Kuehr, and J. Huisman. 2014. *The Global e-Waste Monitor.* Bonn: United Nations University.

Baldé, C.P, V Forti, V Gray, R Kuehr, and P Stegmann. 2017. "The Global e-Waste Monitor." *United Nations University, International Telecommunication and International Solid Waste Association.*

Barbhuiya, S, P Chow, and S Memon. 2015. "Microstructure, Hydration and Nanomechanical Properties of Concrete Containing Metakaolin." *Construction and Building Materials* 696–702.

Baxter, J, Margareta W, M Castell-Rüdenhausen, and A Zu. Fråne. 2015. "WEEE Plastics Recycling: A Guide to Enhancing the Recovery of Plastics from Waste Electrical and Electronic Equipment." *The Nordic Region.*

Bennett, M, L Edwards, L Goyos-Ball, R Hilder, P Hall, L Morrish, R Mortin, and N Myles. 2009. *Separation of Mixed WEEE Plastics.* Axion Consulting. Accessed August 22, 2018. http://www.wrap.org.uk/sites/files/wrap/Separation%20of%20mixed%20WEEE%20plastics%20-%20Final%20report.pdf.

Bensted, J, and P Barnes. 2002. *Structure and Performance of Cements.* London: Taylor & Francis.

Beushausen, H, and M.G Alexander. 2008. "The South African Durability Index Tests in an International Comparison." *Journal of the South African Institution of Civil Engineering* 25–31.

Billmeyer, B.W. 1984. *Textbook of Polymer Science.* New York: John Wiley & Sons, Inc.

Blais, P, D.J Carlsson, G.W Csullg, and D.M Wiles. 1973. "The Chromic Acid Etching of Polyolefin Surfaces and Adhesive Bonding." *Journal of Colloi and Interface Science* (Academic Press) 47 (3): 636-649. Accessed June 5, 2018.

Bodogiannis, E, G Kakali, and S Tsivili. 2005. "Metakaolin as Supplementary Cementitious Material." *Journal of Thermal Analysis and Calorimetry* 457–462.

n.d. *Bonding of Low-energy Plastics and Rubbers.* Accessed June 3, 2018. https://www.smithersrapra.com/SmithersRapra/media/Sample-Chapters/Practical-Guide-to-Adhesive-Bonding.pdf.

Bortrill, R.S. 1991. *Silica Fume Analysis - A Preliminary Report.* Division of Mines and Mineral Resources, Tasmainia Department and Mineral Resources.

BS:2782-0. 2011. *Methods of testing plastic. Introduction.* British Standards Institution.

BS:882. 1992. *Specification for aggregates from natural sources for concrete.* British Standards.

Buekens, A, and J Yang. 2014. "Recycling of WEEE plastics: A Review." *Journal of Material Cycles and Waste* (Springer) 13 (3): 415–434. Accessed August 20, 2018. doi:10.1007/s10163-014-0241-2.

Bulut, H.A, and R Sahin. 2017. "A Study on Mechanical Properties of Polymer Concrete Containing Electronic Plastic Waste." *Composite Structures* (Elsevier, Science Direct) 50-62. doi:10.1016/j.compstruct.2017.06.058.

Bunaciu, A.A, E.G Udri¸Stioiu, and H.Y Aboul-Enein. 2015. "X-Ray Diffraction: Instrumentation and Applications." *Critical Reviews in Analytical Chemistry* (Taylor and Francis Group) 289–299.

Burke, M. 2007. "The Gadget Scrap Heap." (Chemistry World) 45-48.

Callister, William. 2007. *Materials Science and Engineering an Introduction.* 7. John Wiley and Sons, Inc.

Council. 2012. "Waste Electrical and Electronic Equipment. Directive 2012/19/EU of the European Parliament and of the Council." *Official Journal of the European Union.*

Crawford, R.J. 2002. *Plastics Engineering.* Belfast: Butterworth Heinemann.

Cui, T. n.d. "Dry Etching." Accessed June 2, 2018. me.umn.edu/courses/me8254/attfiles/Lecture%2007%20Dry%20Etching_Full.pdf.

Delgardo, C, L Barruetabena, and O Salas. 2007. "Assessment of the Environmental Advantages and Drawbacks of Existing and Emerging Polymers Recovery Processes." Edited by O Wolf. *European Commission* (Institute for Prospective Technological Studies). Accessed August 20, 2018. doi:10.2791/46661.

Desco. 2019. "Images supplied from Desco to the author." Johannesburg, Gauteng: Desco Electronic Recyclers.

Deurwaerder. 2006. "Modification of Polymer Surfaces before Painting." *Gis-surfaces.* Coatings Research Institute . October 26. Accessed June 1, 2018. http://www.gis-surfaces.be/Media_n/H%20De%20Deurwaerder.pdf.

Dhinakaran, G, S Thilgavathi, and J Venkataramana. 2012. "Compressive Strength and Chloride Resistance of Metakaolin Concrete." *KSCE Journal of Civil Engineering* 1209-1217.

Diffo, B.B.K, A Elimbi, M Cyr, J.D Manga, and H.T Kouamo. 2015. "Effect of the Rate of Calcination of Kaolin on the Properties of Metakaolin-Based Geopolymers." *Journal of Asian Ceramic Societies* 130–138.

Doolittle, A. n.d. "Etching Techniques." *Alan.ece.gatech.* Accessed June 1, 2018. http://alan.ece.gatech.edu.

Dumas, O, T Despreaux, F Perros, E Lau, P Andujar, M Humbert, and A Descatha. 2017. "Respratory Effects of Trichloroethylene." *Science Direct, Respiratory Medicine* (Elsevier) 47-53. Accessed June 4, 2018. doi:10.1016/j.rmed.2017.11.021.

2017. *Durability Index Manual.* University of Cape Town. http://www.uct.ac.za/sites/default/files/image_tool/images/333/Downloads/UCT-WITS%20DI%20Manual_2017%20Ver%204.2%202017-07-14.pdf.

Ebbing, D.D, and S.D Gammon. 2009. *General Chemistry.* Boston: Houghton Mifflin Company.

Egerton, R.F. 2005. *Physical Principles of Electron Microscopy.* Edmonton, Alberta: Springer Science and Business Media.

Escadeillas, G, and J.C Maso. 1991. "Approach of the Initial State in Cement Paste, Mortar, and Concrete." *American Ceramic Society* 169-184.

2017. "Etching and Deposition." *Nptel.* Accessed June 2, 2018. https://nptel.ac.in/courses/113106062/Lec26.pdf.

European Commission. 2011. "Plastic Waste in the Environment." *Institute for European Environmental Policy* (Bio-Intelligence Service). Accessed August 21, 2018.

eWasa. 2018. *e-Waste Association of South Africa.* May 28. https://ewasa.org.

Finlay, A, and D. Liechti. 2008. "e-Waste Assessment South Africa." (e-Waste Association of South Africa).

Fulton, F, and G Owens. 2009. *Fulton's Concrete Technology.* Midrand: Cement and Concrete Institute.

Garforth, A.A, S Alib, J Martı´nez H, and A Akah. 2005. "Feedstock Recycling of Polymer Wastes." *Science Direct* (Elsevier Ltd.) 419–425. Accessed August 23, 2018. doi:10.1016/j.cossms.2005.04.003.

Ghutke, V.S, and P.S. Bhandari. 2014. "Influence of Silica Fume on Concrete." *Journal of Mechanical and Civil Engineering* (International Conference on Advances in Engineering & Technology) 44-47.

Godfrey, L. 2016. "Industry Meets Science Workshop Proceedings. Waste electrical and electronic equipment – Seeking alternative solutions to disposal." *Department of Science and Technology* (Department of Science and Technology). http://www.wasteroadmap.co.za.

Gong, F, D Zhang, E Sicat, and T Ueda. 2013. "Empirical Estimation of Pore Size Distribution in Cement, Mortar, and Concrete." *Journal of Materials in Civil Engineering.*

Guneyisi, E, and K Mermerda. 2007. "Comparative Study on Strength, Sorptivity, and Chloride Ingress Characteristics of Air-Cured and Water-Cured Concretes Modified with Metakaolin." *Materials and Structures* 1161–1171.

Gutman, E, A Bobovitch, I Rubinchik, S Shefter, S Lach, L Utevski, and M Muskatel. 1995. "Thermal Degradation of Flame-retardant components in filled and unfilled ABS Plastics." *Polymer Degradation and Stability* (ELSEVIER) 399-402. doi:0141-3910(95)00122-0.

Hansen, H.R, and S.A Pergantis. 2006. "Detection of Antimony Species in Citrus Juices and Drinking Water Stored in Pet Containers." *Journal of Analytical Atomic Spectrometry* (8): 731-733.

Heath, J, and N Taylor. 2015. *Electron Probe Microanalysis.* Chichester: John Wiley & Sons.

Heikal, M, H El-Didamony, and F El-Raoof. 2004. "Electrical Properties, Physico-Chemical and Mechanical Characteristics of Fly Ash-Limestone-Filled Pozzolanic Cement." *Ceramics Silikaty* 49-58.

Heinrich, K. F. J. 1966. "X-Ray Optics and Microanalysis." *Proceedings* (4th International Congress on X-Ray Optics and Microanalysis, eds. R. Castaing, P. Deschamps, and J. Philibert, Hermann, Paris,) 1509.

Holland, T.C. 2005. *Silica Fume User's Manual.* Lovettsville: US Department of Transportation.

Honda, S, D.S Khetriwal, and R. Kuehr. 2016. *Regional e-Waste Monitor: East and Southeast Asia.* Vol. 1. United Nations University and Japanese Ministry of the Environment.

Hora´K, Z, I Fortelny, J Kolar´K, D Hlavat, and A Sikora. 2010. *Encyclopedia of Polymer Blends.* John Wiley & Sons.

Hund, J, J Naumann, and Th. Seelig. 2018. "An Experimental and Constitutive Modeling Study on the Large Strain Deformation and Fracture Behavior of PC/ABS Blends." *Mechanics of Materials* (Science Direct) 132–142.

Hunnicutt, W.A. 2013. *Characterization of Calcium-Silicate-Hydrate and Calciumalumino-Silicate-Hydrate.* Thesis, Urbana, Illinois: University of Illinois.

Imai, T, S Hamm, and K.P Rothenbacher. 2002. *Comparison of the Recyclability of Flame-Retarded Plastics.* Environmental Science and Technology.

Ionas, A.C, A.C Dirtu, T Anthonissen, H Neels, and A., Covaci. 2014. "Downsides of the Recycling Process: Harmful Organic Chemicals in Children's Toys." *Environment International* 54–62.

Jadhav, R, and N.C Debnath. 2011. "Computation of X-ray Powder Diffractograms of Cement Components and its Application to Phase Analysis and Hydration Performance of OPC Cement." *Bulletin of Materials Science* 1137–1150.

Kadri, E, H, S Aggoun, S Kenai, and A Kaci. 2012. "The Compressive Strength of High-Performance Concrete and Ultrahigh-Performance." *Advances in Materials Science and Engineering* (Hindawi Publishing Corporation) 1-7.

Kaech, A. 2013. *An Introduction to Electron Microscopy Instrumentation, Imaging and Preparation.* Zurich: Center for Microscopy and Image Analysis, University of Zurich.

Kaolin-Group. 2017. *Metakaolin KG-K40.* Cape Town: Kaolin-Group.

Kaplan, S.L, and P.W Rose. 1991. "Plasma Surface Treatment of Plastics to Enhance Adhesion." *International Journal Adhesion and Adhesives, Plasma Science* (Butterworth-Heinemann) 11 (2): 109-113. Accessed June 3, 2018. doi:0143-7496/91/020109-05.

Khedr, S.A, and M.N Abou-Zeid. 1994. "Characteristics of Silica-Fume Concrete." *J. Mater. Civ. Eng* 357-375.

Kontoleontos, F, P Tsakiridis, A Marinos, N Katsiotis, V Kaloidas, and M Katsioti. 2013. "Dry-grinded Ultrafine Cements Hydration. Physicochemical and Microstructural Characterization." *Materials Research* 404-416. doi:10.1590/S1516-14392013005000014.

Kumar, A, and R.K Gupta. 2003. *Fundamentals of Polymer Engineering.* New York: Marcel Dekker, Inc.

Kumar, S.K., and K Baskar. 2015. "Recycling of e-Plastic Waste as a Construction Material in Developing Countries." *Journal of Material Cycles and Waste Management* (Springer) 718–724. doi:10.1007/s10163-014-0303-5.

Lakshmi, R, and S Nagan. 2010. "Studies on Concrete Containing e-Plastic Waste." *International Journal of Environmental Sciences* 1 (3): 270-281.

Li, Z. 2011. *Advanced Concrete Technology.* Hoboken, New Jersey: JOHN WILEY & SONS, INC.

Liu, F, Y Yan, L Li, C Lan, and G Chen. 2015. "Performance of Recycled Plastic-Based Concrete." *Journal of Materials in Civil Engineering* (ASCE) A4014004-1-A4014004-9.

Lundgren, K. 2012. *The Global Impact of e-Waste, Addressing the Challenge.* Geneva: International Labour Organization.

Lundstedt, S. 2011. *Recycling and Disposal of Electronic Waste.* Bromma: Swedish Environmental Protection Agency.

Lydall, Marian , Wonder Nyanjowa, and Yulandi James. 2017. *Mapping South Africa's Waste Electrical and Electronic Equipment (WEEE) Dismantling, Pre-Processing and Processing Technology Landscape.* Vol. 7574. Johannesburg, Gauteng: Mintek.

Ma, H. 2014. "Mercury Intrusion Porosimetry in Concrete Technology: Tips in Measurement, Pore Structure Parameter Acquisition and Application." *Journal of Porous Materials* 207–215.

Mahesh, P, P Rajankar, and Vinod Kumar. 2012. *Improving Plastic Management in Delhi. A Report on WEEE Plastic Recycling.* New Delhi: Toxics Link. Accessed 8 20, 2018.

Malvern. 2016. *Particle Size Analysis of Cement Using the Technique of Laser Diffraction.* Worcestershire: Malvern Instruments Limited.

Manhart, A, O Osibanjo, D Rochart, N Isarin, and E Mueller. 2011. *Where are Weee in Africa? Findings from the Basel Convention e-Waste Africa Programme.* SBC, Geneva: Secretariat of the Basel Convention.

Manjunath, Ashwini. 2016. "Partial Replacement of e-Waste as Coarse Aggregate in Concrete." *Science Direct* (ELSEVIER) 731-739. doi:10.1016.

Marikunte, S.S, and S Nacer. 2012. "Interaction of Silica Fume and Water Content on Strength and Permeability of Concrete." *TRB 2012 Annual Meeting* 1-13.

Mehta, P.K, and P.J.M Monteiro. 2006. *Concrete Microstructure, Properties, and Materials.* California: Department of Civil and Environmental Engineering University of California at Berkeley.

2015. *Milton Plastics.* Accessed March 5, 2019. http://www.miltonplastics.com/index.php/Picture/show/6.html.

Mineral, Economics. 2008. *Overview of the South African Sand and Aggregate Industry.* Pretoria: Department of Mineral Resources.

Molewa, E. 2015. "Minister Molewa Leads National Consultative Conference on Electronic and Electrical Waste (e-Waste) Management in South Africa."

NEMA. 2008. "National Environmental Management: Waste Act, 2008." *Government Gazette Republic of South Africa* 525. Accessed August 7, 2018. https://www.environment.co.za/documents/legislation/NEMA-National-Environmental-Management-Act-Waste-Act-59-2008-G32000.pdf.

Newman, J, and B.S Choo, . 2003. *Advanced Concrete Technology.* Oxford: Butterworth-Heinemann.

Nilson, A.H, D Darwin, and C.W Dolan. 2010. *Design of Concrete Structures.* 14th. New York: Mc Graw Hill.

Odian, G. 2004. *Principles of Polymerization.* New Jersey: John Wiley & Sons, Inc.

Olivera, S, H.B Muralidhara, K Venkatesh, K Gopalakrishna, and C.S Vivek. 2016. "Plating on Acrylonitrile–Butadiene–Styrene Plastic: A Review." *Journal of Materials Science* (Springer). doi:10.1007/s10853-015-9668-7.

Oriol, M, and J Pera. 1995. "Pozzolanic Activity of Metakaolin Under Microwave Treatment." *Cement and Concrete Research* 265–270.

Ottavio, D. 1972. "Regeneration of Chromic Acid Etching Solutions." (United States Patents). Accessed June 4, 2018. https://patentimages.storage.googleapis.com/29/06/1b/45804c7a9fc65b/US3650859.pdf.

Owens, G. and Addis, B. 2012. *Fundamentals of Concrete.* Midrand: Cement and Concrete Institute.

Pallon, L.K.H, R.T., Liu, D Olsson, A.M Pourrahimi, M.S Hedenqvist, A.T Hoang, S Gubanski, and U.W Gedde. 2015. "Formation and the Structure of Freeze-Dried Mgo Nanoparticle Foams and their Electrical Behaviour in Polyethylene." *Journal of Materials Chemistry* 7523–7534.

Pathak, P., R Srivastava, and R Ojasvi. 2017. "Assessment of Legislation and Practices for the Sustainable Management of Waste Electrical and Electronic Equipment in India." *Renewable and Sustainable Energy Reviews* 220–232.

Peeters, J.R, P Vanegasa, L Tangec, J Houwelingend, and J.R Dufloua. 2014. "Closed Loop Recycling of Plastics Containing Flame Retardants." *ScienceDirect* (ELSEVIER) 35–43. doi:http://dx.doi.org/10.1016/j.resconrec.2013.12.006.

Pennell, K.D. 2016. "Specific Surface Area." 1-9. Medford: Tufts University.

Poon, C.S, S.C Kou, and L Lam. 2002. "Pore Size Distribution of High Performance Metakaolin Concrete." *Journal of Wuhan University of Technology Material Science* 42-46.

Richardson, M.G. 2002. *Fundamentals of Durable Reinforced Concrete.* London: Spon Press.

SANS:1083. 2013. *Aggregates from natural sources - Aggregates for concrete.* 2.3. Pretoria, Gauteng: South African Bureau of Standards.

SANS:201. 2008. *Sieve analysis, fines content and dust content of aggregates.* Vol. 2.2. Pretoria, Gauteng: South African Bureau of Standards.

SANS:3001-CO3-2. 2015. "Part CO3-2: Concrete durability index testing — Oxygen permeability test." Pretoria, Gauteng: South African Bureau of Standards.

SANS:3001-CO3-3. 2015. "Part CO3-3: Concrete durability index testing — Chloride conductivity test." Pretoria, Gauteng: South African Bureau of Standards.

SANS:5844. 2014. "Particle and relative densities of aggregates." Pretoria, Gauteng: South African Bureau of Standards.

SANS:5845. 2006. "Bulk densities and voids content of aggregates." Pretoria, Gauteng: South African Bureau of Standards.

SANS:5861-3. 2006. "Concrete tests. Part 3: Making and curing of test specimens." Pretoria, Gauteng: South African Bureau of Standards.

SANS:5862-1. 2006. "Concrete Tests. Consistence of Freshly Mixed Concrete: Slump Test." Pretoria, Gauteng: South African Bureau of Standards.

SANS:5863. 2006. "Concrete Tests — Compressive Strength of Hardened Concrete." Pretoria, Gauteng: South African Bureau of Standards.

SANS:6256. 2006. "Concrete Tests — Tensile Splitting Strength of Concrete." Pretoria, Gauteng: South African Bureau of Standards.

Sawant, Mithun, Chetan Pawar, Digvijay Shinde, Nikhil Shid, Suresh Vyavhare, and Sandeep Naykinde. 2017. "Study of Combine Effect of Silica Fume and e-Waste in Concrete." *International Research Journal of Engineering and Technology* 4: 93-95.

Siddique, R. 2008. *Waste Materials and By-Products in Concrete.* Springer.

Sika:3088. 2012. "Sika®ViscoCrete®-3088." Westmead, Gauteng: Sika. doi:02-01-01-01-200-0-000077.

Škvára, F, K Kolár, J Novotný, and Z Zadák. 1981. "The Effect of Cement Particle Size Distribution Upon Properties of Pastes and Mortars with Low Water-to-Cement Ratio." *Cement and Concrete Research* 247–255.

Snyder, K.A, D.P Bentz, E.J Garboczi, and D.N Winslow. 1992. "Interfacial Zone Percolation in Cement-aggregate Composites." *Interface in Cementitios Composites. RILEM Proceedings* 259-268.

Souza, T.M, A.P Luz, T Santos, D.C Gimenes, M.M Miglioli, A.M Correa, and V.C Pandolfelli. 2014. "Phosphate Chemicalbinderasananti-Hydrationadditive for Al2O3–MgO Refractorycastables." *Ceramics International* (Science Direct) 1503–1512.

Stenvall, Erik. 2013. *Electronic Waste Plastics Characterisation and Recycling by Melt-processing.* Gothenburg, Sweden: Department of Materials and Manufacturing Technology: Chalmers University of Technology. Accessed August 9, 2018. http://publications.lib.chalmers.se/records/fulltext/175356/175356.pdf.

Stutzman, P.E, P Feng, and J.W. Bullard. 2016. "Phase Analysis of Portland Cement by Combined Quantitative X-Ray Powder Diffraction and Scanning Electron Microscopy." *Journal of Research of the National Institute of Standards and Technology* 121. http://dx.doi.org/10.6028/jres.121.004.

Swetham, T., K,M,M Reddy, A. Huggi, and M,N., Kumar. 2017. "A critical review on of 3D printing materials and details of materials used in FDM." *International Journal of Scientific Research in Science, Engineering and Technology* 353–361.

Talsness, C.E, A.J.M Andrade, S.N Kuriyama, J.A Taylor, and F.S Saal. 2009. "Components of Plastic: Experimental Studies in Animals and Relevance for Human Health." *The Royal Society* 2079–2096.

Teuten, E.L., J.M. Saquing, and D.R.U Knappe. 2009. *Transport and Release of Chemicals from Plastics to the Environment and to Wildlife.* Philosophical Transactions of the Royal Society. doi:B 364:2027-2045.

2018. *The Concrete Institute.* Accessed October 1, 2018. https://www.theconcreteinstitute.org.za/durability.

Thomas, M.D, R.D Hooton, A Scott, and H Zibara. 2012. "The Effect of Supplementary Cementitious Materials on Chloride Binding in Hardened Cement Paste." *Cem. Concr. Res* 1–7.

Torres, D., S. Guzmán, R. Kuehr, F. Magalini, L Devia, A Cueva, E Herbeck, et al. 2016. *Sustainable Management of Waste Electrical and Electronic Equipment in Latin America.* South America.

2018. *Trading Economics.* April 19. https://tradingeconomics.com/south-africa/population .

Truc, T.T, C.H Lee, B.K Lee, and S.R Mallampati. 2015. "Separation of Hazardous Brominated Plastics from Waste Plastics by Froth Flotation after Surface Modification with Mild Heat-Treatment ." *International Journal of Chemical and Molecular Engineering* (World Academy of Science, Engineering and Technology. International Scholarly and Scientific Research and Innovation) 9 (12): 1388-1391. doi:scholar.waset.org/1307-6892/10003189.

Vahabi, H., R. Sonnier, and L., Ferry. 2015. "Effects Of Ageing on the Fire Behaviour of Flame-Retarded Polymers: A Review." *Polymer International* 313–328.

Vazquez, Y.V, and Barbosa, S.E. 2017. "Process Window for Direct Recycling of Acrylonitrile-Butadiene-Styrene and High-Impact Polystyrene from Electrical and Electronic Equipment Waste." *Waste Management* 403–408.

Walker, P, and W.H Tarn. 1991. *Handbook of Metal Etchants.* CRC Press LLC. https://vector.umd.edu/images/links/Handbook_of_Metal_Etchants.pdf.

Wang, A., C. Zhang, Ningsheng, and Z. 1999. "The Theoretic Analysis of the Influence of the Particle Size Distribution of Cement System on the Property of Cement." *Cement and Concrete Research* 1721–1726.

n.d. *Wet and Dry Etching.* University of Florida Chemical Engineering. Accessed June 3, 2018. http://ww2.che.ufl.edu/unit-ops-lab/experiments/semiconductors/etching/Etching-theory.pdf.

Wild, S, B,B Sabir, and J, M Khatib. 1995. "Factors Influencing Strength Development of Concrete Containing Silica Fume." *Cement and Concrete Research* 1567-1580.

Wong, M.H., S.C. Wu, and W.J. Deng. 2007. "Export of Toxic Chemicals - A Review of the Case of Uncontrolled Electronic Waste Recycling." *Environmental Pollution* 149:131-140.

Zhao, H, and D Darwin. 1990. *Quantitative Backscattered Electron Analysis Techniques For Cement Based Materials.* Lawrence: The University of Kansas.

Zhou, W, R.P Apkarian, Z.L Wang, and D Joy. 2006. *Fundamentals of Scanning Electron Microscopy.* New York: Springer.

Appendix A: Sieve analysis results

Table A1: Sieve analysis for fine natural aggregates.

Sieve size (mm)	Mass on each sieve (g)	Cumulative mass (g)	Cumulative % passing	Lower Limit	Upper limit
6.700	0.0	0.0	100.0	100	100
4.750	34.4	34.4	96.6	100	100
2.360	346.2	380.6	61.9	60	100
2.000	64.5	445.1	55.5	45	95
1.180	156.9	602.0	39.8	30	90
0.600	122.2	724.2	27.6	15	54
0.425	46.8	771.0	22.9	10	47
0.300	32.6	803.6	19.7	5	40
0.150	51.7	855.3	14.5	0	20
0.075	31	886.3	11.4		
Pan	113.9	113.9			
Sum	1 000.2				
Fineness modulus:	3.8				
Dust content (%)	9.9				

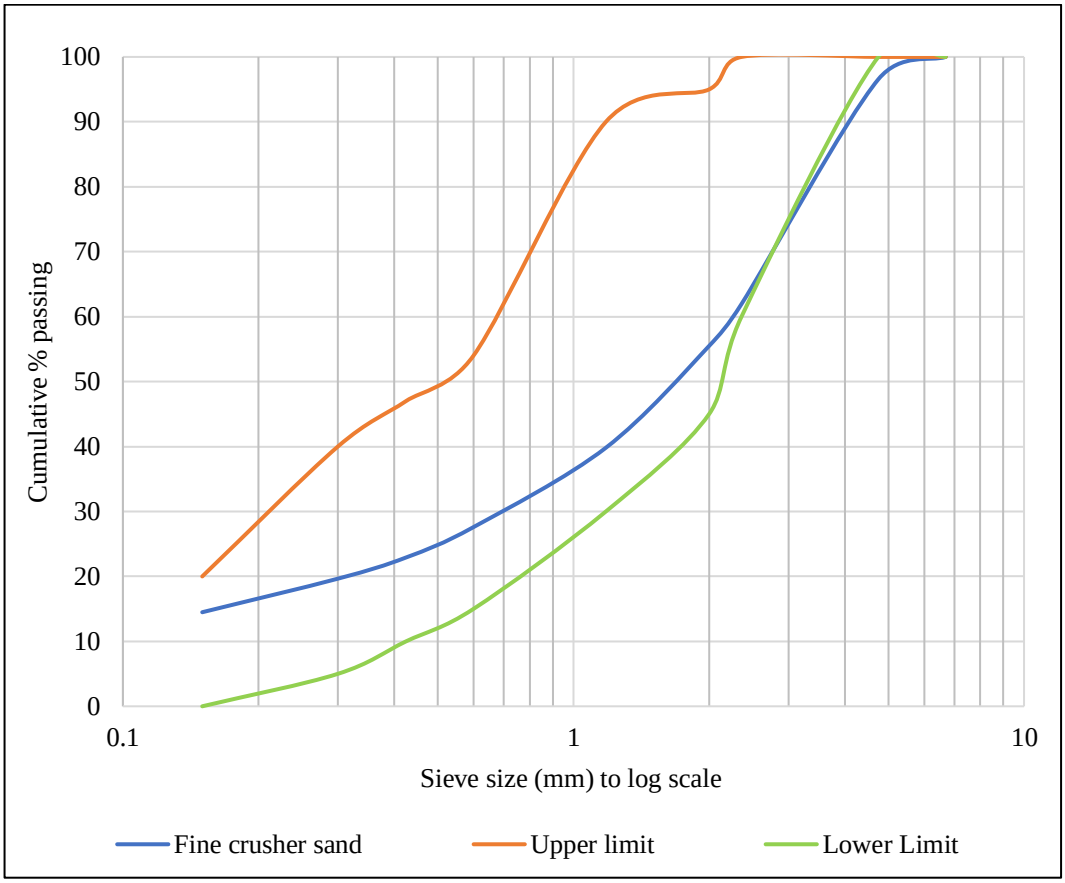

Figure A1: Grading curve for fine natural aggregates.

Table A2: Sieve analysis for 13.2mm natural aggregate.

Sieve size (mm)	Mass on each sieve (g)	Cumulative mass (g)	Cumulative % passing
19.000	0.0	0.0	100.0
16.000	40.3	40.3	98.4
13.200	685.1	725.4	71.0
9.500	1 513.1	2 238.5	10.5
6.700	204.1	2 442.6	2.3
4.750	4.4	2 447.0	2.1
2.360	0.1	2 447.1	2.1
2.000	0.0	2 447.1	2.1
1.180	0.0	2 447.1	2.1
0.600	0.1	2 447.2	2.1
0.425	0.0	2 447.2	2.1
0.300	0.2	2 447.4	2.1
0.150	0.2	2 447.6	2.1
0.075	1.2	2 448.8	2.1
Pan	51.8		
Sum	2 500.6		
Fineness modulus	6.2		
Dust content (%)	2.1		

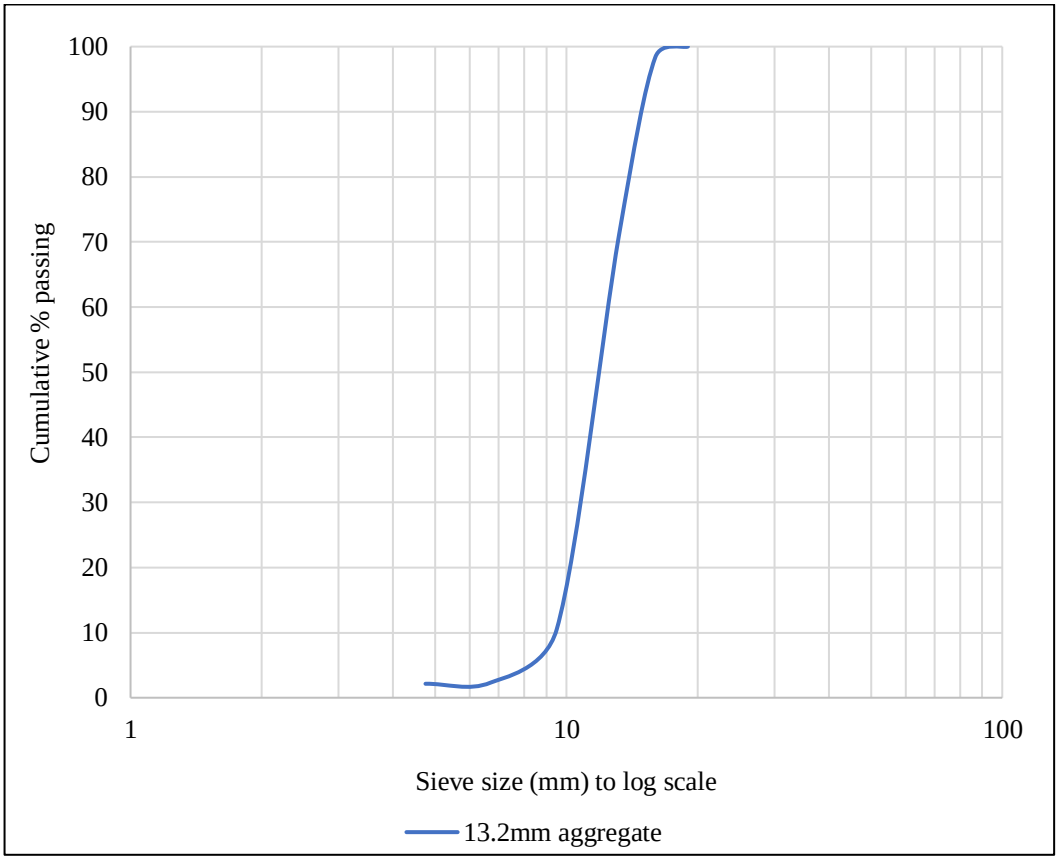

Figure A2: Grading curve for 13.2mm natural aggregates.

Table A3: Sieve analysis for 9.5mm natural aggregate.

Sieve size (mm)	Mass on each sieve (g)	Cumulative mass (g)	Cumulative % passing
13.200	0.0	0.0	100.0
9.500	293.1	293.1	88.3
6.700	1 872.5	2 165.6	13.4
4.750	288.1	2 453.7	1.9
2.360	28.4	2 482.1	0.7
2.000	8.1	2 490.2	0.4
1.180	0.7	2 490.2	0.4
0.600	0.6	2 490.9	0.4
0.425	0.2	2 490.9	0.4
0.300	0.1	2 490.9	0.4
0.150	0.1	2 490.9	0.4
0.075	0.1	2 490.9	0.4
Pan	9.2		
Sum	2 500.1		
Fineness modulus	5.9		
Dust content (%)	0.4		

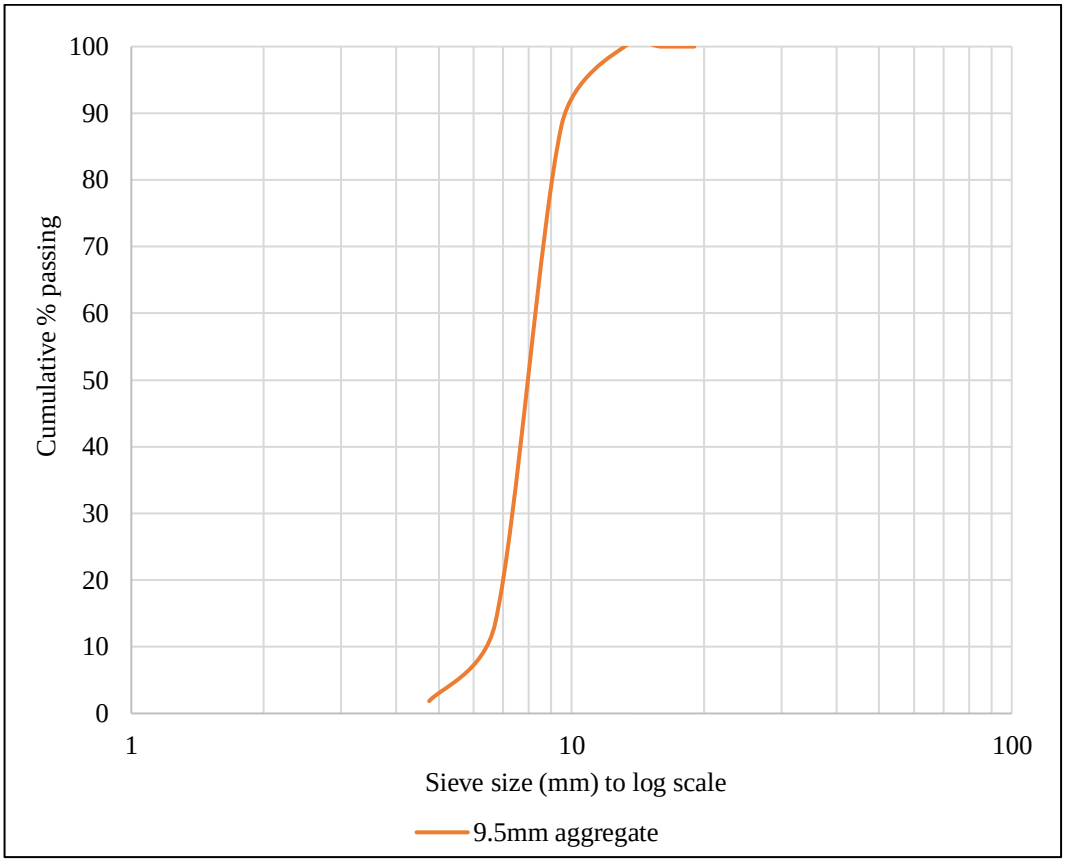

Figure A3: Grading curve for 9.5mm natural aggregates.

Table A4: Sieve analysis for ABS WEEP.

Sieve size (mm)	Mass on each sieve (g)	Cumulative mass (g)	Cumulative % passing	Lower Limit	Upper limit
9.500	0.0	0.0	100.0	100.0	100.0
6.700	7.6	7.6	96.2	72.5	100.0
4.750	57.4	65.0	67.5	45.0	100.0
2.360	112.7	177.7	11.1	0.0	30.0
2.000	0.1	177.8	4.6		
1.180	13.1	190.9	1.6		
0.600	5.9	196.8	1.0		
0.425	1.3	198.1	0.7		
0.300	0.5	198.6	0.5		
0.150	0.5	199.1	0.3		
0.075	0.3	199.4	0.0		
Pan					
Fineness	6.0				

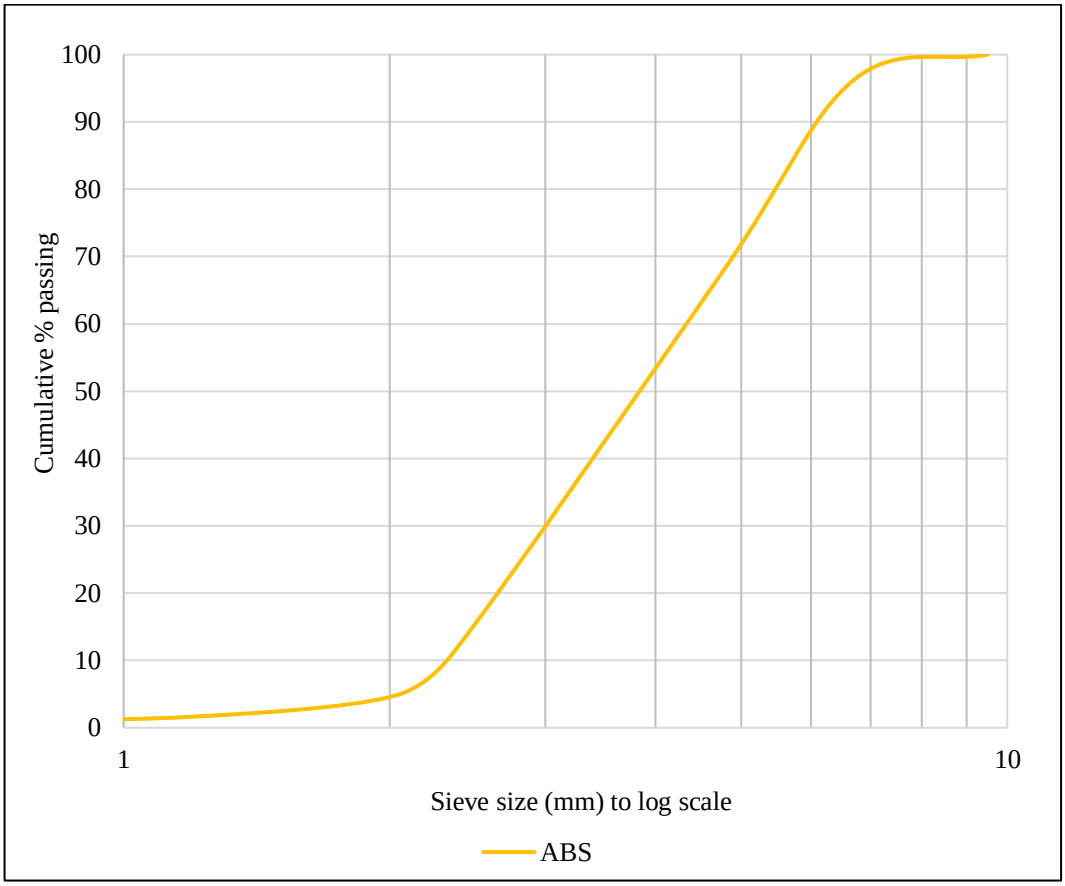

Figure A4: Grading curve for ABS WEEP.

Table A5: Sieve analysis for HIPS WEEP.

Sieve size (mm)	Mass on each sieve (g)	Cumulative mass (g)	Cumulative % passing	Lower Limit	Upper limit
9.500	0.0	0.0	100	100	100
6.700	1.0	1.0	99.5	72.5	100
4.750	43.2	44.2	77.9	45	100
2.360	140.6	184.8	7.6	0	30
2.000	14.1	198.9	0.5		
1.180	0.6	199.5	0.3		
0.600	0.0	199.5	0.3		
0.425	0.1	199.6	0.2		
0.003	0.0	199.6	0.2		
0.150	0.0	199.6	0.1		
0.075	0.0	199.6			
Pan					
Fineness modulus	6.0				

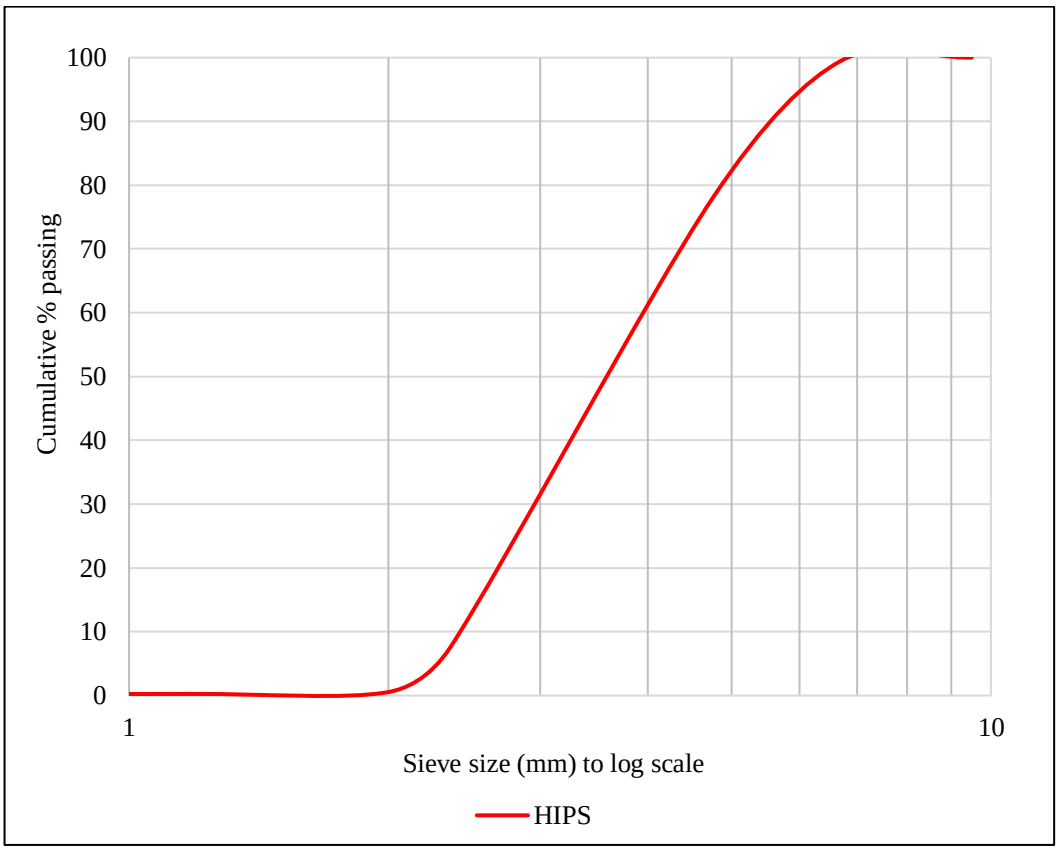

Figure A5: Grading curve for HIPS WEEP.

Table A6: Sieve analysis for PC/ABS WEEP.

Sieve size (mm)	Mass on each sieve (g)	Cumulative mass (g)	Cumulative % passing	Lower Limit	Upper limit
9.500	0.0	0.0	100.0	100.0	100.0
6.700	3.3	3.3	98.3	72.5	100.0
4.750	48.3	51.6	74.2	45.0	100.0
2.360	137.6	189.2	5.4	0.0	30.
2.000	5.0	194.2	2.9		
1.180	4.7	198.9	0.5		
0.600	0.6	199.5	0.2		
0.425	0.0	199.5	0.2		
0.300	0.0	199.5			
0.150	0.0	199.5			
0.075	0.0	199.5			
Pan					
Fineness modulus	6.0				

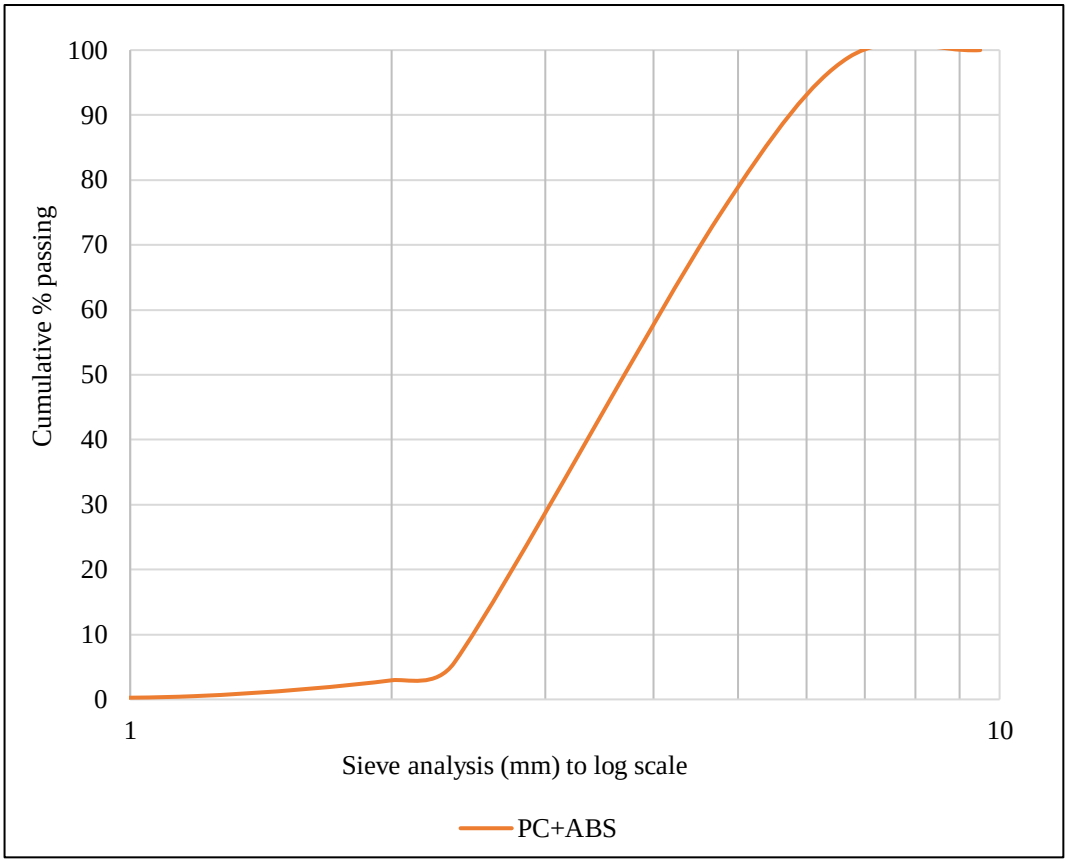

Figure A6: Grading curve for PC/ABS WEEP.

Appendix B: Trial mix designs

Two different trial mix designs were made using a 13.2mm and 9.5mm natural aggregate. This was done as WEEP was granulated into a single sized aggregate as presented in Table 20 and could either replace the fine, coarse or both fine and coarse aggregates. Thus, trial mixes replaced 5% and 20% of the natural aggregate with PC/ABS WEEP by volume. Furthermore, 5% MK and 5% CSF replaced cement by mass respectively to assess the concretes workability's and compressive strength when replaced with a pozzolan. Therefore, based on the strength and workability the final mix design could either use a 13.2mm or 9.5mm aggregate, while WEEP could replace either fine, coarse or both fine and coarse aggregates.

From Tables B2 - B3 it was found that mixes having both their fine and coarse natural aggregates replaced with 20% PC/ABS WEEP yielded the overall highest 28 day compressive strength. Moreover, it was found that TS1(M20) had a higher compressive strength compared to TS2(M20) i.e. (55.9MPa vs 48.5MPa) and had a higher slump for concretes which had both their coarse and fine aggregates replaced i.e. (15mm vs 10mm). Therefore, the 13.2mm aggregate was used as coarse aggregate in this study.

Table B1: Acronyms used for trial mix designs.

Acronym			
TS1	T = Trial mix using 13.2mm stone	ST***2***	2 = Trial mix using 9.5mm stone
T***S***1	S = Control mix	ST1 (***5***F)	5% replacement aggregate
T***M***1	M = 5% replacement of cement with metakaolin	ST1 (10***F***)	Replacement of fine aggregate/sand
T***C***1	C = 5% replacement of cement with condensed silica fume	ST1 (5***C***)	5% replacement of coarse aggregate/stone
TS***1***	1 = Using 13.2mm stone		

Table B2: Compressive strength for trial mixes (1).

		Slump (mm)	3 Day strength (MPa) (test 1)	3 Day strength (MPa) (test 2)	3 Day strength (MPa) (test 3)	3 Day strength (MPa) (average)	7 Day strength (MPa) (test 1)	7 Day strength (MPa) (test 2)	7 Day strength (MPa) (test 3)	7 Day strength (MPa) (average)	14 Day strength (MPa) (test 1)	14 Day strength (MPa) (test 2)	14 Day strength (MPa) (test 3)	14 Day strength (MPa) (average)	28 Day strength (MPa) (test 1)	28 Day strength (MPa) (test 2)	28 Day strength (MPa) (test 3)	28 Day strength (MPa) (average)
Use of 13.2mm stone	TS1	80	42.8	42.2	43.1	42.7	46.7	46.0	46.1	46.3	53.2	52.1	53.0	52.7	54.3	54.6	55.2	54.7
	TM1	55	44.3	43.8	41.9	43.3	55.4	51.4	52.3	53.0	59.5	61.7	58.2	59.8	60.4	60.1	61.4	60.6
	TC1	80	39.1	37.9	40.1	39.0	48.0	48.4	49.1	48.5	53.2	52.5	55.0	53.6	62.6	59.9	62.4	61.6
Trial mix replacing 13.2mm stone with WEEP	TS1 (C5)	70	40.6	41.4	41.9	41.3	47.6	46.3	46.5	46.8	51.5	52.1	48.8	50.8	55.3	54.7	54.8	54.9
	TS1 (C20)	30	38.1	37.6	37.9	37.9	42.6	42.3	41.0	42.0	43.0	44.8	43.4	43.8	48.8	45.4	47.6	47.3
	TM1 (C5)	40	44.2	43.9	43.3	43.8	49.6	51.4	50.9	50.6	54.3	51.7	54.5	53.5	56.3	57.4	56.5	56.7
	TM1 (C20)	10	37.1	37.3	36.7	37.0	41.8	43.0	42.7	42.5	44.7	46.0	45.8	45.5	47.7	46.9	46.5	47.0
	TC1 (C5)	70	38.3	37.5	38.3	38.0	46.5	42.8	47.4	45.6	51.5	54.2	52.7	52.8	54.9	56.9	55.6	55.8
Trial mix replacing sand with WEEP	TS1 (F5)	70	40.7	41.2	39.7	40.5	45.6	47.2	45.2	46.0	49.1	49.7	49.6	49.5	53.7	54.4	53.9	54.0
	TS1 (F20)	10	34.2	33.4	32.5	33.4	37.8	37.2	37.3	37.4	39.9	38.7	40.0	39.5	42.9	42.3	43.0	42.7
	TM1 (F5)	30	41.0	41.2	39.5	40.6	50.3	48.8	50.0	49.7	50.1	51.1	52.2	51.1	55.9	55.1	57.2	56.1
	TM1 (F20)	0	34.7	35.1	35.2	35.0	40.9	41.4	41.1	41.2	42.7	44.4	44.3	43.8	42.7	43.2	42.9	42.9
	TC1 (F5)	60	34.8	34.8	35.4	35.0	43.4	45.8	43.4	44.2	51.2	49.4	49.8	50.1	53.2	54.9	54.0	54.0
Trial mix replacing sand and 13.2mm stone with WEEP	TS1 (M5)	80	40.0	37.2	38.5	38.6	47.9	46.2	47.0	47.0	50.7	52.5	51.4	51.5	55.3	55.7	54.5	55.2
	TS1 (M20)	15	33.2	35.9	34.4	34.5	38.9	39.4	38.4	38.9	42.8	41.8	42.5	42.4	55.1	56.6	56.0	55.9
	TM1 (M5)	50	39.3	39.2	40.2	39.5	51.3	51.4	50.0	50.9	56.0	57.0	54.7	55.9	47.3	42.3	43.9	44.5
	TM1 (M20)	15	34.7	34.2	34.5	34.5	43.3	41.2	41.1	41.9	45.1	49.9	43.8	46.3	46.1	47.0	46.0	46.3
	TC1 (M5)	60	39.4	39.3	37.0	38.6	46.8	49.4	46.6	47.6	56.2	52.2	56.0	54.8	62.0	59.5	61.1	60.9

Table B3: Compressive strength for trial mixes (2).

		Slump (mm)	3 Day strength (MPa) (test 1)	3 Day strength (MPa) (test 2)	3 Day strength (MPa) (test 3)	3 Day strength (MPa) (average)	7 Day strength (MPa) (test 1)	7 Day strength (MPa) (test 2)	7 Day strength (MPa) (test 3)	7 Day strength (MPa) (average)	14 Day strength (MPa) (test 1)	14 Day strength (MPa) (test 2)	14 Day strength (MPa) (test 3)	14 Day strength (MPa) (average)	28 Day strength (MPa) (test 1)	28 Day strength (MPa) (test 2)	28 Day strength (MPa) (test 3)	28 Day strength (MPa) (average)
Use of 9.5mm stone	TS2	70	38.4	38.2	38.4	38.3	51.0	49.5	50.0	50.2	56.2	54.5	55.5	55.4	59.3	60.4	58.8	59.5
	TM2	40	43.8	48.8	44.9	45.8	54.8	54.4	57.1	55.4	60.2	61.8	61.0	61.0	63.0	62.8	63.4	63.1
	TC2	70	39.2	39.8	39.8	39.6	49.6	49.6	48.8	49.3	57.2	57.1	54.5	56.3	61.8	64.5	61.2	62.5
Trial mix Replacing 9.5mm stone with WEEP	TS2 (C5)	35	42.4	43.2	42.0	42.5	47.7	47.3	46.7	47.2	51.4	49.4	49.9	50.2	57.6	57.2	55.1	56.6
	TS2 (C20)	10	38.4	39.1	37.7	38.4	42.7	45.4	42.8	43.6	46.6	45.1	44.7	45.5	46.3	49.3	49.5	48.3
	TM2 (C5)	25	44.3	44.0	46.0	44.8	52.2	51.3	52.4	51.9	55.1	54.7	55.0	54.9	58.9	58.3	55.9	57.7
	TM2 (C20)	5	36.1	37.3	37.8	37.1	41.3	42.3	42.5	42.0	44.5	42.9	44.3	43.9	47.5	44.6	46.5	46.2
	TC2 (C5)	45	37.4	38.7	36.7	37.6	46.3	48.2	46.6	47.0	54.3	54.6	54.8	54.6	59.3	60.1	57.7	59.0
Trial mix Replacing sand with WEEP	TS2 (F5)	50	42.5	41.7	42.6	42.3	47.0	46.2	47.1	46.7	49.8	50.4	50.7	50.3	53.9	55.5	54.8	54.7
	TS2 (F20)	20	35.0	34.2	34.5	34.6	37.4	38.0	37.0	37.5	42.0	40.8	41.8	41.5	42.1	42.3	42.5	42.3
	TM2 (F5)	25	40.1	40.9	42.8	41.3	49.8	51.8	51.0	50.9	52.4	52.8	53.8	53.0	57.6	57.0	56.3	56.9
	TM2 (F20)	0	36.1	37.0	35.1	36.1	40.4	40.3	39.9	40.2	43.5	45.6	43.4	44.1	42.8	43.4	43.6	43.3
	TC2 (F5)	70	37.3	36.4	36.0	36.6	43.3	43.4	43.0	43.2	48.1	49.3	48.9	48.8	53.4	54.5	53.9	53.9
Trial mix replacing sand and 9.5mm stone with WEEP	TS2 (M5)	30	37.8	37.3	38.9	38.0	46.6	46.5	47.3	46.8	49.8	50.4	50.7	50.3	55.7	54.9	56.9	55.8
	TS2 (M20)	10	39.5	35.9	37.3	37.6	40.5	41.5	42.3	41.4	46.0	44.8	45.8	45.5	48.4	47.4	49.9	48.5
	TM2 (M5)	20	37.0	37.2	37.5	37.2	48.8	49.9	48.4	49.0	52.4	52.8	53.8	53.0	58.1	59.4	48.8	55.5
	TM2 (M20)	0	33.1	32.1	32.7	32.7	42.8	42.7	42.7	42.7	43.5	45.6	43.4	44.1	46.5	47.0	47.8	47.1
	TC2 (M5)	30	40.9	40.8	41.4	41.0	50.8	49.5	47.6	49.3	56.7	57.8	59.0	57.8	61.7	63.2	64.2	63.0

Appendix C: Compressive strength results for all mix designs

Table C1: Compressive strength results for all mix designs.

Concrete mix design	3 Day fcu						7 Day fcu						28 Day fcu						90 Day fcu					
	fcu (1)	fcu (2)	fcu (3)	fcu (Ave)	S.D	CoV (%)	fcu (1)	fcu (2)	fcu (3)	fcu (Ave)	S.D	CoV (%)	fcu (1)	fcu (2)	fcu (3)	fcu (Ave)	S.D	CoV (%)	fcu (1)	fcu (2)	fcu (3)	fcu (Ave)	S.D	CoV (%)
PC (Control mix)	36.8	38.4	37.3	37.5	0.8	2.2	46.2	46.9	46.2	46.4	0.4	0.9	58.5	57.7	56.6	57.6	1.0	1.7	61.9	60.2	58.3	60.1	1.8	3.0
PC(ABS-5)	32.4	36.6	36.6	35.2	2.4	6.9	41.0	43.4	43.4	42.6	1.4	3.2	50.1	49.5	49.3	49.6	0.4	0.8	54.7	52.7	52.6	53.3	1.2	2.2
PC(ABS-10)	30.8	32.5	31.1	31.5	0.9	2.8	37.5	38.5	37.4	37.8	0.6	1.7	45.4	43.9	43.2	44.2	1.1	2.6	50.1	50.2	47.3	49.2	1.7	3.4
PC(ABS-20)	29.4	28.4	28.5	28.8	0.5	1.9	34.3	33.3	34.4	34.0	0.6	1.7	39.0	37.8	37.5	38.1	0.8	2.1	42.6	42.0	41.7	42.1	0.5	1.1
PC(ABS-30)	18.8	19.1	19.4	19.1	0.3	1.6	22.4	20.6	23.3	22.1	1.4	6.3	26.5	25.1	23.6	25.1	1.4	5.7	28.8	26.7	25.5	27.0	1.6	6.1
PC(PC/ABS-5)	36.2	37.4	38.6	37.4	1.2	3.2	43.5	44.6	42.4	43.5	1.1	2.5	49.3	51.4	50.4	50.4	1.1	2.2	54.0	52.9	52.5	53.1	0.8	1.4
PC(PC/ABS-10)	35.8	36.6	36.3	36.3	0.4	1.1	40.6	41.4	40.1	40.7	0.6	1.6	46.1	46.3	47.1	46.5	0.5	1.1	46.9	46.5	46.4	46.6	0.3	0.6
PC(PC/ABS-20)	34.0	33.7	34.7	34.2	0.5	1.5	38.6	35.0	38.9	37.5	2.2	5.8	42.3	41.8	40.9	41.6	0.7	1.8	43.1	42.7	45.6	43.8	1.5	3.5
PC(PC/ABS-30)	32.4	35.7	31.6	33.2	2.2	6.6	38.0	34.9	36.4	36.4	1.5	4.2	41.6	41.1	38.7	40.5	1.6	3.8	40.6	40.1	42.1	40.9	1.0	2.5
PC(HIPS-5)	37.4	37.7	36.0	37.0	0.9	2.5	42.2	44.7	39.7	42.2	2.5	5.9	51.4	49.6	50.4	50.5	0.9	1.8	51.7	51.0	50.7	51.1	0.5	1.0
PC(HIPS-10)	33.8	34.1	34.1	34.0	0.2	0.5	39.1	39.8	39.6	39.5	0.4	0.9	46.1	46.2	46.0	46.1	0.1	0.2	48.3	46.1	45.6	46.7	1.4	3.1
PC(HIPS-20)	32.6	31.5	32.9	32.3	0.7	2.2	35.3	36.3	35.1	35.5	0.7	1.8	41.6	39.7	38.2	39.8	1.7	4.3	41.8	40.4	41.0	41.1	0.7	1.8
PC(HIPS-30)	34.6	33.3	34.2	34.0	0.7	2.0	37.8	40.6	37.0	38.5	1.9	4.9	40.2	39.9	38.6	39.5	0.8	2.1	38.7	40.8	42.5	40.7	1.9	4.7
PC(Blend-5)	37.1	37.0	37.2	37.1	0.1	0.3	43.5	43.0	42.2	42.9	0.6	1.5	50.2	49.6	48.3	49.4	1.0	1.9	54.9	52.6	52.5	53.3	1.4	2.6
PC(Blend-10)	35.2	33.9	35.5	34.9	0.9	2.5	41.4	41.8	41.0	41.4	0.4	1.0	47.2	46.4	46.0	46.5	0.6	1.4	51.1	50.0	48.7	49.9	1.2	2.4
PC(Blend-20)	31.0	31.4	31.6	31.3	0.3	0.9	36.1	37.5	36.9	36.8	0.7	1.9	42.5	42.5	41.0	42.0	0.9	2.1	42.9	42.5	42.0	42.5	0.4	1.0
PC(Blend-30)	32.0	31.1	31.8	31.6	0.5	1.6	36.4	34.9	33.3	34.9	1.6	4.5	38.9	36.9	36.7	37.5	1.2	3.1	39.0	38.2	35.3	37.5	1.9	5.1
PCM	41.8	41.3	40.6	41.2	0.6	1.4	59.5	59.6	58.8	59.3	0.4	0.8	71.5	70.2	68.9	70.2	1.3	1.9	74.1	73.4	72.9	73.5	0.6	0.8
PCM(ABS-5)	40.3	39.2	39.1	39.5	0.7	1.7	54.9	53.4	53.8	54.0	0.8	1.4	64.3	64.0	61.7	63.3	1.4	2.3	67.0	64.6	64.1	65.2	1.5	2.4
PCM(ABS-10)	33.7	34.2	31.0	33.0	1.7	5.2	44.5	47.0	47.6	46.4	1.6	3.5	53.5	52.1	51.5	52.4	1.0	2.0	56.4	54.7	53.3	54.8	1.5	2.8
PCM(ABS-20)	28.8	27.9	27.9	28.2	0.6	2.0	33.6	34.1	34.7	34.1	0.5	1.5	41.1	41.5	41.4	41.3	0.2	0.5	44.8	43.3	42.1	43.4	1.3	3.1
PCM(ABS-30)	27.1	26.7	26.6	26.8	0.3	1.0	23.8	22.3	23.0	23.0	0.8	3.3	39.7	38.3	38.2	38.8	0.8	2.2	44.3	39.8	38.5	40.9	3.0	7.4
PCM(PC/ABS-5)	41.2	39.7	39.8	40.2	0.8	2.0	52.6	49.5	50.5	50.8	1.6	3.1	61.4	60.1	58.5	60.0	1.4	2.4	62.9	61.7	61.6	62.1	0.7	1.2

Concrete mix design	3 Day fcu						7 Day fcu						28 Day fcu						90 Day fcu					
	fcu (1)	fcu (2)	fcu (3)	fcu (Ave)	S.D	CoV (%)	fcu (1)	fcu (2)	fcu (3)	fcu (Ave)	S.D	CoV (%)	fcu (1)	fcu (2)	fcu (3)	fcu (Ave)	S.D	CoV (%)	fcu (1)	fcu (2)	fcu (3)	fcu (Ave)	S.D	CoV (%)
PCM(PC/ABS-10)	41.6	41.0	42.5	41.7	0.7	1.8	53.6	50.4	52.2	52.1	1.6	3.0	62.9	60.6	59.6	61.0	1.7	2.7	58.3	64.9	62.0	61.8	3.3	5.4
PCM(PC/ABS-20)	36.8	37.3	38.3	37.5	0.7	2.0	46.6	48.0	45.7	46.7	1.2	2.5	53.6	52.5	53.2	53.1	0.5	1.0	55.0	54.8	54.0	54.6	0.5	1.0
PCM(PC/ABS-30)	35.1	36.5	37.4	36.3	1.1	3.1	44.7	45.1	43.8	44.5	0.7	1.6	49.8	47.6	49.8	49.1	1.3	2.6	52.3	51.7	48.6	50.9	2.0	3.9
PCM(HIPS-5)	41.1	41.1	40.9	41.0	0.1	0.2	55.4	57.5	56.5	56.4	1.1	1.9	61.0	63.7	63.1	62.6	1.4	2.3	57.6	57.1	56.8	57.2	0.4	0.8
PCM(HIPS-10)	35.6	34.4	35.6	35.2	0.7	2.0	48.5	48.8	50.2	49.1	0.9	1.8	55.6	56.3	56.2	56.0	0.4	0.7	59.1	55.3	54.9	56.4	2.3	4.1
PCM(HIPS-20)	36.6	33.4	35.5	35.2	1.6	4.5	48.1	48.6	46.0	47.6	1.4	2.9	52.6	53.3	52.3	52.7	0.5	1.0	55.5	53.1	51.3	53.3	2.1	4.0
PCM(HIPS-30)	39.6	38.4	38.1	38.7	0.8	2.0	46.0	47.0	44.3	45.8	1.4	3.0	50.5	48.6	47.9	49.0	1.3	2.7	51.8	51.4	49.4	50.8	1.3	2.5
PCM(Blend-5)	40.5	41.4	41.0	41.0	0.4	1.1	56.7	56.6	57.5	56.9	0.5	0.9	67.0	66.9	64.3	66.1	1.5	2.3	70.9	70.2	68.3	69.8	1.4	1.9
PCM(Blend-10)	42.3	42.2	41.8	42.1	0.3	0.7	54.0	51.7	57.7	54.5	3.1	5.6	62.7	61.7	60.7	61.7	1.0	1.6	65.3	63.8	61.8	63.6	1.8	2.8
PCM(Blend-20)	36.0	37.0	36.2	36.4	0.5	1.4	46.7	44.0	45.7	45.4	1.4	3.0	52.0	51.1	47.6	50.3	2.3	4.7	51.3	51.2	50.4	51.0	0.5	1.0
PCM(Blend-30)	32.9	35.7	33.8	34.2	1.4	4.2	41.4	44.4	45.3	43.7	2.0	4.6	49.4	47.4	45.6	47.5	1.9	4.1	48.3	46.3	47.5	47.4	1.0	2.2
PCS	38.9	35.7	35.5	36.7	1.9	5.2	47.8	47.6	47.3	47.6	0.2	0.5	60.2	59.4	59.0	59.5	0.6	1.0	65.2	64.8	61.1	63.7	2.3	3.5
PCS(ABS-5)	31.6	30.5	30.0	30.7	0.8	2.6	39.6	39.3	39.0	39.3	0.3	0.7	53.7	52.4	52.4	52.8	0.7	1.4	58.5	58.3	54.3	57.1	2.4	4.2
PCS(ABS-10)	28.7	28.0	28.6	28.4	0.4	1.5	36.7	37.3	37.7	37.2	0.5	1.3	48.4	48.1	47.9	48.1	0.2	0.5	51.7	51.3	51.1	51.4	0.3	0.6
PCS(ABS-20)	25.1	25.2	25.8	25.3	0.4	1.4	25.6	26.1	26.7	26.1	0.5	2.0	41.1	40.5	39.2	40.2	1.0	2.4	42.8	42.2	41.3	42.1	0.8	1.8
PCS(ABS-30)	17.0	17.7	17.0	17.3	0.4	2.2	23.8	22.3	23.0	23.0	0.8	3.3	33.4	31.7	31.0	32.0	1.2	3.8	33.5	33.2	32.2	33.0	0.7	2.1
PCS(PC/ABS-5)	32.0	32.4	31.2	31.9	0.6	1.9	40.9	39.6	39.4	40.0	0.8	2.0	55.9	54.9	53.6	54.8	1.2	2.1	57.4	53.4	56.5	55.8	2.1	3.8
PCS(PC/ABS-10)	34.3	33.5	34.7	34.2	0.6	1.8	43.9	44.0	43.9	43.9	0.0	0.0	55.7	54.6	56.3	55.5	0.9	1.6	57.6	56.5	55.2	56.4	1.2	2.1
PCS(PC/ABS-20)	32.1	30.9	30.6	31.2	0.8	2.6	39.5	39.0	40.5	39.7	0.8	2.0	48.0	47.7	43.9	46.6	2.3	5.0	50.2	46.4	48.3	48.3	1.9	4.0
PCS(PC/ABS-30)	28.4	26.3	27.1	27.3	1.0	3.7	36.9	37.0	37.5	37.1	0.3	0.9	39.4	40.3	40.2	40.0	0.5	1.3	40.1	38.0	48.3	42.1	5.4	12.9
PCS(HIPS-5)	34.5	34.4	34.0	34.3	0.3	0.9	43.4	41.9	43.0	42.8	0.8	1.9	53.1	50.8	54.5	52.8	1.9	3.5	56.8	56.6	56.3	56.5	0.3	0.5
PCS(HIPS-10)	33.4	31.5	33.1	32.7	1.0	3.0	43.9	43.4	43.6	43.6	0.2	0.6	49.0	55.9	52.6	52.5	3.4	6.5	54.9	54.6	54.4	54.7	0.3	0.5
PCS(HIPS-20)	28.9	30.2	29.4	29.5	0.6	2.2	36.6	36.8	38.1	37.1	0.8	2.2	47.0	46.0	46.1	46.4	0.6	1.2	46.0	45.7	47.5	46.4	1.0	2.1
PCS(HIPS-30)	29.3	28.7	27.8	28.6	0.7	2.6	38.9	39.4	37.3	38.5	1.1	2.8	42.7	41.4	41.0	41.7	0.9	2.1	42.2	43.6	43.3	43.0	0.7	1.7
PCS(Blend-5)	34.5	32.8	33.1	33.5	0.9	2.7	40.8	42.0	41.0	41.3	0.7	1.6	53.0	52.5	52.1	52.6	0.5	0.9	58.5	55.7	54.9	56.4	1.9	3.4
PCS(Blend-10)	33.2	33.7	33.3	33.4	0.3	0.8	40.5	40.3	40.2	40.3	0.2	0.5	50.1	50.0	49.6	49.9	0.3	0.5	53.7	53.4	52.2	53.1	0.8	1.5
PCS(Blend-20)	31.1	30.9	31.5	31.2	0.3	1.0	37.1	37.3	37.4	37.3	0.1	0.3	44.9	43.7	43.1	43.9	0.9	2.1	48.6	46.9	43.7	46.4	2.5	5.4
PCS(Blend-30)	27.9	27.8	27.4	27.7	0.3	1.0	33.1	32.7	32.4	32.7	0.4	1.1	40.1	39.3	36.4	38.6	2.0	5.1	40.9	40.8	39.2	40.3	0.9	2.3

Appendix D: Correlation between PC, PCM, PCS and its different types of WEEP substitution

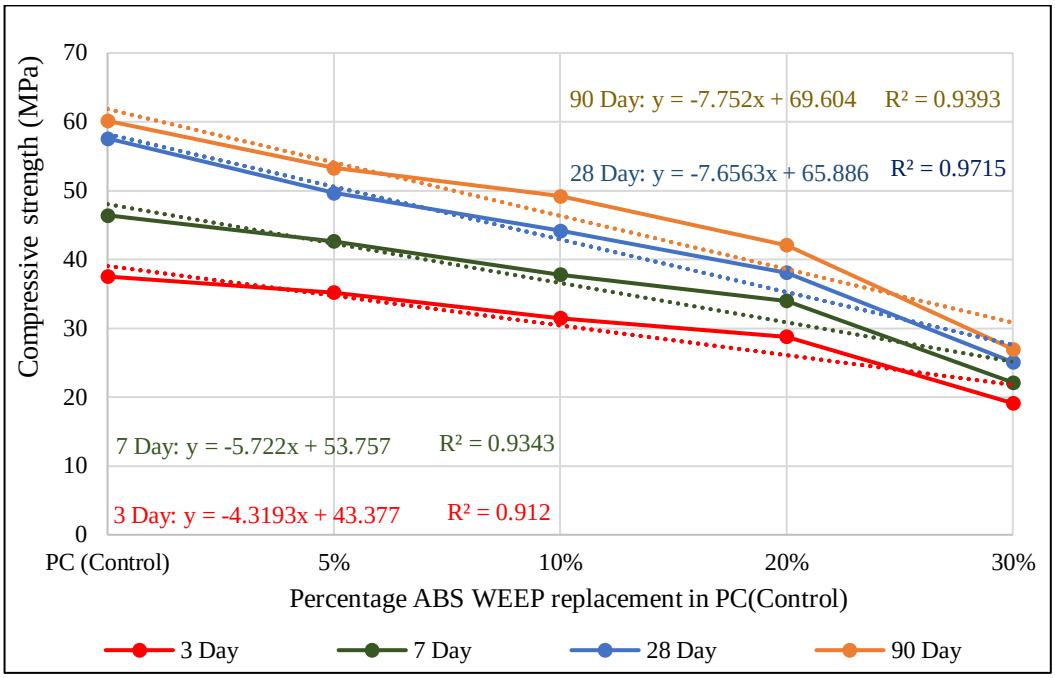

Figure D1: Correlation between PC (Control) and ABS WEEP at different ages.

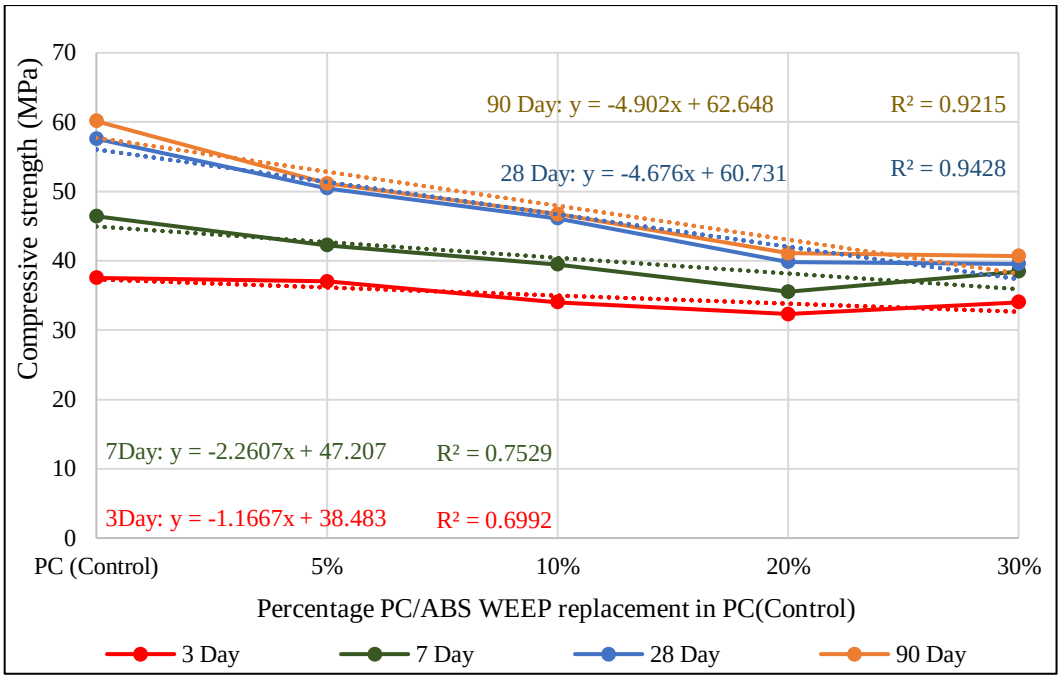

Figure D2: Correlation between PC (Control mix) and PC/ABS WEEP at different ages.

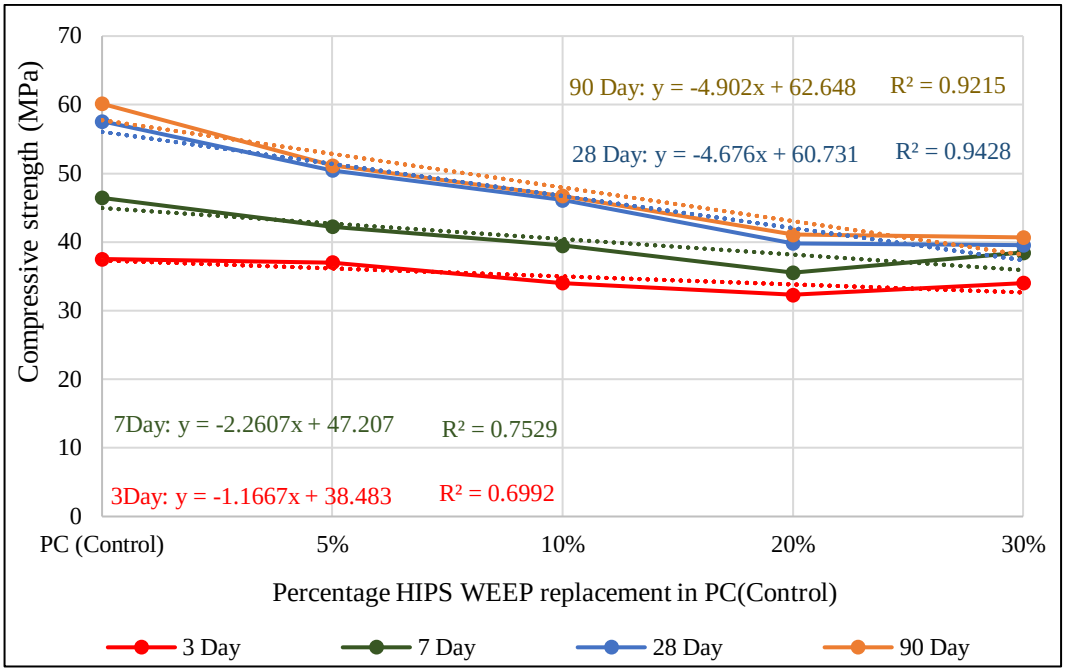

Figure D3: Correlation between PC (Control mix) and HIPS WEEP at different ages.

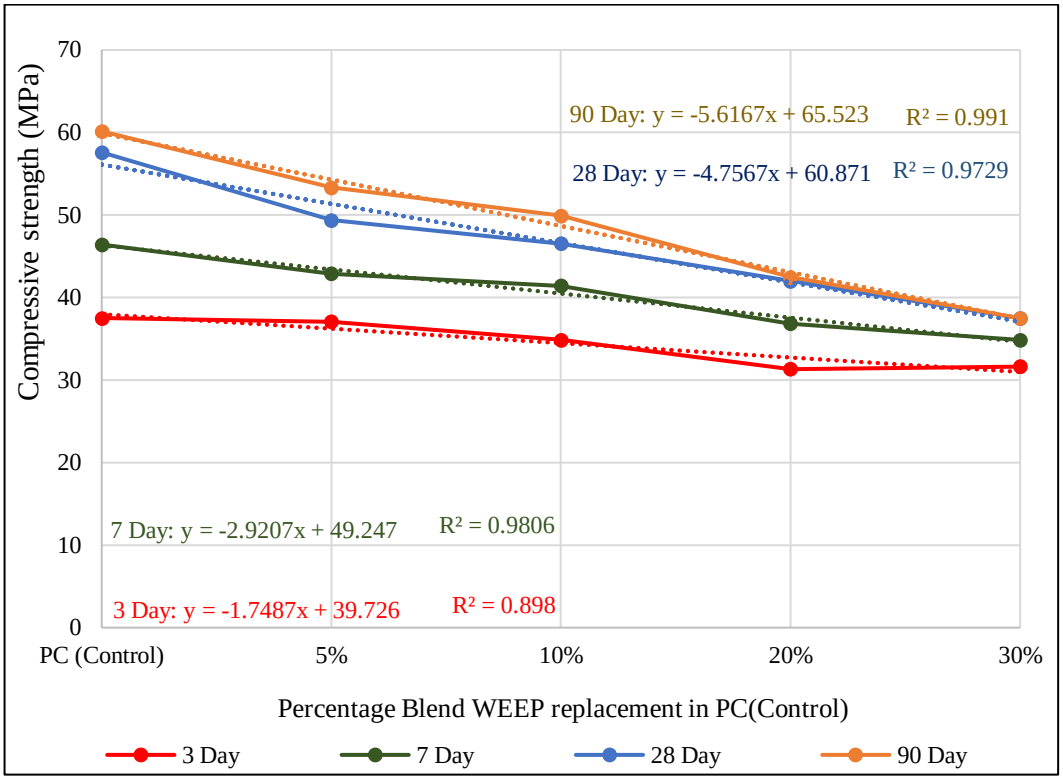

Figure D4: Correlation between PC (Control mix) and Blend WEEP at different ages.

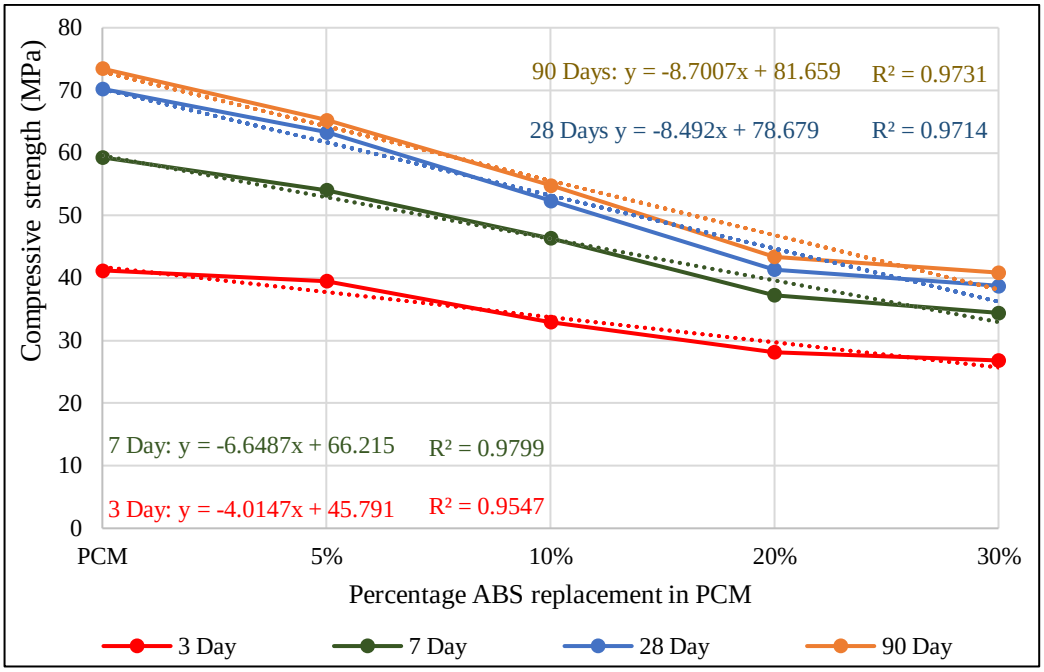

Figure D5: Correlation between PCM and ABS WEEP at different ages.

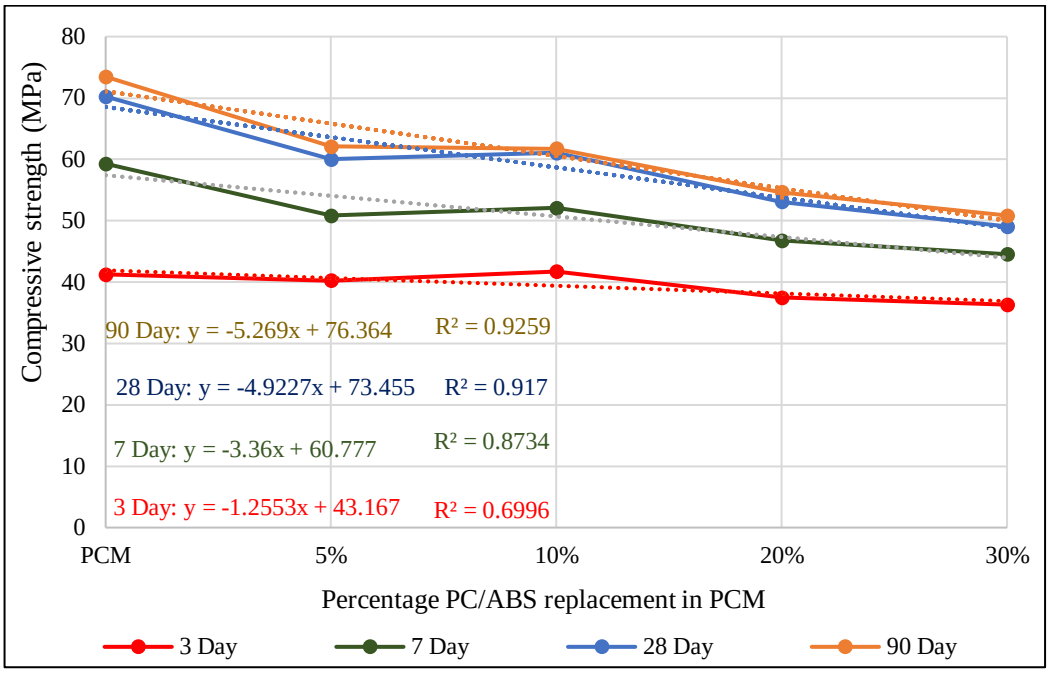

Figure D6: Correlation between PCM and PC/ABS WEEP at different ages.

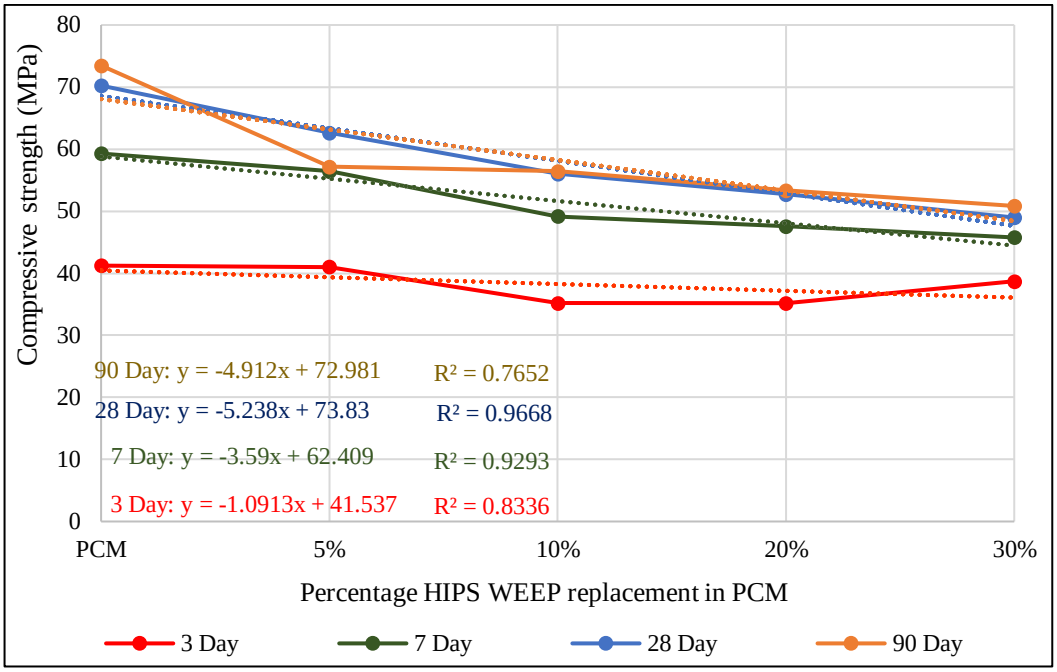

Figure D7: Correlation between PCM and HIPS WEEP at different ages.

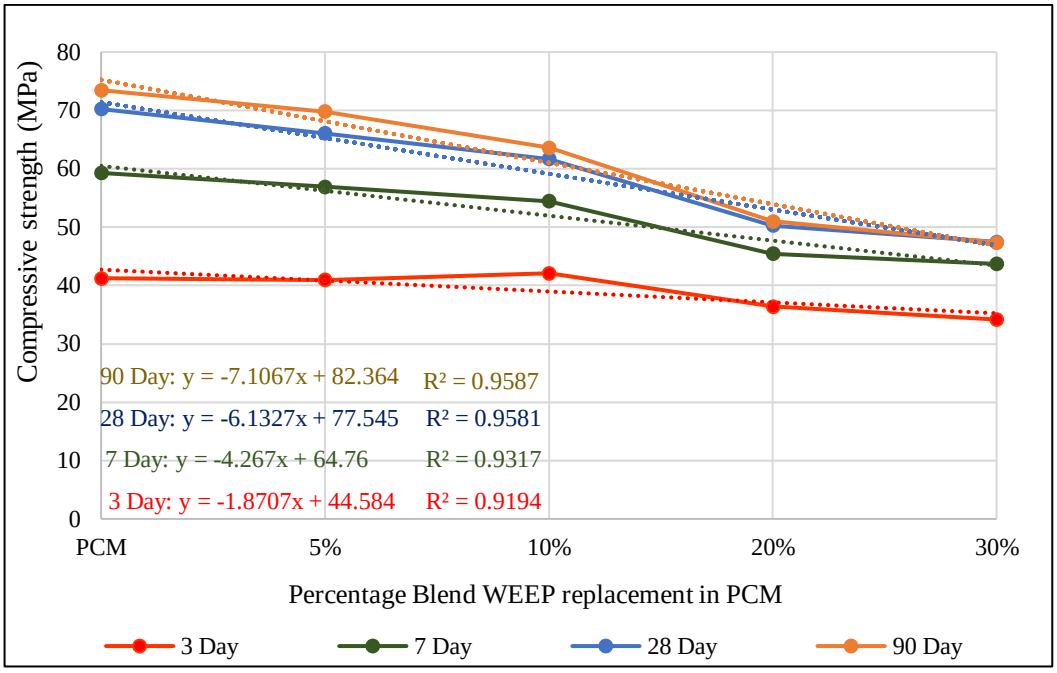

Figure D8: Correlation between PCM and Blend WEEP at different ages.

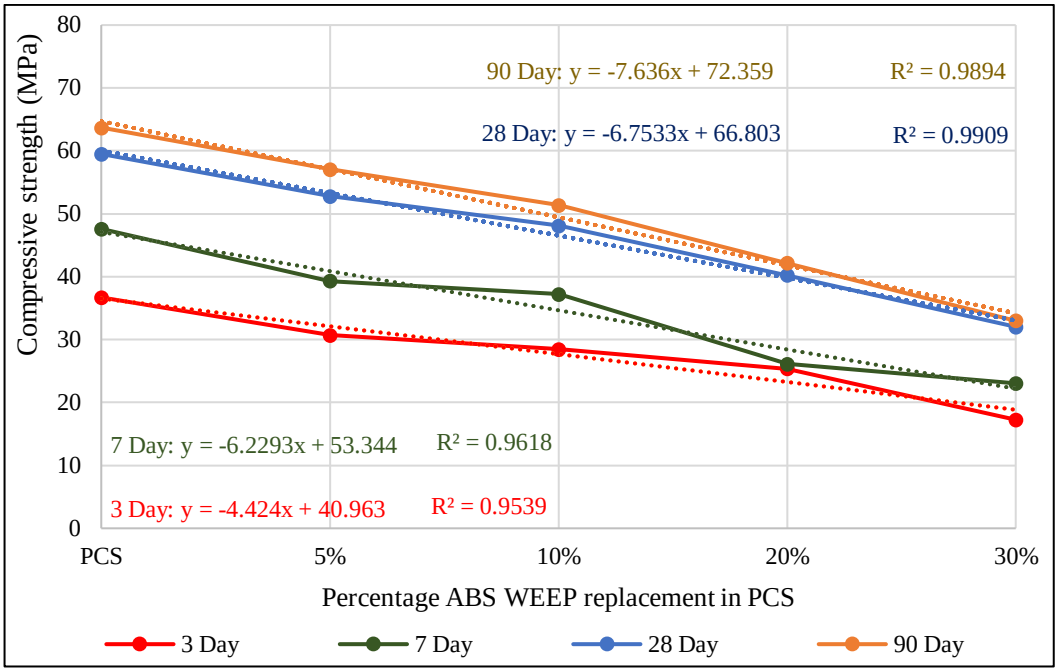

Figure D9: Correlation between PCS and ABS WEEP at different ages.

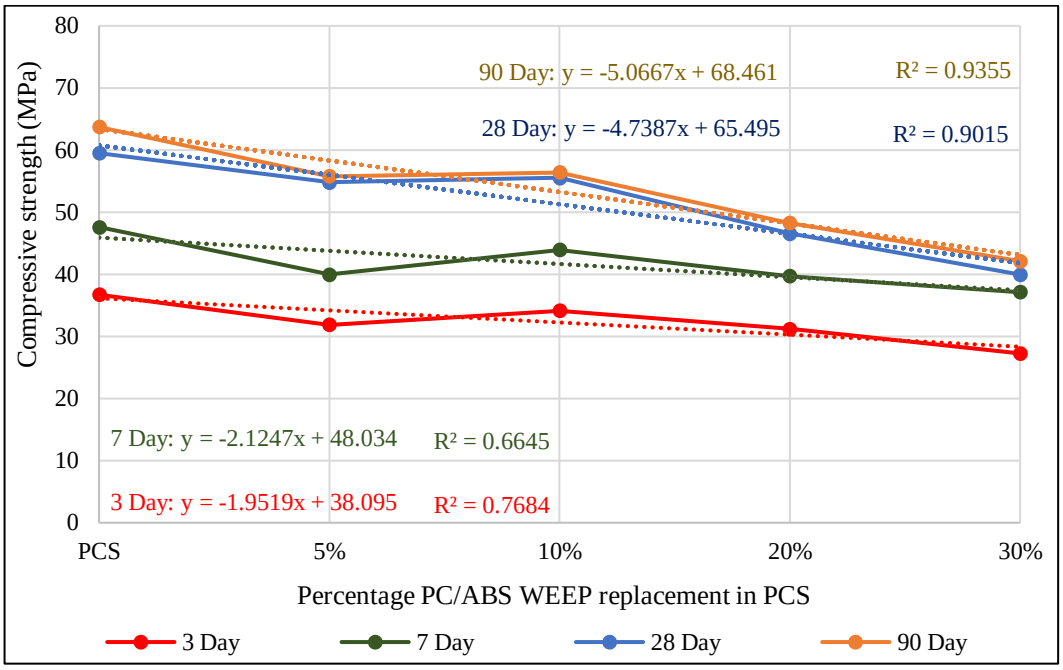

Figure D10: Correlation between PCS and PC/ABS WEEP at different ages.

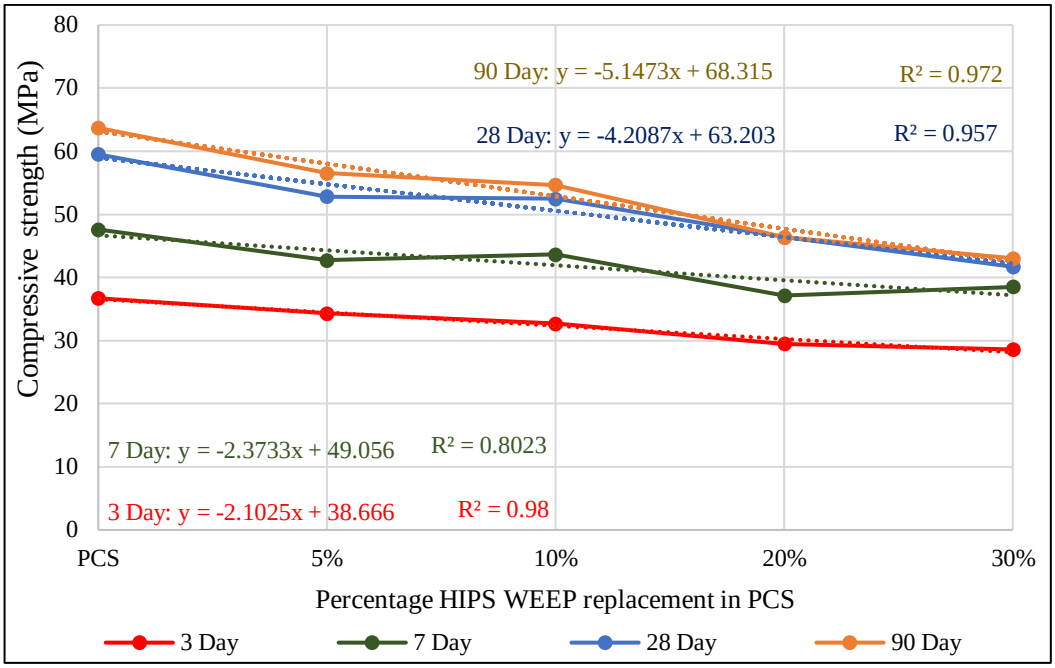

Figure D11: Correlation between PCS and HIPS WEEP at different ages.

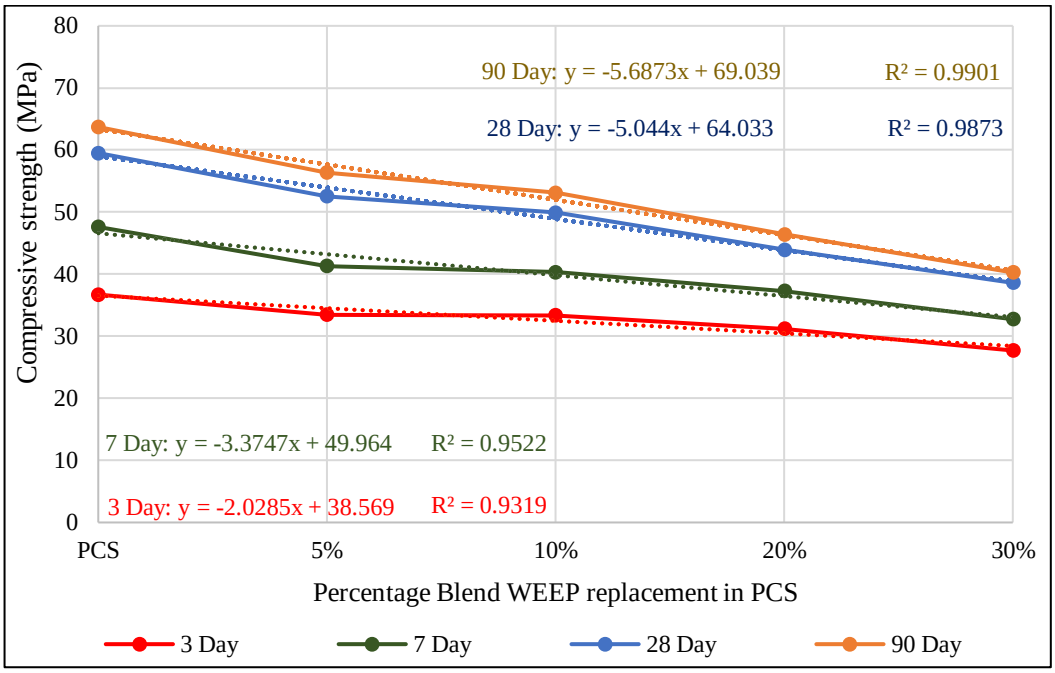

Figure D12: Correlation between PCS and Blend WEEP at different ages.

Appendix E: Durability results

Table E1: Oxygen permeability index test results for the individual disks.

Mix design	1	2	3	4	Mean	S.D	CoV(%)
PC (Control mix)	10.22	10.24	10.24	10.19	10.22	0.02	0.23
PCM	10.92	10.93	10.94	10.98	10.95	0.02	0.22
PCS	10.56	10.55	10.41	*10.32	10.51	0.09	0.81
PC(ABS-30)	9.60	9.57	9.62	9.56	9.59	0.03	0.29
PC(PC/ABS-30)	9.93	*10.11	9.99	9.87	9.93	0.06	0.59
PC(HIPS-30)	10.07	10.08	*9.79	10.02	10.06	0.03	0.31
PC(Blend-30)	9.55	*9.37	9.55	9.63	9.58	0.05	0.52
PCM(ABS-30)	9.43	9.28	*10.55	9.51	9.83	0.11	1.15
PCM(PC/ABS-30)	10.65	10.81	*10.23	10.45	10.63	0.18	1.69
PCM(HIPS-30)	10.35	*10.77	10.31	10.50	10.38	0.10	0.94
PCM(Blend-30)	10.34	10.31	10.41	10.36	10.36	0.04	0.39
PCS(ABS-30)	9.69	9.65	9.74	*9.51	9.69	0.04	0.45
PCS(PC/ABS-30)	*10.20	10.00	9.97	10.08	10.01	0.06	0.60
PCS(HIPS-30)	10.07	*9.89	10.04	10.15	10.08	0.06	0.57
PCS(Blend-30)	9.95	10.07	9.90	9.94	9.96	0.07	0.73

* Omitted results.

Table E2: k-values results for the individual disks (m/s).

Mix design	1	2	3	4	Mean	S.D	CoV (%)
PC (Control mix)	6.0E-11	5.7E-11	5.8E-11	6.5E-11	6.0E-11	3.4E-12	5.60
PCM	1.2E-11	1.2E-11	1.1E-11	1.0E-11	1.1E-11	6.2E-13	5.47
PCS	2.7E-11	2.8E-11	3.9E-11	*4.8E-11	3.2E-11	6.5E-12	20.63
PC(ABS-30)	2.5E-10	2.7E-10	2.4E-10	2.7E-10	2.6E-10	1.6E-11	6.32
PC(PC/ABS-30)	1.2E-10	*7.7E-11	1.0E-10	1.3E-10	1.2E-10	1.6E-11	13.38
PC(HIPS-30)	8.6E-11	8.3E-11	*1.6E-10	9.5E-11	8.8E-11	6.4E-12	7.26
PC(Blend-30)	2.8E-10	4.2E-10	2.8E-10	2.3E-10	2.7E-10	3.0E-11	11.12
PCM(ABS-30)	3.7E-10	5.2E-10	2.8E-11	3.1E-10	4.0E-10	1.1E-10	26.80
PCM(PC/ABS-30)	2.2E-11	1.6E-11	5.9E-11	3.6E-11	2.5E-11	1.0E-11	41.39
PCM(HIPS-30)	4.5E-11	1.7E-11	4.9E-11	3.2E-11	4.2E-11	8.9E-12	21.12
PCM(Blend-30)	4.5E-11	4.9E-11	3.9E-11	4.4E-11	4.4E-11	4.0E-12	9.02
PCS(ABS-30)	2.0E-10	2.2E-10	1.8E-10	*3.1E-10	2.0E-10	2.1E-11	10.06

PCS(PC/ABS-30)	*6.3E-11	1.0E-10	1.1E-10	8.3E-11	9.7E-11	1.3E-11	13.30
PCS(HIPS-30)	8.6E-11	1.3E-10	9.2E-11	7.1E-11	8.3E-11	1.1E-11	12.82
PCS(Blend-30)	1.1E-10	8.6E-11	1.3E-10	1.2E-10	1.1E-10	1.7E-11	15.69

* Omitted results.

Table E3: Water sorptivity test results for the individual disks (mm/√h).

Mix design	1	2	3	4	Mean	S.D	CoV(%)
PC (Control mix)	9.68	9.70	9.04	9.86	9.57	0.36	3.78
PCM	6.20	6.03	6.89	6.53	6.41	0.38	5.95
PCS	7.58	7.50	8.07	8.03	7.80	0.30	3.79
PC(ABS-30)	7.81	9.37	8.29	8.40	8.47	0.65	7.73
PC(PC/ABS-30)	8.42	8.31	6.64	8.70	8.02	0.93	11.63
PC(HIPS-30)	7.51	8.34	8.28	8.21	8.09	0.39	4.81
PC(Blend-30)	7.96	7.71	9.49	8.17	8.33	0.80	9.55
PCM(ABS-30)	5.42	5.80	5.26	5.54	5.50	0.23	4.11
PCM(PC/ABS-	4.83	4.15	5.77	4.78	4.88	0.67	13.67
PCM(HIPS-30)	3.36	4.23	4.81	3.64	4.01	0.64	15.98
PCM(Blend-30)	5.53	5.59	5.49	5.07	5.42	0.24	4.39
PCS(ABS-30)	7.39	6.68	7.84	7.49	7.35	0.49	6.64
PCS(PC/ABS-30)	6.03	6.61	6.00	6.17	6.20	0.28	4.53
PCS(HIPS-30)	6.46	5.96	6.26	6.23	6.23	0.21	3.35
PCS(Blend-30)	6.61	6.81	6.48	7.86	6.94	0.63	9.08

Table E4: Porosity (%) obtained from the water sorptivity test results for the individual disks.

Mix design	1	2	3	4	Mean	S.D	CoV(%)
PC (Control mix)	12.02	11.89	11.49	12.23	11.91	0.31	2.64
PCM	8.83	9.12	8.59	8.27	8.70	0.36	4.14
PCS	15.22	15.12	15.20	15.22	15.19	0.05	0.32
PC(ABS-30)	11.57	11.14	11.49	11.43	11.41	0.19	1.66
PC(PC/ABS-30)	11.59	8.93	10.97	9.00	10.12	1.36	13.42
PC(HIPS-30)	11.03	10.52	10.08	10.27	10.48	0.41	3.91
PC(Blend-30)	10.10	10.21	9.14	9.88	9.83	0.48	4.90
PCM(ABS-30)	13.21	12.84	12.34	12.70	12.77	0.36	2.81
PCM(PC/ABS-	8.89	10.79	9.16	8.47	9.33	1.02	10.89
PCM(HIPS-30)	12.86	11.10	12.07	10.96	11.75	0.89	7.61
PCM(Blend-30)	13.16	12.78	14.01	13.35	13.33	0.51	3.86
PCS(ABS-30)	7.20	7.55	7.70	7.49	7.48	0.21	2.79
PCS(PC/ABS-30)	10.09	10.13	10.29	10.18	10.17	0.09	0.86
PCS(HIPS-30)	15.24	11.15	11.07	11.29	12.19	2.04	16.73
PCS(Blend-30)	7.84	8.60	8.25	8.36	8.26	0.31	3.80

Table E5: Chloride conductivity test results for the individual disks (mS/cm).

Mix design	1	2	3	4	Mean	S.D	CoV (%)
PC (Control mix)	0.99	1.11	1.03	1.04	1.05	0.05	4.95
PCM	0.69	0.70	0.62	0.62	0.66	0.04	6.31
PCS	0.96	0.96	0.89	0.96	0.94	0.03	3.46
PC(ABS-30)	3.07	3.16	3.36	2.87	3.11	0.2	6.53
PC(PC/ABS-30)	1.76	1.75	1.95	1.95	1.85	0.11	5.94
PC(HIPS-30)	2.29	2.44	2.69	2.36	2.45	0.17	7.12
PC(Blend-30)	2.48	2.71	2.78	2.55	2.63	0.14	5.27
PCM(ABS-30)	0.96	1.08	1.03	1.12	1.04	0.07	6.8
PCM(PC/ABS-	0.76	0.77	0.71	0.71	0.74	0.03	4.59
PCM(HIPS-30)	0.78	0.87	0.73	0.80	0.79	0.06	7.72
PCM(Blend-30)	0.79	0.85	0.89	0.86	0.85	0.04	5.28
PCS(ABS-30)	1.30	1.19	1.26	1.31	1.27	0.05	4.29
PCS(PC/ABS-30)	1.10	1.09	1.20	1.15	1.13	0.05	4.71
PCS(HIPS-30)	0.99	1.04	1.11	1.00	1.03	0.05	5.31
PCS(Blend-30)	1.14	1.03	1.16	1.15	1.12	0.06	5.55

Table E6: Porosity obtained from the chloride conductivity tests for the individual disks.

Mix design	1	2	3	4	Mean	S.D	CoV(%)
PC (Control mix)	3.61	3.78	3.77	3.57	3.68	0.11	2.85
PCM	3.53	3.33	3.40	3.22	3.37	0.13	3.82
PCS	3.49	3.36	3.56	3.41	3.54	0.09	2.58
PC(ABS-30)	4.61	4.58	4.44	4.70	4.58	0.11	2.37
PC(PC/ABS-30)	5.22	4.91	5.16	5.60	5.22	0.29	5.45
PC(HIPS-30)	4.20	3.94	4.06	3.88	4.02	0.14	3.54
PC(Blend-30)	4.58	4.38	4.92	4.24	4.53	0.30	6.49
PCM(ABS-30)	4.51	4.33	4.22	4.51	4.39	0.14	3.24
PCM(PC/ABS-30)	3.43	3.42	3.83	3.59	3.57	0.19	5.35
PCM(HIPS-30)	3.06	3.05	3.23	3.00	3.08	0.10	3.20
PCM(Blend-30)	3.57	3.40	3.45	3.79	3.55	0.17	4.87
PCS(ABS-30)	5.35	5.39	4.87	5.20	5.20	0.24	4.52
PCS(PC/ABS-30)	4.65	4.48	5.08	5.01	4.89	0.29	3.92
PCS(HIPS-30)	4.32	4.46	4.77	4.61	4.54	0.19	4.24
PCS(Blend-30)	5.18	4.90	4.64	5.07	4.95	0.24	4.75

Appendix F: Equations

F.1 Calculation for the oxygen permeability index

Determine the best fit line using linear regression:

$$t = \ln\frac{P_0}{P_t} \tag{F.1}$$

time since the start of the test (s);

$P_0 =$ initial pressure at the start of the test (kPa); and

$P_t =$ pressure reading at time t (kPa).

Determine the slope of the linear regression line forced through (0,0):

$$z = \frac{\sum\left[(\ln(\frac{P_0}{P_t})^2\right]}{\sum\left[\ln(\frac{P_0}{P_t})t\right]} \tag{F.2}$$

$z =$ slope of linear regression (s^{-1}).

The correlation coefficient r^2 is calculated as:

$$r^2 = 1 - \frac{\sum\left[t_i - t_{p,i}\right]^2}{\sum t_i^2 - \left(\sum t_{p,i}\right)^2 \Big/ n} \tag{F.3}$$

$t_i =$ time at any given pressure reading, recorded to the nearest minute (s);

$t_{p,i} =$ predicted time at the same pressure reading, (s);

where $t_{p,i} = \frac{\ln(P_o/P_t)}{z}$; and

$n =$ number of data points being considered.

The D'arcy coefficient of permeability is calculated as:

$$k = \frac{\omega x V x g x d x z}{R x A x T} \tag{F.4}$$

$k =$ coefficient of permeability (*m/s*);

$\omega =$ molecular mass of oxygen (*kg/mol*);

$V =$ volume of the permeability cell (m^3);

g = gravitational acceleration ($^{m}/_{s^2}$);

d = average specimen thickness *(m)*;

k = slope of linear regression ((s^{-1});

R = universal gas constant (*Nm/Kmol*);

A = crossectional area of the specimen (m^2); and

T = absolute temperature in Kelvin (K).

The OPI is calculated as:

$$OPI = -\log_{10} k$$
$$OPI = \frac{OPI_1 + OPI_2 + OPI_3 + OPI_4}{4} \quad \text{(F.5)}$$

F.2 Calculation for water porosity and sorptivity

The porosity of concrete can be determined with the following equation (Durability Index Manual, 2017):

$$n = \frac{M_{sv} - M_{s0}}{Ad\rho_w} \quad \text{(F.6)}$$

M_{sv} = vacuum saturated mass of the specimen (g);

M_{s0} = mass of specimen at the start of the test (g);

A = cross-sectional area of the specimen (mm²);

d = average specimen thickness (mm); and

ρ_w = density of water (g/mm³).

The water sorptivity of the specimen can be calculated as such:

$$S = \frac{Fd}{M_{sv} - M_{s0}} \quad \text{(F.7)}$$

Where:

$$F = \frac{\sum\left(\sqrt{t_i} - t\right)\left(M_{wti} - \overline{M_{wt}}\right)}{\sum(\sqrt{t_i} - T)^2} \quad \text{(F.8)}$$

F = slope of the best fit line;

M_{wti} = mass gained at any given time (g);

$\overline{M_{wt}}$ = sum of M_{wti} over a given number of data points;

t_i = time corresponding to the mass gain M_{wti} (h); and

T = sum of $\sqrt{t_i}$ over a given number of data points (h).

F.3 Calculation for the porosity and chloride conductivity

The chloride conductivity can be calculated as (Durability Index Manual, 2017):

The porosity is calculated as:

$$n = \frac{M_s - M_d}{Ad\rho_s}.100 \tag{F.9}$$

n = porosity (%);

M_s = vacuum saturated mass (g);

M_d = mass of the dried specimen (g);

A = cross-sectional area (mm²);

d = average specimen thickness (mm); and

ρ_s = density of the salt solution (g/mm³).

$$\sigma = \frac{id}{VA} \tag{F.10}$$

σ = chloride conductivity (mS/cm);

i = electric current (mA);

d = average thickness of specimen (cm);

V= voltage difference (V); and

A = cross-sectional area of the specimen (cm²).

F.4 Calculation of the BET

The BET may be calculated as follows (Lowell, 2004):

$$\frac{1}{W((P/Po)-1)} = \frac{1}{WmC} + \frac{C-1}{WmC}(P/Po) \tag{F.11}$$

W = weigh of gas adsorbed;

$P/Po =$ relative pressure;

$Wm =$ weight of adsorbate as monolayer; and

$C =$ BET constant related to the heat of adsorption.

The slope can be calculated as:

$$s = \frac{C - 1}{WmC} \tag{F.12}$$

The intercept can be calculated as:

$$i = \frac{1}{WmC} \tag{F.13}$$

The weight absorbed in a monolayer as:

$$Wm = \frac{1}{s + i} \tag{F.14}$$

Therefore, the total surface area can be calculated as:

$$St = \frac{Wm \cdot \bar{N} \cdot Ax}{\bar{M}} \tag{F.15}$$

$\bar{N} =$ Avogadro's number (6.023×10^{23});

$\bar{M} =$ molecular weight of adsorbate; and

$Acx =$ adsorbate cross-sectional area (16.2Å² for nitrogen).

Therefore, the specific surface area can be calculated as:

$$S = \frac{St}{W} \tag{F.16}$$

F.5 Calculation for the atomic number and backscatter coefficient

$$\eta = \frac{n_{bs}}{n_b} \tag{F.17}$$

$\eta =$ backscattered electron coefficient (function of the atomic number Z);

$n_{bs} =$ number of backscattered electrons; and

$n_b =$ number of electrons incident on the target.

For a pure element, η can be determined as (Heinrich, 1966):

$$\eta = -0.0254 + 0.016Z - 1.86 * 10^{-4} * Z^2 + 8.3 * 10^{-7} * Z^3 \quad \text{(F.18)}$$

For a homogeneous mixture, η_{mix} can be calculated as (Heinrich, 1966):

$$n = \sum_i C_i \eta_i \quad \text{(F.19)}$$

$C_i =$ weight fraction of element i.

Thus, the mean atomic number of a mixture can be calculated as:

$$\bar{Z} = \sum_i C_i Z_i \quad \text{(F.20)}$$

F.6 Calculation for the confidence intervals

$$\mu = \bar{X} \pm t_{\frac{\alpha}{2}}(s/\sqrt{n}) \quad \text{(F.21)}$$

$\mu =$ population mean;
$\bar{X} =$ sample mean;
$s =$ sample standard deviation;
$n =$ Sample size;
$\alpha =$ Type 1 error, the portion of the time the confidence interval does not overlap the population mean; and
$t_{\frac{\alpha}{2}} =$ Critical value of the Student's t-distribution for a two-tail confidence interval.

Appendix G: Elemental and oxide compositions for binder materials and elemental compositions for WEEP

Table G1: Cement WDS quantification results.

	Beam curr (nA)	Peak cnt (cps)	Peak (cts)	Pk-Bg (cps)	Bg cnt (cps)	Bg1 cnt (cps)	Bg2 cnt (cps)	Ix/Istd	Ix/Ipure	Weight %	Norm Weight %	Atomic %	Det.Lim ppm	StdDev wt%
Mg	20.302	169.39	1693	144.39	25.002	19.2012	30.803	0.0099	0.00454	0.740	0.743	0.7617	415	0.06798
Al	20.302	170.6	1705	145.49	25.10	27.4025	22.802	0.0204	0.00382	0.536	0.539	0.4974	299	0.04934
Ca	20.302	26526	243910	26329	196.93	232.779	161.09	1.2089	0.44271	47.923	48.136	29.89	412	0.72966
Fe	20.302	70.516	705	48.815	21.701	21.2015	22.202	0.0061	0.00387	0.474	0.477	0.2126	733	0.08876
S	20.302	9.7003	97	4.1002	5.6001	6.20013	5.0001	0.0011	0.00023	0.026	0.026	0.0205	248	0.02383
Si	20.302	4937.5	48583	4886.1	51.408	54.4098	48.408	0.2844	0.11308	13.797	13.858	12.28	327	0.21756
O										36.059	36.219	56.338		
Total										99.558	100	100		

Table G2: Metakaolin WDS quantification results.

	Beam curr (nA)	Peak cnt (cps)	Peak (cts)	Pk-Bg (cps)	Bg cnt (cps)	Bg1 cnt (cps)	Bg2 cnt (cps)	Ix/Istd	Ix/Ipure	Weight %	Norm Weight %	Atomic %	Det.Lim ppm	StdDev wt%
O	21.001	2368.3	23499	2303.851	64.413	72.0171	56.810	0.52441	0.1092	28.627	44.166	57.7290	1610	0.69051
Al	21.001	6654.7	65117	6588.284	66.415	86.0244	46.807	0.99662	0.1167	14.774	22.793	17.6667	295	0.20901
Si	21.001	5687.7	55829	5637.079	50.608	55.0099	46.207	0.37357	0.1485	21.416	33.041	24.6036	436	0.31799
Total										64.817	100	100		

Table G3: Condensed silica fume WDS quantification results.

	Beam curr (nA)	Peak cnt (cps)	Peak (cts)	Pk-Bg (cps)	Bg cnt (cps)	Bg1 cnt (cps)	Bg2 cnt (cps)	Ix/Istd	Ix/Ipure	Weight%	Norm Weight %	Atomic %	Det.Lim ppm	StdDev wt%
Si	19.871	14227	135889	14155	71.417	77.0196	65.814	0.84186	0.3347	40.09	45.148	32.472	386	0.44784
S	19.871	8.3	83	3.1001	5.2001	3.80005	6.6001	0.00082	0.0002	0.0243	0.0274	0.0172	293	0.02733
Cl	19.871	48.31	483	40.708	7.6002	7.60019	7.6002	0.03977	0.0024	0.3155	0.3553	0.2024	348	0.05525
Fe	19.871	35.3	353	23.204	12.1	13.6006	10.6	0.00294	0.0019	0.2358	0.2655	0.096	574	0.06642
Na	19.871	14.1	141	8.2005	5.9001	6.60014	5.2001	0.00913	0.0004	0.0834	0.0939	0.0825	404	0.0433
Mg	19.871	136.7	1366	125.96	10.7	11.8005	9.6003	0.00612	0.0028	0.4123	0.4643	0.3859	174	0.03787
Al	19.871	72.22	722	51.716	20.501	23.8019	17.201	0.00827	0.001	0.1256	0.1414	0.1059	178	0.0222
P	19.871	25.4	254	3.4005	22.002	22.2016	21.802	0.00111	1E-04	0.0154	0.0173	0.0113	343	0.02951
K	19.871	439.6	4390	419.54	20.101	23.6018	16.601	0.08205	0.0088	1.0741	1.2097	0.625	186	0.05984
O										46.421	52.277	66.002		
Total										88.797	100	100		

Table G4: ABS WEEP WDS quantification results.

	Beam curr (nA)	Peak cnt (cps)	Peak (cts)	Pk-Bg (cps)	Bg cnt (cps)	Bg1 cnt (cps)	Bg2 cnt (cps)	Ix/Istd	Ix/Ipure	Weight%	Norm Weight%	Atomic %	Det.Lim ppm	StdDev wt%
C	20.467	8400.7	81741	7434	967.01	697.401	1236.6	3.54181	0.22511	70.4644	77.1947	93.2968	4753	3.019838
O	20.467	67.115	671	59.41	7.7002	9.80032	5.6001	0.02225	0.00524	2.97696	3.2613	2.9589	2265	0.413275
Cl	20.467	34.504	345	33.1	1.4	1.20001	1.6	0.21708	0.01286	1.60227	1.7553	0.71872	976	0.277059
Br	20.467	78.02	780	63.92	14.101	12.2005	16.001	0.65416	0.08614	13.2236	14.4867	2.63184	12598	4.319521
Sb	20.467	290.58	2903	267.4	23.202	23.2018	23.202	0.03356	0.02111	3.01418	3.30207	0.39371	879	1.808054
Total										91.2814	100	100		

Table G5: PC/ABS WEEP WDS quantification results.

	Beam curr (nA)	Peak cnt (cps)	Peak (cts)	Pk-Bg (cps)	Bg cnt (cps)	Bg1 cnt (cps)	Bg2 cnt (cps)	Ix/Istd	Ix/Ipure	Weight %	Norm Weight %	Atomic %	Det.Lim ppm	StdDev wt%
C	20.043	24531	226942	21799	2732.8	1967.7	3497.9	10.61	0.6741	76.87	91.65	92.85	2972	3.202454
N	20.043	8.1002	81	5.5	2.6	2.6	2.6	0.03	0.0045	6.145	7.326	6.365	29940	3.467301
O	20.043	82.623	826	25.71	56.913	85.424	28.403	0.005	0.0011	0.861	1.027	0.781	4081	0.375528
Total										83.87	100	100		

Table G6: HIPS WEEP WDS quantification results.

	Beam curr (nA)	Peak cnt (cps)	Peak (cts)	Pk-Bg (cps)	Bg cnt (cps)	Bg1 cnt (cps)	Bg2 cnt (cps)	Ix/Istd	Ix/Ipure	Weight %	Norm Weight %	Atomic %	Det.Lim ppm	StdDev wt%
C	21.773	15981	151805	14181	1800.2	1274	2326.5	6.351	0.4037	65.375	81.473	85.779	3154	2.745476
O	21.773	289.48	2892	276.7	12.801	16.2	9.4003	0.097	0.023	14.086	17.554	13.874	2956	0.862803
Cl	21.773	180.01	1799	173.9	6.1001	5.2	7.0002	0.108	0.0064	0.7809	0.9732	0.3471	181	0.058802
Total										80.241	100	100		

Appendix H: X-ray mapping results

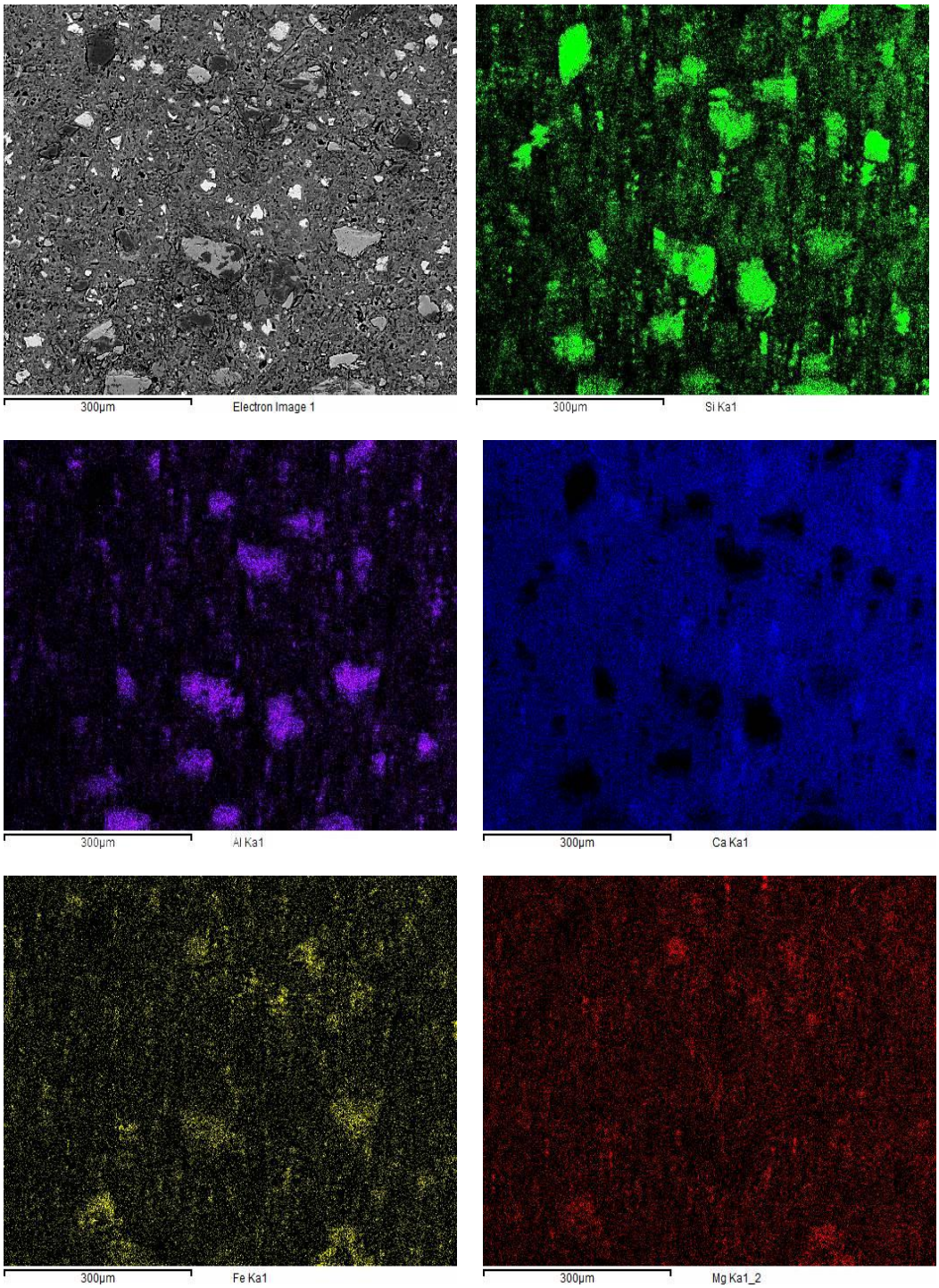

Figure H1: X-ray maps for PC (Control mix) at 28 days of curing.

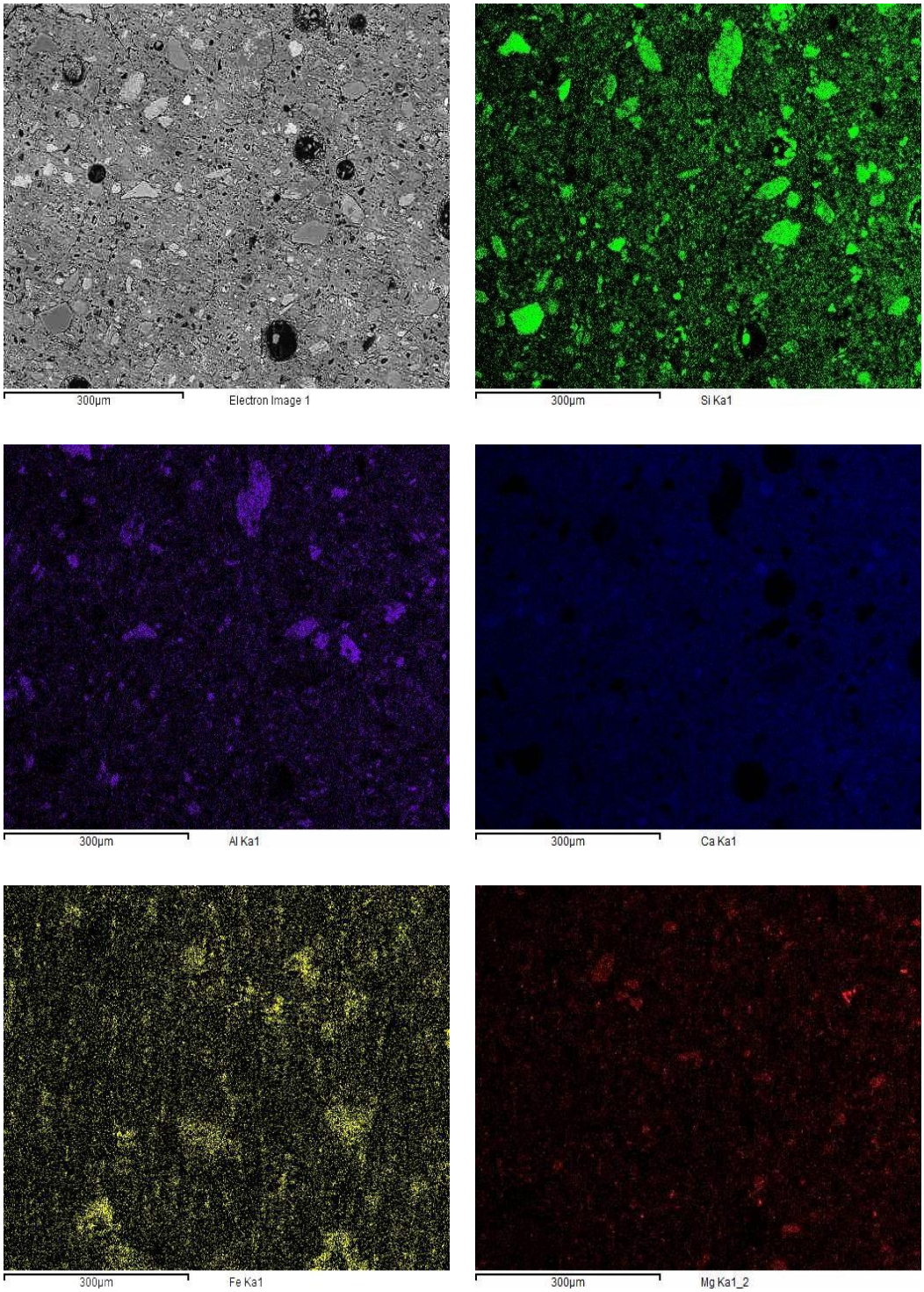

Figure H2: X-ray maps for PCM at 28 days of curing.

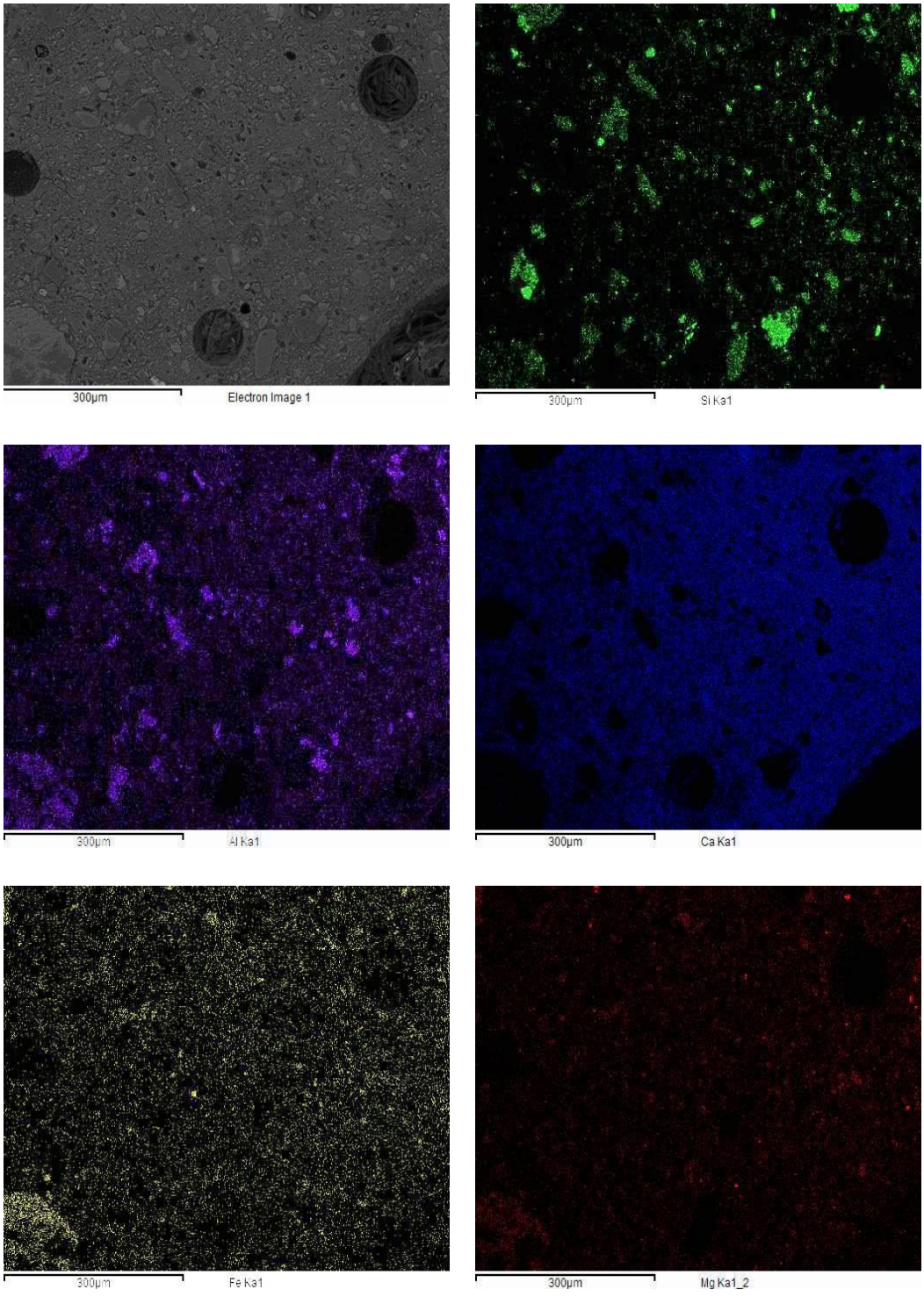

Figure H3: X-ray maps for PCS at 28 days of curing.

Appendix I: XRD results for the binder material and hardened concrete

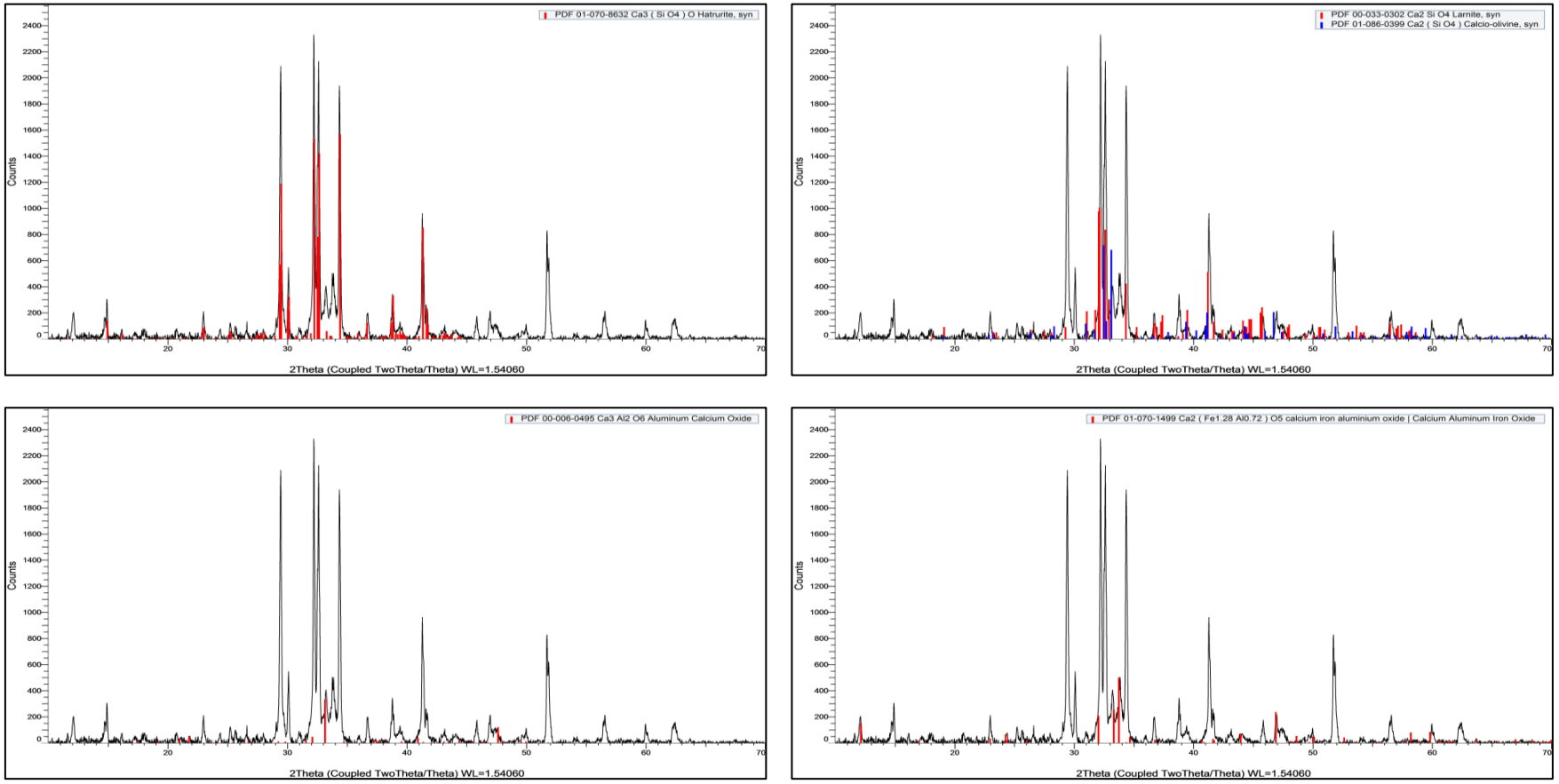

Figure I1: XRD results for the cement (1).

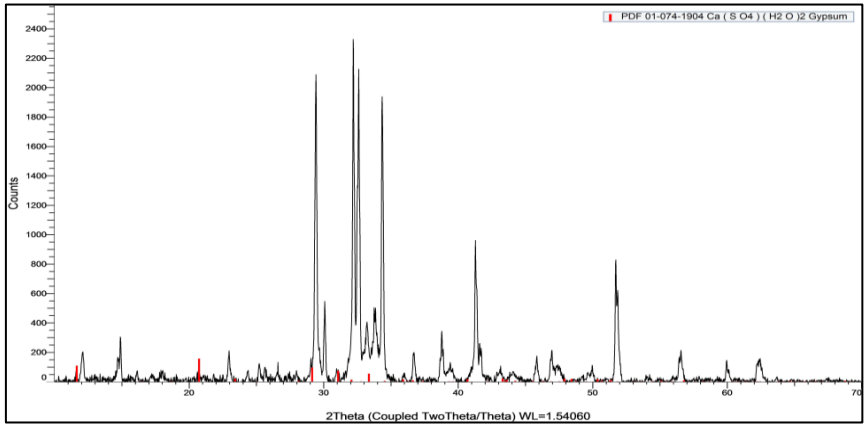

Figure I2: XRD results for the cement (2).

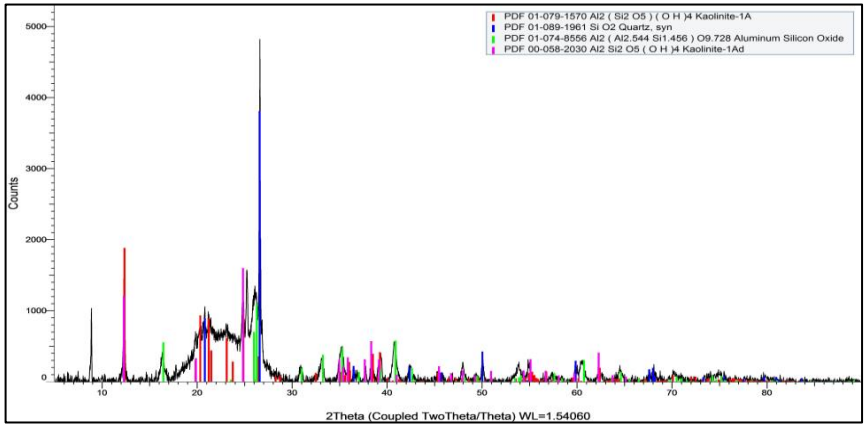

Figure I3: XRD results for the metakaolin.

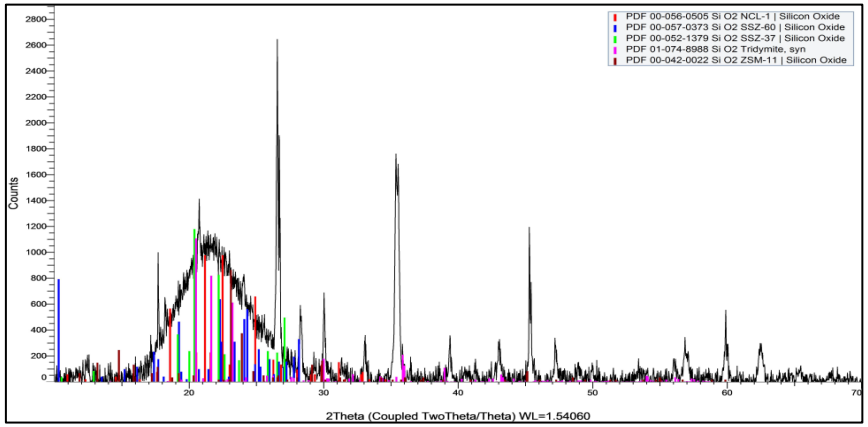

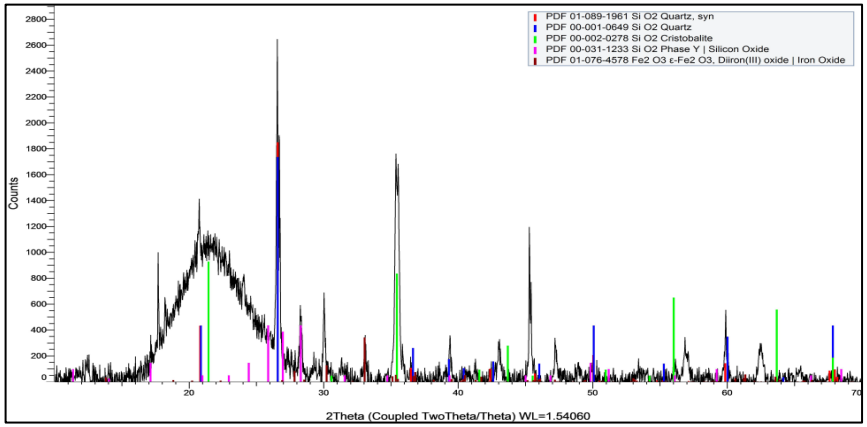

Figure I4: XRD results for the condensed silica fume.

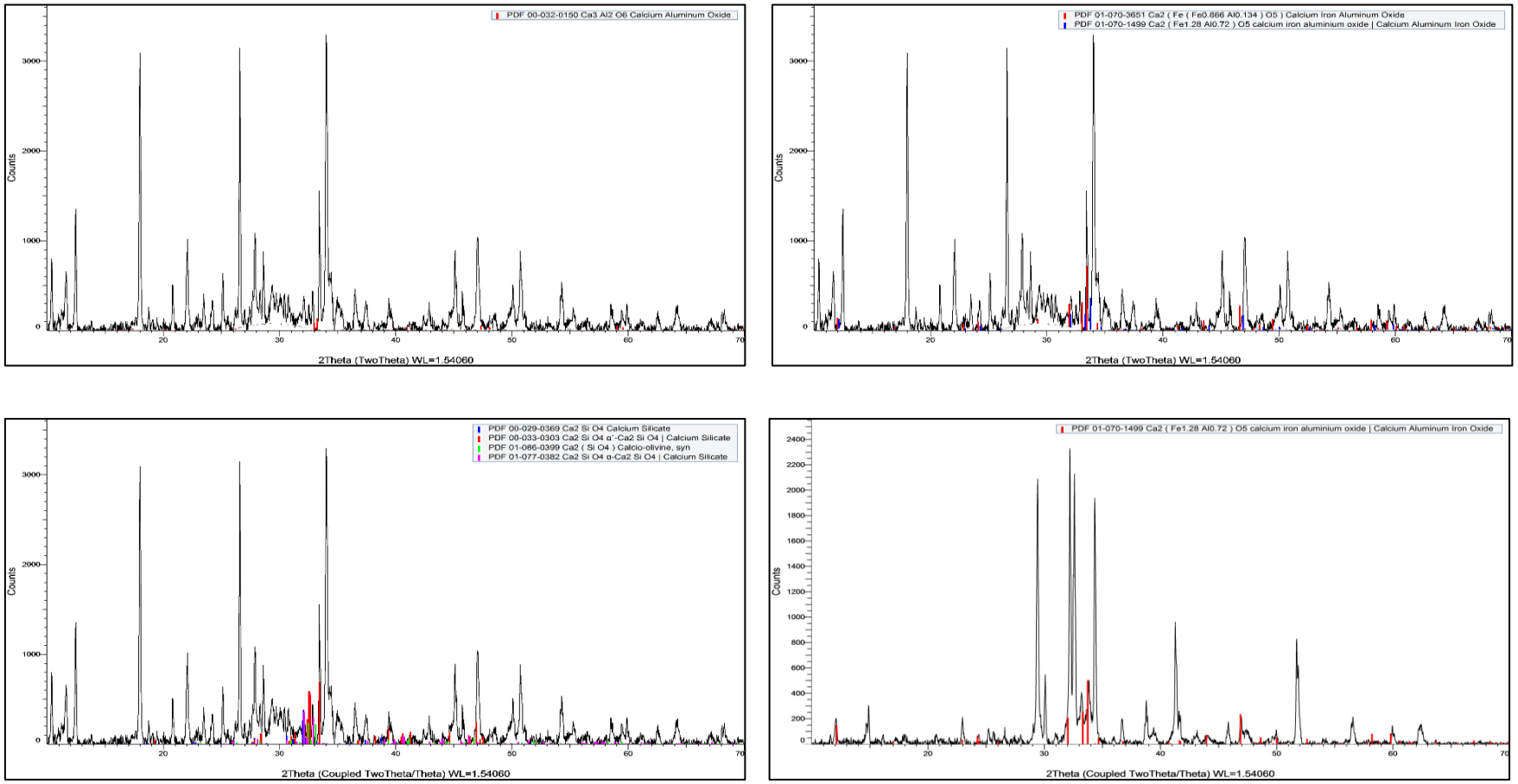

Figure I5: XRD results for PC (Control mix) at 28 days of curing (1).

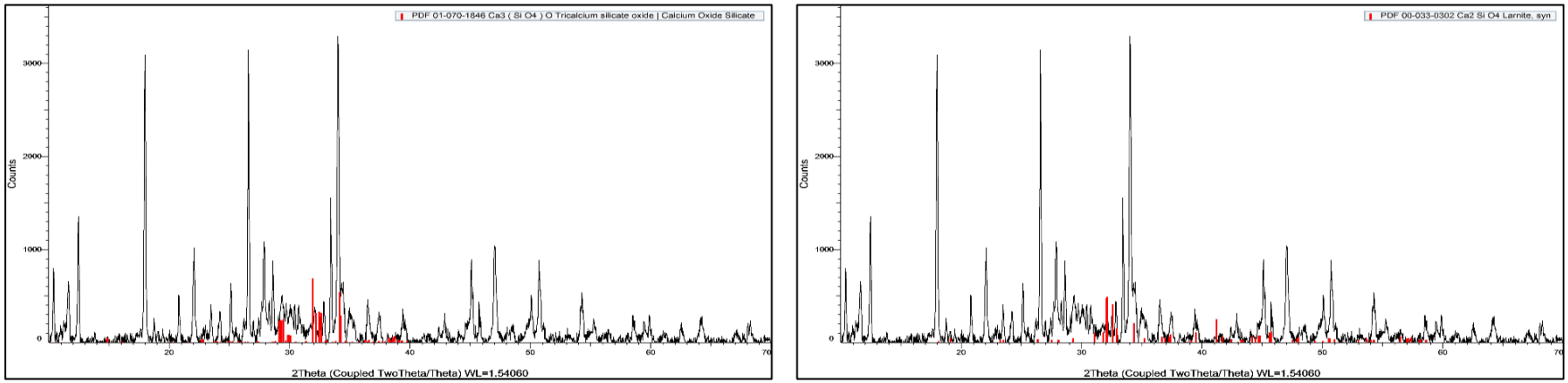

Figure I6: XRD results for PC (Control mix) at 28 days of curing (2).

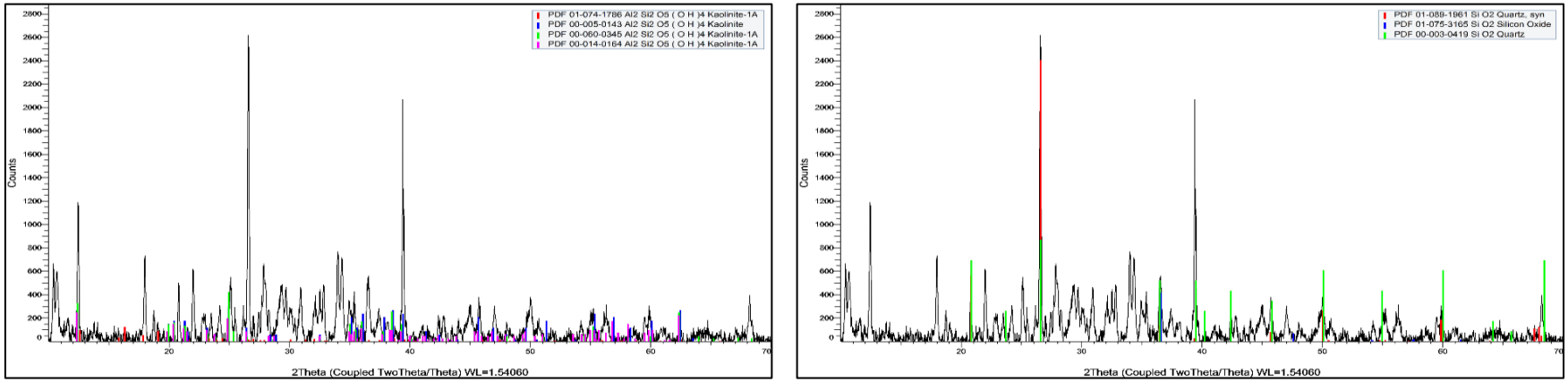

Figure I7: XRD results for PCM at 28 days of curing (1).

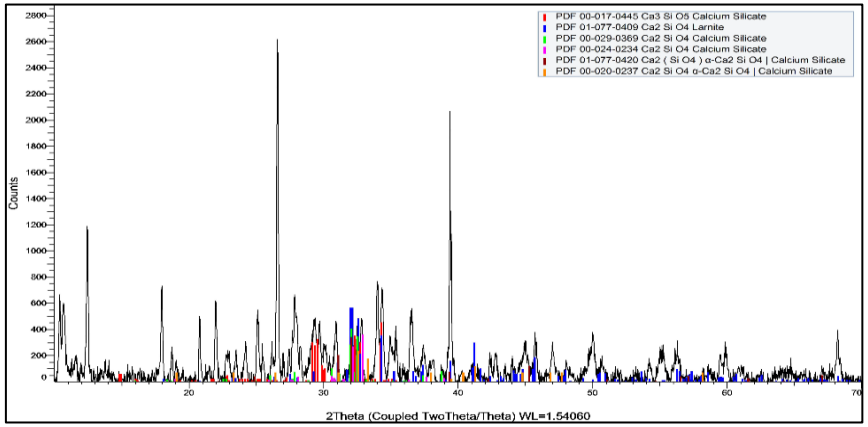

Figure I8: XRD results for PCM at 28 days of curing (2).

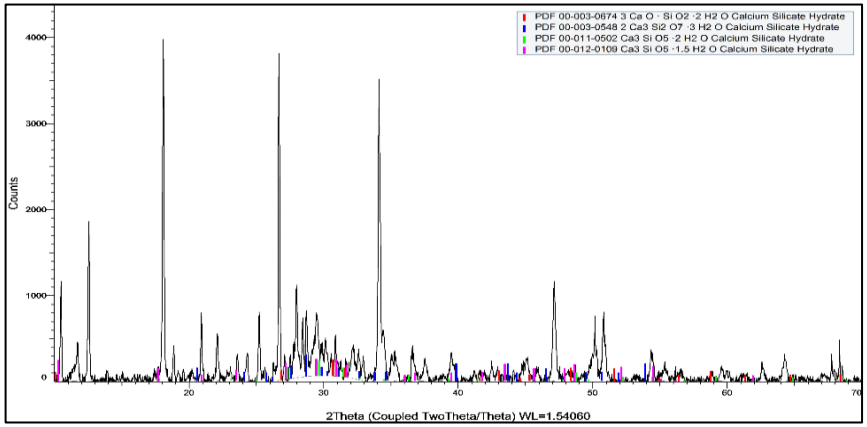

Figure I9: XRD results for PCS at 28 days of curing (1).

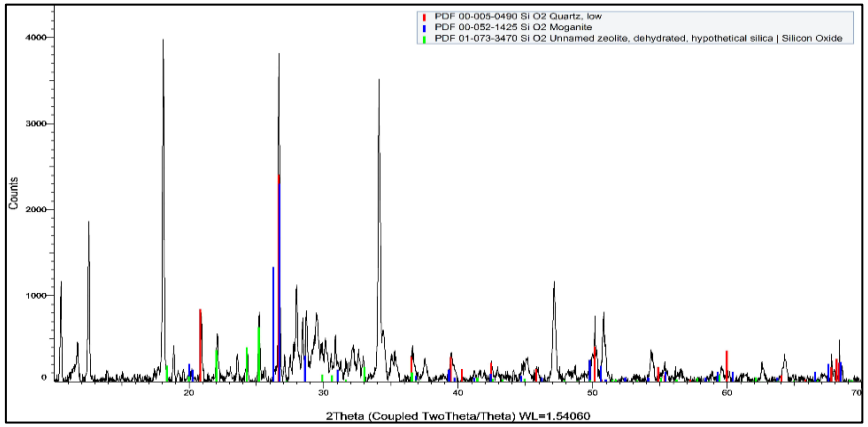

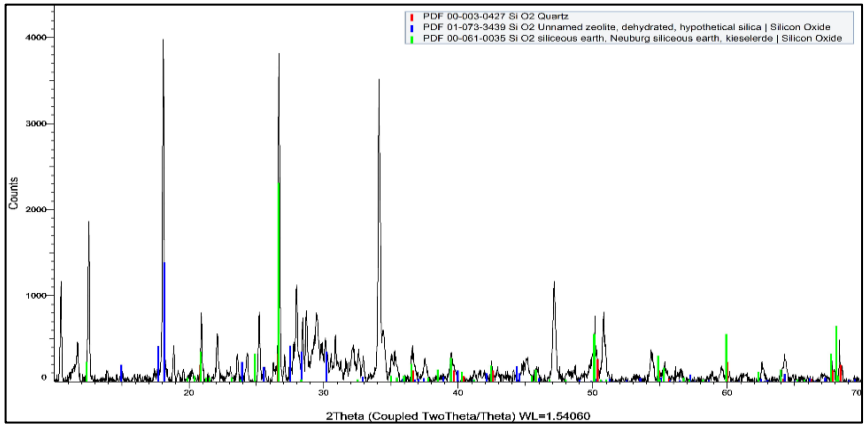

Figure I10: XRD results for PCS at 28 days of curing (2).

Appendix J: EDS results for PC (Control mix), PCM and PCS

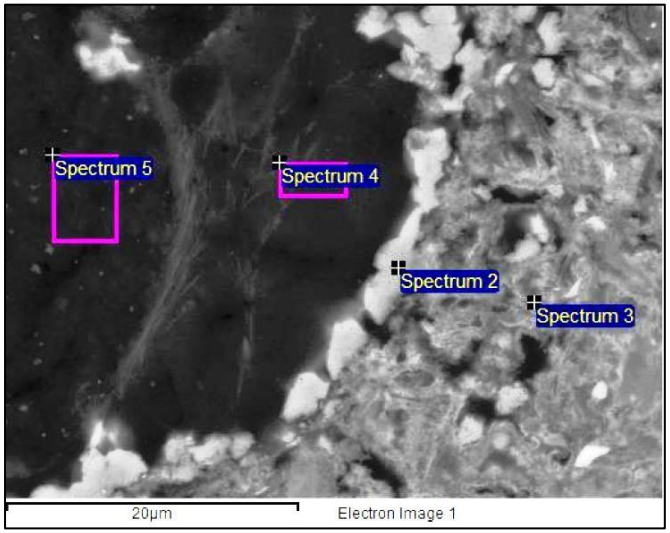

Figure J1: EDS spectrum for the ITZ between ABS WEEP and hcp in PC(Blend-30) at 28 days of curing.

Table J1: EDS results for the ITZ between ABS WEEP and hcp in PC(Blend-30).

PCS	C	O	Na	Mg	Al	Si	S	Cl	K	Ca	Ti	Fe	Total
Spectrum 1	55.01	30.63	0.00	0.27	1.27	2.40	0.16	0.14	0.26	9.45	0.09	0.33	100
Spectrum 2	0.00	41.28	0.28	1.16	5.85	13.44	0.00	0.48	1.52	32.47	0.00	3.52	100
Spectrum 3	22.69	33.34	0.00	0.00	4.42	8.40	0.00	0.00	1.16	28.47	0.00	1.53	100
Spectrum 4	7.45	14.70	0.00	0.00	0.00	0.00	0.00	0.34	0.00	8.51	0.00	0.00	100
Spectrum 5	88.62	10.44	0.00	0.00	0.00	0.00	0.00	0.31	0.00	0.40	0.24	0.00	100

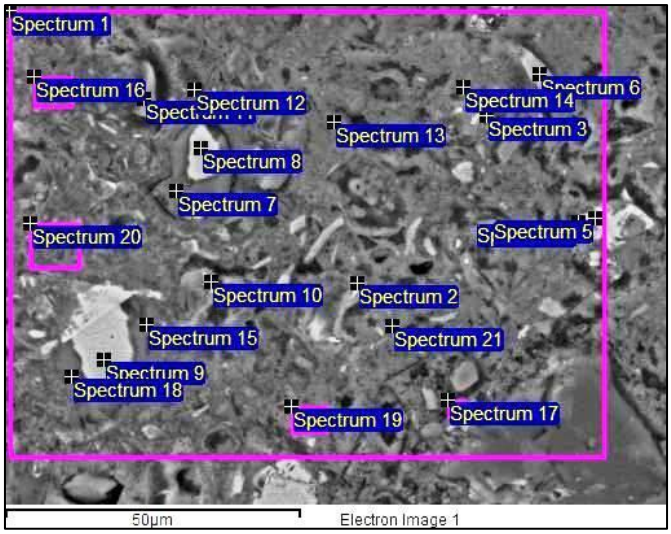

Figure J2: EDS spectrum for PC (Control mix) at 28 days of curing.

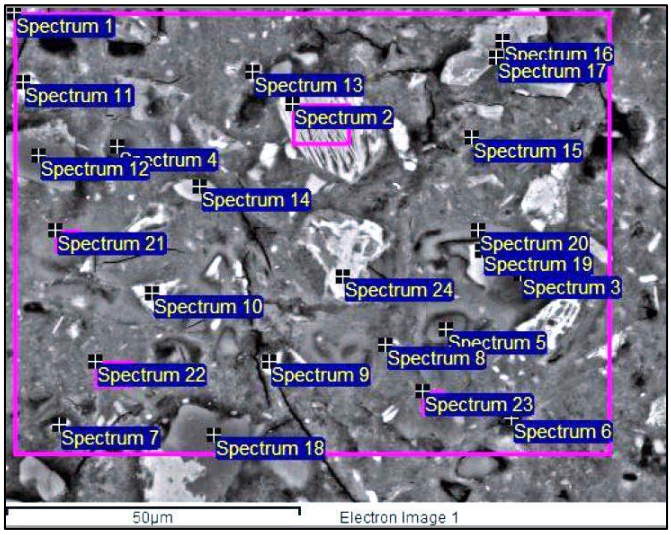

Figure J3: EDS spectrum for PCM at 28 days of curing.

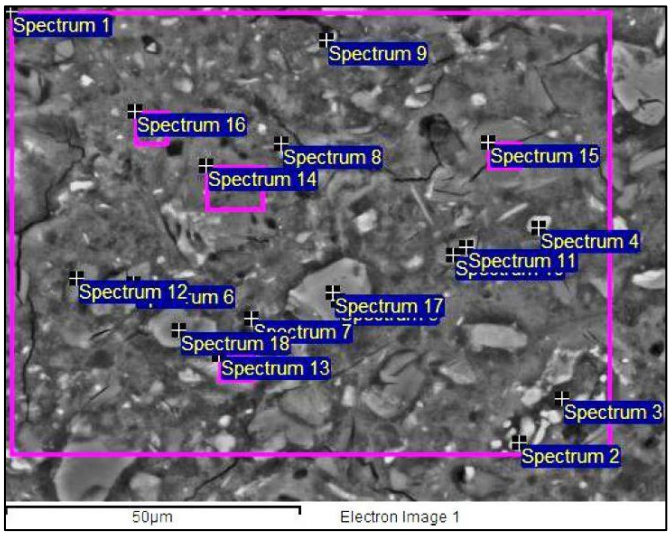

Figure J4: EDS spectrum for PCS at 28 days of curing.

Table J2: EDS results for the weight (%) at different spectrums for PC (Control mix) at 28 days of curing.

PCS	O	Na	Mg	Al	Si	S	Cl	K	Ca	Ti	Mn	Fe	Total
Spectrum 1	57.49	0.98	1.14	2.52	9.95	0.70	0.00	1.13	24.38	0.00	0.00	1.73	100
Spectrum 2	54.40	0.00	2.38	6.45	3.69	1.00	0.00	0.18	23.00	0.70	0.29	7.91	100
Spectrum 3	52.40	0.00	2.51	9.29	3.71	0.47	0.00	0.24	24.03	0.43	0.00	6.93	100
Spectrum 4	46.68	0.00	2.50	8.98	2.82	0.29	0.00	0.34	27.21	1.03	0.62	9.54	100
Spectrum 5	44.29	0.00	2.08	10.97	2.15	0.00	0.00	0.46	29.50	0.99	0.53	9.03	100
Spectrum 6	52.00	0.46	5.32	3.21	21.28	0.00	0.00	0.34	7.17	0.00	0.00	10.21	100
Spectrum 7	55.13	0.00	1.39	1.14	15.87	0.68	0.00	1.14	23.71	0.26	0.00	0.68	100
Spectrum 8	45.00	0.00	0.82	0.45	12.09	0.00	0.00	0.00	40.73	0.00	0.00	0.29	100
Spectrum 9	45.07	0.00	0.85	0.46	11.93	0.00	0.00	0.00	41.29	0.00	0.00	0.40	100
Spectrum 10	48.44	0.33	1.67	4.01	5.05	2.89	0.00	0.71	31.22	0.45	0.32	4.90	100
Spectrum 11	65.31	0.00	0.00	0.23	33.66	0.00	0.00	0.00	0.80	0.00	0.00	0.00	100
Spectrum 12	63.74	0.00	0.45	5.48	9.84	0.36	0.00	0.33	17.32	0.00	0.00	2.48	100
Spectrum 13	58.10	0.43	0.36	1.11	7.67	0.33	0.00	1.57	29.86	0.00	0.00	0.57	100
Spectrum 14	54.22	0.00	2.94	2.70	6.08	0.69	0.00	0.66	24.19	1.46	0.39	6.66	100
Spectrum 15	56.99	0.00	11.17	1.30	15.01	0.98	0.00	0.50	23.19	0.24	0.00	0.61	100
Spectrum 16	58.11	0.00	0.69	1.50	9.40	0.59	0.00	0.69	28.14	0.00	0.00	0.88	100
Spectrum 17	52.97	2.27	0.92	5.68	19.76	0.00	0.00	1.61	11.59	2.84	0.00	2.36	100
Spectrum 18	55.02	0.00	1.44	1.30	14.55	0.89	0.00	0.56	25.30	0.32	0.00	0.62	100
Spectrum 19	59.01	0.00	0.83	1.55	7.55	0.84	0.00	0.85	27.84	0.00	0.00	1.54	100
Spectrum 20	57.78	0.00	1.37	2.51	7.93	1.61	0.00	0.38	26.65	0.00	0.00	1.77	100
Spectrum 21	54.98	0.00	0.59	1.22	7.93	0.37	0.00	1.19	32.36	0.00	0.00	1.36	100

Table J3: EDS results for the atomic (%) at different spectrums for PC (Control mix) at 28 days of curing.

PCS	O	Na	Mg	Al	Si	S	Cl	K	Ca	Ti	Mn	Fe	Total
Spectrum 1	74.55	0.88	0.97	1.94	7.35	0.45	0.00	0.60	12.62	0.00	0.00	0.64	100
Spectrum 2	73.28	0.00	2.11	5.15	2.83	0.67	0.00	0.10	12.37	0.32	0.11	3.05	100
Spectrum 3	71.08	0.00	2.24	7.46	2.87	0.32	0.00	0.13	13.01	0.19	0.00	2.69	100
Spectrum 4	67.02	0.00	2.36	7.65	2.30	0.21	0.00	0.20	15.59	0.49	0.26	3.92	100
Spectrum 5	64.73	0.00	2.00	9.51	1.79	0.00	0.00	0.27	17.21	0.48	0.23	3.78	100
Spectrum 6	68.62	0.43	4.62	2.51	16.00	0.00	0.00	0.18	3.78	0.00	0.00	3.86	100
Spectrum 7	72.24	0.00	1.20	0.88	11.85	0.44	0.00	0.61	12.40	0.11	0.00	0.26	100
Spectrum 8	65.48	0.00	0.78	0.38	9.89	0.00	0.00	0.00	23.35	0.00	0.00	0.12	100
Spectrum 9	65.04	0.00	0.81	0.39	9.81	0.00	0.00	0.00	23.78	0.00	0.00	0.17	100
Spectrum 10	68.35	0.33	1.55	3.35	4.06	2.04	0.00	0.41	17.59	0.21	0.13	1.98	100
Spectrum 11	76.89	0.00	0.00	0.16	22.52	0.00	0.00	0.00	0.38	0.00	0.00	0.00	100
Spectrum 12	78.86	0.00	0.37	4.02	6.93	0.22	0.00	0.17	8.55	0.00	0.00	0.88	100
Spectrum 13	75.89	0.39	0.31	0.86	5.71	0.21	0.00	0.84	15.57	0.00	0.00	0.21	100
Spectrum 14	73.26	0.00	2.62	2.16	4.68	0.47	0.00	0.36	13.05	0.66	0.16	2.58	100
Spectrum 15	73.74	0.00	1.00	1.00	11.06	0.64	0.00	0.27	11.97	0.10	0.00	0.23	100
Spectrum 16	75.60	0.00	0.59	1.15	6.96	0.38	0.00	0.37	14.61	0.00	0.00	0.33	100
Spectrum 17	69.07	2.06	0.79	4.39	14.68	0.00	0.00	0.86	6.03	1.24	0.00	0.88	100
Spectrum 18	72.30	0.00	1.24	1.01	10.90	0.58	0.00	0.30	13.27	0.14	0.00	0.23	100
Spectrum 19	76.55	0.00	0.71	1.19	5.58	0.54	0.00	0.45	14.41	0.00	0.00	0.57	100
Spectrum 20	75.24	0.00	1.17	1.94	5.88	1.05	0.00	0.20	13.85	0.00	0.00	0.66	100
Spectrum 21	73.71	0.00	0.52	0.97	6.06	0.25	0.00	0.65	17.32	0.00	0.00	0.52	100

Table J4: EDS results for the weight (%) at different spectrums for PCM at 28 days of curing.

PCM	O	Na	Mg	Al	Si	S	Cl	K	Ca	Ti	Mn	Fe	Total
Spectrum 1	56.99	0.56	1.24	2.57	11.46	0.84	0.18	0.23	23.75	0.19	0.00	2.00	100
Spectrum 2	46.74	0.00	0.41	0.59	14.45	0.00	0.00	0.29	37.08	0.00	0.00	0.44	100
Spectrum 3	48.08	0.00	1.64	1.39	15.80	0.58	0.00	0.00	31.77	0.00	0.00	0.74	100
Spectrum 4	48.30	0.00	0.64	1.09	12.04	0.61	0.00	0.42	35.69	0.33	0.00	0.88	100
Spectrum 5	59.84	0.00	0.34	7.80	5.06	1.00	0.63	0.00	24.24	0.00	0.00	1.09	100
Spectrum 6	23.19	0.00	0.59	3.17	12.61	1.32	0.57	0.00	56.44	0.00	0.00	2.11	100
Spectrum 7	55.98	0.00	5.16	1.05	18.74	0.00	0.00	0.00	8.91	3.61	0.17	6.36	100
Spectrum 8	58.93	0.30	3.73	2.10	15.34	0.50	0.00	0.16	12.44	0.39	0.00	6.10	100
Spectrum 9	47.54	0.00	0.24	0.31	15.31	0.00	0.00	0.14	36.46	0.00	0.00	0.00	100
Spectrum 10	44.79	0.00	3.69	11.28	2.69	0.00	0.00	0.31	28.29	0.62	0.32	8.02	100
Spectrum 11	50.92	0.00	0.46	0.52	14.45	0.00	0.00	0.36	32.96	0.00	0.00	0.32	100
Spectrum 12	55.10	7.38	0.00	8.85	27.66	0.00	0.00	0.55	0.47	0.00	0.00	0.00	100
Spectrum 13	60.42	0.29	1.60	4.29	13.73	0.20	0.00	1.57	9.73	4.63	0.00	3.55	100
Spectrum 14	53.39	0.00	6.48	9.25	12.10	0.00	0.00	0.00	1.81	0.00	0.00	16.9	100
Spectrum 15	47.36	0.31	1.00	1.46	14.28	1.18	0.00	0.25	32.24	0.00	0.00	1.92	100
Spectrum 16	48.00	0.00	5.84	10.27	12.75	0.00	0.00	0.00	2.05	0.00	0.32	20.7	100
Spectrum 17	57.28	0.30	2.82	5.07	10.14	0.62	0.00	0.26	14.70	0.44	0.00	8.38	100
Spectrum 18	54.74	7.50	0.00	8.85	28.36	0.00	0.00	0.14	0.42	0.00	0.00	0.00	100
Spectrum 19	36.00	0.00	0.78	0.38	12.91	0.00	0.00	0.00	49.49	0.00	0.00	0.43	100
Spectrum 20	53.43	0.00	0.47	0.94	13.17	0.93	0.29	0.00	30.15	0.00	0.00	0.63	100
Spectrum 21	56.58	0.00	1.09	1.24	13.23	0.74	0.00	0.00	26.41	0.00	0.00	0.71	100
Spectrum 22	56.24	0.00	0.84	1.63	12.13	0.96	0.25	0.00	26.89	0.00	0.00	1.05	100
Spectrum 23	55.49	0.43	0.45	1.81	13.24	0.98	0.00	0.00	26.13	0.00	0.00	1.47	100
Spectrum 24	45.31	0.00	2.18	11.83	1.92	0.00	0.00	0.00	28.46	0.59	0.26	9.45	100

Table J5: EDS results for the atomic (%) at different spectrums for PCM at 28 days of curing.

PCM	O	Na	Mg	Al	Si	S	Cl	K	Ca	Ti	Mn	Fe	Total
Spectrum 1	74.06	0.51	1.06	1.98	8.48	0.54	0.11	0.12	12.32	0.08	0.00	0.75	100
Spectrum 2	66.17	0.00	0.38	0.49	11.65	0.00	0.00	0.17	20.95	0.00	0.00	0.18	100
Spectrum 3	66.62	0.00	1.50	1.15	12.47	0.40	0.00	0.00	17.57	0.00	0.00	0.29	100
Spectrum 4	67.73	0.00	0.59	0.91	9.62	0.42	0.00	0.24	19.98	0.16	0.00	0.36	100
Spectrum 5	76.38	0.00	0.29	5.90	3.68	0.64	0.36	0.00	12.35	0.00	0.00	0.40	100
Spectrum 6	40.90	0.00	0.69	3.31	12.67	1.16	0.45	0.00	39.74	0.00	0.00	1.07	100
Spectrum 7	72.41	0.00	4.39	0.81	13.81	0.00	4.60	0.00	0.00	1.56	0.07	2.36	100
Spectrum 8	74.84	0.27	3.12	1.58	11.10	0.32	0.00	0.08	6.31	0.17	0.00	2.22	100
Spectrum 9	66.76	0.00	0.22	0.25	12.25	0.00	0.00	0.08	20.44	0.00	0.00	0.00	100
Spectrum 10	64.49	0.00	3.50	9.63	2.21	0.00	0.00	0.18	16.26	0.36	0.14	3.31	100
Spectrum 11	69.60	0.00	0.41	0.42	11.25	0.00	0.00	0.20	17.98	0.00	0.00	0.13	100
Spectrum 12	67.48	6.29	0.00	6.43	19.30	0.00	0.00	0.28	0.23	0.00	0.00	0.00	100
Spectrum 13	76.26	0.25	1.33	3.21	9.87	0.13	0.00	0.81	4.90	1.95	0.00	1.28	100
Spectrum 14	70.60	0.00	5.64	7.25	9.12	0.00	0.00	0.00	0.96	0.00	0.00	6.43	100
Spectrum 15	66.38	0.30	0.92	1.22	11.40	0.83	0.00	0.14	18.04	0.00	0.00	0.77	100
Spectrum 16	66.61	0.00	5.33	8.45	10.08	0.00	0.00	0.00	1.14	0.00	0.13	8.26	100
Spectrum 17	74.44	0.27	2.42	3.91	7.50	0.40	0.00	0.14	7.62	0.19	0.00	3.12	100
Spectrum 18	67.09	6.40	0.00	6.43	19.80	0.00	0.00	0.07	0.20	0.00	0.00	0.00	100
Spectrum 19	56.27	0.00	0.80	0.36	11.49	0.00	0.00	0.00	30.88	0.00	0.00	0.19	100
Spectrum 20	71.61	0.00	0.42	0.75	10.05	0.62	0.17	0.00	16.13	0.00	0.00	0.24	100
Spectrum 21	73.79	0.00	0.94	0.96	9.82	0.48	0.00	0.00	13.75	0.00	0.00	0.26	100
Spectrum 22	73.71	0.00	0.72	1.27	9.06	0.63	0.15	0.00	14.07	0.00	0.00	0.40	100
Spectrum 23	72.98	0.39	0.39	1.41	9.92	0.64	0.00	0.00	13.72	0.00	0.00	0.55	100
Spectrum 24	65.48	0.00	2.08	10.14	1.58	0.00	0.00	0.00	16.42	0.28	0.11	3.91	100

Table J6: EDS results for the weight (%) at different spectrums for PCS at 28 days of curing.

PCS	O	Na	Mg	Al	Si	S	Cl	K	Ca	Ti	Fe	Total
Spectrum 1	56.92	0.44	1.05	5.31	12.55	0.54	0.00	0.26	21.35	0.00	1.59	100
Spectrum 2	48.04	0.00	0.37	1.14	14.58	0.00	0.00	0.26	35.09	0.00	0.52	100
Spectrum 3	37.42	0.00	1.71	4.25	14.08	0.46	0.00	0.40	39.64	0.00	2.04	100
Spectrum 4	43.19	0.00	0.00	0.81	19.25	0.00	0.00	0.00	36.75	0.00	0.00	100
Spectrum 5	52.62	0.00	0.00	13.01	17.11	0.00	0.00	0.00	13.65	0.00	3.61	100
Spectrum 6	58.95	0.00	0.00	10.55	3.04	1.50	0.00	0.00	25.17	0.00	0.79	100
Spectrum 7	48.01	0.00	0.79	6.82	10.13	1.40	0.31	0.00	28.87	0.00	3.67	100
Spectrum 8	46.45	0.00	1.08	5.36	15.69	0.58	0.00	0.00	23.94	2.88	4.02	100
Spectrum 9	22.13	0.00	0.00	0.80	73.26	0.00	0.00	0.00	3.81	0.00	0.00	100
Spectrum 10	54.93	0.00	0.60	9.42	2.72	0.90	0.00	0.00	30.84	0.00	0.59	100
Spectrum 11	50.28	0.00	9.75	3.92	9.21	0.37	0.00	0.00	25.37	0.31	0.78	100
Spectrum 12	57.22	0.00	0.34	10.31	5.48	1.19	0.00	0.00	24.58	0.00	0.89	100
Spectrum 13	51.27	0.00	0.27	2.49	12.49	0.37	0.00	0.00	32.62	0.00	0.49	100
Spectrum 14	60.57	0.00	1.08	10.83	7.44	0.58	0.00	0.00	18.45	0.00	1.05	100
Spectrum 15	57.65	0.00	0.43	11.00	7.46	0.35	0.00	0.26	21.10	0.00	1.76	100
Spectrum 16	56.83	0.00	0.55	3.61	13.64	0.43	0.00	0.00	23.78	0.00	1.17	100
Spectrum 17	50.76	0.00	0.00	13.39	17.37	0.00	0.00	0.00	14.26	0.00	4.22	100
Spectrum 18	56.00	8.07	0.00	8.61	26.86	0.00	0.00	0.00	0.45	0.00	0.00	100

Table J7: EDS results for the atomic (%) at different spectrums for PCS at 28 days of curing.

PCS	O	Na	Mg	Al	Si	S	Cl	K	Ca	Ti	Fe	Total
Spectrum 1	73.39	0.39	0.89	4.06	9.21	0.35	0.00	0.14	10.99	0.00	0.59	100.01
Spectrum 2	67.16	0.00	0.34	0.95	11.61	0.00	0.00	0.15	19.59	0.00	0.21	100.01
Spectrum 3	56.80	0.00	1.71	3.82	12.17	0.35	0.00	0.25	24.01	0.00	0.89	100
Spectrum 4	62.32	0.00	0.00	0.69	15.82	0.00	0.00	0.00	21.17	0.00	0.00	100
Spectrum 5	68.73	0.00	0.00	10.07	12.73	0.00	0.00	0.00	7.12	0.00	1.35	100
Spectrum 6	75.61	0.00	0.00	8.02	2.22	0.96	0.00	0.00	12.89	0.00	0.29	99.99
Spectrum 7	66.90	0.00	0.73	5.63	8.04	0.97	0.20	0.00	16.06	0.00	1.46	99.99
Spectrum 8	65.21	0.00	0.99	4.46	12.55	0.41	0.00	0.00	0.00	1.35	1.62	86.59
Spectrum 9	33.61	0.00	0.00	0.72	63.36	0.00	0.00	0.00	2.31	0.00	0.00	100
Spectrum 10	72.86	0.00	0.52	7.41	2.06	0.60	0.00	0.00	16.33	0.00	0.23	100.01
Spectrum 11	67.12	0.00	8.56	3.11	7.00	0.25	0.00	0.00	13.52	0.14	0.30	100
Spectrum 12	73.99	0.00	0.29	7.90	4.03	0.77	0.00	0.00	12.69	0.00	0.33	100
Spectrum 13	69.86	0.00	0.24	2.01	9.69	0.25	0.00	0.00	17.74	0.00	0.19	99.98
Spectrum 14	75.81	0.00	0.89	8.03	5.31	0.36	0.00	0.00	9.22	0.00	0.38	100
Spectrum 15	74.00	0.00	0.36	8.37	5.45	0.22	0.00	0.14	10.81	0.00	0.65	100
Spectrum 16	73.67	0.00	0.47	2.77	10.07	0.28	0.00	0.00	12.30	0.00	0.43	99.99
Spectrum 17	67.24	0.00	0.00	10.51	13.11	0.00	0.00	0.00	7.54	0.00	1.60	100
Spectrum 18	68.12	6.83	0.00	6.21	18.62	0.00	0.00	0.00	0.22	0.00	0.00	100

Appendix K: Particle size distribution for cement, MK and CSF

Table K1: Particle size distribution for cement.

Particle dia-meter (μm)	Test 1		Test 2		Test 3		Average	
	Volume weight-ted (%)	Cumu-lative (%)	Volume weight-ted (%)	Cumu-lative (%)	Volume weight-ted (%)	Cumu-lative (%)	Volume weight-ted (%)	Cumu-lative (%)
0.000	0.000	0.000	0.000	0.000	0.000	0.000	0.000	0.000
0.100	0.000	0.000	0.000	0.000	0.000	0.000	0.000	0.000
0.200	0.000	0.000	0.000	0.000	0.000	0.000	0.000	0.000
0.300	0.000	0.000	0.000	0.000	0.000	0.000	0.000	0.000
0.400	0.045	0.045	0.051	0.051	0.077	0.077	0.000	0.058
0.500	0.151	0.196	0.160	0.211	0.196	0.273	0.058	0.226
0.600	0.052	0.248	0.055	0.266	0.065	0.338	0.169	0.284
0.700	0.000	0.248	0.000	0.266	0.000	0.338	0.057	0.284
0.800	0.000	0.248	0.000	0.266	0.000	0.338	0.000	0.284
0.900	0.000	0.248	0.000	0.266	0.000	0.338	0.000	0.284
1.000	0.000	0.248	0.000	0.266	0.000	0.338	0.000	0.284
1.100	0.779	1.026	0.829	1.094	1.031	1.368	0.000	1.163
1.200	1.124	2.150	1.175	2.269	1.403	2.771	0.879	2.397
1.300	1.373	3.523	1.397	3.666	1.572	4.343	1.234	3.844
1.400	1.507	5.030	1.481	5.148	1.532	5.875	1.447	5.351
1.500	1.526	6.557	1.446	6.594	1.351	7.226	1.507	6.792
1.600	1.451	8.008	1.296	7.890	0.891	8.117	1.441	8.005
1.700	1.255	9.263	1.068	8.958	0.616	8.733	1.213	8.984
1.800	0.961	10.224	0.764	9.721	0.318	9.051	0.979	9.666
2.000	0.423	10.647	0.244	9.966	0.000	9.051	0.681	9.888
2.200	0.000	10.647	0.000	9.966	0.000	9.051	0.222	9.888
2.400	0.000	10.647	0.000	9.966	0.000	9.051	0.000	9.888
2.600	0.000	10.647	0.000	9.966	0.000	9.051	0.000	9.888
3.000	0.000	10.647	0.000	9.966	0.000	9.051	0.000	9.888
4.000	4.036	14.683	4.103	14.069	4.247	13.298	0.000	14.017
5.000	2.331	17.014	2.279	16.347	2.275	15.574	4.129	16.312
6.000	1.785	18.799	1.629	17.976	1.688	17.262	2.295	18.012
6.500	1.644	20.443	1.382	19.358	1.480	18.743	1.701	19.515
7.000	1.719	22.162	1.417	20.775	1.521	20.264	1.502	21.067
7.500	1.931	24.093	1.608	22.382	1.713	21.977	1.552	22.817
8.000	2.236	26.328	1.913	24.295	2.015	23.992	1.751	24.872
8.500	2.708	29.037	2.424	26.720	2.511	26.503	2.055	27.420
9.000	3.026	32.062	2.786	29.506	2.837	29.340	2.548	30.303
10.000	3.384	35.447	3.226	32.732	3.202	32.542	2.883	33.574
11.000	3.662	39.109	3.642	36.375	3.481	36.023	3.271	37.169
12.000	3.841	42.950	3.947	40.321	3.688	39.712	3.595	40.994
13.000	3.950	46.900	4.167	44.489	3.842	43.554	3.825	44.981
14.000	3.999	50.899	4.290	48.779	3.934	47.488	3.987	49.055
15.000	4.007	54.906	4.337	53.115	3.976	51.464	4.074	53.162
16.000	3.981	58.887	4.317	57.432	3.971	55.436	4.106	57.252
17.000	3.963	62.850	4.283	61.715	3.967	59.403	4.090	61.323

18.000	3.949	66.800	4.233	65.948	3.952	63.355	4.071	65.368
19.000	3.944	70.743	4.167	70.115	3.938	67.293	4.045	69.384
20.000	3.937	74.681	4.104	74.219	3.915	71.208	4.016	73.369
22.000	3.931	78.612	4.006	78.225	3.874	75.082	3.985	77.306
25.000	3.913	82.525	3.846	82.071	3.781	78.863	3.937	81.153
28.000	3.717	86.242	3.558	85.629	3.550	82.413	3.847	84.761
32.000	3.199	89.441	3.073	88.703	3.106	85.519	3.608	87.888
36.000	2.566	92.007	2.523	91.225	2.594	88.113	3.126	90.448
38.000	2.153	94.159	2.173	93.398	2.270	90.384	2.561	92.647
40.000	1.901	96.060	1.956	95.354	2.083	92.467	2.199	94.627
45.000	1.499	97.559	1.605	96.959	1.801	94.268	1.980	96.262
50.000	0.972	98.531	1.133	98.091	1.456	95.725	1.635	97.449
53.000	0.661	99.191	0.820	98.911	1.218	96.942	1.187	98.348
56.000	0.481	99.673	0.624	99.536	1.058	98.000	0.899	99.069
63.000	0.250	99.923	0.347	99.882	0.823	98.824	0.721	99.543
71.000	0.077	100.00	0.118	100.000	0.517	99.340	0.474	99.780
75.000	0.000	100.00	0.000	100.000	0.296	99.636	0.237	99.879
80.000	0.000	100.00	0.000	100.000	0.194	99.830	0.099	99.943
85.000	0.000	100.00	0.000	100.000	0.112	99.942	0.065	99.981
90.000	0.000	100.00	0.000	100.000	0.058	100.000	0.037	100.000
95.000	0.000	100.00	0.000	100.000	0.000	100.000	0.019	100.000
100.00	0.000	100.00	0.000	100.000	0.000	100.000	0.000	100.000

Table K2: Particle size distribution for metakaolin.

Particle dia-meter (μm)	Test 1		Test 2		Test 3		Average	
	Volume weight-ted (%)	Cumu-lative (%)	Volume weight-ted (%)	Cumu-lative (%)	Volume weight-ted (%)	Cumu-lative (%)	Volume weight-ted (%)	Cumu-lative (%)
0.000	0.000	0.000	0.000	0.000	0.000	0.000	0.000	0.000
0.100	0.043	0.043	0.041	0.041	0.034	0.034	0.050	0.039
0.200	0.123	0.166	0.119	0.160	0.103	0.137	0.132	0.154
0.300	0.143	0.309	0.141	0.301	0.121	0.257	0.156	0.289
0.400	0.190	0.499	0.188	0.489	0.165	0.422	0.203	0.470
0.500	0.353	0.852	0.345	0.833	0.310	0.732	0.358	0.806
0.600	0.583	1.435	0.565	1.398	0.521	1.253	0.578	1.362
0.700	0.919	2.354	0.885	2.284	0.841	2.094	0.896	2.244
0.800	1.169	3.523	1.123	3.406	1.105	3.199	1.138	3.376
0.900	1.387	4.911	1.332	4.739	1.355	4.553	1.354	4.734
1.000	1.587	6.498	1.523	6.261	1.609	6.162	1.557	6.307
1.100	1.739	8.236	1.672	7.933	1.795	7.958	1.712	8.042
1.200	1.858	10.095	1.793	9.726	1.938	9.896	1.837	9.905
1.300	1.951	12.045	1.888	11.614	2.043	11.938	1.934	11.866
1.400	2.016	14.061	1.962	13.576	2.113	14.051	2.007	13.896
1.500	2.052	16.114	2.010	15.586	2.137	16.188	2.050	15.962
1.600	2.080	18.193	2.048	17.634	2.157	18.344	2.085	18.057
1.700	2.094	20.288	2.071	19.705	2.158	20.502	2.105	20.165
1.800	2.093	22.381	2.087	21.792	2.130	22.631	2.112	22.268
2.000	2.057	24.437	2.080	23.872	2.051	24.682	2.090	24.331
2.200	2.019	26.456	2.052	25.924	1.971	26.653	2.056	26.344

2.400	1.980	28.436	2.014	27.938	1.890	28.543	2.014	28.306
2.600	1.926	30.362	1.946	29.884	1.785	30.328	1.947	30.191
3.000	1.765	32.127	1.728	31.612	1.609	31.937	1.756	31.892
4.000	1.380	33.507	1.324	32.937	1.413	33.351	1.388	33.265
5.000	0.887	34.394	0.943	33.880	1.039	34.389	0.944	34.221
6.000	0.477	34.871	0.712	34.592	0.617	35.007	0.573	34.823
6.500	0.416	35.287	0.666	35.257	0.474	35.481	0.491	35.342
7.000	0.484	35.771	0.682	35.940	0.414	35.895	0.510	35.869
7.500	0.648	36.419	0.746	36.686	0.435	36.330	0.606	36.478
8.000	1.011	37.431	0.878	37.564	0.557	36.887	0.837	37.294
8.500	1.245	38.675	0.970	38.534	0.683	37.570	1.000	38.260
9.000	1.512	40.187	1.090	39.624	0.924	38.494	1.213	39.435
10.000	1.703	41.890	1.216	40.840	1.301	39.795	1.428	40.842
11.000	1.730	43.620	1.327	42.167	1.572	41.368	1.546	42.385
12.000	1.630	45.250	1.432	43.599	1.755	43.123	1.588	43.991
13.000	1.522	46.772	1.540	45.139	1.859	44.982	1.619	45.631
14.000	1.432	48.204	1.649	46.789	1.905	46.888	1.649	47.293
15.000	1.360	49.564	1.756	48.545	1.898	48.786	1.678	48.965
16.000	1.347	50.912	1.826	50.371	1.872	50.658	1.695	50.647
17.000	1.383	52.295	1.866	52.238	1.826	52.484	1.704	52.339
18.000	1.452	53.747	1.875	54.113	1.752	54.236	1.696	54.032
19.000	1.562	55.309	1.890	56.003	1.720	55.956	1.719	55.756
20.000	1.777	57.086	1.915	57.917	1.716	57.672	1.783	57.558
22.000	2.225	59.312	1.979	59.896	1.827	59.498	1.971	59.569
25.000	2.543	61.854	2.080	61.976	2.000	61.498	2.154	61.776
28.000	2.435	64.290	2.188	64.164	2.155	63.653	2.207	64.036
32.000	2.193	66.483	2.175	66.339	2.239	65.892	2.168	66.238
36.000	2.076	68.559	2.020	68.359	2.223	68.115	2.101	68.344
38.000	2.047	70.605	1.978	70.337	2.214	70.329	2.091	70.424
40.000	2.064	72.670	2.023	72.360	2.207	72.537	2.134	72.522
45.000	2.184	74.854	2.298	74.658	2.225	74.761	2.289	74.758
50.000	2.222	77.076	2.436	77.095	2.230	76.991	2.324	77.054
53.000	2.214	79.290	2.479	79.573	2.228	79.220	2.302	79.361
56.000	2.147	81.437	2.451	82.025	2.208	81.428	2.197	81.630
63.000	2.055	83.492	2.257	84.281	2.101	83.528	2.060	83.767
71.000	1.988	85.481	2.022	86.303	1.971	85.499	1.968	85.761
75.000	1.928	87.409	1.872	88.175	1.882	87.381	1.896	87.655
80.000	1.852	89.261	1.733	89.908	1.787	89.168	1.813	89.446
85.000	1.767	91.027	1.614	91.523	1.695	90.863	1.724	91.137
90.000	1.671	92.698	1.527	93.050	1.613	92.476	1.630	92.741
95.000	1.554	94.252	1.416	94.466	1.507	93.983	1.514	94.233
100.00	1.405	95.657	1.285	95.751	1.379	95.361	1.371	95.590
106.00	1.223	96.879	1.131	96.883	1.219	96.580	1.195	96.781
112.00	0.935	97.815	0.890	97.773	0.966	97.546	0.920	97.711
125.00	0.696	98.510	0.679	98.452	0.741	98.287	0.688	98.417
130.00	0.529	99.039	0.526	98.978	0.578	98.864	0.525	98.961
140.00	0.345	99.384	0.357	99.335	0.392	99.257	0.344	99.325
145.00	0.274	99.658	0.287	99.622	0.319	99.576	0.274	99.618
150.00	0.186	99.844	0.201	99.823	0.224	99.800	0.188	99.822
160.00	0.104	99.947	0.116	99.939	0.130	99.930	0.105	99.939
170.00	0.053	100.00	0.061	100.00	0.070	100.000	0.054	100.000

Table K3: Particle size distribution for condense silica fume.

Particle dia-meter (μm)	Test 1 Volume weight-ted (%)	Test 2 Cumu-lative (%)	Test 3 Volume weight-ted (%)	Averag Cumu-lative (%)	Test 1 Volume weight-ted (%)	Test 2 Cumu-lative (%)	Test 3 Volume weight-ted (%)	Average Cumu-lative (%)
0.000	0.000	0.000	0.000	0.000	0.000	0.000	0.000	0.000
0.100	0.017	0.017	0.158	0.158	0.020	0.020	0.065	0.065
0.200	0.031	0.048	0.197	0.355	0.034	0.054	0.087	0.152
0.300	0.074	0.121	0.327	0.683	0.102	0.156	0.168	0.320
0.400	0.133	0.254	0.465	1.148	0.197	0.353	0.265	0.585
0.500	0.170	0.424	0.396	1.543	0.231	0.584	0.266	0.850
0.600	0.192	0.616	0.228	1.772	0.227	0.811	0.216	1.066
0.700	0.199	0.815	0.000	1.772	0.193	1.005	0.131	1.197
0.800	0.190	1.004	0.000	1.772	0.149	1.154	0.113	1.310
0.900	0.169	1.174	0.000	1.772	0.098	1.251	0.089	1.399
1.000	0.140	1.314	0.000	1.772	0.000	1.251	0.047	1.446
1.100	0.115	1.429	0.000	1.772	0.000	1.251	0.038	1.484
1.200	0.091	1.520	0.000	1.772	0.000	1.251	0.030	1.515
1.300	0.073	1.593	0.000	1.772	0.000	1.251	0.024	1.539
1.400	0.055	1.648	0.000	1.772	0.000	1.251	0.018	1.557
1.500	0.038	1.685	0.000	1.772	0.000	1.251	0.013	1.570
1.600	0.029	1.715	0.000	1.772	0.000	1.251	0.010	1.579
1.700	0.025	1.740	0.000	1.772	0.000	1.251	0.008	1.588
1.800	0.023	1.763	0.000	1.772	0.000	1.251	0.008	1.595
2.000	0.037	1.800	0.369	2.141	0.005	1.257	0.137	1.733
2.200	0.071	1.870	0.513	2.654	0.047	1.304	0.210	1.943
2.400	0.124	1.994	0.539	3.193	0.130	1.434	0.264	2.207
2.600	0.224	2.218	0.387	3.580	0.301	1.734	0.304	2.511
3.000	0.405	2.623	0.000	3.580	0.659	2.393	0.355	2.866
4.000	0.191	2.814	0.000	3.580	0.177	2.570	0.123	2.988
5.000	0.000	2.814	0.000	3.580	0.000	2.570	0.000	2.988
6.000	0.064	2.878	0.616	4.196	0.000	2.570	0.227	3.215
6.500	0.183	3.061	0.982	5.178	0.000	2.570	0.388	3.603
7.000	0.344	3.404	1.126	6.304	0.000	2.570	0.490	4.093
7.500	0.508	3.912	1.070	7.374	0.000	2.570	0.526	4.619
8.000	0.746	4.658	0.796	8.170	0.590	3.161	0.711	5.330
8.500	0.827	5.485	0.606	8.777	0.751	3.912	0.728	6.058
9.000	0.789	6.274	0.337	9.114	0.797	4.709	0.641	6.699
10.000	0.563	6.837	0.000	9.114	0.579	5.288	0.381	7.079
11.000	0.501	7.338	0.000	9.114	0.373	5.661	0.292	7.371
12.000	0.578	7.916	0.006	9.119	0.211	5.872	0.265	7.636
13.000	0.674	8.589	0.109	9.228	0.255	6.127	0.346	7.982
14.000	0.762	9.351	0.245	9.473	0.453	6.581	0.486	8.468
15.000	0.849	10.200	0.447	9.920	0.906	7.486	0.734	9.202
16.000	0.961	11.161	0.618	10.538	1.306	8.792	0.962	10.164
17.000	1.096	12.257	0.787	11.326	1.691	10.483	1.191	11.355
18.000	1.269	13.525	0.953	12.279	2.167	12.650	1.463	12.818
19.000	1.400	14.925	1.157	13.436	2.336	14.986	1.631	14.449
20.000	1.546	16.471	1.522	14.958	2.220	17.206	1.763	16.212

22.000	1.639	18.111	2.242	17.200	1.065	18.270	1.649	17.860
25.000	1.282	19.392	2.127	19.327	0.166	18.437	1.192	19.052
28.000	0.353	19.745	0.525	19.852	0.000	18.437	0.292	19.344
32.000	0.018	19.763	0.000	19.852	0.000	18.437	0.006	19.350
36.000	0.485	20.248	1.150	21.001	0.697	19.133	0.777	20.127
38.000	0.890	21.138	1.914	22.916	1.118	20.251	1.307	21.435
40.000	1.583	22.721	2.744	25.659	1.833	22.084	2.053	23.488
45.000	2.367	25.088	2.754	28.413	2.657	24.741	2.593	26.081
50.000	2.483	27.571	2.260	30.672	2.567	27.307	2.436	28.517
53.000	2.325	29.896	1.735	32.408	2.157	29.465	2.073	30.590
56.000	1.786	31.683	0.701	33.109	1.134	30.599	1.207	31.797
63.000	1.430	33.112	0.016	33.125	0.710	31.309	0.719	32.515
71.000	1.423	34.536	0.000	33.125	0.976	32.286	0.800	33.315
75.000	1.514	36.049	0.118	33.243	1.303	33.589	0.978	34.294
80.000	1.674	37.723	0.527	33.770	1.727	35.316	1.309	35.603
85.000	1.862	39.585	1.062	34.832	2.135	37.451	1.686	37.289
90.000	2.108	41.693	2.645	37.477	2.601	40.052	2.451	39.741
95.000	2.275	43.968	3.372	40.849	2.834	42.886	2.827	42.568
100.00	2.411	46.378	3.875	44.724	2.923	45.809	3.070	45.637
106.00	2.507	48.885	4.053	48.777	2.826	48.635	3.129	48.766
112.00	2.570	51.455	3.895	52.672	2.511	51.147	2.992	51.758
125.00	2.563	54.019	3.540	56.212	2.229	53.376	2.778	54.536
130.00	2.538	56.556	3.184	59.396	2.057	55.433	2.593	57.128
140.00	2.441	58.997	2.664	62.060	1.860	57.293	2.322	59.450
145.00	2.467	61.465	2.471	64.530	1.870	59.163	2.269	61.719
150.00	2.559	64.024	2.248	66.779	1.986	61.149	2.265	63.984
160.00	2.804	66.828	2.094	68.873	2.340	63.489	2.413	66.397
170.00	3.147	69.975	2.116	70.989	2.858	66.347	2.707	69.104
180.00	3.680	73.655	2.313	73.302	3.724	70.072	3.239	72.343
190.00	4.053	77.708	2.633	75.934	4.318	74.389	3.668	76.011
200.00	4.400	82.108	3.130	79.065	4.874	79.264	4.135	80.146
212.00	4.797	86.905	4.400	83.464	5.520	84.784	4.906	85.051
242.00	4.939	91.845	5.547	89.011	5.783	90.567	5.423	90.474
250.00	4.703	96.547	5.906	94.917	5.538	96.105	5.382	95.856
300.00	2.866	99.413	3.464	98.381	3.276	99.380	3.202	99.058
400.00	0.587	100.00	1.416	99.798	0.620	100.000	0.874	99.933
500.00	0.000	100.00	0.202	100.00	0.000	100.000	0.067	100.000

Appendix L: Pore-size and distribution for PC (Control mix), PCM and PCS

Table L1: Pore-size and distribution for PC (Control mix), PCM and PCS at 28 days of curing.

PC				PCM				PCS			
Pressure	Pore Diameter	Volume Intruded	-dV/d(log	Pressure	Pore Diameter	Volume Intruded	-dV/d(log	Pressure	Pore Diameter	Volume Intruded	-dV/d(log
(PSI)	(µm)	(cc/g)	(cc/g)	(PSI)	(µm)	(cc/g)	(cc/g)	(PSI)	(µm)	(cc/g)	(cc/g)
3.736	5.71E+01	0	5.27E-04	4.674	4.56E+01	0.0007	2.43E-03	4.2	5.08E+01	0	2.38E-04
3.864	5.52E+01	0	5.09E-04	4.775	4.47E+01	0.0008	2.36E-03	5.831	3.66E+01	0.0001	2.77E-04
4.135	5.16E+01	0.0001	4.87E-04	4.894	4.36E+01	0.0008	2.27E-03	8.554	2.49E+01	0.0001	2.76E-04
4.396	4.85E+01	0.0001	4.68E-04	5.025	4.25E+01	0.0008	2.16E-03	11.961	1.78E+01	0.0002	2.84E-04
4.647	4.59E+01	0.0001	4.56E-04	5.142	4.15E+01	0.0008	2.06E-03	15.872	1.34E+01	0.0002	2.96E-04
4.923	4.33E+01	0.0001	4.44E-04	5.286	4.04E+01	0.0009	1.97E-03	20.103	1.06E+01	0.0002	3.14E-04
5.266	4.05E+01	0.0001	4.71E-04	5.443	3.92E+01	0.0009	2.05E-03	24.013	8.88E+00	0.0003	3.64E-04
5.666	3.77E+01	0.0001	3.73E-04	5.608	3.80E+01	0.0009	1.65E-03	33.585	6.35E+00	0.0003	3.99E-04
6.11	3.49E+01	0.0001	3.52E-04	5.78	3.69E+01	0.0009	1.45E-03	43.557	4.90E+00	0.0004	4.46E-04
6.552	3.26E+01	0.0001	3.35E-04	5.972	3.57E+01	0.0009	1.28E-03	54.136	3.94E+00	0.0004	4.97E-04
7.081	3.01E+01	0.0001	3.16E-04	6.179	3.45E+01	0.001	1.15E-03	64.7	3.30E+00	0.0004	5.51E-04
7.705	2.77E+01	0.0002	3.00E-04	6.406	3.33E+01	0.001	1.07E-03	75.706	2.82E+00	0.0005	6.10E-04
8.39	2.54E+01	0.0002	2.88E-04	6.633	3.22E+01	0.001	9.55E-04	86.808	2.46E+00	0.0005	6.62E-04
9.285	2.30E+01	0.0002	2.86E-04	6.88	3.10E+01	0.001	8.60E-04	98.03	2.18E+00	0.0005	8.51E-04
10.255	2.08E+01	0.0002	2.85E-04	7.132	2.99E+01	0.001	7.97E-04	109.131	1.96E+00	0.0006	1.05E-03
11.37	1.88E+01	0.0002	2.79E-04	7.404	2.88E+01	0.001	7.43E-04	120.179	1.78E+00	0.0006	1.29E-03
12.65	1.69E+01	0.0002	2.77E-04	7.692	2.77E+01	0.001	7.01E-04	131.224	1.63E+00	0.0007	1.55E-03
13.91	1.53E+01	0.0002	2.81E-04	7.987	2.67E+01	0.001	6.83E-04	142.153	1.50E+00	0.0007	1.85E-03
15.155	1.41E+01	0.0002	2.89E-04	8.315	2.57E+01	0.0011	6.61E-04	147.51	1.45E+00	0.0007	2.18E-03
16.513	1.29E+01	0.0002	3.09E-04	8.677	2.46E+01	0.0011	6.43E-04	152.733	1.40E+00	0.0008	2.53E-03
18.035	1.18E+01	0.0003	3.34E-04	9.034	2.36E+01	0.0011	6.22E-04	157.303	1.36E+00	0.0008	2.87E-03
19.548	1.09E+01	0.0003	3.68E-04	9.394	2.27E+01	0.0011	6.06E-04	161.712	1.32E+00	0.0009	3.24E-03

20.975	1.02E+01	0.0003	4.14E-04	9.753	2.19E+01	0.0011	5.95E-04	165.611	1.29E+00	0.0009	3.64E-03
22.351	9.54E+00	0.0003	4.64E-04	10.149	2.10E+01	0.0011	5.97E-04	169.271	1.26E+00	0.0009	4.06E-03
23.535	9.06E+00	0.0003	5.10E-04	10.563	2.02E+01	0.0011	6.17E-04	172.653	1.24E+00	0.001	4.37E-03
24.636	8.66E+00	0.0003	5.63E-04	11.001	1.94E+01	0.0011	6.39E-04	175.955	1.21E+00	0.001	4.70E-03
25.606	8.33E+00	0.0003	6.36E-04	11.475	1.86E+01	0.0011	6.61E-04	179.117	1.19E+00	0.001	4.98E-03
26.405	8.08E+00	0.0003	7.14E-04	11.945	1.79E+01	0.0011	6.75E-04	182.165	1.17E+00	0.0011	5.22E-03
27.149	7.86E+00	0.0003	7.96E-04	12.39	1.72E+01	0.0012	6.85E-04	185.041	1.15E+00	0.0011	5.41E-03
27.933	7.64E+00	0.0003	8.76E-04	12.797	1.67E+01	0.0012	6.99E-04	187.989	1.14E+00	0.0012	5.56E-03
28.664	7.44E+00	0.0004	9.37E-04	13.219	1.61E+01	0.0012	7.09E-04	190.786	1.12E+00	0.0012	5.68E-03
29.278	7.29E+00	0.0004	9.91E-04	13.656	1.56E+01	0.0012	7.15E-04	193.705	1.10E+00	0.0012	5.73E-03
29.866	7.14E+00	0.0004	1.04E-03	14.143	1.51E+01	0.0012	7.28E-04	196.98	1.08E+00	0.0013	5.72E-03
30.451	7.01E+00	0.0004	1.08E-03	14.666	1.45E+01	0.0012	7.34E-04	200.325	1.07E+00	0.0013	5.67E-03
31.06	6.87E+00	0.0004	1.11E-03	15.199	1.40E+01	0.0012	7.31E-04	203.754	1.05E+00	0.0014	5.59E-03
31.758	6.72E+00	0.0004	1.15E-03	15.796	1.35E+01	0.0012	7.05E-04	207.261	1.03E+00	0.0014	5.53E-03
32.478	6.57E+00	0.0004	1.20E-03	16.469	1.30E+01	0.0013	6.79E-04	211.583	1.01E+00	0.0015	5.40E-03
33.204	6.43E+00	0.0004	1.25E-03	17.102	1.25E+01	0.0013	6.54E-04	216.015	9.88E-01	0.0015	5.30E-03
33.915	6.29E+00	0.0004	1.29E-03	17.817	1.20E+01	0.0013	6.38E-04	220.565	9.67E-01	0.0016	5.21E-03
34.665	6.15E+00	0.0005	1.32E-03	18.576	1.15E+01	0.0013	6.22E-04	225.219	9.47E-01	0.0016	5.10E-03
35.386	6.03E+00	0.0005	1.34E-03	19.448	1.10E+01	0.0013	6.08E-04	229.995	9.28E-01	0.0016	5.01E-03
36.016	5.92E+00	0.0005	1.39E-03	20.363	1.05E+01	0.0013	6.07E-04	234.862	9.08E-01	0.0017	4.93E-03
36.624	5.83E+00	0.0005	1.46E-03	21.296	1.00E+01	0.0013	6.17E-04	239.859	8.89E-01	0.0017	4.96E-03
37.226	5.73E+00	0.0005	1.52E-03	22.219	9.60E+00	0.0013	6.22E-04	244.64	8.72E-01	0.0018	4.98E-03
37.842	5.64E+00	0.0005	1.56E-03	23.209	9.19E+00	0.0013	6.44E-04	249.62	8.55E-01	0.0018	5.04E-03
38.498	5.54E+00	0.0005	1.62E-03	24.189	8.82E+00	0.0013	6.66E-04	254.667	8.38E-01	0.0019	5.08E-03
39.095	5.46E+00	0.0005	1.66E-03	25.109	8.50E+00	0.0014	7.07E-04	259.919	8.21E-01	0.0019	5.07E-03
39.655	5.38E+00	0.0005	1.69E-03	25.992	8.21E+00	0.0014	7.49E-04	264.505	8.07E-01	0.0019	5.09E-03
40.244	5.30E+00	0.0006	1.71E-03	26.873	7.94E+00	0.0014	7.91E-04	269.279	7.92E-01	0.002	5.08E-03
40.89	5.22E+00	0.0006	1.74E-03	27.658	7.71E+00	0.0014	8.18E-04	274.112	7.78E-01	0.002	5.08E-03
41.531	5.14E+00	0.0006	4.47E-03	28.431	7.50E+00	0.0014	8.54E-04	279.161	7.64E-01	0.0021	5.11E-03
42.203	5.06E+00	0.0006	7.87E-03	29.148	7.32E+00	0.0014	8.90E-04	284.865	7.49E-01	0.0021	5.15E-03
42.873	4.98E+00	0.0006	1.15E-02	29.878	7.14E+00	0.0014	9.14E-04	290.728	7.34E-01	0.0022	5.16E-03

43.57	4.90E+00	0.0006	1.22E-02	30.618	6.97E+00	0.0014	9.32E-04	296.74	7.19E-01	0.0022	5.15E-03
44.267	4.82E+00	0.0006	1.27E-02	31.481	6.78E+00	0.0014	9.42E-04	302.882	7.04E-01	0.0022	5.16E-03
45.013	4.74E+00	0.0009	1.33E-02	32.299	6.61E+00	0.0015	9.37E-04	309.158	6.90E-01	0.0023	5.17E-03
45.683	4.67E+00	0.0011	1.40E-02	33.111	6.44E+00	0.0015	9.29E-04	315.574	6.76E-01	0.0023	5.19E-03
46.325	4.61E+00	0.0014	1.46E-02	33.94	6.29E+00	0.0015	9.10E-04	322.154	6.62E-01	0.0024	5.27E-03
49.599	4.30E+00	0.0016	1.53E-02	34.795	6.13E+00	0.0015	8.95E-04	328.899	6.49E-01	0.0024	5.36E-03
53.276	4.00E+00	0.0019	1.59E-02	35.743	5.97E+00	0.0015	8.77E-04	335.827	6.35E-01	0.0025	5.46E-03
57.245	3.73E+00	0.0021	1.67E-02	36.811	5.80E+00	0.0015	8.84E-04	342.917	6.22E-01	0.0025	5.51E-03
61.297	3.48E+00	0.0024	1.39E-02	37.951	5.62E+00	0.0015	8.19E-04	350.182	6.09E-01	0.0026	5.55E-03
65.334	3.27E+00	0.0026	1.04E-02	39.173	5.45E+00	0.0015	7.52E-04	356.999	5.98E-01	0.0026	5.57E-03
69.792	3.06E+00	0.0029	6.64E-03	40.353	5.29E+00	0.0015	6.88E-04	364.062	5.86E-01	0.0027	5.60E-03
74.323	2.87E+00	0.0031	5.94E-03	41.598	5.13E+00	0.0016	6.20E-04	371.201	5.75E-01	0.0027	5.63E-03
78.961	2.70E+00	0.0034	5.28E-03	42.723	4.99E+00	0.0016	5.61E-04	378.654	5.63E-01	0.0028	5.64E-03
83.765	2.55E+00	0.0034	4.63E-03	47.353	4.51E+00	0.0016	5.08E-04	386.213	5.52E-01	0.0028	5.64E-03
88.827	2.40E+00	0.0034	3.95E-03	52.556	4.06E+00	0.0016	4.63E-04	394.102	5.41E-01	0.0029	5.66E-03
94.073	2.27E+00	0.0035	3.22E-03	58.403	3.65E+00	0.0016	4.25E-04	402.078	5.31E-01	0.0029	5.65E-03
96.87	2.20E+00	0.0035	2.53E-03	67.668	3.15E+00	0.0016	3.87E-04	410.363	5.20E-01	0.003	5.62E-03
99.296	2.15E+00	0.0035	1.82E-03	77.491	2.75E+00	0.0016	3.55E-04	418.696	5.10E-01	0.003	5.59E-03
101.703	2.10E+00	0.0035	1.06E-03	87.914	2.43E+00	0.0016	3.13E-04	427.317	4.99E-01	0.0031	5.62E-03
104.087	2.05E+00	0.0035	1.05E-03	98.989	2.16E+00	0.0017	3.56E-04	436.021	4.89E-01	0.0031	5.66E-03
106.52	2.00E+00	0.0035	1.12E-03	110.775	1.93E+00	0.0017	4.11E-04	445.073	4.79E-01	0.0032	5.71E-03
108.632	1.96E+00	0.0035	1.21E-03	123.408	1.73E+00	0.0017	4.73E-04	454.222	4.70E-01	0.0032	5.75E-03
110.82	1.93E+00	0.0035	1.27E-03	136.905	1.56E+00	0.0017	5.73E-04	463.72	4.60E-01	0.0033	5.78E-03
113.115	1.89E+00	0.0035	1.31E-03	151.413	1.41E+00	0.0017	6.80E-04	473.264	4.51E-01	0.0033	5.81E-03
115.461	1.85E+00	0.0036	1.36E-03	163.499	1.31E+00	0.0018	7.87E-04	483.121	4.42E-01	0.0034	5.85E-03
117.803	1.81E+00	0.0036	1.41E-03	176.255	1.21E+00	0.0018	8.97E-04	492.982	4.33E-01	0.0034	5.84E-03
120.273	1.77E+00	0.0036	1.45E-03	189.649	1.13E+00	0.0018	1.01E-03	503.148	4.24E-01	0.0035	5.85E-03
122.866	1.74E+00	0.0036	1.47E-03	200.933	1.06E+00	0.0018	1.13E-03	513.351	4.16E-01	0.0035	5.88E-03
125.567	1.70E+00	0.0036	1.50E-03	213.049	1.00E+00	0.0019	1.25E-03	523.927	4.07E-01	0.0036	5.89E-03
128.078	1.67E+00	0.0036	1.53E-03	226.096	9.44E-01	0.0019	1.37E-03	534.591	3.99E-01	0.0036	5.89E-03
130.654	1.63E+00	0.0036	1.58E-03	240.099	8.89E-01	0.002	1.49E-03	545.616	3.91E-01	0.0037	5.89E-03

133.289	1.60E+00	0.0037	1.63E-03	255.036	8.36E-01	0.002	1.60E-03	556.664	3.83E-01	0.0037	5.86E-03
136.002	1.57E+00	0.0037	1.69E-03	270.96	7.87E-01	0.002	1.71E-03	568.033	3.76E-01	0.0038	5.85E-03
138.656	1.54E+00	0.0037	1.74E-03	287.959	7.41E-01	0.0021	1.80E-03	579.373	3.68E-01	0.0038	5.83E-03
141.241	1.51E+00	0.0037	1.81E-03	305.989	6.97E-01	0.0021	1.88E-03	591.053	3.61E-01	0.0039	5.83E-03
143.729	1.48E+00	0.0037	1.86E-03	325.007	6.56E-01	0.0022	1.96E-03	602.738	3.54E-01	0.0039	5.84E-03
146.165	1.46E+00	0.0037	1.92E-03	345.104	6.18E-01	0.0022	2.04E-03	614.813	3.47E-01	0.004	5.88E-03
148.481	1.44E+00	0.0037	2.00E-03	366.339	5.82E-01	0.0023	2.11E-03	626.933	3.40E-01	0.004	5.91E-03
150.724	1.42E+00	0.0038	2.08E-03	388.742	5.49E-01	0.0024	2.18E-03	639.412	3.34E-01	0.0041	5.93E-03
152.973	1.40E+00	0.0038	2.16E-03	412.266	5.17E-01	0.0024	2.25E-03	651.854	3.27E-01	0.0041	5.96E-03
155.31	1.37E+00	0.0038	2.21E-03	436.913	4.88E-01	0.0025	2.30E-03	664.582	3.21E-01	0.0042	5.97E-03
157.705	1.35E+00	0.0038	2.26E-03	462.729	4.61E-01	0.0025	2.36E-03	677.22	3.15E-01	0.0042	5.97E-03
160.172	1.33E+00	0.0038	2.30E-03	489.646	4.36E-01	0.0026	2.39E-03	690.152	3.09E-01	0.0043	6.04E-03
162.703	1.31E+00	0.0038	2.34E-03	517.543	4.12E-01	0.0027	2.41E-03	703.027	3.03E-01	0.0043	6.07E-03
165.345	1.29E+00	0.0038	2.38E-03	546.387	3.90E-01	0.0027	2.42E-03	716.277	2.98E-01	0.0044	6.10E-03
168.366	1.27E+00	0.0039	2.43E-03	576.243	3.70E-01	0.0028	2.43E-03	729.488	2.92E-01	0.0044	6.13E-03
171.462	1.24E+00	0.0039	2.46E-03	607.011	3.51E-01	0.0028	2.44E-03	743.053	2.87E-01	0.0045	6.15E-03
174.649	1.22E+00	0.0039	2.49E-03	638.514	3.34E-01	0.0029	2.45E-03	756.518	2.82E-01	0.0045	6.15E-03
177.919	1.20E+00	0.0039	2.48E-03	670.729	3.18E-01	0.0029	2.45E-03	771.442	2.77E-01	0.0046	6.15E-03
181.271	1.18E+00	0.0039	2.49E-03	703.637	3.03E-01	0.003	2.44E-03	786.474	2.71E-01	0.0046	6.16E-03
184.744	1.16E+00	0.004	2.48E-03	737.145	2.89E-01	0.003	2.42E-03	801.629	2.66E-01	0.0047	6.19E-03
188.339	1.13E+00	0.004	2.50E-03	771.143	2.77E-01	0.0031	2.40E-03	817.002	2.61E-01	0.0047	6.24E-03
192.033	1.11E+00	0.004	2.50E-03	805.671	2.65E-01	0.0031	2.37E-03	834.098	2.56E-01	0.0048	6.29E-03
195.862	1.09E+00	0.004	2.50E-03	840.805	2.54E-01	0.0032	2.35E-03	851.183	2.51E-01	0.0049	6.28E-03
199.772	1.07E+00	0.0041	2.49E-03	876.478	2.43E-01	0.0032	2.34E-03	868.644	2.46E-01	0.0049	6.30E-03
203.784	1.05E+00	0.0041	2.48E-03	912.564	2.34E-01	0.0033	2.32E-03	886.001	2.41E-01	0.005	6.34E-03
207.599	1.03E+00	0.0041	2.45E-03	949.204	2.25E-01	0.0033	2.31E-03	903.697	2.36E-01	0.005	6.37E-03
211.579	1.01E+00	0.0041	2.44E-03	986.488	2.16E-01	0.0033	2.29E-03	922.92	2.31E-01	0.0051	6.40E-03
215.65	9.89E-01	0.0041	2.43E-03	1024.76	2.08E-01	0.0034	2.28E-03	942.339	2.26E-01	0.0051	6.44E-03
219.898	9.70E-01	0.0042	2.47E-03	1063.36	2.01E-01	0.0034	2.27E-03	960.807	2.22E-01	0.0052	6.48E-03
224.243	9.51E-01	0.0042	2.51E-03	1102.59	1.94E-01	0.0034	2.26E-03	979.228	2.18E-01	0.0052	6.51E-03
228.768	9.33E-01	0.0042	2.55E-03	1142.4	1.87E-01	0.0035	2.26E-03	998.03	2.14E-01	0.0053	6.51E-03

233.365	9.14E-01	0.0042	2.58E-03	1182.83	1.80E-01	0.0035	2.28E-03	1016.691	2.10E-01	0.0053	6.51E-03
238.133	8.96E-01	0.0042	2.60E-03	1223.73	1.74E-01	0.0035	2.30E-03	1034.404	2.06E-01	0.0054	6.53E-03
242.982	8.78E-01	0.0043	2.62E-03	1265.21	1.69E-01	0.0036	2.32E-03	1052.551	2.03E-01	0.0054	6.51E-03
248.049	8.60E-01	0.0043	2.65E-03	1307.25	1.63E-01	0.0036	2.34E-03	1070.912	1.99E-01	0.0055	6.51E-03
253.254	8.42E-01	0.0043	2.69E-03	1349.66	1.58E-01	0.0036	2.36E-03	1089.728	1.96E-01	0.0055	6.49E-03
258.665	8.25E-01	0.0043	2.74E-03	1392.75	1.53E-01	0.0037	2.40E-03	1108.743	1.92E-01	0.0056	6.48E-03
264.802	8.06E-01	0.0044	2.79E-03	1436.39	1.49E-01	0.0037	2.43E-03	1126.275	1.89E-01	0.0056	6.48E-03
271.096	7.87E-01	0.0044	2.85E-03	1480.21	1.44E-01	0.0037	2.47E-03	1145.789	1.86E-01	0.0057	6.49E-03
277.558	7.69E-01	0.0044	2.88E-03	1525.02	1.40E-01	0.0038	2.50E-03	1165.5	1.83E-01	0.0057	6.52E-03
284.171	7.51E-01	0.0045	2.92E-03	1570.11	1.36E-01	0.0038	2.54E-03	1185.213	1.80E-01	0.0058	6.60E-03
290.973	7.33E-01	0.0045	2.97E-03	1615.56	1.32E-01	0.0038	2.57E-03	1205.317	1.77E-01	0.0058	6.68E-03
297.981	7.16E-01	0.0045	3.04E-03	1661.74	1.28E-01	0.0039	2.61E-03	1225.6	1.74E-01	0.0059	6.73E-03
305.211	6.99E-01	0.0045	3.18E-03	1708.46	1.25E-01	0.0039	2.64E-03	1245.558	1.71E-01	0.0059	6.78E-03
312.646	6.82E-01	0.0046	3.32E-03	1755.63	1.22E-01	0.0039	2.69E-03	1265.517	1.69E-01	0.006	6.93E-03
320.276	6.66E-01	0.0046	3.47E-03	1803.44	1.18E-01	0.004	2.74E-03	1285.475	1.66E-01	0.006	7.07E-03
328.068	6.50E-01	0.0046	3.61E-03	1852.25	1.15E-01	0.004	2.80E-03	1305.252	1.63E-01	0.0061	7.26E-03
336.065	6.35E-01	0.0047	3.75E-03	1901.42	1.12E-01	0.004	2.87E-03	1325.12	1.61E-01	0.0061	7.44E-03
343.604	6.21E-01	0.0047	3.89E-03	1950.68	1.09E-01	0.0041	2.94E-03	1345.169	1.59E-01	0.0062	7.59E-03
351.434	6.07E-01	0.0048	4.04E-03	2000.4	1.07E-01	0.0041	3.01E-03	1363.767	1.56E-01	0.0062	7.76E-03
359.421	5.94E-01	0.0048	4.20E-03	2050.2	1.04E-01	0.0041	3.12E-03	1382.002	1.54E-01	0.0063	7.95E-03
367.709	5.80E-01	0.0049	4.35E-03	2100.46	1.02E-01	0.0042	3.24E-03	1400.872	1.52E-01	0.0063	8.05E-03
376.146	5.67E-01	0.0049	4.51E-03	2151.18	9.92E-02	0.0042	3.38E-03	1419.469	1.50E-01	0.0064	8.17E-03
384.832	5.54E-01	0.0049	4.65E-03	2201.89	9.69E-02	0.0042	3.53E-03	1438.702	1.48E-01	0.0064	8.31E-03
393.628	5.42E-01	0.005	4.77E-03	2253.15	9.47E-02	0.0043	3.70E-03	1457.572	1.46E-01	0.0064	8.48E-03
402.688	5.30E-01	0.005	4.89E-03	2304.04	9.26E-02	0.0043	3.88E-03	1476.805	1.44E-01	0.0065	8.63E-03
411.856	5.18E-01	0.0051	5.02E-03	2354.93	9.06E-02	0.0043	4.07E-03	1498.033	1.42E-01	0.0066	8.82E-03
421.327	5.06E-01	0.0051	5.16E-03	2405.83	8.87E-02	0.0044	4.26E-03	1519.625	1.40E-01	0.0066	8.96E-03
430.93	4.95E-01	0.0052	5.31E-03	2456.72	8.68E-02	0.0044	4.49E-03	1542.94	1.38E-01	0.0067	9.17E-03
440.854	4.84E-01	0.0052	5.44E-03	2507.89	8.51E-02	0.0045	4.73E-03	1566.527	1.36E-01	0.0067	9.51E-03
450.874	4.73E-01	0.0053	5.55E-03	2558.33	8.34E-02	0.0045	4.99E-03	1590.205	1.34E-01	0.0068	9.80E-03
461.124	4.63E-01	0.0054	5.63E-03	2609.13	8.18E-02	0.0045	5.25E-03	1613.974	1.32E-01	0.0068	1.01E-02

471.441	4.53E-01	0.0054	5.68E-03	2660.3	8.02E-02	0.0046	5.55E-03	1637.833	1.30E-01	0.0069	1.04E-02
482.003	4.43E-01	0.0055	5.70E-03	2711.74	7.87E-02	0.0046	5.85E-03	1661.693	1.28E-01	0.007	1.08E-02
492.728	4.33E-01	0.0055	5.69E-03	2763.08	7.72E-02	0.0047	6.18E-03	1685.371	1.27E-01	0.0071	1.13E-02
503.823	4.23E-01	0.0056	5.65E-03	2814.43	7.58E-02	0.0047	6.52E-03	1709.684	1.25E-01	0.0071	1.19E-02
515.114	4.14E-01	0.0056	5.56E-03	2866.51	7.44E-02	0.0048	6.88E-03	1733.906	1.23E-01	0.0072	1.25E-02
526.796	4.05E-01	0.0057	5.42E-03	2918.22	7.31E-02	0.0048	7.28E-03	1757.947	1.21E-01	0.0073	1.32E-02
538.637	3.96E-01	0.0057	5.23E-03	2969.47	7.18E-02	0.0049	7.70E-03	1782.079	1.20E-01	0.0074	1.39E-02
550.853	3.87E-01	0.0058	4.99E-03	3020.91	7.06E-02	0.005	8.13E-03	1804.487	1.18E-01	0.0074	1.46E-02
563.239	3.79E-01	0.0058	4.76E-03	3072.17	6.94E-02	0.005	8.58E-03	1826.804	1.17E-01	0.0075	1.53E-02
576.001	3.70E-01	0.0059	4.52E-03	3123.79	6.83E-02	0.0051	9.07E-03	1848.94	1.15E-01	0.0076	1.62E-02
588.949	3.62E-01	0.0059	4.32E-03	3174.96	6.72E-02	0.0052	9.60E-03	1871.348	1.14E-01	0.0077	1.73E-02
602.344	3.54E-01	0.006	4.11E-03	3225.67	6.61E-02	0.0052	1.01E-02	1893.302	1.13E-01	0.0078	1.89E-02
615.938	3.46E-01	0.006	3.91E-03	3276.29	6.51E-02	0.0053	1.07E-02	1915.166	1.11E-01	0.0079	2.05E-02
629.9	3.39E-01	0.006	3.74E-03	3326.91	6.41E-02	0.0054	1.13E-02	1936.757	1.10E-01	0.008	2.23E-02
643.943	3.31E-01	0.0061	3.59E-03	3376.72	6.32E-02	0.0054	1.19E-02	1958.258	1.09E-01	0.0081	2.41E-02
658.252	3.24E-01	0.0061	3.49E-03	3426.25	6.23E-02	0.0055	1.26E-02	1979.033	1.08E-01	0.0082	2.62E-02
672.584	3.17E-01	0.0061	3.42E-03	3476.51	6.14E-02	0.0056	1.34E-02	1998.175	1.07E-01	0.0083	2.88E-02
687.176	3.10E-01	0.0062	3.39E-03	3526.68	6.05E-02	0.0057	1.41E-02	2016.773	1.06E-01	0.0084	3.18E-02
701.769	3.04E-01	0.0062	3.42E-03	3576.39	5.97E-02	0.0058	1.50E-02	2035.461	1.05E-01	0.0086	3.49E-02
716.635	2.98E-01	0.0062	3.44E-03	3626.47	5.88E-02	0.0059	1.59E-02	2053.605	1.04E-01	0.0087	3.85E-02
731.543	2.92E-01	0.0062	3.50E-03	3676.64	5.80E-02	0.006	1.69E-02	2071.477	1.03E-01	0.0088	4.25E-02
746.752	2.86E-01	0.0063	3.54E-03	3726.72	5.72E-02	0.0061	1.80E-02	2090.075	1.02E-01	0.009	4.68E-02
761.969	2.80E-01	0.0063	3.62E-03	3776.52	5.65E-02	0.0062	1.91E-02	2108.4	1.01E-01	0.0092	5.11E-02
777.418	2.74E-01	0.0063	3.73E-03	3826.24	5.58E-02	0.0063	2.04E-02	2126.454	1.00E-01	0.0094	5.57E-02
792.827	2.69E-01	0.0064	3.84E-03	3875.86	5.50E-02	0.0064	2.16E-02	2145.596	9.94E-02	0.0096	6.06E-02
808.479	2.64E-01	0.0064	3.97E-03	3927.75	5.43E-02	0.0065	2.29E-02	2165.463	9.85E-02	0.0099	6.57E-02
824.135	2.59E-01	0.0064	4.09E-03	3981.37	5.36E-02	0.0067	2.43E-02	2186.329	9.76E-02	0.0102	7.06E-02
840.097	2.54E-01	0.0065	4.24E-03	4034.62	5.29E-02	0.0068	2.57E-02	2207.739	9.66E-02	0.0105	7.54E-02
856.12	2.49E-01	0.0065	4.38E-03	4087.88	5.22E-02	0.007	2.71E-02	2230.147	9.57E-02	0.0109	8.01E-02
872.457	2.45E-01	0.0066	4.51E-03	4141.22	5.15E-02	0.0072	2.86E-02	2252.737	9.47E-02	0.0113	8.48E-02
888.811	2.40E-01	0.0066	4.66E-03	4194.11	5.09E-02	0.0073	3.01E-02	2276.233	9.37E-02	0.0117	8.92E-02

905.382	2.36E-01	0.0066	4.79E-03	4247	5.02E-02	0.0075	3.16E-02	2300.546	9.27E-02	0.0121	9.33E-02
921.888	2.31E-01	0.0067	4.93E-03	4299.44	4.96E-02	0.0077	3.31E-02	2324.587	9.18E-02	0.0126	9.70E-02
938.572	2.27E-01	0.0067	5.08E-03	4351.87	4.90E-02	0.0078	3.46E-02	2349.445	9.08E-02	0.013	1.00E-01
955.173	2.23E-01	0.0067	5.20E-03	4403.76	4.84E-02	0.008	3.61E-02	2375.028	8.98E-02	0.0135	1.04E-01
972.068	2.20E-01	0.0068	5.32E-03	4455.38	4.79E-02	0.0082	3.77E-02	2400.067	8.89E-02	0.014	1.06E-01
988.946	2.16E-01	0.0068	5.43E-03	4505.01	4.74E-02	0.0084	3.92E-02	2425.015	8.80E-02	0.0145	1.09E-01
1006.11	2.12E-01	0.0069	5.53E-03	4552.09	4.69E-02	0.0086	4.07E-02	2449.691	8.71E-02	0.015	1.11E-01
1023.23	2.09E-01	0.0069	5.61E-03	4599.18	4.64E-02	0.0088	4.22E-02	2474.094	8.62E-02	0.0155	1.12E-01
1040.42	2.05E-01	0.007	5.71E-03	4645.99	4.59E-02	0.009	4.36E-02	2498.407	8.54E-02	0.016	1.13E-01
1057.89	2.02E-01	0.007	5.78E-03	4692.35	4.55E-02	0.0092	4.50E-02	2522.993	8.46E-02	0.0165	1.14E-01
1075.40	1.98E-01	0.007	5.85E-03	4738.61	4.50E-02	0.0094	4.63E-02	2547.669	8.37E-02	0.017	1.14E-01
1092.96	1.95E-01	0.0071	5.92E-03	4784.61	4.46E-02	0.0096	4.75E-02	2572.163	8.29E-02	0.0175	1.14E-01
1110.78	1.92E-01	0.0071	6.00E-03	4830.79	4.42E-02	0.0098	4.86E-02	2596.748	8.22E-02	0.0179	1.13E-01
1128.65	1.89E-01	0.0072	6.06E-03	4876.69	4.37E-02	0.01	4.98E-02	2621.515	8.14E-02	0.0184	1.12E-01
1146.90	1.86E-01	0.0072	6.15E-03	4922.69	4.33E-02	0.0102	5.08E-02	2646.373	8.06E-02	0.0189	1.11E-01
1165.00	1.83E-01	0.0072	6.24E-03	4968.86	4.29E-02	0.0104	5.17E-02	2670.867	7.99E-02	0.0193	1.09E-01
1183.48	1.80E-01	0.0073	6.33E-03	5014.58	4.25E-02	0.0106	5.25E-02	2695.724	7.91E-02	0.0198	1.06E-01
1202.08	1.78E-01	0.0073	6.43E-03	5060.67	4.22E-02	0.0108	5.16E-02	2721.398	7.84E-02	0.0202	1.04E-01
1220.77	1.75E-01	0.0074	6.53E-03	5106.12	4.18E-02	0.011	5.07E-02	2747.254	7.77E-02	0.0206	1.01E-01
1239.55	1.72E-01	0.0074	6.63E-03	5151.84	4.14E-02	0.0113	4.97E-02	2773.291	7.69E-02	0.021	9.89E-02
1258.15	1.70E-01	0.0075	6.76E-03	5197.57	4.10E-02	0.0115	4.86E-02	2799.599	7.62E-02	0.0214	9.65E-02
1277.02	1.67E-01	0.0075	6.87E-03	5243.11	4.07E-02	0.0117	4.76E-02	2826.362	7.55E-02	0.0218	9.39E-02
1296.07	1.65E-01	0.0076	7.01E-03	5309.61	4.02E-02	0.0119	4.65E-02	2853.85	7.48E-02	0.0222	9.17E-02
1315.12	1.62E-01	0.0076	7.17E-03	5376.2	3.97E-02	0.0121	4.54E-02	2881.701	7.40E-02	0.0225	9.02E-02
1334.08	1.60E-01	0.0076	7.30E-03	5442.97	3.92E-02	0.0123	4.42E-02	2909.916	7.33E-02	0.0229	8.88E-02
1353.22	1.58E-01	0.0077	7.43E-03	5509.65	3.87E-02	0.0125	4.30E-02	2938.764	7.26E-02	0.0233	8.79E-02
1372.64	1.55E-01	0.0077	7.54E-03	5576.33	3.83E-02	0.0127	4.17E-02	2968.43	7.19E-02	0.0236	8.72E-02
1391.87	1.53E-01	0.0078	7.63E-03	5643.28	3.78E-02	0.0129	4.05E-02	2998.005	7.12E-02	0.024	8.67E-02
1411.19	1.51E-01	0.0078	7.69E-03	5710.5	3.74E-02	0.0132	4.26E-02	3027.308	7.05E-02	0.0244	8.65E-02
1430.70	1.49E-01	0.0079	7.75E-03	5777.82	3.69E-02	0.0134	4.46E-02	3057.245	6.98E-02	0.0247	8.67E-02
1450.38	1.47E-01	0.0079	7.79E-03	5845.31	3.65E-02	0.0136	4.66E-02	3087.093	6.91E-02	0.0251	8.69E-02

1470.34	1.45E-01	0.008	7.81E-03	5913.17	3.61E-02	0.0138	4.85E-02	3117.302	6.84E-02	0.0255	8.72E-02
1490.66	1.43E-01	0.008	7.83E-03	5981.3	3.57E-02	0.014	5.03E-02	3147.422	6.78E-02	0.0258	8.76E-02
1510.99	1.41E-01	0.0081	7.82E-03	6028.57	3.54E-02	0.0142	5.21E-02	3177.994	6.71E-02	0.0262	8.79E-02
1531.58	1.39E-01	0.0081	7.76E-03	6076.01	3.51E-02	0.0144	5.39E-02	3208.295	6.65E-02	0.0266	8.76E-02
1552.45	1.37E-01	0.0082	7.75E-03	6123.73	3.48E-02	0.0146	5.56E-02	3238.777	6.59E-02	0.0269	8.75E-02
1573.31	1.36E-01	0.0082	7.74E-03	6171.45	3.46E-02	0.0148	5.74E-02	3269.531	6.53E-02	0.0273	8.70E-02
1594.45	1.34E-01	0.0082	7.77E-03	6219.17	3.43E-02	0.015	5.91E-02	3300.739	6.46E-02	0.0277	8.65E-02
1615.86	1.32E-01	0.0083	7.83E-03	6267.16	3.40E-02	0.0152	6.09E-02	3332.309	6.40E-02	0.028	8.59E-02
1637.45	1.30E-01	0.0083	7.96E-03	6315.43	3.38E-02	0.0154	6.08E-02	3364.606	6.34E-02	0.0284	8.52E-02
1659.22	1.29E-01	0.0084	8.13E-03	6363.78	3.35E-02	0.0156	6.09E-02	3397.265	6.28E-02	0.0287	8.41E-02
1680.72	1.27E-01	0.0084	8.31E-03	6411.95	3.33E-02	0.0158	6.10E-02	3430.741	6.22E-02	0.0291	8.29E-02
1702.68	1.25E-01	0.0085	8.59E-03	6460.31	3.30E-02	0.016	6.10E-02	3464.308	6.16E-02	0.0294	8.17E-02
1724.27	1.24E-01	0.0085	8.95E-03	6508.84	3.28E-02	0.0162	6.11E-02	3498.419	6.10E-02	0.0298	8.05E-02
1746.04	1.22E-01	0.0086	9.36E-03	6557.47	3.25E-02	0.0164	6.11E-02	3532.711	6.04E-02	0.0301	7.92E-02
1767.63	1.21E-01	0.0086	9.88E-03	6606.37	3.23E-02	0.0166	6.08E-02	3568.092	5.98E-02	0.0304	7.82E-02
1789.59	1.19E-01	0.0087	1.04E-02	6655.35	3.21E-02	0.0168	6.04E-02	3603.836	5.92E-02	0.0308	7.73E-02
1811.45	1.18E-01	0.0087	1.11E-02	6704.71	3.18E-02	0.017	5.96E-02	3640.033	5.86E-02	0.0311	7.64E-02
1833.32	1.16E-01	0.0088	1.18E-02	6754.06	3.16E-02	0.0172	5.86E-02	3676.775	5.80E-02	0.0314	7.54E-02
1855.09	1.15E-01	0.0088	1.26E-02	6803.5	3.14E-02	0.0174	5.71E-02	3714.333	5.74E-02	0.0318	7.44E-02
1876.68	1.14E-01	0.0089	1.34E-02	6852.76	3.11E-02	0.0176	5.52E-02	3752.255	5.69E-02	0.0321	7.34E-02
1898.27	1.12E-01	0.009	1.43E-02	6902.57	3.09E-02	0.0178	5.15E-02	3790.176	5.63E-02	0.0324	7.26E-02
1920.14	1.11E-01	0.0091	1.54E-02	6952.56	3.07E-02	0.0179	4.76E-02	3827.008	5.57E-02	0.0327	7.16E-02
1941.09	1.10E-01	0.0091	1.65E-02	7002.36	3.05E-02	0.0181	4.35E-02	3864.566	5.52E-02	0.033	7.07E-02
1962.50	1.09E-01	0.0092	1.76E-02	7052.8	3.03E-02	0.0182	3.92E-02	3902.85	5.47E-02	0.0333	6.97E-02
1983.55	1.08E-01	0.0093	1.89E-02	7103.15	3.00E-02	0.0183	3.48E-02	3941.316	5.41E-02	0.0336	6.88E-02
2004.6	1.06E-01	0.0094	2.03E-02	7186.34	2.97E-02	0.0184	3.05E-02	3978.421	5.36E-02	0.0339	6.77E-02
2025.01	1.05E-01	0.0095	2.17E-02	7269.71	2.93E-02	0.0185	2.63E-02	4016.433	5.31E-02	0.0341	6.63E-02
2045.51	1.04E-01	0.0096	2.32E-02	7353.36	2.90E-02	0.0186	2.23E-02	4054.716	5.26E-02	0.0344	6.51E-02
2065.47	1.03E-01	0.0097	2.47E-02	7437.46	2.87E-02	0.0187	1.85E-02	4093.273	5.21E-02	0.0347	6.37E-02
2085.34	1.02E-01	0.0098	2.64E-02	7521.73	2.84E-02	0.0187	1.50E-02	4131.829	5.16E-02	0.0349	6.23E-02
2104.93	1.01E-01	0.0099	2.82E-02	7606.38	2.81E-02	0.0188	1.20E-02	4171.202	5.11E-02	0.0352	6.07E-02

2124.26	1.00E-01	0.01	3.00E-02	7691.11	2.77E-02	0.0188	1.12E-02	4211.209	5.07E-02	0.0354	5.90E-02
2143.58	9.95E-02	0.0102	3.18E-02	7775.93	2.74E-02	0.0189	1.04E-02	4253.304	5.02E-02	0.0357	5.75E-02
2162.99	9.86E-02	0.0103	3.37E-02	7861.21	2.71E-02	0.0189	9.98E-03	4295.852	4.97E-02	0.0359	5.59E-02
2181.59	9.78E-02	0.0104	3.56E-02	7946.22	2.69E-02	0.019	9.70E-03	4338.853	4.92E-02	0.0362	5.43E-02
2200.19	9.70E-02	0.0106	3.77E-02	8031.68	2.66E-02	0.019	9.58E-03	4382.671	4.87E-02	0.0364	5.25E-02
2218.42	9.62E-02	0.0107	3.98E-02	8084.84	2.64E-02	0.019	9.48E-03	4428.485	4.82E-02	0.0366	5.09E-02
2236.66	9.54E-02	0.0108	4.19E-02	8138.09	2.62E-02	0.0191	9.49E-03	4474.571	4.77E-02	0.0368	4.94E-02
2254.44	9.46E-02	0.011	4.42E-02	8191.16	2.60E-02	0.0191	9.59E-03	4521.383	4.72E-02	0.0371	4.77E-02
2272.31	9.39E-02	0.0111	4.66E-02	8244.5	2.59E-02	0.0191	9.78E-03	4568.83	4.67E-02	0.0373	4.62E-02
2291.09	9.31E-02	0.0113	4.90E-02	8297.94	2.57E-02	0.0191	9.99E-03	4616.912	4.62E-02	0.0375	4.48E-02
2309.69	9.24E-02	0.0115	5.15E-02	8351.28	2.55E-02	0.0192	1.02E-02	4664.993	4.57E-02	0.0377	4.35E-02
2328.10	9.16E-02	0.0117	5.40E-02	8404.72	2.54E-02	0.0192	9.90E-03	4713.529	4.53E-02	0.0378	4.22E-02
2347.52	9.09E-02	0.0119	5.66E-02	8458.69	2.52E-02	0.0192	9.71E-03	4762.427	4.48E-02	0.038	4.10E-02
2368.11	9.01E-02	0.0121	5.92E-02	8512.95	2.51E-02	0.0192	9.54E-03	4811.96	4.43E-02	0.0382	3.98E-02
2389.89	8.93E-02	0.0124	6.20E-02	8567.11	2.49E-02	0.0193	9.39E-03	4861.675	4.39E-02	0.0384	3.86E-02
2412.57	8.84E-02	0.0126	6.45E-02	8621.54	2.47E-02	0.0193	9.23E-03	4912.025	4.34E-02	0.0385	3.77E-02
2436.52	8.76E-02	0.0129	6.72E-02	8675.7	2.46E-02	0.0193	9.11E-03	4962.919	4.30E-02	0.0387	3.67E-02
2461.74	8.67E-02	0.0132	6.99E-02	8730.13	2.44E-02	0.0193	9.00E-03	5014.267	4.25E-02	0.0389	3.57E-02
2487.77	8.58E-02	0.0136	7.26E-02	8784.93	2.43E-02	0.0194	8.86E-03	5065.706	4.21E-02	0.039	3.49E-02
2514.72	8.48E-02	0.0139	7.52E-02	8839.63	2.41E-02	0.0194	8.70E-03	5117.507	4.17E-02	0.0392	3.41E-02
2541.48	8.39E-02	0.0143	7.77E-02	8894.43	2.40E-02	0.0194	8.55E-03	5169.762	4.13E-02	0.0393	3.33E-02
2569.24	8.30E-02	0.0146	8.00E-02	8950.22	2.38E-02	0.0194	8.40E-03	5222.47	4.09E-02	0.0395	3.26E-02
2598.00	8.21E-02	0.015	8.22E-02	9006.01	2.37E-02	0.0195	8.23E-03	5275.451	4.04E-02	0.0396	3.19E-02
2625.94	8.12E-02	0.0154	8.45E-02	9061.9	2.35E-02	0.0195	8.11E-03	5328.885	4.00E-02	0.0397	3.12E-02
2653.97	8.04E-02	0.0159	8.63E-02	9117.6	2.34E-02	0.0195	7.96E-03	5382.683	3.96E-02	0.0399	3.05E-02
2681.91	7.95E-02	0.0163	8.79E-02	9174.03	2.33E-02	0.0195	7.82E-03	5436.752	3.92E-02	0.04	3.00E-02
2710.04	7.87E-02	0.0167	8.95E-02	9230.73	2.31E-02	0.0195	7.73E-03	5490.73	3.89E-02	0.0401	2.95E-02
2738.07	7.79E-02	0.0171	9.06E-02	9287.43	2.30E-02	0.0196	7.71E-03	5545.163	3.85E-02	0.0402	2.89E-02
2765.74	7.71E-02	0.0175	9.11E-02	9344.4	2.28E-02	0.0196	7.72E-03	5599.958	3.81E-02	0.0404	2.85E-02
2792.78	7.64E-02	0.0179	9.04E-02	9401.73	2.27E-02	0.0196	7.77E-03	5655.297	3.77E-02	0.0405	2.80E-02
2819.99	7.57E-02	0.0183	8.91E-02	9459.25	2.26E-02	0.0196	7.87E-03	5710.637	3.74E-02	0.0406	2.76E-02

2847.21	7.49E-02	0.0187	8.56E-02	9517.04	2.24E-02	0.0196	7.96E-03	5766.158	3.70E-02	0.0407	2.72E-02
2874.51	7.42E-02	0.0191	8.15E-02	9574.47	2.23E-02	0.0197	8.08E-03	5822.313	3.66E-02	0.0408	2.69E-02
2902.00	7.35E-02	0.0194	7.68E-02	9632.62	2.22E-02	0.0197	8.22E-03	5878.651	3.63E-02	0.0409	2.65E-02
2930.58	7.28E-02	0.0198	7.13E-02	9690.77	2.20E-02	0.0197	8.33E-03	5934.988	3.59E-02	0.041	2.62E-02
2958.79	7.21E-02	0.0201	6.57E-02	9749.37	2.19E-02	0.0197	8.45E-03	5991.417	3.56E-02	0.0411	2.59E-02
2995.72	7.12E-02	0.0203	5.94E-02	9807.89	2.18E-02	0.0198	8.62E-03	6048.479	3.53E-02	0.0413	2.56E-02
3032.73	7.03E-02	0.0206	5.26E-02	9866.58	2.16E-02	0.0198	8.74E-03	6105.634	3.49E-02	0.0414	2.53E-02
3070.29	6.95E-02	0.0208	4.55E-02	9925.73	2.15E-02	0.0198	8.83E-03	6162.878	3.46E-02	0.0415	2.51E-02
3108.12	6.86E-02	0.021	3.86E-02	9984.98	2.14E-02	0.0198	8.91E-03	6220.304	3.43E-02	0.0416	2.48E-02
3147.49	6.78E-02	0.0211	3.23E-02	10044.3	2.12E-02	0.0199	8.95E-03	6277.821	3.40E-02	0.0417	2.46E-02
3186.95	6.69E-02	0.0213	2.67E-02	10104.1	2.11E-02	0.0199	8.96E-03	6335.52	3.37E-02	0.0418	2.45E-02
3227.05	6.61E-02	0.0214	2.32E-02	10164.2	2.10E-02	0.0199	8.99E-03	6393.581	3.34E-02	0.0418	2.43E-02
3267.97	6.53E-02	0.0215	2.02E-02	10226.7	2.09E-02	0.0199	9.01E-03	6451.461	3.31E-02	0.0419	2.42E-02
3309.16	6.45E-02	0.0215	1.77E-02	10289.1	2.07E-02	0.0199	9.03E-03	6509.794	3.28E-02	0.042	2.41E-02
3349.25	6.37E-02	0.0216	1.56E-02	10352.3	2.06E-02	0.02	9.04E-03	6568.58	3.25E-02	0.0421	2.40E-02
3390.08	6.29E-02	0.0216	1.37E-02	10415.5	2.05E-02	0.02	9.03E-03	6627.004	3.22E-02	0.0422	2.39E-02
3422.83	6.23E-02	0.0217	1.23E-02	10478.9	2.04E-02	0.02	8.99E-03	6685.609	3.19E-02	0.0423	2.37E-02
3456.12	6.17E-02	0.0217	1.14E-02	10542.6	2.02E-02	0.02	8.94E-03	6744.668	3.16E-02	0.0424	2.35E-02
3489.51	6.11E-02	0.0218	1.09E-02	10606.6	2.01E-02	0.0201	8.92E-03	6803.908	3.14E-02	0.0425	2.34E-02
3522.17	6.06E-02	0.0218	1.05E-02	10671	2.00E-02	0.0201	8.90E-03	6863.058	3.11E-02	0.0426	2.32E-02
3554.92	6.00E-02	0.0219	1.03E-02	10735.5	1.99E-02	0.0201	8.90E-03	6922.571	3.08E-02	0.0427	2.30E-02
3587.03	5.95E-02	0.0219	1.01E-02	10800.4	1.98E-02	0.0201	8.91E-03	6982.356	3.06E-02	0.0428	2.27E-02
3619.42	5.89E-02	0.022	9.60E-03	10865.6	1.96E-02	0.0202	8.89E-03	7042.412	3.03E-02	0.0428	2.25E-02
3651.99	5.84E-02	0.022	9.23E-03	10928.8	1.95E-02	0.0202	8.83E-03	7102.469	3.00E-02	0.0429	2.23E-02
3685.46	5.79E-02	0.022	8.92E-03	10992.3	1.94E-02	0.0202	8.74E-03	7162.708	2.98E-02	0.043	2.19E-02
3721.03	5.73E-02	0.0221	8.70E-03	11055.8	1.93E-02	0.0202	8.64E-03	7222.946	2.95E-02	0.0431	2.17E-02
3757.31	5.68E-02	0.0221	8.54E-03	11120.1	1.92E-02	0.0202	8.57E-03	7283.457	2.93E-02	0.0432	2.15E-02
3794.24	5.62E-02	0.0221	8.45E-03	11187.3	1.91E-02	0.0203	8.51E-03	7343.967	2.91E-02	0.0432	2.14E-02
3831.80	5.57E-02	0.0222	8.41E-03	11254.6	1.90E-02	0.0203	8.48E-03	7404.661	2.88E-02	0.0433	2.13E-02
3870.08	5.51E-02	0.0222	8.35E-03	11322.4	1.88E-02	0.0203	8.42E-03	7465.715	2.86E-02	0.0434	2.13E-02
3910.72	5.46E-02	0.0222	8.39E-03	11390.3	1.87E-02	0.0203	8.34E-03	7527.042	2.83E-02	0.0435	2.12E-02

3951.82	5.40E-02	0.0223	8.41E-03	11458.5	1.86E-02	0.0204	8.27E-03	7588.278	2.81E-02	0.0435	2.11E-02
3994.91	5.34E-02	0.0223	8.45E-03	11527	1.85E-02	0.0204	8.21E-03	7649.877	2.79E-02	0.0436	2.11E-02
4038.82	5.28E-02	0.0224	8.49E-03	11595.5	1.84E-02	0.0204	8.17E-03	7711.567	2.77E-02	0.0437	2.11E-02
4083.55	5.22E-02	0.0224	8.49E-03	11664.4	1.83E-02	0.0204	8.23E-03	7773.347	2.74E-02	0.0438	2.10E-02
4128.54	5.17E-02	0.0224	8.51E-03	11733.2	1.82E-02	0.0204	8.31E-03	7835.219	2.72E-02	0.0438	2.11E-02
4173.54	5.11E-02	0.0225	8.49E-03	11802	1.81E-02	0.0205	8.48E-03	7897.361	2.70E-02	0.0439	2.11E-02
4216.81	5.06E-02	0.0225	8.46E-03	11871.1	1.80E-02	0.0205	8.61E-03	7960.05	2.68E-02	0.044	2.11E-02
4258.64	5.01E-02	0.0226	8.43E-03	11937.9	1.79E-02	0.0205	8.75E-03	8022.919	2.66E-02	0.044	2.11E-02
4300.64	4.96E-02	0.0226	8.41E-03	12004.9	1.78E-02	0.0205	8.89E-03	8085.607	2.64E-02	0.0441	2.10E-02
4343.01	4.91E-02	0.0226	8.34E-03	12072.1	1.77E-02	0.0205	9.03E-03	8148.295	2.62E-02	0.0442	2.09E-02
4385.73	4.86E-02	0.0227	8.21E-03	12139.4	1.76E-02	0.0206	9.14E-03	8210.892	2.60E-02	0.0443	2.09E-02
4428.74	4.82E-02	0.0227	8.08E-03	12206.9	1.75E-02	0.0206	9.26E-03	8274.033	2.58E-02	0.0443	2.08E-02
4472.19	4.77E-02	0.0227	7.97E-03	12274.4	1.74E-02	0.0206	9.38E-03	8336.993	2.56E-02	0.0444	2.07E-02
4515.92	4.72E-02	0.0228	7.81E-03	12342	1.73E-02	0.0206	9.50E-03	8400.406	2.54E-02	0.0445	2.06E-02
4559.65	4.68E-02	0.0228	7.70E-03	12410	1.72E-02	0.0207	9.53E-03	8464.183	2.52E-02	0.0445	2.07E-02
4603.83	4.63E-02	0.0228	7.59E-03	12478.6	1.71E-02	0.0207	9.56E-03	8528.142	2.50E-02	0.0446	2.05E-02
4648.55	4.59E-02	0.0229	7.47E-03	12550.5	1.70E-02	0.0207	9.51E-03	8592.28	2.48E-02	0.0447	2.03E-02
4695.82	4.54E-02	0.0229	7.34E-03	12622.3	1.69E-02	0.0207	9.48E-03	8656.421	2.46E-02	0.0447	2.01E-02
4745.35	4.50E-02	0.0229	7.22E-03	12694.2	1.68E-02	0.0208	9.44E-03	8720.74	2.45E-02	0.0448	1.99E-02
4795.52	4.45E-02	0.023	7.08E-03	12766.6	1.67E-02	0.0208	9.37E-03	8785.151	2.43E-02	0.0449	1.97E-02
4845.96	4.40E-02	0.023	7.02E-03	12842.3	1.66E-02	0.0208	9.31E-03	8849.654	2.41E-02	0.0449	1.94E-02
4894.31	4.36E-02	0.023	7.03E-03	12918.2	1.65E-02	0.0208	9.23E-03	8914.973	2.39E-02	0.045	1.93E-02
4942.85	4.32E-02	0.023	7.12E-03	12994.9	1.64E-02	0.0208	9.13E-03	8980.109	2.38E-02	0.045	1.92E-02
4989.39	4.28E-02	0.0231	7.18E-03	13074.5	1.63E-02	0.0209	8.99E-03	9045.7	2.36E-02	0.0451	1.89E-02
5036.02	4.24E-02	0.0231	7.29E-03	13154.5	1.62E-02	0.0209	8.82E-03	9111.11	2.34E-02	0.0452	1.88E-02
5083.28	4.20E-02	0.0231	7.39E-03	13234.8	1.61E-02	0.0209	8.71E-03	9176.61	2.33E-02	0.0452	1.85E-02
5130.73	4.16E-02	0.0232	7.47E-03	13318.5	1.60E-02	0.0209	8.53E-03	9242.384	2.31E-02	0.0453	1.83E-02
5178.45	4.12E-02	0.0232	7.58E-03	13399.6	1.59E-02	0.021	8.36E-03	9307.883	2.29E-02	0.0453	1.83E-02
5226.17	4.08E-02	0.0232	7.72E-03	13481.3	1.58E-02	0.021	8.19E-03	9373.837	2.28E-02	0.0454	1.83E-02
5274.25	4.05E-02	0.0233	7.82E-03	13566.1	1.57E-02	0.021	8.01E-03	9439.79	2.26E-02	0.0454	1.84E-02
5322.61	4.01E-02	0.0233	7.94E-03	13654.3	1.56E-02	0.021	7.82E-03	9506.108	2.24E-02	0.0455	1.84E-02

5370.96	3.97E-02	0.0233	8.01E-03	13740.1	1.55E-02	0.0211	7.61E-03	9573.06	2.23E-02	0.0455	1.85E-02
5421.58	3.94E-02	0.0233	8.02E-03	13829.1	1.54E-02	0.0211	7.45E-03	9639.738	2.21E-02	0.0456	1.85E-02
5472.84	3.90E-02	0.0234	7.97E-03	13921.5	1.53E-02	0.0211	7.27E-03	9706.689	2.20E-02	0.0457	1.85E-02
5526.73	3.86E-02	0.0234	7.97E-03	14015.1	1.52E-02	0.0211	7.13E-03	9773.732	2.18E-02	0.0457	1.85E-02
5580.98	3.82E-02	0.0235	7.94E-03	14111.8	1.51E-02	0.0211	6.99E-03	9840.865	2.17E-02	0.0458	1.86E-02
5635.23	3.79E-02	0.0235	7.90E-03	14211.8	1.50E-02	0.0212	6.83E-03	9908.271	2.15E-02	0.0458	1.86E-02
5689.84	3.75E-02	0.0235	7.87E-03	14309.1	1.49E-02	0.0212	6.70E-03	9975.858	2.14E-02	0.0459	1.87E-02
5744.73	3.71E-02	0.0235	7.79E-03	14410.3	1.48E-02	0.0212	6.58E-03	10044.17	2.12E-02	0.0459	1.88E-02
5799.98	3.68E-02	0.0236	7.67E-03	14514.6	1.47E-02	0.0212	6.43E-03	10112.3	2.11E-02	0.046	1.89E-02
5855.50	3.64E-02	0.0236	7.60E-03	14616.4	1.46E-02	0.0212	6.27E-03	10180.61	2.10E-02	0.046	1.89E-02
5910.84	3.61E-02	0.0236	7.50E-03	14718.5	1.45E-02	0.0213	6.13E-03	10249.38	2.08E-02	0.0461	1.89E-02
5966.81	3.58E-02	0.0237	7.43E-03	14823.9	1.44E-02	0.0213	6.01E-03	10318.06	2.07E-02	0.0462	1.89E-02
6023.15	3.54E-02	0.0237	7.36E-03	14930.4	1.43E-02	0.0213	5.86E-03	10386.91	2.05E-02	0.0462	1.89E-02
6079.76	3.51E-02	0.0237	7.31E-03	15036.7	1.42E-02	0.0213	5.76E-03	10455.68	2.04E-02	0.0463	1.90E-02
6136.37	3.48E-02	0.0238	7.15E-03	15143.7	1.41E-02	0.0213	5.61E-03	10524.99	2.03E-02	0.0463	1.90E-02
6193.16	3.44E-02	0.0238	7.00E-03	15251	1.40E-02	0.0213	5.50E-03	10594.57	2.01E-02	0.0464	1.90E-02
6250.04	3.41E-02	0.0238	6.87E-03	15359.3	1.39E-02	0.0214	5.37E-03	10664.34	2.00E-02	0.0464	1.91E-02
6307.28	3.38E-02	0.0238	6.74E-03	15468	1.38E-02	0.0214	5.27E-03	10734.19	1.99E-02	0.0465	1.91E-02
6364.62	3.35E-02	0.0239	6.64E-03	15576.3	1.37E-02	0.0214	5.18E-03	10804.23	1.97E-02	0.0465	1.91E-02
6422.32	3.32E-02	0.0239	6.59E-03	15685.3	1.36E-02	0.0214	5.09E-03	10874.72	1.96E-02	0.0466	1.90E-02
6479.83	3.29E-02	0.0239	6.48E-03	15797.9	1.35E-02	0.0214	5.01E-03	10945.39	1.95E-02	0.0466	1.89E-02
6538.08	3.26E-02	0.0239	6.42E-03	15911.1	1.34E-02	0.0214	4.92E-03	11016.15	1.94E-02	0.0467	1.89E-02
6596.32	3.23E-02	0.024	6.32E-03	16024.4	1.33E-02	0.0214	4.84E-03	11086.64	1.92E-02	0.0467	1.89E-02
6654.74	3.21E-02	0.024	6.20E-03	16138.2	1.32E-02	0.0215	4.79E-03	11157.77	1.91E-02	0.0468	1.89E-02
6713.26	3.18E-02	0.024	6.10E-03	16252.6	1.31E-02	0.0215	4.72E-03	11229.25	1.90E-02	0.0469	1.89E-02
6772.05	3.15E-02	0.024	6.08E-03	16378	1.30E-02	0.0215	4.67E-03	11300.29	1.89E-02	0.0469	1.89E-02
6831.29	3.12E-02	0.0241	6.03E-03	16504.4	1.29E-02	0.0215	4.58E-03	11371.68	1.88E-02	0.047	1.88E-02
6890.71	3.10E-02	0.0241	5.98E-03	16630.8	1.28E-02	0.0215	4.55E-03	11443.35	1.86E-02	0.047	1.88E-02
6950.13	3.07E-02	0.0241	5.90E-03	16760.9	1.27E-02	0.0215	4.45E-03	11515.2	1.85E-02	0.0471	1.88E-02
7009.82	3.04E-02	0.0241	5.84E-03	16903.2	1.26E-02	0.0216	4.35E-03	11587.14	1.84E-02	0.0471	1.86E-02
7069.79	3.02E-02	0.0242	5.77E-03	17057.1	1.25E-02	0.0216	4.30E-03	11658.99	1.83E-02	0.0472	1.86E-02

7130.03	2.99E-02	0.0242	5.72E-03	17211.1	1.24E-02	0.0216	4.26E-03	11731.3	1.82E-02	0.0472	1.86E-02
7189.81	2.97E-02	0.0242	5.64E-03	17365.6	1.23E-02	0.0216	4.25E-03	11803.69	1.81E-02	0.0473	1.85E-02
7250.32	2.94E-02	0.0242	5.58E-03	17521.1	1.22E-02	0.0216	4.21E-03	11876.36	1.80E-02	0.0473	1.84E-02
7310.74	2.92E-02	0.0242	5.52E-03	17676.5	1.21E-02	0.0216	4.14E-03	11949.21	1.79E-02	0.0474	1.83E-02
7371.62	2.89E-02	0.0243	5.47E-03	17832.7	1.20E-02	0.0217	4.06E-03	12022.15	1.77E-02	0.0474	1.82E-02
7432.58	2.87E-02	0.0243	5.39E-03	17989.6	1.19E-02	0.0217	4.01E-03	12095.45	1.76E-02	0.0474	1.82E-02
7493.54	2.85E-02	0.0243	5.36E-03	18147.2	1.18E-02	0.0217	3.98E-03	12168.48	1.75E-02	0.0475	1.81E-02
7554.87	2.82E-02	0.0243	5.30E-03	18316.5	1.17E-02	0.0217	3.93E-03	12241.78	1.74E-02	0.0475	1.79E-02
7616.38	2.80E-02	0.0243	5.31E-03	18486.3	1.15E-02	0.0217	3.90E-03	12315.45	1.73E-02	0.0476	1.79E-02
7677.98	2.78E-02	0.0243	5.25E-03	18656.9	1.14E-02	0.0217	3.87E-03	12388.84	1.72E-02	0.0476	1.79E-02
7739.40	2.76E-02	0.0244	5.18E-03	18828	1.13E-02	0.0217	3.79E-03	12462.78	1.71E-02	0.0477	1.79E-02
7801.54	2.73E-02	0.0244	5.14E-03	19000.4	1.12E-02	0.0218	3.75E-03	12536.44	1.70E-02	0.0477	1.80E-02
7864.14	2.71E-02	0.0244	5.11E-03	19172.9	1.11E-02	0.0218	3.65E-03	12610.47	1.69E-02	0.0478	1.80E-02
7926.28	2.69E-02	0.0244	5.10E-03	19357.4	1.10E-02	0.0218	3.62E-03	12684.77	1.68E-02	0.0478	1.79E-02
7989.15	2.67E-02	0.0244	5.09E-03	19554.2	1.09E-02	0.0218	3.58E-03	12758.8	1.67E-02	0.0479	1.80E-02
8052.11	2.65E-02	0.0245	5.05E-03	19763.2	1.08E-02	0.0218	3.54E-03	12833.01	1.66E-02	0.0479	1.80E-02
8114.89	2.63E-02	0.0245	5.04E-03	19961.7	1.07E-02	0.0218	3.48E-03	12907.49	1.65E-02	0.048	1.79E-02
8177.58	2.61E-02	0.0245	4.99E-03	20172.2	1.06E-02	0.0219	3.41E-03	12982.15	1.64E-02	0.048	1.79E-02
8240.63	2.59E-02	0.0245	4.97E-03	20372	1.05E-02	0.0219	3.36E-03	13057	1.63E-02	0.048	1.79E-02
8303.95	2.57E-02	0.0245	4.90E-03	20572.3	1.04E-02	0.0219	3.29E-03	13132.02	1.62E-02	0.0481	1.78E-02
8367.36	2.55E-02	0.0245	4.90E-03	20773.9	1.03E-02	0.0219	3.23E-03	13207.41	1.62E-02	0.0481	1.78E-02
8431.05	2.53E-02	0.0246	4.90E-03	20976.7	1.02E-02	0.0219	3.22E-03	13289.61	1.61E-02	0.0482	1.78E-02
8500.36	2.51E-02	0.0246	4.89E-03	21179.6	1.01E-02	0.0219	3.16E-03	13372.43	1.60E-02	0.0482	1.77E-02
8569.67	2.49E-02	0.0246	4.84E-03	21383.5	9.98E-03	0.0219	3.13E-03	13454.99	1.59E-02	0.0483	1.77E-02
8639.34	2.47E-02	0.0246	4.81E-03	21588.7	9.88E-03	0.0219	3.06E-03	13537.73	1.58E-02	0.0483	1.77E-02
8709.02	2.45E-02	0.0246	4.78E-03	21795.3	9.79E-03	0.022	3.00E-03	13620.37	1.57E-02	0.0484	1.77E-02
8778.78	2.43E-02	0.0246	4.78E-03	21990.3	9.70E-03	0.022	2.97E-03	13703.47	1.56E-02	0.0484	1.76E-02
8849.00	2.41E-02	0.0247	4.75E-03	22185.9	9.62E-03	0.022	2.96E-03	13786.93	1.55E-02	0.0485	1.75E-02
8919.85	2.39E-02	0.0247	4.75E-03	22395.3	9.53E-03	0.022	2.94E-03	13870.58	1.54E-02	0.0485	1.76E-02
8990.70	2.37E-02	0.0247	4.72E-03	22617.1	9.43E-03	0.022	2.92E-03	13961.12	1.53E-02	0.0486	1.75E-02
9061.56	2.35E-02	0.0247	4.70E-03	22839.7	9.34E-03	0.022	2.90E-03	14051.84	1.52E-02	0.0486	1.75E-02

9132.59	2.34E-02	0.0247	4.64E-03	23050.2	9.26E-03	0.022	2.89E-03	14142.83	1.51E-02	0.0487	1.74E-02
9203.44	2.32E-02	0.0247	4.59E-03	23249.5	9.18E-03	0.022	2.86E-03	14230.28	1.50E-02	0.0487	1.73E-02
9268.94	2.30E-02	0.0247	4.54E-03	23462.2	9.09E-03	0.0221	2.85E-03	14317.83	1.49E-02	0.0487	1.72E-02
9334.90	2.29E-02	0.0248	4.52E-03	23675.3	9.01E-03	0.0221	2.82E-03	14405.65	1.48E-02	0.0488	1.71E-02
9401.03	2.27E-02	0.0248	4.46E-03	23902.3	8.93E-03	0.0221	2.81E-03	14497.46	1.47E-02	0.0488	1.70E-02
9467.08	2.25E-02	0.0248	4.40E-03	24130.2	8.84E-03	0.0221	2.79E-03	14593.08	1.46E-02	0.0489	1.70E-02
9533.48	2.24E-02	0.0248	4.37E-03	24372.2	8.75E-03	0.0221	2.74E-03	14688.69	1.45E-02	0.0489	1.69E-02
9605.97	2.22E-02	0.0248	4.30E-03	24614.4	8.67E-03	0.0221	2.69E-03	14788.03	1.44E-02	0.049	1.69E-02
9684.62	2.20E-02	0.0248	4.26E-03	24858.5	8.58E-03	0.0221	2.66E-03	14888.01	1.43E-02	0.049	1.68E-02
9763.46	2.19E-02	0.0248	4.23E-03	25117.8	8.49E-03	0.0221	2.63E-03	14984.63	1.42E-02	0.0491	1.67E-02
9842.57	2.17E-02	0.0249	4.21E-03	25389.9	8.40E-03	0.0221	2.61E-03	15092.04	1.41E-02	0.0491	1.67E-02
9921.95	2.15E-02	0.0249	4.21E-03	25681.1	8.31E-03	0.0222	2.56E-03	15202.99	1.40E-02	0.0492	1.67E-02
10008.1	2.13E-02	0.0249	4.18E-03	25972.7	8.21E-03	0.0222	2.52E-03	15314.39	1.39E-02	0.0492	1.67E-02
10094.0	2.11E-02	0.0249	4.16E-03	26265.2	8.12E-03	0.0222	2.47E-03	15426.34	1.38E-02	0.0493	1.66E-02
10180.0	2.10E-02	0.0249	4.13E-03	26558.9	8.03E-03	0.0222	2.44E-03	15541.83	1.37E-02	0.0493	1.67E-02
10266.3	2.08E-02	0.0249	4.13E-03	26845.2	7.95E-03	0.0222	2.41E-03	15657.77	1.36E-02	0.0494	1.66E-02
10353.0	2.06E-02	0.0249	4.11E-03	27164	7.85E-03	0.0222	2.40E-03	15770.9	1.35E-02	0.0495	1.66E-02
10439.7	2.04E-02	0.025	4.05E-03	27487.2	7.76E-03	0.0222	2.39E-03	15887.84	1.34E-02	0.0495	1.65E-02
10527.0	2.03E-02	0.025	4.07E-03	27811.5	7.67E-03	0.0222	2.37E-03	16004.96	1.33E-02	0.0496	1.64E-02
10608.5	2.01E-02	0.025	4.04E-03	28131.5	7.58E-03	0.0223	2.37E-03	16125.62	1.32E-02	0.0496	1.63E-02
10696.3	1.99E-02	0.025	4.01E-03	28448.7	7.50E-03	0.0223	2.36E-03	16247.18	1.31E-02	0.0497	1.62E-02
10784.2	1.98E-02	0.025	3.99E-03	28776.9	7.41E-03	0.0223	2.34E-03	16361.49	1.30E-02	0.0497	1.61E-02
10872.7	1.96E-02	0.025	3.95E-03	29110.9	7.33E-03	0.0223	2.34E-03	16477.16	1.30E-02	0.0498	1.60E-02
10954.9	1.95E-02	0.025	3.96E-03	29450.1	7.24E-03	0.0223	2.35E-03	16592.65	1.29E-02	0.0498	1.59E-02
11037.5	1.93E-02	0.0251	3.96E-03	29781.7	7.16E-03	0.0223	2.37E-03	16712.03	1.28E-02	0.0499	1.59E-02
11126.7	1.92E-02	0.0251	3.94E-03	30118	7.08E-03	0.0223	2.39E-03	16832.06	1.27E-02	0.0499	1.58E-02
11215.8	1.90E-02	0.0251	3.93E-03	30460	7.00E-03	0.0223	2.42E-03	16952.35	1.26E-02	0.05	1.57E-02
11304.8	1.89E-02	0.0251	3.92E-03	30781.7	6.93E-03	0.0223	2.46E-03	17076.37	1.25E-02	0.05	1.56E-02
11394.1	1.87E-02	0.0251	3.93E-03	31110.9	6.86E-03	0.0224	2.48E-03	17200.84	1.24E-02	0.0501	1.55E-02
11477.5	1.86E-02	0.0251	3.89E-03	31445	6.78E-03	0.0224	2.51E-03	17325.31	1.23E-02	0.0501	1.55E-02
11567.3	1.84E-02	0.0251	3.88E-03	31763.3	6.72E-03	0.0224	2.53E-03	17450.68	1.22E-02	0.0502	1.54E-02

11651.3	1.83E-02	0.0252	3.88E-03	32063.7	6.65E-03	0.0224	2.51E-03	17575.87	1.21E-02	0.0502	1.54E-02
11742.2	1.82E-02	0.0252	3.89E-03	32385.3	6.59E-03	0.0224	2.52E-03	17702.25	1.21E-02	0.0502	1.53E-02
11832.7	1.80E-02	0.0252	3.92E-03	32709	6.52E-03	0.0224	2.52E-03	17828.35	1.20E-02	0.0503	1.52E-02
11923.5	1.79E-02	0.0252	3.90E-03	33033.2	6.46E-03	0.0224	2.52E-03	17955.63	1.19E-02	0.0503	1.51E-02
12014.6	1.78E-02	0.0252	3.87E-03	33377.9	6.39E-03	0.0224	2.50E-03	18082.91	1.18E-02	0.0504	1.50E-02
12099.7	1.76E-02	0.0252	3.88E-03	33763.4	6.32E-03	0.0224	2.47E-03	18211.01	1.17E-02	0.0504	1.49E-02
12191.4	1.75E-02	0.0252	3.86E-03	34169.7	6.24E-03	0.0225	2.45E-03	18338.65	1.16E-02	0.0505	1.48E-02
12290.2	1.74E-02	0.0252	3.87E-03	34598.1	6.17E-03	0.0225	2.40E-03	18467.2	1.16E-02	0.0505	1.49E-02
12388.9	1.72E-02	0.0253	3.89E-03	35028.8	6.09E-03	0.0225	2.36E-03	18595.93	1.15E-02	0.0506	1.48E-02
12494.6	1.71E-02	0.0253	3.89E-03	35500.9	6.01E-03	0.0225	2.32E-03	18725.48	1.14E-02	0.0506	1.48E-02
12594.2	1.69E-02	0.0253	3.87E-03	35973.8	5.93E-03	0.0225	2.29E-03	18855.39	1.13E-02	0.0507	1.48E-02
12700.6	1.68E-02	0.0253	3.84E-03	36448.3	5.85E-03	0.0225	2.29E-03	18985.67	1.12E-02	0.0507	1.47E-02
12800.6	1.67E-02	0.0253	3.79E-03	36946.2	5.77E-03	0.0225	2.28E-03	19115.58	1.12E-02	0.0507	1.47E-02
12907.8	1.65E-02	0.0253	3.72E-03	37446.4	5.70E-03	0.0226	2.27E-03	19246.04	1.11E-02	0.0508	1.46E-02
13021.9	1.64E-02	0.0253	3.65E-03	37947.5	5.62E-03	0.0226	2.26E-03	19376.86	1.10E-02	0.0508	1.45E-02
13142.8	1.62E-02	0.0254	3.63E-03	38452.3	5.55E-03	0.0226	2.27E-03	19508.4	1.09E-02	0.0509	1.45E-02
13263.9	1.61E-02	0.0254	3.56E-03	38960.4	5.48E-03	0.0226	2.26E-03	19639.58	1.09E-02	0.0509	1.45E-02
13379.3	1.59E-02	0.0254	3.53E-03	39431.7	5.41E-03	0.0226	2.25E-03	19771.85	1.08E-02	0.051	1.44E-02
13494.8	1.58E-02	0.0254	3.50E-03	39906	5.35E-03	0.0226	2.28E-03	19903.76	1.07E-02	0.051	1.43E-02
13618.0	1.57E-02	0.0254	3.44E-03	40361.3	5.29E-03	0.0226	2.31E-03	20036.48	1.07E-02	0.051	1.42E-02
13737.7	1.55E-02	0.0254	3.38E-03	40820.5	5.23E-03	0.0226	2.31E-03	20169.03	1.06E-02	0.0511	1.41E-02
13868.4	1.54E-02	0.0254	3.35E-03	41280.5	5.17E-03	0.0226	2.31E-03	20314	1.05E-02	0.0511	1.40E-02
13992.5	1.53E-02	0.0254	3.31E-03	41763	5.11E-03	0.0227	2.32E-03	20460.06	1.04E-02	0.0512	1.39E-02
14119.8	1.51E-02	0.0255	3.30E-03	42229	5.05E-03	0.0227	2.30E-03	20606.66	1.04E-02	0.0512	1.38E-02
14240.8	1.50E-02	0.0255	3.31E-03	42675.2	5.00E-03	0.0227	2.31E-03	20765.88	1.03E-02	0.0513	1.38E-02
14373.3	1.48E-02	0.0255	3.36E-03	43189.3	4.94E-03	0.0227	2.30E-03	20925.55	1.02E-02	0.0513	1.37E-02
14499.7	1.47E-02	0.0255	3.32E-03	43704.4	4.88E-03	0.0227	2.30E-03	21084.94	1.01E-02	0.0513	1.35E-02
14629.3	1.46E-02	0.0255	3.33E-03	44178.8	4.83E-03	0.0227	2.30E-03	21245.7	1.00E-02	0.0514	1.35E-02
14762.7	1.45E-02	0.0255	3.30E-03	44699.1	4.77E-03	0.0227	2.29E-03	21419.15	9.96E-03	0.0514	1.34E-02
14900.0	1.43E-02	0.0255	3.26E-03	45200.9	4.72E-03	0.0227	2.28E-03	21593.06	9.88E-03	0.0515	1.33E-02
15034.0	1.42E-02	0.0256	3.23E-03	45755	4.66E-03	0.0227	2.24E-03	21767.16	9.80E-03	0.0515	1.33E-02

15187.0	1.41E-02	0.0256	3.23E-03	46267.5	4.61E-03	0.0228	2.24E-03	21955.22	9.72E-03	0.0516	1.33E-02
15333.0	1.39E-02	0.0256	3.21E-03	46815.2	4.56E-03	0.0228	2.26E-03	22130.76	9.64E-03	0.0516	1.31E-02
15483.1	1.38E-02	0.0256	3.19E-03	47343	4.51E-03	0.0228	2.25E-03	22306.94	9.56E-03	0.0517	1.30E-02
15634.0	1.36E-02	0.0256	3.13E-03	47885.3	4.46E-03	0.0228	2.28E-03	22483.4	9.49E-03	0.0517	1.30E-02
15789.0	1.35E-02	0.0256	3.04E-03	48486.6	4.40E-03	0.0228	2.27E-03	22648.05	9.42E-03	0.0518	1.29E-02
15929.4	1.34E-02	0.0256	2.95E-03	49057.9	4.35E-03	0.0228	2.30E-03	22825.68	9.35E-03	0.0518	1.28E-02
16073.8	1.33E-02	0.0256	2.91E-03	49642.7	4.30E-03	0.0228	2.31E-03	23004.22	9.27E-03	0.0518	1.29E-02
16230.2	1.31E-02	0.0257	2.86E-03	50264	4.24E-03	0.0228	2.33E-03	23182.85	9.20E-03	0.0519	1.29E-02
16398.4	1.30E-02	0.0257	2.83E-03	50877.6	4.19E-03	0.0229	2.35E-03	23348.96	9.14E-03	0.0519	1.29E-02
16559.7	1.29E-02	0.0257	2.79E-03	51534.8	4.14E-03	0.0229	2.36E-03	23516.43	9.07E-03	0.052	1.28E-02
16721.9	1.28E-02	0.0257	2.77E-03	52148.7	4.09E-03	0.0229	2.37E-03	23683.81	9.01E-03	0.052	1.27E-02
16877.3	1.26E-02	0.0257	2.73E-03	52769.6	4.04E-03	0.0229	2.37E-03	23838.76	8.95E-03	0.052	1.26E-02
17032.9	1.25E-02	0.0257	2.69E-03	53364.3	4.00E-03	0.0229	2.35E-03	23994.62	8.89E-03	0.0521	1.27E-02
17189.0	1.24E-02	0.0257	2.66E-03	53996.1	3.95E-03	0.0229	2.33E-03	24150.38	8.83E-03	0.0521	1.27E-02
17368.1	1.23E-02	0.0257	2.66E-03	54577.6	3.91E-03	0.0229	2.34E-03	24306.61	8.78E-03	0.0521	1.27E-02
17558.7	1.22E-02	0.0257	2.66E-03	55200.4	3.87E-03	0.0229	2.32E-03	24463.37	8.72E-03	0.0522	1.27E-02
17750.5	1.20E-02	0.0258	2.67E-03	55827.2	3.82E-03	0.0229	2.25E-03	24607.52	8.67E-03	0.0522	1.26E-02
17953.9	1.19E-02	0.0258	2.66E-03	56457.8	3.78E-03	0.023	2.20E-03	24752.4	8.62E-03	0.0522	1.25E-02
18146.9	1.18E-02	0.0258	2.61E-03	57048.7	3.74E-03	0.023	2.17E-03	24897.2	8.57E-03	0.0523	1.25E-02
18340.4	1.16E-02	0.0258	2.56E-03	57559.3	3.71E-03	0.023	2.15E-03	25042.98	8.52E-03	0.0523	1.24E-02
18546.5	1.15E-02	0.0258	2.51E-03	58215.4	3.66E-03	0.023	2.11E-03	25202.1	8.46E-03	0.0523	1.24E-02
18752.5	1.14E-02	0.0258	2.43E-03	59087.9	3.61E-03	0.023	2.09E-03	25376.02	8.41E-03	0.0524	1.24E-02
18971.6	1.12E-02	0.0258	2.33E-03	59765.2	3.57E-03	0.023	2.07E-03	25549.47	8.35E-03	0.0524	1.23E-02
19216.2	1.11E-02	0.0258	2.24E-03					25724.2	8.29E-03	0.0525	1.23E-02
19460.7	1.10E-02	0.0259	2.15E-03					25912.72	8.23E-03	0.0525	1.22E-02
19695.7	1.08E-02	0.0259	2.04E-03					26115.93	8.17E-03	0.0525	1.20E-02
19956.2	1.07E-02	0.0259	1.97E-03					26318.69	8.11E-03	0.0526	1.19E-02
20242.2	1.05E-02	0.0259	1.88E-03					26523.18	8.04E-03	0.0526	1.20E-02
20529.7	1.04E-02	0.0259	1.79E-03					26727.21	7.98E-03	0.0527	1.20E-02
20817.9	1.03E-02	0.0259	1.73E-03					26945.93	7.92E-03	0.0527	1.19E-02
21120.7	1.01E-02	0.0259	1.66E-03					27179.36	7.85E-03	0.0527	1.18E-02

21412.5	9.96E-03	0.0259	1.61E-03					27413.42	7.78E-03	0.0528	1.18E-02
21756.1	9.81E-03	0.0259	1.59E-03					27634.68	7.72E-03	0.0528	1.17E-02
22102.2	9.65E-03	0.0259	1.59E-03					27871.1	7.65E-03	0.0529	1.17E-02
22463.2	9.50E-03	0.026	1.58E-03					28107.06	7.59E-03	0.0529	1.16E-02
22865.0	9.33E-03	0.026	1.58E-03					28344.3	7.53E-03	0.053	1.15E-02
23268.0	9.17E-03	0.026	1.58E-03					28587.16	7.46E-03	0.053	1.14E-02
23662.4	9.02E-03	0.026	1.56E-03					28845.62	7.40E-03	0.053	1.14E-02
24045.8	8.87E-03	0.026	1.54E-03					29127.94	7.32E-03	0.0531	1.13E-02
24471.3	8.72E-03	0.026	1.53E-03					29415.89	7.25E-03	0.0531	1.12E-02
24897.9	8.57E-03	0.026	1.51E-03					29714.36	7.18E-03	0.0532	1.12E-02
25353.8	8.41E-03	0.026	1.49E-03					30020.9	7.11E-03	0.0532	1.11E-02
25837.4	8.26E-03	0.0261	1.46E-03					30318.56	7.04E-03	0.0533	1.11E-02
26330.6	8.10E-03	0.0261	1.43E-03					30640.7	6.96E-03	0.0533	1.11E-02
26849.1	7.95E-03	0.0261	1.39E-03					30974.1	6.89E-03	0.0534	1.10E-02
27353.7	7.80E-03	0.0261	1.35E-03					31313.12	6.81E-03	0.0534	1.11E-02
27881.2	7.65E-03	0.0261	1.30E-03					31643.44	6.74E-03	0.0535	1.11E-02
28434.9	7.50E-03	0.0261	1.27E-03					31958.6	6.68E-03	0.0535	1.12E-02
29001.7	7.36E-03	0.0261	1.24E-03					32262.33	6.61E-03	0.0536	1.13E-02
29581.2	7.21E-03	0.0261	1.23E-03					32547.46	6.55E-03	0.0536	1.15E-02
30171.9	7.07E-03	0.0261	1.23E-03					32833.5	6.50E-03	0.0537	1.16E-02
30788.5	6.93E-03	0.0262	1.20E-03					33101.04	6.45E-03	0.0537	1.18E-02
31397.5	6.79E-03	0.0262	1.21E-03					33352.88	6.40E-03	0.0537	1.19E-02
32025.9	6.66E-03	0.0262	1.22E-03					33626.22	6.34E-03	0.0538	1.20E-02
32601.4	6.54E-03	0.0262	1.23E-03					33880.06	6.30E-03	0.0538	1.21E-02
33232.3	6.42E-03	0.0262	1.23E-03					34115.2	6.25E-03	0.0539	1.23E-02
33967.6	6.28E-03	0.0262	1.25E-03					34350.98	6.21E-03	0.0539	1.24E-02
34648.2	6.16E-03	0.0262	1.26E-03					34607.36	6.16E-03	0.0539	1.24E-02
35400.9	6.03E-03	0.0262	1.27E-03					34866.36	6.12E-03	0.054	1.25E-02
36205.8	5.89E-03	0.0262	1.29E-03					35127.1	6.07E-03	0.054	1.26E-02
37056.5	5.76E-03	0.0263	1.30E-03					35408.97	6.03E-03	0.0541	1.26E-02
37915.0	5.63E-03	0.0263	1.32E-03					35712.06	5.97E-03	0.0541	1.27E-02

38842.3	5.49E-03	0.0263	1.38E-03					36016.52	5.92E-03	0.0542	1.26E-02
39732.2	5.37E-03	0.0263	1.41E-03					36320.8	5.87E-03	0.0542	1.27E-02
40584.2	5.26E-03	0.0263	1.44E-03					36605.75	5.83E-03	0.0542	1.28E-02
41459.8	5.15E-03	0.0263	1.50E-03					36891.43	5.78E-03	0.0543	1.28E-02
42238.5	5.05E-03	0.0263	1.56E-03					37177.92	5.74E-03	0.0543	1.28E-02
42919.7	4.97E-03	0.0263	1.62E-03					37486.01	5.69E-03	0.0544	1.29E-02
43647.2	4.89E-03	0.0264	1.68E-03					37774.41	5.65E-03	0.0544	1.31E-02
44317.8	4.81E-03	0.0264	1.73E-03					38063.45	5.60E-03	0.0545	1.32E-02
44951.2	4.75E-03	0.0264	1.77E-03					38354.3	5.56E-03	0.0545	1.32E-02
45567.4	4.68E-03	0.0264	1.81E-03					38625.19	5.52E-03	0.0546	1.33E-02
46126.0	4.63E-03	0.0264	1.84E-03					38897.26	5.48E-03	0.0546	1.33E-02
46765.2	4.56E-03	0.0264	1.82E-03					39169.51	5.45E-03	0.0546	1.35E-02
47411.0	4.50E-03	0.0264	1.81E-03					39442.49	5.41E-03	0.0547	1.36E-02
48093.4	4.44E-03	0.0264	1.81E-03					39716.29	5.37E-03	0.0547	1.37E-02
48849.3	4.37E-03	0.0264	1.78E-03					39990.98	5.33E-03	0.0548	1.39E-02
49642.1	4.30E-03	0.0265	1.77E-03					40265.95	5.30E-03	0.0548	1.40E-02
50450.0	4.23E-03	0.0265	1.73E-03					40520.07	5.27E-03	0.0548	1.42E-02
51432.3	4.15E-03	0.0265	1.66E-03					40796.85	5.23E-03	0.0549	1.43E-02
52304.7	4.08E-03	0.0265	1.64E-03					41074.45	5.19E-03	0.0549	1.45E-02
53313.1	4.00E-03	0.0265	1.61E-03					41374.38	5.16E-03	0.055	1.47E-02
54172.4	3.94E-03	0.0265	1.59E-03					41674.84	5.12E-03	0.055	1.49E-02
55216.5	3.86E-03	0.0265	1.57E-03					41955.17	5.09E-03	0.0551	1.51E-02
57204.0	3.73E-03	0.0265	1.56E-03					42235.59	5.05E-03	0.0551	1.52E-02
								42517.36	5.02E-03	0.0551	1.53E-02
								42798.51	4.98E-03	0.0552	1.53E-02
								43081.1	4.95E-03	0.0552	1.54E-02
								43386.38	4.92E-03	0.0553	1.54E-02
								43692.74	4.88E-03	0.0553	1.53E-02
								44000.65	4.85E-03	0.0554	1.53E-02
								44308.64	4.81E-03	0.0554	1.52E-02
								44595.77	4.78E-03	0.0555	1.52E-02

								44883.9	4.75E-03	0.0555	1.51E-02
								45172.3	4.72E-03	0.0555	1.51E-02
								45461.88	4.69E-03	0.0556	1.51E-02
								45752.09	4.66E-03	0.0556	1.53E-02
								46043.22	4.63E-03	0.0557	1.55E-02
								46335.07	4.60E-03	0.0557	1.56E-02
								46605.05	4.58E-03	0.0558	1.58E-02
								46875.94	4.55E-03	0.0558	1.60E-02
								47124.34	4.53E-03	0.0558	1.62E-02
								47374	4.50E-03	0.0559	1.63E-02
								47647.15	4.48E-03	0.0559	1.59E-02
								47902.13	4.45E-03	0.056	1.60E-02
								48160.38	4.43E-03	0.056	1.60E-02
								48425.86	4.41E-03	0.056	1.60E-02
								48710.67	4.38E-03	0.0561	1.59E-02
								49132.8	4.34E-03	0.0561	1.56E-02